# INTERACTIONS BETWEEN PLATELETS AND PLATELET DERIVED MICROVESICLES IN INFLAMMATION

**By**

**Clare Louise Box**

**A thesis submitted to**
**The University of Birmingham**
**For the degree of**
**DOCTOR OF PHILOSOPHY**

School of Clinical and Experimental Medicine
College of Medical and Dental Sciences
University of Birmingham
Date: Oct 2014

## Abstract

Atherosclerosis is a chronic inflammatory disease, characterised by infiltration of leukocytes and accumulation of fatty deposits in the artery wall. Early events in this disease process include recruitment of platelets to the artery wall, which in turn aid in leukocyte recruitment. However, upon activation platelets release microvesicles (PMV), we are interested in whether PMV have a role in enhancing leukocyte recruitment.

We demonstrated using whole blood that upon activation, platelets form aggregates with monocytes and neutrophils. The data suggests that upon platelet activation, PMV may be generated and subsequently may have a role in heterotypic aggregate formation observed. Interestingly, lymphocytes did not form aggregates with platelets (or PMV) as readily. We showed that blocking P-selectin leads to a significant reduction in heterotypic aggregate formation. We also demonstrated the presence of P-selectin glycoprotein ligand-1 (PSGL1), the ligand with the highest binding affinity for P-selectin, on monocytes and neutrophils.

Monocytes preferentially bound platelets or PMV. However, we found no significant increase in recruitment of these heterotypic aggregates to von Willebrand factor, under conditions of low shear stress compared to monocytes alone. These heterotypic aggregates provide a mechanism for cross-talk between cell types and have a potential role in inflammatory and thrombotic diseases.

## Acknowledgements

*I would first like to thank my supervisor Prof Ed Rainger for giving me the opportunity to work on this project and for your advice, guidance and support. I would also like to thank my second and third supervisors, Prof Lorraine Harper and Prof Steve Watson, and also Prof Gerard Nash and Dr Paul Harrison for your advice and guidance.*

*I would also like to thank Samantha Tull, Myriam Chimen, Matthew Harrison and Clara Yates for your contributions to the project and for help in the lab with platelet adhesion assays, monocyte isolations, flow assays and for help with the Nanosight. Thank you to Dr Eduard Shantsila for your advice with regards to setting up the flow cytometry protocol. Also thanks to Phil Kitchen for your help with western blots. Thank you to members of the Watson group particularly Craig Hughes, Monica Armen Albert, Marie Lordkipanidze and Stef Watson for lending me reagents and for all your help and advice.*

*I would also like to say a massive thank you to everyone in the Rainger/Nash group and the downstairs office. Particularly Stacey, Bon, Jas, Hafsa, Arjun, Emma, Andy and Mike for putting up with my endless moaning and providing cups of much needed tea. I also want to thank all the blood donors who made this project possible.*

*Last but not least I want to say a massive thank you to all my family and friends for putting up with me over the last four years! Particularly my Mom, my brother Kev and my friends Amanda, Cathy, Lou, Judith, Heather and Rach. Thank you for always being there for me I couldn't have achieved this without you.*

## Table of contents

## Table of figures

## List of tables

## Abbreviations

AA: Arachidonic acid
ACS: Acute coronary syndrome
ADP: Adenosine diphosphate
ang1: Angiopoietin
APC: Allophycocyanin
APES: (3-aminopropyl)triethoxysilane
APOB-100: Apolipoprotein B-100
APOE: Apolipoprotein E
ATP: Adenosine triphosphate
BCR: B-cell receptor
BSA: Bovine serum albumin
C2GnT: Core 2 N-acetylglucosamine transferase
CC-CKR-1: CC-chemokine receptor-1
CCL1: Chemokine (CC motif) ligand 1
CCR1: Chemokine (CC motif) receptor 1
CD: Cluster of differentiation
$CD4^+$: Helper T-cells
$CD8^+$: Cytotoxic T cell
CD40L: Cluster of differentiation 40 ligand
CD99L2: Cluster of differentiation 99 Like 2
CLEC-2: C -type lectin receptor
$CO_2$: Carbon dioxide
COX-1: Cyclooxygenase-1
CPDA: Citrate phosphate dextrose solution
CRP-XL: Collegen related peptide (cross linked form)
CTH: Calf thymus histones
CXCL1: Chemokine (CX motif) ligand 1
CXCR1: Chemokine (CX motif) receptor 1
CX3CL1: Fractalkine
CX3CL1: Fractalkine receptor
DC: Dendritic cells
δ: Dense (platelet storage granules)
D: Diversity chains
DAMPS: Damage- associated molecular pattern molecules
DM: Diabetes mellitus
DMSO: Dimethyl sulphoxide hybri-max
EC: Endothelial cells
EDTA: Ethylenediaminetetraacetic acid
EGM2-MV: Endothelial cell growth medium (Lonza)
ENA-78: Epithelial derived activating peptide
eNOS: Endothelial nitric oxide synthase
ESAM: Endothelial cell selective adhesion molecule
E-selectin: Endothelial-selectin
ET-1: Endothilin-1
FA: Formaldehyde
FCS: Foetal Calf Serum

FITC: Fluorescein isothiocyanate
fMLP-R: Formyl-methionyl-leucyl-phenylalanine receptor
FucT-VII: Fucosyltransferase VII
FXII: Factor XII
GAGS: Glycosaminoglycans
GCP-2: Granulocyte chemotactic protein-2
GBM: Glomerular basement membrane
G-CSF: Granulocyte cell stimulating factor
GEnC: Glomerular endothelial cells
GFB: Glomerular filtration barrier
GM-CSF: Granulocyte/macrophage cell stimulating factor
GPCRs: G-protein coupled receptors
GPIb: Glycoprotein Ib-IX-V
GPVI: Glycoprotein VI
GROα: Chemokine (CX motif) ligand 1
GROβ: Chemokine (CX motif) ligand 2
GROγ: Chemokine (CX motif) ligand 3
H3: Histone 3
HRP: Horseradish peroxidase
HUVEC: Human umbilical vein endothelial cells
ICAM-1: Intracellular adhesion molecule-1
IFN-γ: Interferon γ
Ig: Immunoglobulin
IL-1β: Interlukin-1β
IL-8RA: Interlukin-8 receptor A
IP-10: Interferon gamma induced protein-10
I-TAC: Interferon-inducible T-cell alpha chemoattractant
J: Joining chains
JAMs: Junction adhesion molecules
JAM-A: Junction adhesion molecule-A
LDL: Low density-lipoprotein
LFA-1: Lymphocyte function associated antigen-1 (or CD11a/CD18 or αL integrin/ β2 integrin)
LOX-1: Lectin like oxidised low-density lipoprotein receptor-1
LPA: Lymphocyte-platelet aggregate
LRR: Leucine rich repeats
L-selectin: Leukocyte-selectin
LPS: Lipopolysaccharide
$Ly6C^{hi}$: mouse monocyte subset
$Ly6C^{lo}$: mouse monocyte subset
MAC-1: Macrophage antigen-1 (or CD11b/CD18 αM integrin/β2 integrin)
M-CSF: Macrophage stimulating factor
MCP-1: Monocyte chemotactic protein-1
MFI: Median fluorescent intensity
MHC: Major histocompatibitly complex
MI: Myocardial infarction
MIG: Monokine induced by gamma interferon
MIP1α: Macrophage inflammatory protein-1 alpha

miRNA: micro-RNA
Mon1: Classical monocytes
Mon2: Intermediate monocytes
Mon3: Non classical monocytes
MPA: Monocyte-platelet aggregate
NAP-2: Neutrophil activating peptide-2
NETs: Neutrophil extracellular traps
NK: Natural killer cells
NLRs: Nucleotide binding oligomerization domain like receptors
NO: Nitric oxide
NPA: Neutrophil platelet aggregate
OLR1: Lectin like oxidised low-density lipoprotein receptor-1
oxLDL: Oxidised low-density lipoprotein
P41: Passage 41
PAMPS: Pathogen associated molecular patterns
PAR1: Protease activated receptor 1
PBMC: Peripheral blood mononuclear cells
PBS: Phosphate buffered saline
PBSA: PBS and BSA
PBS-t: PBS tween
PDGF: Platelet derived growth factor
PE: Phycoerythrin
PECAM-1: Platelet endothelial cell adhesion molecule (CD31)
PEcy7: PEcyanine7
PF4: Platelet factor 4
PGI2: Prostaglandin-I2
PKA: Protein kinase A
PLC-γ2: Phospholipase C-γ2
PMN: Polymorphic nuclear cells
PMV: Platelet microvesicles
PPP: Platelet poor plasma
PRP: Platelet rich plasma
PRRs: Pattern recognition receptors
P-selectin: Platelet-selectin
PSGL1: P-selectin glycoprotein ligand 1
PVDF: Polyvinylidene fluoride
RA: Rheumatoid arthritis
RANTES: Regulated on activation normal T-cell expressed and secreted
RBC: Red blood cells
RPMI: Roswell Park Memorial Institute
ROS: Reactive oxygen species
RT: Room temperature
SD: Standard deviation
SDF-1: Stromal cell derived factor-1
SEM: Standard error of mean
SFK: Src family kinase
SLE: Systemic lupus erythematosus

SMC: Smooth muscle cells
SRA: Scavenger receptor A
SV40LT: Temperature sensitive simian virus 40 large tumour antigen
SYK: Spleen tyrosine kinase
TCR: T-cell receptor
TEER: Transepithelial electrical resistance
TF: Tissue factor
TFPI: Tissue factor pathway inhibitor
TGFβ: Transforming growth factor-β
TGFβR1: Transforming growth factor-β receptor 1
$T_H1$: Helper T-cell 1
$T_H2$: Helper T-cell
Tie2: Angiopoietin receptor
TLRs: Toll like receptors
TLR1: Toll like receptor 1
TNFα: Tumour necrosis factor-α
TP: Thromboxane A2 receptor
TRAP: Thrombin receptor activating peptide
TxA2: Thromboxane
U46619: Thromboxane mimetic
v: Variable chains
VCAM-1: Vascular cell adhesion molecule-1
VE-cadherin: Vascular endothelial-cadherin
VEGF: Vascular endothelial growth factor
VEGFR2: Vascular endothelial growth factor receptor 2
VLA-4: Very late antigen 4
VLDL: Very low density lipoproteins
vWf: von Willebrand factor
WHO: World Health Organisation
XCL1: Chemokine (XC) ligand 1
XCR1: Chemokine (XC) receptor 1

# 1. Chapter 1-GENERAL INTRODUCTION

### 1.1.0 The blood vasculature

### 1.1.1 Endothelial cells

The lumens of all of the blood vessels of the vasculature are lined with a monolayer of endothelial cells (EC), which are in constant contact with the blood. Endothelial cells are joined by tight and adherens junctions and are supported by a subendothelial protein matrix, produced by EC themselves, as well as other cells such as smooth muscles cells and pericytes (**Figure 1-1**) (Michiels, 2003). The subendothelial matrix consists of molecules such as collagen III, IV and V, laminins, heparan sulphate, proteoglycans and fibronectin (Eldor et al., 1985). It provides a surface for anchorage of EC as well as their proliferation and migration, should the monolayer be damaged and an angiogenic response be required (Michiels, 2003). Indeed, fibronectin has also been shown to play a role in EC migration through an integrin dependent mechanism (Roy et al., 2003). EC also regulate the haemostatic process as well as playing an important role in the inflammatory response. These aspects of EC function will be discussed in more detail later.

The EC of veins and arteries form a continuous and poorly permeable barrier, which guards against loss of the cellular and fluid constituents of the blood into the tissues. However, blood is supplied to tissues and organs through capillary beds and the EC lining capillaries need to allow for the passage of nutrients from the blood into the surrounding tissue and for the removal of waste products from the tissue. In some tissues where specialised functions occur the EC and the subendothelial basement membrane have become specially adapted. For example, glomerular endothelial cells (GEnC) of the kidney are fenestrated (60-80nm wide pores), which allows for the efficient passage of solutes and water out of the blood and into the Bowman's capsule (Satchell, 2004). Water and some salts are actively reabsorbed at distal sites, while waste metabolites are excreted from the body in the urine. The subendothelial matrix

below the glomerular EC is highly negatively charged this, coupled with the small size of the fenestrations, prevents large proteins passing through (Satchell et al., 2006). The liver sinusoids, which also require passage of solutes and large macromolecules such as lipoproteins, have discontinuous, fenestrated EC which support the transport of these molecules (Braet and Wisse, 2002).

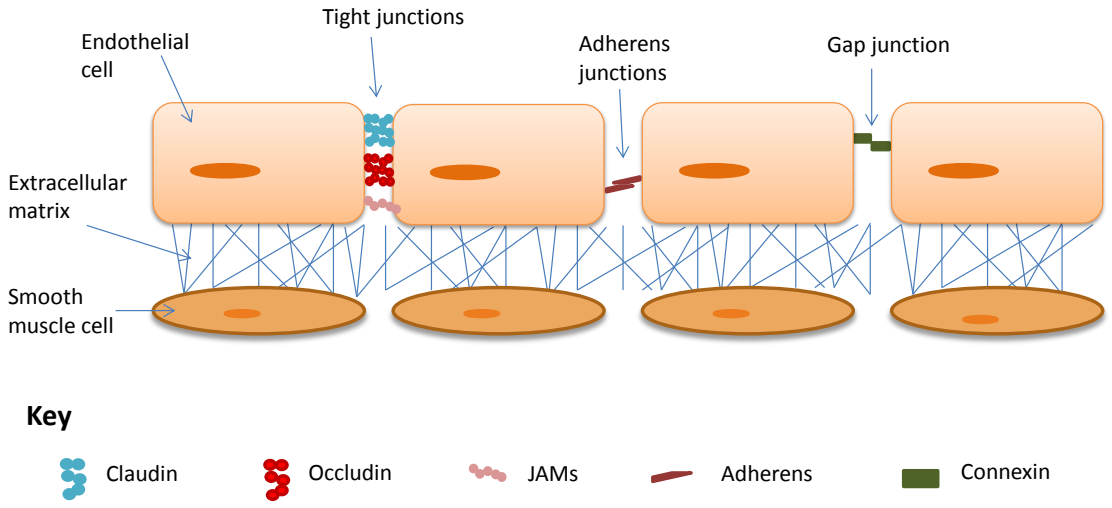


**Figure 1-1: Endothelium lining the blood vasculature**

Endothelial cells lining the blood vessel wall are supported by their own extracellular matrix, which forms above a layer of smooth muscle cells. The endothelial cells are held together to make a poorly permeable barrier through tight junctions made of claudin, occludin, or junction adhesion molecules (JAMs), (including JAM-A, JAM-B and JAM-C), as well as adherens junctions. There are also gap junctions formed from connexin which, allow the passage of nutrients into the tissue and for the removal of waste products. (Image adapted from Otsuka et al., 2012).

### 1.2.0 Blood

Blood has two major components. The first is cellular in nature and includes specialised cells of the immune and haemostatic systems as well as erythrocytes. These are transported in the second, the blood plasma. Plasma is a complex mixture of solutes including proteins such as albumin and clotting factors, metabolites such as glucose and waste products, carbon dioxide ($CO_2$), urea, lactic acid and lipids, which are solubilised by association with lipoproteins.

### 1.2.1 Lineage and development of blood cells

The cells of the blood; leukocytes, erythrocytes and platelets develop in the bone marrow through the process of haematopoesis. This leads to the production of $10^{11}$-$10^{12}$ new blood cells in a healthy adult every day. Haemopoietic stem cells are able to differentiate into multipotent progenitor cells, which in turn differentiate to produce either common lymphoid progenitor cells or common myeloid progenitor cells through the process of mitosis (**Figure 1-2**) (Beerman et al., 2010). Cell fate is determined by the haemopoietic microenvironment, the presence of glycoprotein growth factors (colony stimulating factors) such as granulocyte/macrophage cell stimulating factor (GM-CSF), granulocyte cell stimulating factor (G-CSF) and macrophage stimulating factor (M-CSF), which are able to initiate signal transduction pathways to alter transcription (Krause, 2002). Common myeloid progenitor cells are able to differentiate to form erythrocytes, platelets and cells of the innate immune system (**Figure 1-2**) (Chotinantakul and Leeanansaksiri, 2012). Each of these cells has its own characteristic appearance, and specialised function.

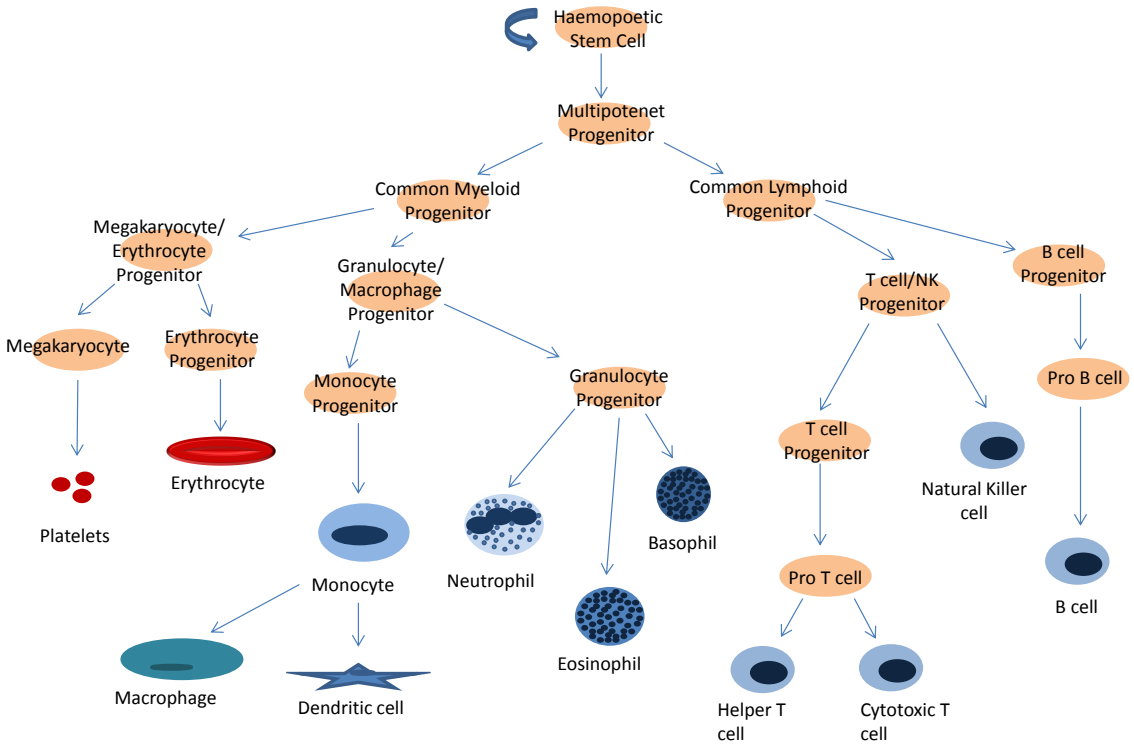


**Figure 1-2: Blood cell development**

Figure 1-2 demonstrates how self renewing haemopoietic stem cells found within the bone marrow are able to differentiate in response to the haemopoietic microenvironment, to form blood cells through the process of haematopoesis. Cells produced from common myeloid progenitor cells platelets, erythrocytes, monocytes, neutrophils, basophils, eosinophils and also a subset of cells produced from common lymphoid progenitor cells -natural killer cells mature in the bone marrow and then are released into the blood stream. Pro T-cells and Pro-B cells are released into the blood where they travel to the thymus and spleen respectively to differentiate into mature T- and B-lymphocytes. Monocytes are capable of migrating into tissues, where they further differentiate to form macrophages and dendritic cells. (Image adapted from Stirewalt and Radich, 2003.)

### 1.2.2 Erythrocytes

Erythrocytes or red blood cells (RBC) are the largest population of blood cells constituting ≈40% of the blood volume, meaning a healthy haematocrit is considered to be between 0.35 and 0.4 (World Health Organisation WHO). They are produced in the red bone marrow and differentiate from common myeloid progenitor cells to produce erythrocyte

progenitor cells (reticulocytes), which are released into the blood to further differentiate to form RBC. Their main function is to transport oxygen to tissues and organs and $CO_2$ from tissues to the lungs. RBC are approximately 4µm in diameter, anucleate, highly deformable and shaped like biconcave discs, characteristics which aid in their ability to travel through small capillaries thereby giving easy access to tissues and organs. They contain haemoglobin, a molecule, which is able to bind oxygen in regions of high concentration (the lungs) and release it in regions of low concentration (metabolising tissues) (Clark et al., 1985).

### 1.2.3 Granulocytes

Granulocyte populations are constituted of neutrophils, basophils and eosinophils. As the name suggests, these cells contain granules which give them a distinct staining phenotype. Eosinophils and basophils are both present in low numbers (i.e. constituting ≈1% of the total leukocyte population in blood). They both have important roles in immunity against multicellular parasites, but also appear to be important in allergic responses (Chirumbolo, 2012; Rosenberg et al., 2013). Eosinophils have a short half life and were thought to have evolved to protect the host from parasitic infections such as helminths, but they may also have a role in protecting the host from infections which occur due to mRNA viruses (Rosenberg et al., 2013). There is also some debate in the literature as to whether eosinophils are able to act as antigen presenting cells, allowing them to play a role in activating the adaptive immune system (Rothenberg and Hogan, 2006).

The most common leukocyte is the neutrophil. These are short lived cells with an average lifespan in the blood, of 5-7 hours (Summers et al., 2010). They are 'the first responders' to an infection and to inflammatory signals (Witko-Sarsat et al., 2000). They contain three types of granules, azurophilic (or primary) granules, specific (or secondary) granules and

tertiary granules, which contain many cytotoxic and bactericidal components (**Table 1-1**). They are most effective at destroying bacterial and fungal cells. When neutrophils come in to contact with bacterial or fungal cells they become activated through pattern recognition receptors (PRR) interaction with pathogen associated molecular patterns (PAMPS). Once activated, neutrophils phagocytose the pathogen. This process involves the pathogen being engulfed and taken up inside a phagocytotic vacuole. Once inside the vacuole the azurophilic and specific granules fuse with the phagocytotic vacuole and degranulate at roughly the same time, followed later by the tertiary granules (Segal, 2005). This leads to the pH inside the vacuole being lowered giving optimal conditions for enzymes (such as serine protease, also released from the granules) to degrade the pathogen (Segal, 2005). The release of nitric oxide and other oxidising agents also help in destroying the pathogen (Witko-Sarsat et al., 2000).

Another way in which neutrophils kill pathogens is through the formation of neutrophil extracellular traps (NETs). NETs are composed mainly of DNA and histones as well as some of the contents from the azurophilic, specific and tertiary granules (Carestia et al., 2013). Histones themselves have been shown to have antimicrobial properties (Huang et al., 2011). This means that NETs provide a way of immobilizing pathogens and exposing them to high concentrations of antimicrobials.

| | |
|---|---|
| **Azurophilic granules** | Myeloperoxidase<br>Defensins<br>Serine protease<br>Lysosomes |
| **Specific granules** | Lactoferrin<br>Lysosome<br>Macrophage antigen-1 MAC-1 (CD11b/CD18)<br>Gelatinase<br>Collagenase<br>Formyl-Methionyl-Leucyl-Phenylalanine receptor (fMLP-R) |
| **Tertiary granules** | MAC-1<br>Lysosomes<br>Acetyltransferase<br>Gelatinase |

**Table 1-1: Contents of Neutrophil Granules**

Table 1-1 shows neutrophil granules and the contents of each (Eyles et al., 2006). Myeloperoxidase produces hypochlorous acid lowering the pH. Defensins, serine proteases, collagenase, and gelatinase damage bacteria or fungi cell membranes and walls, some are even effective against enveloped viruses, these enzymes are most effective at low pH. Lactoferrin targets DNA/RNA and polysaccharide, while MAC-1 and fMLP-R are part of the complement cascade. Lysosmes contain hydrolytic enzymes which also aid in destroying pathogens.

### 1.2.4 Monocytes

Monocytes play a role in both the innate and adaptive immune responses. They are the largest of the leukocytes and possess a distinctive kidney shaped or horseshoe shaped nucleus. Monocytes account for between 5-8% of circulating leukocytes (Ghattas et al., 2013). Monocytes develop from the haemopoietic stem cell precursor known as monoblasts, these later develop into promonocytes and finally monocytes. Monocytes migrate from the bone marrow and enter the blood stream using interactions between chemokine (CC motif) ligand 2 (CCL2), expressed by the bone marrow and monocyte chemokine (CC motif) receptor 2 (CCR2) (Serbina and Pamer, 2006). Once present in the blood stream they circulate for between 1-3 days (Whitelaw and Bell, 1966). Unlike other leukocytes they can migrate into tissues in the absence of inflammation to further differentiate into either macrophages (innate immune cells)

or dendritic cells (DC) (adaptive immune cells) (Serbina and Jia, 2008). As part of the innate immune system, the main function of monocyte derived macrophages is to protect the host from invading pathogens. This is achieved through phagocytosis of exogenous bacteria, fungi and viruses. Macrophages are also important regulators of the inflammatory response, being a major source of inflammatory cytokines (**Table 1-2**) (Murray and Wynn, 2011). Monocytes that differentiate into DC are professional antigen presenting cells and are involved in cross talk with helper T-cells, which leads to activation of the acquired immune response (Randolph et al., 1999). This aspect of their function is discussed in greater detail later.

| | |
|---|---|
| Inflammatory cytokines | TNFα |
| | TGFβ |
| | IL-6 |
| Inflammatory chemokines | CCL2 |
| | CCL3 |
| | CCL4 |
| | CXCL8 |
| Anti-inflammatory cytokines | IL-10 |

**Table 1-2: Cytokines (including chemokines) produced by macrophages**

Table 1-2 shows some of the cytokines (including chemokines) produced by macrophages during the inflammatory response (Yoshida and Tuder, 2007). (Tumour necrosis factor-α, TNFα, transforming growth factor-β, TGFβ, IL, interlukin and CXCL, chemokine CXC motif ligand.)

Monocytes are not a homogenous population, to date three subpopulations have been identified; these include the 'classical monocytes' (or mon1), 'intermediate monocytes' (mon2) or 'non classical monocytes' (mon3) (**Figure 1-3**) (Shantsila et al., 2011). The largest of the monocyte populations (~90%) is the classical monocytes which can be identified by the following markers $CD14^{+}CD16^{-}CCR2^{+}$ (**Figure 1-3**) (Shantsila et al., 2011). Other markers

expressed by this subset include expression of Leucocyte (L)-selectin (Cluster of differentiation 62L, CD62L), CD64 and low level expression of vascular cell adhesion molecule (VCAM) receptor and fractalkine receptor; CX3CR1 (**Figure1-3**) (Strauss-Ayali et al., 2007; Geissmann et al., 2003; Ghattas et al., 2013). This subset produce high levels of CCL2, interlukin-10 (IL-10), CXCL8, reactive oxygen species (ROS) and IL-6 (Woollard, 2013). Intermediate monocytes are the most recent subset to be identified these express $CD14^{+}$, $CD16^{+}$ (low) and $CCR2^{+}$ (**Figure 1-3**). They are the smallest population of monocytes. This subset express the highest levels of angiopoietin receptor (Tie2) (Strauss-Ayali et al., 2007; Ghattas et al., 2013; Jaipersad et al., 2014). They are known to secrete high levels of tumour necrosis factor α (TNFα), IL-1β and IL-6 (Woollard, 2013).

Non classical monocytes can be identified by their expression of $CD14^{+}$ (low), $CD16^{+}$ and $CCR2^{-}$. They express the highest amount of CD16, CX3CR1 and VCAM, however they express no L-selectin (Strauss-Ayali et al., 2007; Ghattas et al., 2013; Shantsila et al., 2011). The subtle variation of expression of different surface markers between monocyte subsets leads to differences in their behaviour. $Ly6C^{hi}$ (equivalent mouse population of Mon1) with higher CCR2 expression are known to arrive earlier in the inflammatory process, followed later by $Ly6C^{lo}$ (equivalent mouse population of Mon3), which are more responsive to (CX3CL1) fractalkine (Nahrendorf et al., 2007). The ability of monocytes to respond to and release cytokines and chemokines during the inflammatory response enables them to fulfil their role, in protecting the host from invading pathogens.

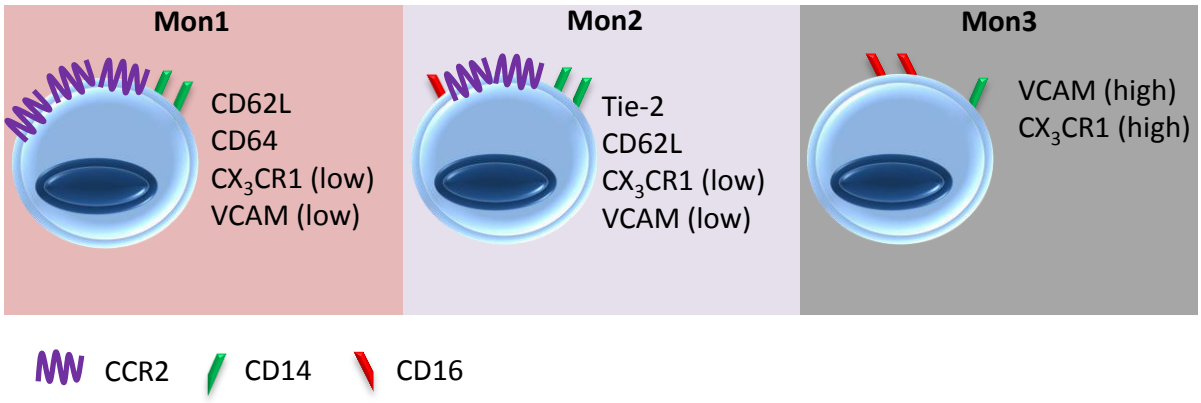


**Figure 1-3: Monocyte Subsets**

Figure 1-3 demonstrates the differences in receptor expression by mon1 (classical), mon2 (intermediate) and mon3 (non-classical) monocytes (Geissmann et al., 2003; Ghattas et al., 2013; Shantsila et al., 2011; Strauss-Ayali et al., 2007).

### 1.2.5 Lymphocytes and the acquired immune system

Lymphoid stem cells are able to differentiate to form either lymphocytes or natural killer cells (Chotinantakul and Leeanansaksiri, 2012) (**Figure 1-1**). T- and B-cells constitute the effector cells of the acquired immune system and are able to recognise and mount an immune response against specific pathogens (or other antigens). This is due to a large repertoire of receptors, which mediate recognition of antigens (Ogle, B. M., Cascalho Marilia, Joao Cristina, Taylor William, 2003). They also confer lasting immunity to the host by producing memory cells, giving a quicker response if a specific pathogen invades again.

Diversity of T-cell receptors (TCR) and immunoglobulins (Ig) is achieved through genomic rearrangements of the variable (v) joining (J) and diversity (D) chains (Boyd et al., 2013). Once formed these receptors go through a negative selection process to remove any receptors that have a high affinity for self antigens (Boyd et al., 2013). T-cells leave the bone marrow and travel to the thymus where they reach maturity. There are two types of T-cell, which can be

distinguished through their expression of either $CD4^+$ (helper T-cells) or $CD8^+$ (cytotoxic T cells) (Janssen et al., 2003).

All cells of the body express major histocompatibitly complex (MHC) class I receptors, which if the cell becomes infected (especially by a virus), can be used to present antigens to immune cells (**Figure 1-4**) (Greene et al., 2011). A specific $CD8^+$ TCR can recognise antigen peptide displayed by MHC class I, leading to T-cell activation and destruction of the infected cell (**Figure 1-4**) (Masopust et al., 2007).

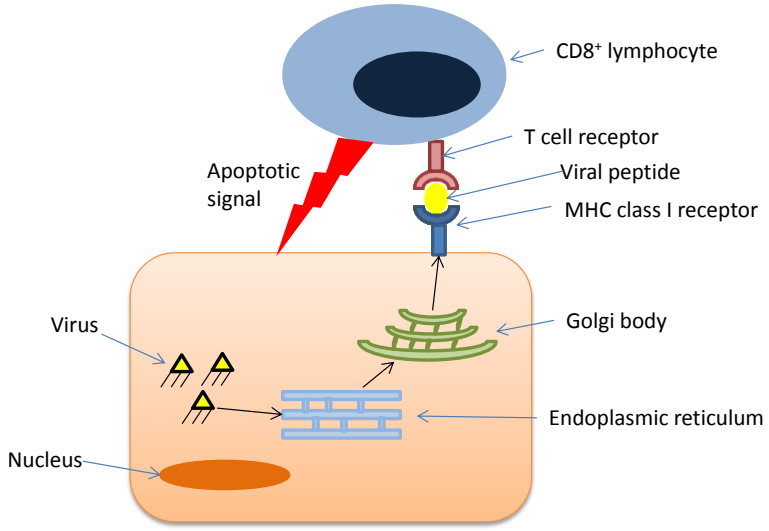


**Figure 1-4: MHC Class I signalling to $CD8^+$ cytotoxic T-cells**

Viral proteins of an infected cell are processed by the endoplasmic reticulum and become associated with MCH class I receptors, these are trafficked to the surface of the cell via the golgi body and expressed on the cell surface. The T-cell receptor of a specific clone of $CD8^+$ cytotoxic T-cells can bind to the MCH class I receptor, which is associated with viral peptide. This then signals to the cell to undergo apoptosis. (Figure adapted from Vyas et al., 2008.)

Helper T-cells provide the mechanism for cross talk between the innate and the acquired immune system. Phagocytotic cells of the innate immune system, macrophages or dendritic

cells are antigen presenting cells, which express MHC class II receptors (Geissmann et al., 2008). After engulfing and destroying an invading pathogen an antigen (usually a short peptide) is expressed in association with the MHC class II receptor. The TCR on $CD4^+$ T-cell, which is specific for a given antigen, for each 'clone' of T-cells, recognises and binds to the antigen (**Figure 1-5**). This is accompanied by simultaneous binding of the CD80 or CD86 (antigen presenting cell receptors) to the CD28 receptor (expressed on T-cells) leading to the activation of the $CD4^+$ T-cell and its differentiation into an effector cell (**Figure 1-5**) (Luckheeram et al., 2012). $CD4^+$ effector cells secrete IL-2, which act as autocrine signalling in a positive feedback loop, this is effective in areas where these cells are highly concentrated, such as the lymph nodes (Sojka et al., 2004).

The effector cells of $CD4^+$ can be either of two subclasses $T_H1$ or $T_H2$ (Luckheeram et al., 2012). $T_H1$ cells mainly secrete interferon γ (IFN-γ) and TNFα. TNFα will activate surrounding EC by triggering the inflammatory response, leading to increased leukocyte recruitment (this will be discussed in more detail later). Binding of $T_H1$, CD40 ligand (CD40L) (also known as CD154) to CD40 on the macrophage or secretion of IFN-γ by the $T_H1$ and its interaction with the macrophage; are both mechanisms which promote macrophage activation (Mosser, 2003). $T_H1$ cells are also able to aid in activation of $CD8^+$ T cells leading to a cytotoxic T cell response (Huang et al., 2007).

$T_H2$ will produce IL-4, IL-5, IL-10 and IL-13 these are responsible for the activation of B-cell lymphocytes and the humoral response (Mosmann and Sad, 1996). B-cells reach maximal activation through a two step process; the first step involves the B-cell binding specifically recognised antigen to its antigen specific B-cell receptor (BCR) (**Figure 1-5**) (Linsley et al., 1991). The second step involves an effector $CD4^+$ (either $T_H1$ or $T_H2$), which specifically recognises the same antigen. The effector $CD4^+$ binds its CD40L to the B-cell CD40 receptor leading to B-cell

activation (**Figure 1-5**) (Mosmann and Sad, 1996). Upon activation a naive B-cells will form a plasma cell, which is short lived but able to produce large quantities of antibodies (IgA, IgE, IgD, IgG or IgM) or a memory B-cell (Tobón et al., 2013).

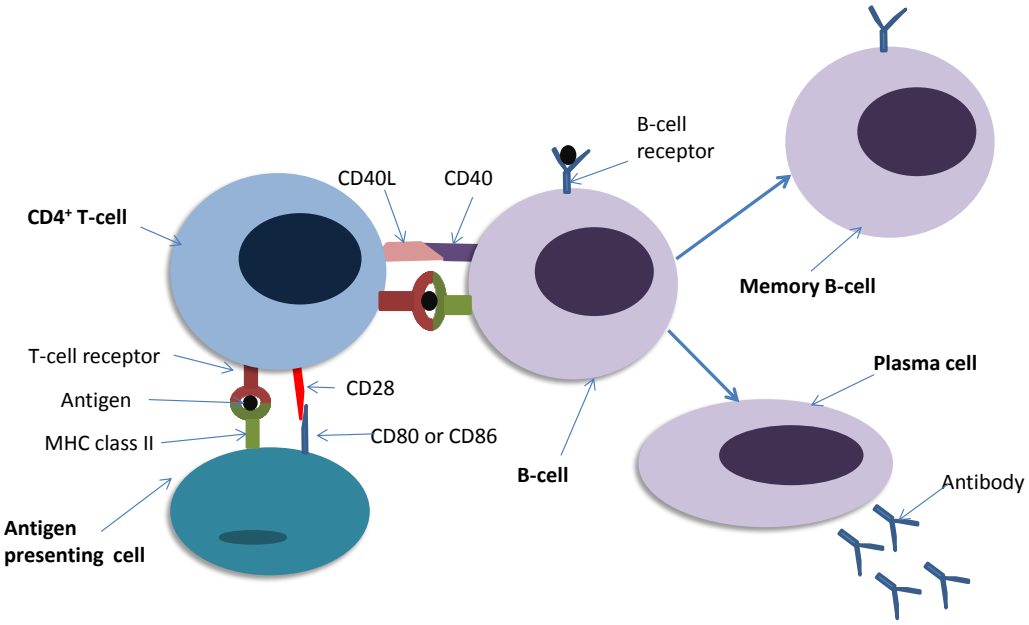


**Figure 1-5: CD4$^+$ helper T cells activate B cells**

Antigen presenting cells (such as a macrophages) engulf and destroy invading pathogens, they then display antigen via their MHC class II receptor. A specific CD4$^+$ helper T-cell receptor, which recognises the antigen, binds to the antigen and MHC class II. The T-cell CD28 simultaneously binds to the CD80/CD86 expressed by the antigen presenting cell. This leads to activation of the CD4$^+$ T cell, which now becomes an effector cell. The B-cell has two receptors, which will recognise the same specific antigen; B-cell receptor and MHC class II receptor. Antigen binding to the B-cell receptor leads to downstream signalling and partial B-cell activation. The effector T-cell receptor interacts with B-cell, MHC class II, bound to antigen. These interactions coupled with the interaction between T-cell CD40L and B-cell CD40 leads to full B-cell activation. Active B-cells can now differentiate into either plasma cells, which, secrete large quantities of antibody, or memory B cells. (Image adapted from King, 2009.)

B-cells are produced in the bone marrow but reach maturity in the spleen (Tobón et al., 2013). They can be identified through the presence of a BCR, which like TCR goes through a developmental process which includes VJD rearrangement (Tobón et al., 2013). Any B-cells with self recognising BCR will be destroyed through apoptosis. Although maximal activation of B-cells

can only be achieved through interactions with $CD4^+$ cells (**Figure 1-5**); there are other routes through which partial B-cell activation can be achieved, this however, will not result in the production of long lived memory B-cells (Tobón et al., 2013). B-cell activation can be achieved through BCR binding to antigen, this can be internalised and processed and later expressed on the MHC class II receptor on the B-cell surface (Wang and Zheng, 2013). However B-cells also express toll like receptors (TLRs) including TLR9, these are able to non specifically recognise invading pathogens, resulting in partial B-cell activation (Wang and Zheng, 2013).

### 1.2.6 Platelets

Platelets are anucleate cells and the smallest of all the blood cells being only 3µM in diameter (or smaller) (Rivera et al., 2009). Platelets are derived from bone marrow resident progenitor cells called megakaryocytes and are shed into the blood from proplatelets, membrane processes which are extruded across the EC of the bone marrow sinusoids (Chotinantakul and Leeanansaksiri, 2012). Platelets have an extensive cytoskeleton and dense tubular system. They posses glycogen granules, a small number of mitochondria and dense (δ) and alpha (α) storage granules (Rivera et al., 2009). δ granules contain nucleotides (mainly ADP and ATP), serotonin, histamine, pyrophosphate and calcium (McNicol and Israels, 1999), while α granules contain molecules needed for both autocrine and paracrine signalling events during platelet activation such as; von Willebrand factor (vWf), fibrinogen, Platelet (P)-selectin, platelet endothelial cell adhesion molecule (PECAM-1 or CD31), CD40L, platelet factor 4 (CXCL4), β-thromboglobulin, thrombospondin, platelet derived growth factor (PDGF), clotting factor V and $\alpha_{IIb}\beta_3$ (Blair and Flaumenhaft, 2009; Rivera et al., 2009). The major role of platelets is regulation of haemostasis and thrombosis (Huo and Ley, 2004). Platelets are present in the blood stream in an inactive state, but can be quickly activated to form a thrombus upon vascular injury. Platelet

activation and thrombosis is achieved through the interaction of platelet receptors with components of the exposed subendothelial matrix; molecules such as collagen, thrombospondin, laminins and fibronectin (Nieswandt et al., 2011). This is an example of cross-talk between platelets, EC and the subendothelial matrix.

The role platelets have in clot formation depends upon where the injury occurs within the blood circulation system. Venous clots are dependent on activation of the coagulation cascade (**Figure 1-6**). The coagulation cascade is triggered through two pathways; the extrinsic (or tissue factor - TF) pathway, which starts when TF is released from damaged EC, or activated monocytes or macrophages (**Figure 1-6**) (Levi et al., 2004). The lesser pathway, the contact activation pathway, begins with the exposure of collagen followed by subsequent activation of FXII (**Figure 1-6**) (Davie et al., 1991). Activation of the coagulation cascade, through either pathway results in activation of serine protease enzymes from their zymogen form (**Figure 1-6**) (Levi et al., 2004). One by-product of this cascade is thrombin (**Figure 1-6**) (Coughlin, 2000). The end product of this cascade is fibrin, which platelets use for crosslinking to form a stable clot (**Figure 1-6**) (Schulz et al., 2013).

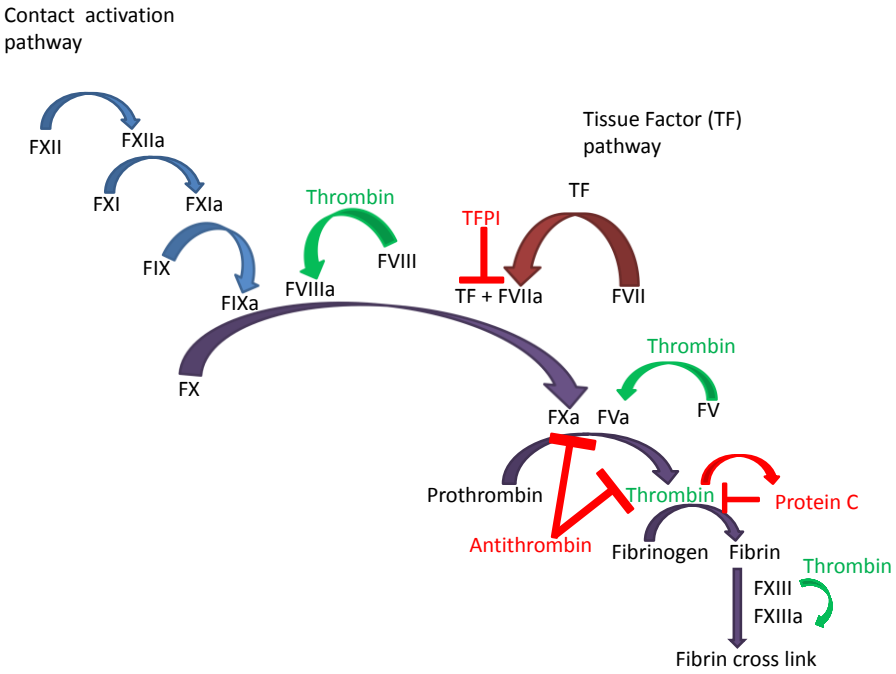


**Figure 1-6: The coagulation cascade**

Schematic of the coagulation cascade; contact activation pathway is triggered upon the exposure of collagen in the subendothelial matrix, this activates the serine protease factor XII (FXII) to its active form FXIIa. The extrinsic (or tissue factor -TF) pathway, starts when tissue factor cleaves FVII into its active form FVIIa. Activation of both pathways leads to the conversion of zymogens into their active serine protease form, resulting in thrombin generation and eventual fibrin deposition. Antithrombin, protein C and tissue factor pathway inhibitor (TFPI) all regulate the coagulation cascade by inhibiting zymogen activation.

Thrombin is a potent platelet agonist which stimulates platelets through cleavage of the N terminus of protease activated receptor 1 (PAR1) and PAR4 the new terminus acts as a ligand for its own receptor (Coughlin, 2000). Signalling of thrombin through PAR1 and PAR4 expressed on the platelet surface leads to irreversible platelet activation inducing shape change, release of platelet granules, P-selectin expression and activation of $\alpha_{IIb}\beta_3$ integrin (**Figure 1-8**) (Coughlin, 2000).

However, arteries are subject to a high shear rate, which limits fibrin deposition and limits the effect of the coagulation cascade on initial platelet capture and activation (Falati et al.,

2002). Under these conditions platelets have a more crucial role in thrombus formation. Upon vascular injury collagen I, III and VI of the subendothelial matrix are exposed. EC are activated and release von Willebrand factor (vWf) from internal stores (Weibel Palade bodies) (Tull et al., 2006). Von Willebrand factor is a large molecular weight molecule, which can be cleaved into a smaller soluble form (Kanaji et al., 2012). Von Willebrand factor can either be expressed on the surface of damaged EC or captured by the exposed collagen, which has a high binding affinity for soluble vWf (**Figure 1-7**) (Kanaji et al., 2012). The platelet receptor Glycoprotein Ib-IX-V (GPIb also known as CD42b) has a high affinity for the cleaved form of vWf (Kanaji et al., 2012). The interaction between CD42b and vWf allows platelets to be captured to the vessel wall, however, the short lived nature of these interactions results in a platelet rolling phenotype being observed (**Figure 1-7**) (Nieswandt et al., 2011). These short lived interactions result in transient calcium $Ca^{2+}$ release, and a reversible form of platelet activation (Nieswandt et al., 2011).

Rolling platelets will eventually come into contact with collagen (**Figure 1-7**). Collagen is able to activate platelets through interactions with the GPVI receptor (Gibbins et al., 1997). This leads to downstream signalling events through Src family kinase (SFK) and phospholipase C-γ2 (PLC-γ2) (**Figure 1-8**) (Yanaga et al., 1995; Blake et al., 1994). This results in an increase in intracellular $Ca^{2+}$ levels, platelet shape change through rearrangement of the actin cytoskeleton and degranulation (Nieswandt and Watson, 2003). Collagen is one of the most effective platelet activators (Nieswandt and Watson, 2003).

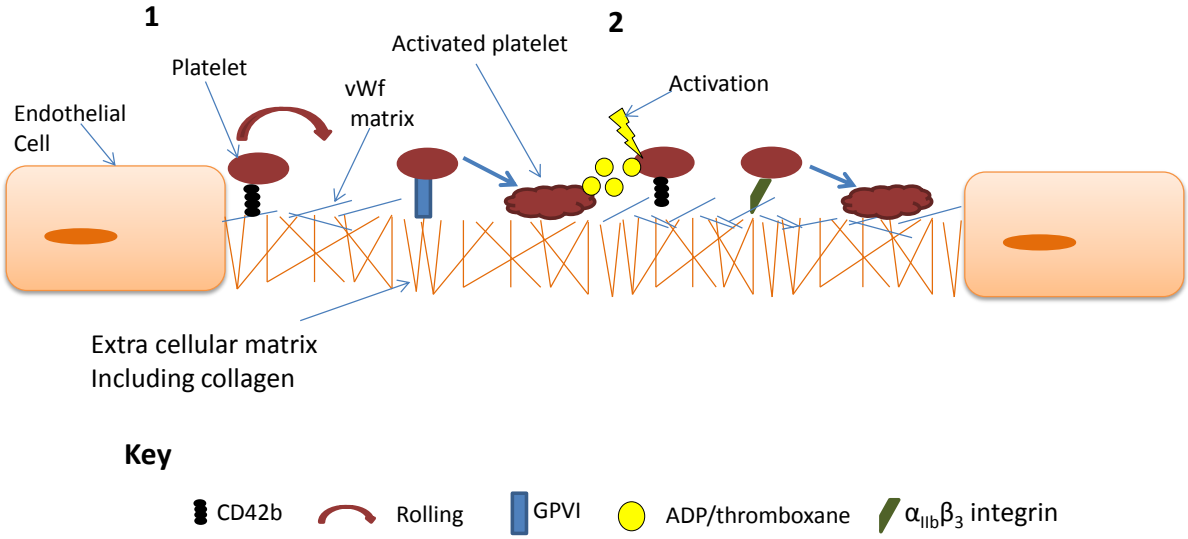


**Figure 1-7: Platelet capture upon endothelium damage**

Soluble von Willebrand factor (vWf) is captured by collagen in the subendothelial matrix. The platelet receptor CD42b is able to form short lived interactions with vWf, allowing platelets to roll along the vWf matrix. Eventually either 1) platelet receptor GPVI will come into contact with collagen and firm platelet adhesion will occur. Or 2) paracrine signalling through ADP/thromboxane will result in conformational shape change of αIIbβ3 integrin, allowing the platelet to firmly adhere to vWf using this receptor.

Platelet degranulation will result in the release of ADP from δ granules, this is part of a positive feedback loop for platelet activation resulting in signalling through an autocrine or paracrine fashion (**Figure 1-7**). ADP stimulates platelet activation through the P2Y1 and P2Y12 receptors (**Figure 1-8**) (Jin and Kunapuli, 1998). Signalling through P2Y1 results in reversible $Ca^{2+}$ mediated platelet shape change through cytoskeletal rearrangement and formation of filopodia and lamellipodia, increasing their surface area (**Figure 1-8**), whilst signalling through P2Y12 involves inhibition of adenylyl cyclase resulting in irreversible activation (**Figure 1-8**) (Jin and Kunapuli, 1998). Signalling through both receptors is required to achieve full platelet activation (Daniel et al., 1998). Patients with a defect in P2Y12 have been identified as having a mild

bleeding disorder, showing the importance of platelet activation through this pathway (Hollopeter et al., 2001).

Upon activation platelets synthesis thromboxane (TxA2) from arachidonic acid (AA) through a Cyclooxygenase-1 (COX-1) dependent pathway (Liu et al., 2012). TxA2 also has a role in a positive feedback loop and signals through the thromboxane A2 receptor (TP) with downstream signalling including activation of PLC-β resulting in an increase in $Ca^{2+}$ (**Figure 1-8**), (Offermanns et al., 1994, 1997).

More recently other platelet receptors have been identified which may have a role in platelet activation. C-type lectin receptor (CLEC-2) has been found to be expressed by platelets and subpopulations of haemopoetic cells (Hughes et al., 2010). Its only known endogenous ligand to date is podoplanin, which is expressed by kidney podocytes, lung type I alveolar cells and lymphatic endothelial cells (Hughes et al., 2010). The interaction between CLEC-2 and podoplanin is thought to play a key role in lymphatic angiogenesis (Suzuki-Inoue et al., 2006). Activation through this receptor can also occur upon binding of rhodocytin from the Malayan pit viper *Calloselasma rhodostoma,* a commonly used agent for activating platelets through this signalling pathway (Suzuki-Inoue et al., 2006). Like GPVI, CLEC-2 also signals through the SFK; spleen tyrosine kinase (SYK) (**Figure 1-8**) (Hughes et al., 2010; Suzuki-Inoue et al., 2006).

Other molecules, which are known to activate platelets are histones and oxidised low-density lipoprotein (oxLDL). Histones have been shown to activate platelets, with histone 4 (H4) being the most potent platelet activator (Semeraro et al., 2011). It was first thought histones activated platelets through a charge based interaction. However, it has now been demonstrated that histones H3 and H4 stimulate platelets at least in part, through the TLR-2 and TLR-4

receptors (Fuchs et al., 2011; Semeraro et al., 2011). Oxidised LDL plays a significant role in the development of atherosclerosis. It is thought to be a potential platelet activator acting through lectin like oxidized receptor 1 (LOX-1) or CD36, scavenger receptors expressed on the platelet cell surface (Korporaal et al., 2007; Chen et al., 2001; Zhao et al., 1995).

Upon platelet activation $\alpha_{IIb}\beta_3$ undergoes a conformational shape change, when this occurs it is able to bind to vWf and fibrinogen. Binding of $\alpha_{IIb}\beta_3$ to vWf on the subendothelial matrix will result in firm adhesion (**Figure 1-7**). Platelet crosslinking through $\alpha_{IIb}\beta_{3,}$ vWf and fibrinogen will allow stable clot formation to occur (Peterson et al., 1987; Rivera et al., 2009). The developing clot provides a procoagulant surface allowing for the production of more fibrin from fibrinogen via the action of thrombin (Falati et al., 2002). P-selectin will also be released from α granules and expressed on the platelet surface, this can be important for interactions with platelets and leukocytes (Kuckleburg et al., 2011). It is often used as a measurement of platelet activation.

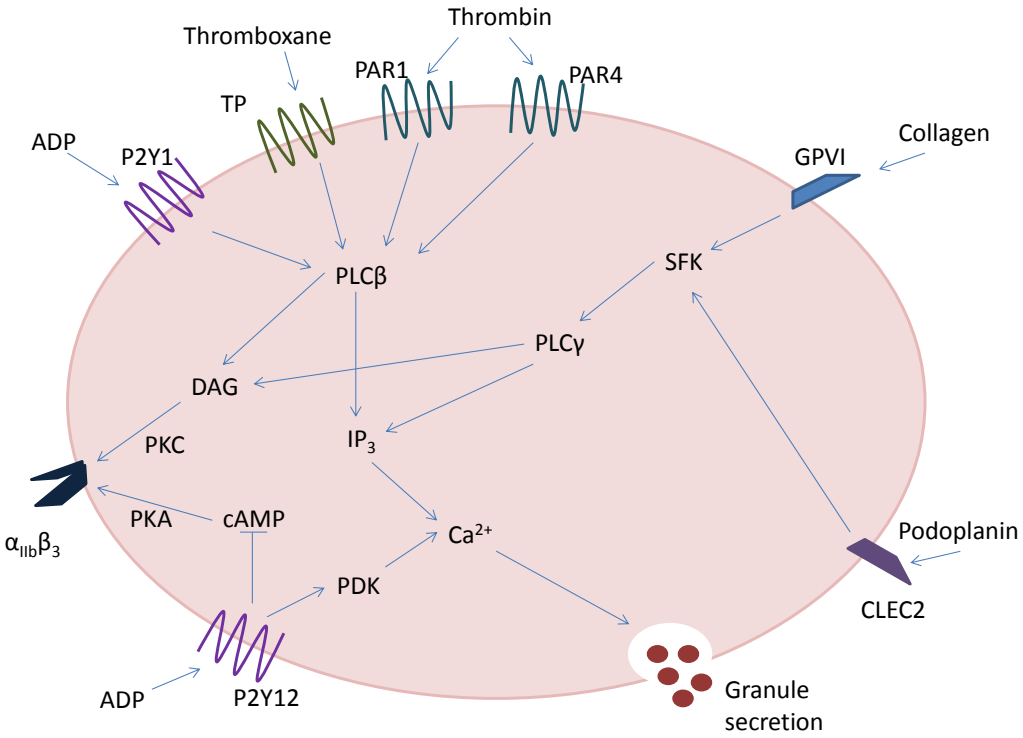


**Figure 1-8: Platelet activation**

Platelet receptors include G-protein coupled receptors P2Y1, P2Y12, (Protease activating receptor 1 and 4) PAR1 and PAR4 and prostanoid TP receptor (TP). Activation through ADP occurs first through the P2Y1 receptor, resulting in reversible shape change and an increase in cytosolic $Ca^{2+}$. For full platelet activation signalling must also occur through P2Y12, which leads to inhibition of adenylyl cyclase and a decrease in cAMP production and a subsequent conformational change of the $\alpha_{IIb}\beta_3$ integrin into its active form. Signalling through the thromboxane receptor (TP) occurs in a PLCβ dependent manner leading to a rise in cytosolic $Ca^{2+}$ and shape change, degranulation and $\alpha_{IIb}\beta_3$ integrin activation. Activation by thrombin occurs through the PAR1 and PAR4 receptors also in a PLCβ dependent manner leading to irreversible platelet activation. The integrin receptor GPVI and the C-type lectin domain 2, (CLEC-2) receptor, both signal through a Src family kinase dependent pathway, resulting in full platelet activation upon collagen or podoplanin binding to its receptor. (Figure adapted from Pignone and Williams, 2010).

Mechanisms need to be in place to make sure that clot formation is a localised process and that unwanted thrombus formation does not take place in the circulation. This is mainly achieved through crosstalk between platelets and EC. But it is also aided by Soluble vWf having a much lower affinity for CD42b (Kanaji et al., 2012). One mechanism for preventing platelet activation is nitric oxide (NO) signalling. Endothelial nitric oxide synthase (eNOS) oxidises L-

arginine through a $Ca^{2+}$ dependent pathway producing NO (Chou et al., 2008). Prostacyclin (prostaglandin-I2; PGI2) is also synthesised from arachidonic acid (AA) through COX-1, and prostacyclin synthase (McAdam et al., 1999). Prostacyclin and NO are able to increase the concentration of cyclic nucleotides (cAMP and cGMP) within the platelet (Mellion et al., 1981; Best et al., 1977). This leads to phosphorylation of protein kinase A (PKA) and a decrease in intracellular $Ca^{2+}$. Thus, cyclic nucleotides inhibit all of the known activatory pathways in platelets including the $Ca^{2+}$ sensitive conformational changes of $\alpha_{IIb}\beta_{3,}$ thereby preventing inappropriate thrombus formation. (Gkaliagkousi et al. 2007 Antl et al. (2007). EC also express CD39 an integral membrane protein, which metabolises ADP into AMP thereby preventing activation of platelets through the P2Y1 and P2Y12 receptors (Marcus et al., 1997).

### 1.2.7 Platelet microvesicles

Microvesicles are cell derived lipid vesicles shed from the plasma membrane of cells. They are 0.1-1μm in size and have a lipid membrane, but lack a nucleus or synthetic capacity (Hargett and Bauer, 2013). However, microvesicles are thought to contain proteins, mRNA and micro-RNA (miRNA) and could play an important role in cell signalling if this cargo was transferred to recipient cells (Garzetti et al., 2013; Hunter et al., 2008; Mause et al., 2005). Several cell types are known to be able to generate microvesicles upon activation and during apoptosis, including EC, epithelial cells, leukocytes, erythrocytes, megakaryocytes and platelets (Hargett and Bauer, 2013). Microvesicles are released by budding directly from the plasma membrane (**Figure 1-9**). Therefore, they should not contain any internal protein markers, unlike exosomes, which originate from multivesicular endosomes inside the cell and are trafficked to the plasma membrane and released (**Figure 1-9**) (Bobrie et al., 2011). Exosomes are 40-100nm in size and although purifying methods (such as ultracentrifugation) are used to separate plasma

membrane derived microvesicles from exosomes, these methods are still not fully effective and require further development.

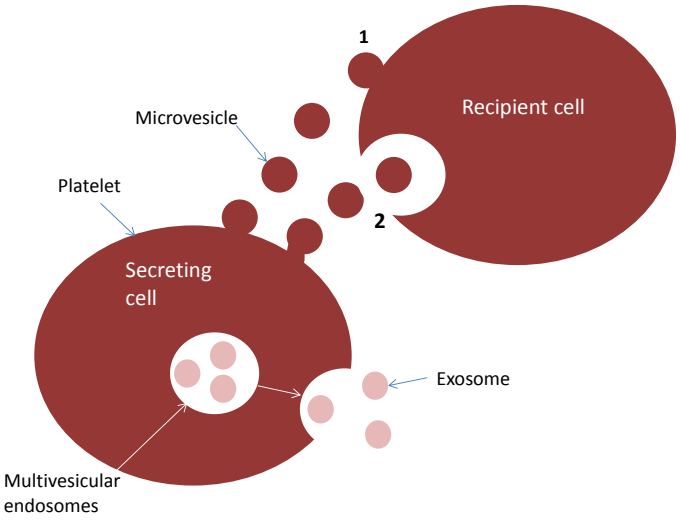


**Figure 1-9: Platelet microvesicle production**

Platelet microvesicles are released from the cell surface, whereas, exosomes originate in multivesicular endosomes, which fuse with the plasma membrane allowing for exosome release. Platelet microvesicles are believed to be taken up by recipient cells, through 1) fusion with the plasma membrane or 2) through receptor mediated endocytosis.

Microvesicles express markers from the parent cell. Thus, platelet microvesicles (PMV) are known to express CD42b, CD41 and CD62P (Flaumenhaft et al., 2009). However microvesicles shed from megakaryocytes also express CD42b and CD41 (Flaumenhaft et al., 2009). These two populations have not been systematically separated in most studies of microvesicles in patient plasma. Shai et al (2012) showed, there may be differences in the overall number and the proteome of PMV, depending on the route of platelet stimulation. Platelets stimulated through the thrombin pathway produce PMV with an increase in regulatory

proteins compared to PMV produced by platelets subjected to high shear stress (Shai et al., 2012).

Although PMV are produced in healthy individuals elevated levels have been observed in cases of inflammatory diseases such as rheumatoid arthritis (RA), systemic lupus erythematosus (SLE) and atherosclerosis (Beyer and Pisetsky, 2010). Nomura et al, (1995) demonstrated diabetes mellitus (DM) patients with high LDL or triglyceride levels have increased plasma levels of microvesicles. It has also been demonstrated that PMV and endothelial microvesicles are increased within 1 day of onset of acute coronary syndrome (ACS) (Biasucci et al., 2012). The elevated levels of microvesicles detected in disease states suggest that microvesicles may play a role in disease progression, although this hypothesis has not been tested in atherosclerosis.

Microvesicles have been shown to regulate thrombosis, coagulation, angiogenesis and inflammation (Yang et al., 2012; Hargett and Bauer, 2013). Scholz et al, (2002) demonstrated that platelets could transfer TF to monocytes via PMV, indicating a role for PMV in initiating coagulation. This is further confirmed by the observation that patients with Scott syndrome are deficient in PMV production and as a consequence suffer from impaired coagulation response (Simss et al., 1989). A role for PMV in inflammation has been shown by their ability to deliver RANTES (CCL5) to endothelial cells and promote monocyte recruitment, this could potentially have major implications in inflammatory diseases such as atherosclerosis, where the recruitment of monocytes is a major contributor to the cellular pathology of the disease (Mause et al., 2005).

Although it is widely agreed that microvesicles have a role in regulating the function of target cells both in health and disease, there is some debate in the literature as to how vesicles deliver their molecular cargo (e.g. proteins and microRNA, miRNA) to other cells. Del Conde et al, (2005) believe that vesicle membranes simply fuse with the plasma membrane of the cell and

release their contents (**Figure 1-9**). Whereas others believe MV are taken up through receptor mediated endocytosis (**Figure 1-9**) (Yang et al., 2012). Of course, both options may operate simultaneously.

### 1.2.8 The innate immune system

The body needs to defend itself from invading pathogens such as bacteria, fungi and viruses to prevent infection from occurring. The first line of defence is the presence of physical barriers such as specialized epithelium which forms the skin and lines orifices such as the nose, throat and GI tract (Sun et al., 2012; Shaykhiev and Crystal, 2013). The epithelium lining the nose and throat is created by a monolayer of specialized epithelial cells connected by impermeable tight junctions, some of these cells are mucous producing or have cilia which help to prevent pathogens adhering and thus, protect the lungs from infection (Shaykhiev and Crystal, 2013). Damage to the epithelium will allow pathogens to penetrate. When this occurs, the next line of the body's defence is the leukocytes, which constitute the innate immune system (Geremia et al., 2014). Leukocytes of the innate immune system, appear to be evolutionary conserved between a wide range of species separated by significant periods of evolutionary time (Beutler, 2004). Innate immune cells recognise and destroy invading pathogens in a non-specific manner, which does not confer any lasting protection to the host (Geremia et al., 2014).

Leukocytes of the innate immune system express PRRs which are able to recognise essential, highly conserved molecular patterns expressed by pathogens (but not by the host cells), known as PAMPS (Uematsu and Akira, 2006). Pattern recognition receptors include TLRs, which are type I integral membrane glycoproteins, containing 19-25 extracellular leucine rich repeats (LRR) motifs. 10 different TLRs have been identified in humans (**Table 1-3**) (Lu et al., 2013). Each TLR has a small repertoire of molecular patterns it can recognise. For example TLR1,

TLR2 and TLR6 are able to target lipids, whereas TLR 7, TLR8 and TLR9 are able to target DNA (**Table 1-3**) (Akira et al., 2006). Other PRRs include nucleotide binding oligomerization domain like receptors (NLRs) 22 of which have been identified in humans (Chaput et al., 2013). NLRs are intracytoplasmic receptors, able to bind to PAMPS on phagocytosed pathogens (Uematsu and Akira, 2006). Stimulation of NLRS and TLRs leads to the release of cytokines and chemokines through a downstream signalling cascade (Akira et al., 2006; Geremia et al., 2014) and are thus important and early initiators of the inflammatory response.

In the event of an infection the body needs to signal to circulating cells of the innate immune system, so that they accumulate at the site of infection. This is done through the release of chemical signals known as cytokines and chemokines (a family of chemotactic-cytokines). These are released as part of a carefully controlled process, known as the inflammatory response, which will be discussed in more detail below. However, at a basic level, cells of the innate immune system are able to migrate towards these signals within a matter of minutes to hours.

| Toll Like Receptor | Cell expressing TLR | PAMPs |
|---|---|---|
| **TLR1** | Monocyte/macrophages<br>Dendritic cells<br>B-lymphocytes<br>Neutrophils | Triacyl lipopeptides (bacteria) |
| **TLR2** | Monocytes/macrophages<br>Neutrophils<br>Dendritic cells<br>Mast cells | Glycolipids (bacteria)<br>Lipopeptides (bacteria)<br>Lipoproteins (bacteria)<br>Lipoteichoic acid (bacteria) |
| **TLR3** | Dendritic cells<br>B-lymphocytes | Double stranded RNA (viruses) |
| **TLR4** | Monocytes/macrophages<br>Neutrophils<br>Dendritic cells<br>Mast cells | Lipopolysaccharide (bacteria) |
| **TLR5** | Monocytes/macrophages<br>Dendritic cells<br>Neutrophils | Flagellin (bacteria) |
| **TLR6** | Monocytes/macrophages<br>mast cells<br>B-Lymphocytes<br>Neutrophils | Diacyl lipopeptides (mycobacteria) |
| **TLR7** | Monocytes/macrophages<br>Dendritic cells<br>B-lymphocytes<br>Neutrophils | Single stranded RNA (viruses) |
| **TLR8** | Monocytes/macrophages<br>Dendritic cells<br>Mast cells<br>Neutrophils | Single stranded RNA (viruses) |
| **TLR9** | Monocytes/macrophages<br>Dendritic cells<br>B-lymphocytes | DNA (Bacteria) |
| **TLR10** | Monocytes/macrophages<br>B-lymphocytes<br>Neutrophils | Unknown |

**Table 1-3: Table of toll like receptors (TLRs) expressed by leukocytes**

Table 1-3: shows the TLRs expressed on leukocyte subsets of the innate and acquired immune system and their known target pathogen associated molecular patterns (PAMPs).
(Table adapted from Waltenbaugh C, Doan T, Melvold R, 2008.)

### 1.3.0 Inflammation

Inflammation is the response of the vasculature to trauma. There are four classic signs of inflammation, redness, swelling, heat and pain. Vasodilatation of the blood vessels

surrounding the site allows an increase in blood flow which accounts for the redness and heat. The swelling and pain is caused by an increase in the permeability of the surrounding blood vessel walls, allowing excess blood plasma to enter the tissue, this is accompanied by leukocyte infiltration.

Leukocyte infiltration has many roles such as preventing infection, aiding in tissue remodelling and also providing signals to resolve the inflammatory process. Inflammation should be an acute response, which ceases as tissue homeostasis is restored, preventing any further infiltration by leukocytes. When inflammation does not resolve, there is continuous infiltration of the tissue by leukocytes resulting in pathological tissue remodelling, which is observed in chronic inflammatory diseases such as atherosclerosis.

### 1.3.1 The leukocyte adhesion cascade

Upon damage to the endothelium leukocytes need to be captured to the site of inflammation, this is achieved through a complex signalling cascade, known as the leukocyte adhesion cascade. Upon tissue injury cytokines (e.g. TNF-α, IL1-β and IFN-γ) are released from surrounding tissues, macrophages and mast cells to activate EC and trigger the start of the leukocyte adhesion cascade (Ley et al., 2007).

There are 3 main steps to leukocyte recruitment, the first includes capture and rolling, which is a selectin or vascular cell adhesion molecule-1 (VCAM-1 or CD106) mediated event (**Figure 1-10**) (Tedder et al., 1995). The second step is activation of leukocytes and EC by chemokines (**Figure 1-10**). Chemokine signalling leads to up regulation of integrin receptors for EC-borne adhesion molecules such as intracellular adhesion molecule-1 (ICAM-1 or CD54) and VCAM-1 and leukocyte β1 and/or β2 integrins (**Figure 1-10**) (Ley et al., 2007). Interaction between leukocyte integrins and EC adhesion molecules results in leukocyte movement being

arrested and leukocytes becoming firmly adherent (**Figure 1-10**) (Ley et al., 2007). Firmly adherent leukocytes are ready to transmigrate across the EC barrier and enter the vessel wall (**Figure 1-10**).

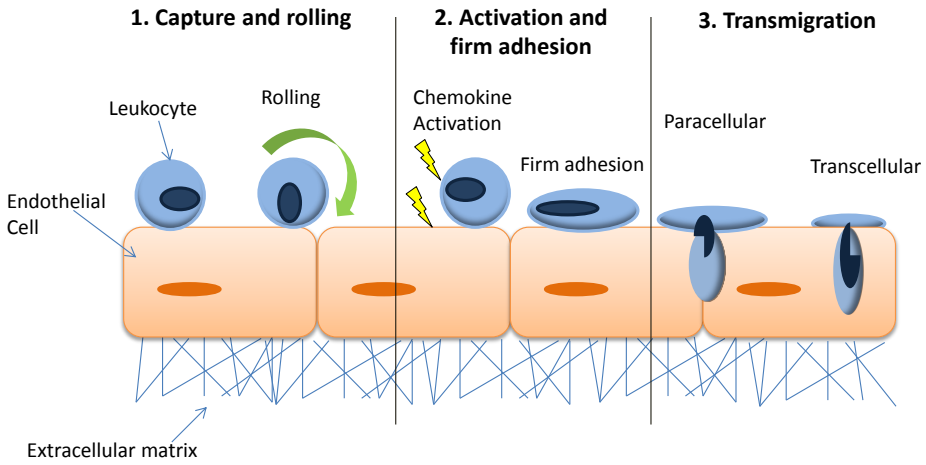


**Figure 1-10: Leukocyte adhesion cascade**

1) Leukocytes are captured by the vessel wall through short lived selectin based interactions, which result in leukocyte rolling. 2) Chemokines released from surrounding activated cells activate both leukocytes and EC resulting in leukocyte β1/β2 integrin expression and EC ICAM-1 and VCAM-1 receptor expression. Interaction of these leukocyte receptors with the EC receptors results in firm adhesion of leukocytes to EC. 3) Activated, adherent leukocytes are now ready to transmigrate through either the transcellular or paracellular route. (Image adapted from (Ley et al., 2007).

### 1.3.2 Capture and rolling

The process of margination allows leukocytes to come into contact with the endothelium. This is a physical characteristic of flowing blood, where the low shear environment in the central flow encourages red cell aggregation. These aggregated red cells behave like large particles in the bulk flow and force the smaller leukocytes to the vessel wall allowing contact to

occur with EC (Schmid-Schönbein et al., 1980; Abbitt and Nash, 2003). This process mainly occurs in post capillary venules, due to the permissive fluid dynamics in this vascular bed.

Once in close proximity to the vessel wall, capture of leukocytes to the activated EC is mediated by selectins. There are 3 different classes of selectins, endothelial (E)-selectin, Platelet (P)-selectin and leukocyte (L)-selectin (**Figure 1-11**) (Carlos and Harlan, 1994). The extracellular regions of selectins are highly conserved and consist of an amino terminal, a $Ca^{2+}$ dependent lectin domain and 2-9 short consensus repeats (**Figure 1-11**) (Carlos and Harlan, 1994).

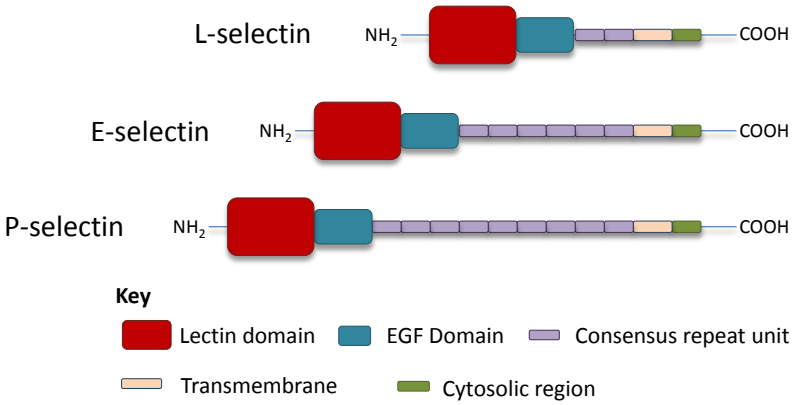


**Figure 1-11: Selectins**

The smallest selectin is leukocyte (L)-selectin has only 2 consensus repeats, endothelial (E)-selectin contains 6 consensus repeats and the largest selectin; platelet (P)-selectin contains 9 consensus repeats. (Figure adapted from Hanley et al., 2004.)

Under normal circumstances EC do not express selectins, however, in response to cytokine signals of inflammation activated EC display E-selectin and P-selectin on their surface (**Figure 1-12**) (Ley et al., 2007). HUVEC stimulated in vitro with TNFα has been shown to have maximum expression of E-selectin after 4-6hrs but this decreases back to baseline within 24-48hrs (Bevilacqua et al., 1987). P-selectin is stored in Weibel Palade bodies of resting EC,

however it is trafficked to the surface upon EC activation (McEver et al., 1989). Another source of P-Selectin is platelets, where it was first identified and gets its name. P-selectin is stored within the α-granules of platelets and is released upon activation (Rivera et al., 2009). It is therefore possible for activated platelets, adherent to the EC surface to deliver P-selectin here and aid in leukocyte recruitment (Pitchford S.C et al., 2005).

L-selectin is constitutively expressed by all leukocytes except a subset of memory T cells and NK cells (Tedder et al., 1995a). Expression of L-selectin may be highly concentrated in certain regions such as on the microvilli projections of unstimulated neutrophils, allowing for early contact with EC-borne selectin ligands (Tedder et al., 1995a). A decrease in leukocyte infiltration was seen under inflammatory conditions in mice deficient in L-selectin, demonstrating the importance of its role in the inflammatory response (Tedder et al., 1995b). Leukocytes also express P-selectin glycoprotein ligand 1 (PSGL-1), which after undergoing post translational glycosylation is known to bind to all selectins allowing leukocyte-endothelial, leukocyte-platelet and leukocyte-leukocyte interactions to occur (**Figure 1-12**) (Hanley et al., 2004). It should be noted however that PSGL-1 is the highest affinity ligand for P-selectin and these molecules will bind preferentially (Mehta, P. Cummings, 1998).

Selectin mediated interactions are weak and continually break and reform, often the new bonds form before the old ones are broken (**Figure 1-12**) (Alón et al., 1995). This results in the phenomenon of leukocytes rolling along the endothelium in the direction of flowing blood (**Figure 1-12**) (Alón et al., 1995; Ley et al., 2007). L-selectin interactions require shear stress to form, if the shear stress is too low then leukocyte capture and rolling is not supported (Marshall et al., 2003; Finger et al., 1996). L-selectin interactions requiring shear stress to form, helps to prevent leukocyte aggregation from occurring in areas of low shear stress (Cines et al., 1998).

There are reports that interactions through selectins cause further activation of EC and allow them to express integrin receptors on their surface, while simultaneously causing partial activation of leukocyte integrins (Zarbock et al., 2007a). It has been shown that integrins may also play a role in leukocyte capture and slow the rolling process, before leukocyte firm adhesion takes place (Dunne et al., 2002). Mice deficient in macrophage antigen-1 (MAC-1 or CD11b/CD18 αM integrin/β2 integrin) or lymphocyte function associated antigen-1 (LFA-1 or CD11a/CD18 or αL integrin/ β2 integrin) had significantly increased leukocyte rolling velocities (Dunne et al., 2002). Huo et al. (2000) demonstrated monocyte very late antigen 4 (VLA-4) interaction with VCAM-1 allowed slow rolling to occur, blocking this interaction significantly increased rolling velocities.

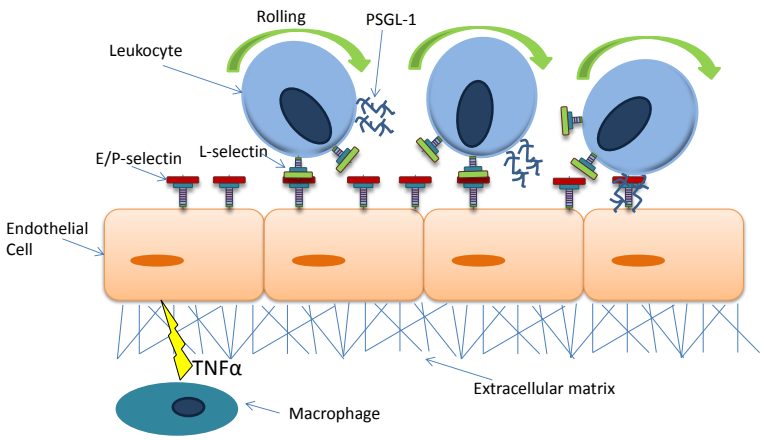


**Figure 1-12: Leukocyte capture and rolling**

During the inflammatory response activated cells, such as macrophages secrete TNFα, this will activate surrounding endothelial (EC) cells, resulting in their surface expression of platelet (P)-selectin and endothelial (E)-selectin. Leukocytes in the flowing blood are forced to the endothelial cell wall due to the process of margination. Constitutively expressed leukocyte (L)-selectin and PSGL-1 are able to interact with surface expressed EC selectins. The bonds which form are weak. Often new bonds form as old ones break resulting in the phenomenon of leukocyte rolling.

### 1.3.3 Activation and firm adhesion

Activated EC produce chemokines, chemokines belong to 4 subfamilies CXC, CC, CX3C and XC, which have been classified depending on the position of cystine residues (Zlotnik and Yoshie, 2012). Chemokines bind to glycosaminoglycans (GAGS) on the EC surface, which is thought to aid in prolonging their stability by preventing their degradation (Johnson et al., 2005). Some chemokines have been reported to activate EC leading to upregulation of surface expression of Ig superfamily members such as ICAM-1 and VCAM-1, which act as integrin receptors for leukocyte β2 and β1 integrins, respectively (**Figure 1-13**). Lymphocytes are known to be high in β2 integrin expression, in contrast to monocytes, which are high in β1 expression (Chan et al., 2001).

Chemokines activate leukocytes causing a conformational change to occur to constitutively expressed integrins, through a complex signalling cascade involving G-protein coupled receptors (GPCRs) (**Figure 1-13**). Binding of a chemokine to its receptor expressed on the leukocyte is referred to as outside-in signalling, this induces a conformational change to occur to the integrin receptor resulting in opening of the ligand binding pockets (Chigaev et al., 2003; Nahrendorf et al., 2007; Ley et al., 2007). In contrast inside-out signalling occurs downstream of ligand binding to activate integrins and aids in stabilisation (Constantin et al., 2000). These two signalling pathways are able to occur simultaneously leading to leukocyte firm adhesion and activation (Constantin et al., 2000).

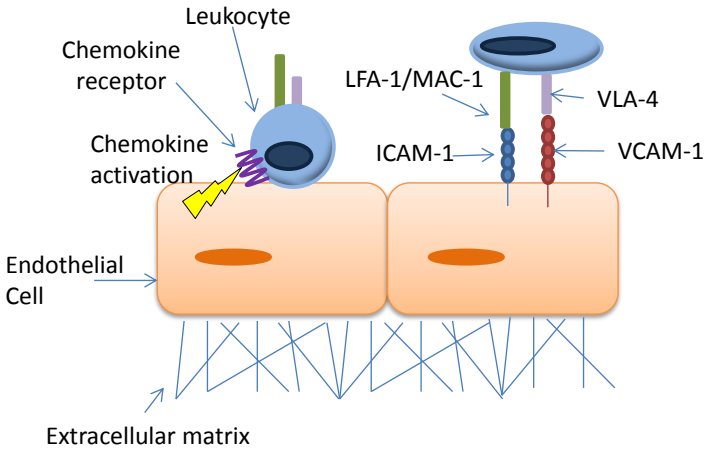


**Figure 1-13: Leukocyte activation and firm adhesion**

Endothelial cells and leukocytes become activated by the binding of chemokine ligands to their relevant receptors. This results in EC expression of Ig superfamily members ICAM-1 and VCAM-1, which are able to interact with LFA-1/MAC-1 or VLA4 respectively, resulting in firm stationary adhesion of the leukocyte.

Each chemokine is only able to bind to certain chemokine receptors (**Table 1-4 and Table 1-5**). This allows for some discrimination between recruitment of leukocyte subsets, as each will respond to different chemotactic signals. Chan et al, (2001) showed that monocyte VLA-4 affinity for VCAM-1 was increased in response to CXCL12. CXCL12 is a ligand known to bind to the chemokine receptors CXCR4 which is expressed by monocytes (**Table 1-5**) (Zlotnik and Yoshie, 2012). The largest monocyte subset ($CD14^{+}CD16^{-}$), are known to express high levels of CCR2 (**Table 1-5**). This has a high affinity for monocyte chemotactic protein-1 (MCP-1 or CCL2) which is produced by EC and indeed by monocytes themselves in response to TNFα, lipopolysaccharide (LPS) and IL-1 (**Table 1-4**). The ability of the classical $CD14^{+}CD16^{-}$ monocyte subset to respond to CCL2, one of the most abundant inflammatory chemokines makes them the most prevalent monocyte subset at the site of inflammation, earning them the reputation of being the most proinflammatory of the monocyte subsets (Strauss-Ayali et al., 2007). Non-classical monocytes ($CD14^{+}CD16^{++}$) lack CCR2 completely however they express high levels of

CXC3R1 (fractalkine receptor) meaning they are highly responsive to fractalkine and migrate towards this (Geissmann et al., 2003). As fractalkine is released downstream of CCR2 this means this monocyte subset arrive later than the classical subset (Nahrendorf et al., 2007).

Platelets are also thought to aid in monocyte recruitment to endothelium during the inflammatory response. Upon activation platelets will release the contents of their α granules, including the chemokines CXCL4 (platelet factor 4), CXCL7 and CCL5 (RANTES) (**Table 1-4**) (Zlotnik and Yoshie, 2012). CCL5 is known to bind to the receptors CCR1 and CCR5 and has been demonstrated to have an active role in inducing monocyte arrest on inflamed endothelium (von Hundelshausen et al., 2005, 2001). Evidence is beginning to emerge which suggests that CXCL4 binds to CXCR3b expressed by endothelial cells (Kuckleburg et al., 2011). This interaction, combined with the interaction of CCL5, may enhance monocyte adhesion and transmigration (Kuckleburg et al., 2011). However CXCL4 signalling alone has no effect on monocyte recruitment (Kuckleburg et al., 2011). This demonstrates a role for crosstalk between platelets and monocytes in monocyte recruitment to EC. Once firmly adherent, monocytes are now ready to transmigrate across the endothelium.

| **Chemokine** | Alternative name | Cells producing chemokine | Chemokine Ligands |
|---|---|---|---|
| **CXC subfamily** | | | |
| CXCL1 | GROα | Epithelial cells Endothelial cells | CXCR2 |
| CXCL2 | GROβ | Monocytes Macrophages | CXCR2 |
| CXCL3 | GROγ | Epithelial cells | CXCR2 |
| CXCL4 | Platelet factor 4 (PF4) | Platelets | CXCR3b |
| CXCL5 | Epithelial-derived neutrophil-activating peptide 78 (ENA-78) | Endothelial cells | CXCR2 |
| CXCL6 | Granulocyte chemotactic protein 2 (GCP2) | Endothelial Cells | CXCR1 CXCR2 |
| CXCL7 | Neutrophil-activating peptide-2 (NAP-2) | Platelets | CXCR1 CXCR2 |
| CXCL8 | Interlukin-8 (IL-8) | Endothelial cells Monocytes Lymphocytes | CXCR1 CXCR2 |
| CXCL9 | Monokine Induced by Gamma interferon (MIG) | Epithelial cells | CXCR3 |
| CXCL10 | Interferon gamma-induced protein 10 (IP-10) | Monocytes Endothelial cells Fibroblasts | CXCR3 |
| CXCL11 | Interferon-inducible T-cell alpha chemoattractant (I-TAC) | Epithelial cells | CXCR3 CXCR7 |
| CXCL12 | Stromal cell derived-factor1 (SDF-1) | Endothelial precursor cells | CXCR4 CXCR7 |
| **CC subfamily** | | | |
| CCL1 | | Lymphatic endothelial cells Lymphocytes | CCR8 |
| CCL2 | Monocyte chemotactic protein 1 (MCP-1) | Endothelial cells Monocytes Macrophages Dendritic cells | CCR2 |
| CCL3 | Macrophage inflammatory protein 1α (MIP1-α) | Monocytes Lymphocytes | CCR1 CCR5 |
| CCL4 | MIP-1β | Monocytes Lymphocytes | CCR5 |
| CCL5 | Regulated on activation, normal T cell expressed and secreted (RANTES) | Platelets | CCR1 CCR3 CCR5 |
| CCL7 | MCP-3 | Fibroblasts | CCR1 CCR2 CCR3 |
| CCL8 | MCP-2 | Endothelial cells | CCR1 CCR2 CCR5 |
| CCL13 | MCP-4 | Fibroblasts | CCR2 CCR3 |
| **XC subfamily** | | | |
| XCL1 | | Lymphocytes | XCR1 |
| **CX3C subfamily** | | | |
| CX3CL1 | Fractalkine | Endothelial cells | CX3CR1 |

**Table 1-4: Chemokine ligands**

Table 1-4 shows chemokines and their alternative names, some examples of cell types which are known to express them and their relevant receptors. (Table adapted from Zlotnik and Yoshie, 2012).

| Chemokine Receptor | Alternative name | Cells expressing receptor | Chemokine ligand |
|---|---|---|---|
| **CXCR subfamily** | | | |
| CXCR1 | Interlukin-8 receptor A (IL8RA) | Neutrophils | CXCL6 CXCL7 CXCL8 |
| CXCR2 | IL8RB | Neutrophils | CXCL1 CXCL2 CXCL3 CXCL5 CXCL6 CXCL7 CXCL8 |
| CXCR3 | G protein coupled receptor-9 (GPCR-9) | Lymphocytes | CXCL4 CXCL9 CXCL10 CXCL11 |
| CXCR3b | | Endothelial cells | CXCL4 |
| CXCR4 | | Monocytes | CXCL12 |
| CXCR7 | | Monocytes | CXCL12 |
| **CC subfamily** | | | |
| CCR1 | CC-chemokine receptor-1 (CC-CKR-1) | Monocytes | CCL3 CCL5 CCL7 CCL8 CCL13 |
| CCR2 | CC-CKR-2 | Monocytes | CCL2 CCL7 CCL8 CCL13 |
| CCR3 | CC-CKR-3 | Basophils Eosinophils | CCL5 CCL7 CCL11 CCL13 |
| CCR5 | CC-CKR-5 | Monocytes Lymphocytes Dendritic cells | CCL3 CCL4 CCL5 CCL8 CCL11 |
| **XCR subfamily** | | | |
| XCR1 | GPCR-5 | Dendritic cells | XCL1 XCL2 |
| **CX3CR1 subfamily** | | | |
| CX3CR1 | Fractalkine receptor | Monocytes Lymphocytes | CX3CL1 |

**Table 1-5: Chemokine receptors**

Table 1-5: shows chemokine receptors and their alternative names an example of the cells which are known to express them and the relevant chemokine receptors. (Table adapted from Zlotnik and Yoshie, 2012).

### 1.3.4 Leukocyte transmigration

Once a leukocyte has been activated and stationary adhesion to the EC has occurred, it can transmigrate across the vessel wall and enter the surrounding tissue (**Figure 1-14**). This occurs through a process known as diapedesis, where activated leukocytes transmigrate across the EC barrier (~2-5mins), the EC basement membrane (~5-15mins) and finally across the surrounding pericytes, leaving the vessel and entering the surrounding tissue (Ley et al., 2007).

There are two main routes, which activated leukocytes may take to cross the EC barrier, either transmigrating through the EC junctions (paracellular) or through the EC themselves (transcellular) (Muller, 2011). The most common route of diapedesis is the paracellular route and many of the molecules which form the tight and adherens junctions of the endothelium play a role in leukocyte transmigration (**Figure 1-14**) (Muller, 2011).

However the first step in initiating paracellular transmigration starts with the clustering of VCAM-1 and ICAM-1 at the site of diapedesis (Matheny et al., 2000; Shaw et al., 2004). Interaction of these molecules with the EC cytoskeleton leads to an increase in cytosolic $Ca^{2+}$ levels and rearrangement of the actin cytoskeleton, resulting in EC contraction (Cook-Mills et al. 2004; Etienne-Manneville et al. 2000; Matheny et al. 2000). This is thought to be one of the first steps in the leukocyte transmigration process. However this may not be the only role for these Ig super family molecules; both play a role in redistributing vascular endothelial-cadherin (VE-cadherin), a molecule which inhibits leukocyte diapedesis (Turowski et al., 2008; van Wetering et al., 2003).

VE-cadherin is a molecule which forms homophilic interactions in order to stabilise adherens junctions, it associates with β-catenin and α-catenin (Schulte et al., 2011). Phosphorylation of β-catenin through ICAM-1 signalling allows the homophilic interaction between VE-cadherin to be broken, allowing disassembly of the junction (Turowski et al., 2008). VE-cadherin-α-cadherin knock in mice, (which could not be phosphorylated at the β-catenin site,) showed stabilised VE-cadherin interactions and decreased transmigration during the inflammatory response (Schulte et al., 2011).

Other EC adhesion molecules, which under homeostatic conditions interact to maintain cell junction integrity have been shown to interact with leukocytes and aid in their

transmigration under inflammatory conditions (Muller, 2011). Junctional adhesion Molecules (JAMs) such as JAM-A, which is capable of homophilic adhesion or can form heterophilic bonds with JAM-C, or JAM-B, also aid in maintaining EC junctions (Chavakis et al., 2004; Ostermann et al., 2002). However, under inflammatory conditions JAM-A has been observed to interact with LFA-1 but not MAC-1 on leukocytes and aid in transmigration (**Figure 1-14**), (Ostermann et al., 2002). In vivo studies have revealed that JAM-A knockout mice show significantly reduced neutrophil transmigration (Woodfin et al., 2009). Likewise JAM-C has been found to interact with MAC-1 and also aid in leukocyte transmigration (**Figure 1-14**) (Chavakis et al., 2004). Chavakis et al, (2004) showed that by inhibiting JAM-C interaction with MAC-1, neutrophil transmigration was significantly reduced. Evidence suggests that a molecule closely related to JAMS, which consists of a longer cytoplasmic domain, endothelial cell selective adhesion molecule (ESAM) also aids in leukocyte transmigration (Wegmann et al., 2006), however, its leukocyte ligand is yet to be identified (Wegmann et al., 2006).

Platelet endothelial cell adhesion molecule-1 also an Ig superfamily member expressed by EC, leukocytes and platelets has been shown to be required for paracellular leukocyte migration (**Figure 1-14**) (Muller et al., 1993). Muller et al, (1993) demonstrated that PECAM-1 blocking antibodies prevented monocyte transmigration in vitro. Other molecules shown to have a role in transmigration include ICAM-2, CD99 and CD99Like2 (CD99L2) (Issekutz et al., 1999; Schenkel et al., 2002; Bixel et al., 2007). CD99 forms homophilic interactions between adjacent EC. However, under inflammatory conditions endothelial cell CD99 is able to form interactions with CD99 expressed on monocytes and neutrophils (Schenkel et al., 2002; Lou et al., 2007). Woodfin et al, (2009) amongst others have suggested that the interactions involved in transmigration may occur in a specific order. It was observed that leukocyte transmigration through EC was halted at specific points in ICAM-$2^{-/-}$, JAM-$A^{-/-}$ and PECAM-$1^{-/-}$ knock-out mice,

with the leukocyte migrating further through the EC barrier in each respective knock out mouse (Woodfin et al., 2009).

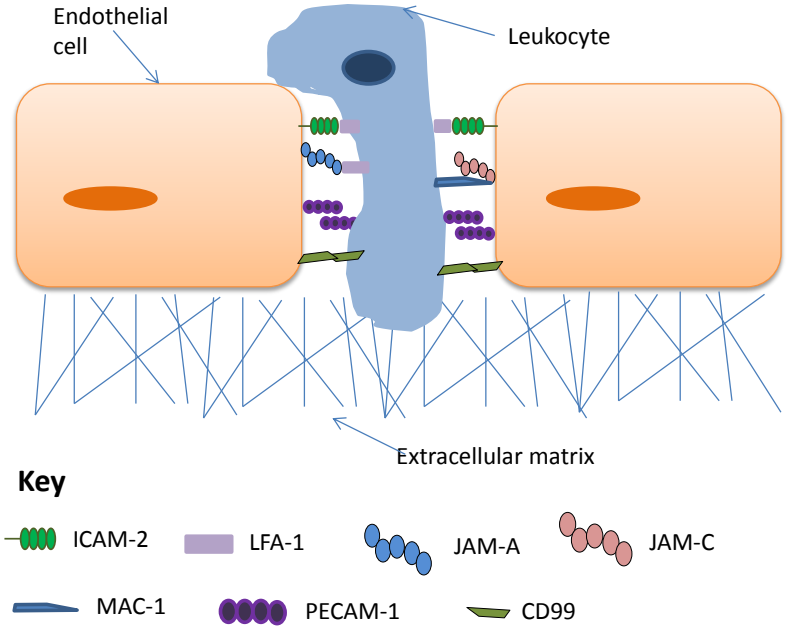


**Figure 1-14: Leukocyte transmigration**

Transmigrating leukocytes may use junctional adhesion molecules such as ICAM-2, JAM-A, JAM-C, PECAM-1 and CD99 to aid in their movement across the EC barrier. This is through interaction with molecules such as LFA-1, MAC-1 and PECAM-1 and CD99 expressed by leukocytes. (Figure adapted from (Ley et al., 2007)

The transcellular route of transmigration is used by 5-20% of leukocytes, it is a rapid response which can occur in ~1min (Ley et al., 2007). Many of the same molecules, which are responsible for paracellular migration have been implicated to play a role in this pathway, including ICAM-1, PECAM-1, CD99 (Mamdouh et al., 2009). ICAM-1 has been shown to cluster at the site of transmigration and throughout the channel the leukocyte passes through (Shaw et al., 2004). It is not entirely clear why cells, which are captured and activated through the same pathways use different routes of transmigration.

### 1.4.0 Atherosclerosis

Atherosclerosis, a chronic inflammatory disease, is one of the leading causes of morbidity and mortality in the western world (Dahlöf, 2010). The risk factors for this disease include aging, smoking, hypertension, elevated circulating levels of cholesterol and triglycerides and diabetes mellitus (as well as many other chronic inflammatory or auto-immune conditions) (Favero et al., 2014). Atherosclerosis involves the accumulation of fatty deposits in the wall of large and medium sized arteries (Ross, 1999). The disease is initiated by endothelial dysfunction, which usually occurs at predilection sites where laminar blood flow is disturbed and the endothelium is under increased stress (**Figure 1-15**), (Moore and Tabas, 2011). Damage or at least a change in phenotype, which compromises barrier function leads to accumulation of low density lipoproteins and associated lipids in the intimal layer of the artery (**Figure 1-15**). Oxidation of LDL occurs in situ, rendering it inflammatory in nature and driving the process of monocyte recruitment to the vessel wall (**Figure 1-15**). The earliest stage of atheroma formation is called the fatty streak (Eriksson et al., 2001). Over time more lipid accumulation and further leukocyte infiltration leads to the formation of a plaque, with a lipid core, at which point smooth muscle cells infiltrate the plaque forming a protective fibrous cap (**Figure 1-15**), (Libby, 2012). Eventually the lipid core can become necrotic and the fibrous cap thinned (**Figure 1-15**), (Moore and Tabas, 2011). This is now termed an unstable plaque, with an associated risk of rupturing (**Figure 1-15**), (Moore and Tabas, 2011). If the plaque ruptures a platelet thrombus will form at the site (**Figure 1-15**), (Cosemans et al., 2013). The mural thrombus, or embolizing fragments have the potential to block blood flow to the heart or brain, causing either a heart attack or stroke (Cosemans et al., 2013).

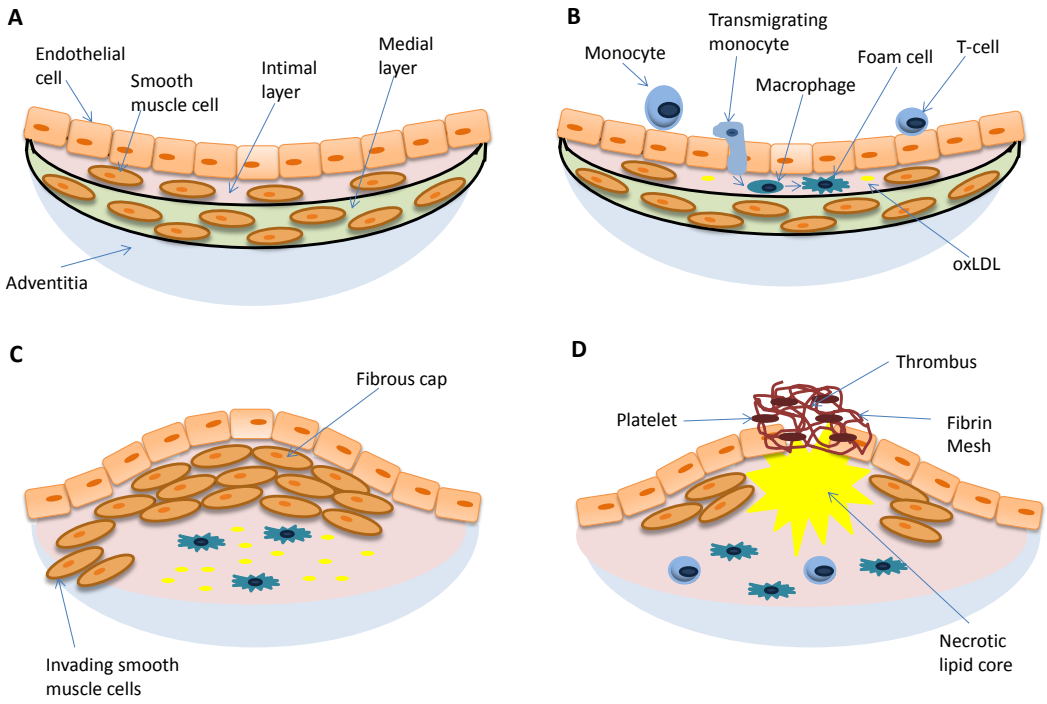


**Figure 1-15: Atherosclerotic plaque formation**

A) Healthy endothelium; endothelial cells and their basement membrane are found above the tunica intima, here resident Smooth muscle cells (SMC) can be found. Below the intimal layer is the medial layer, this contains the majority of the SMC in their own matrix. The outer layer, the adventitia contains mast cells and nerve endings. B) Phenotypic changes to endothelial cells (EC) results in recruitment of monocytes from the blood, this is accompanied by uptake of LDL, these accumulate in the intimal layer. LDL is oxidised in situ, its proinflammatory nature drives recruitment of monocytes. Monocytes differentiate to become macrophages and uptake oxLDL, resulting in the formation of foam cells. As the disease progresses monocytes will recruit T-cells through interactions with MHC-II receptors. C) As foam cells and lipids accumulate forming an atheroma, SMC migrate from the medial layer to form a protective fibrous cap. D) Over time the lipid core can become necrotic, the fibrous plaque may thin, if this happens it is prone to rupture at which point a thrombus may form. (Figure adapted from Libby et al., 2011).

### 1.4.1 The cellular pathology of atherosclerosis

Dietary lipids are processed to form triacylglycerols, cholesteryl esters, phospholipids, free cholesterol all of which are packaged with apolipoproteins. These can be used by cells of the small intestine to synthesise chylomicrons which are eventually released into the circulating blood, after passage into the circulation in the lymph (Beisiegel et al., 1989). Chylomicrons can

be taken up by the liver in an apolipoprotein E (ApoE) dependent manner and used to synthesise very low density lipoproteins (VLDL) (Tiwari and Siddiqi, 2012). VLDL is released back into the blood stream where it is degraded by lipoprotein lipase to produce LDL (Beisiegel et al., 1989). LDL is mainly composed of cholesteryl esters associated with ApoB-100 (Tiwari and Siddiqi, 2012). However, LDL is susceptible to oxidative damage, leading to the production of oxidised LDL (oxLDL) (Twigg et al., 2012). Oxidised LDL has been shown to play a major role in atherosclerosis disease progression as it activates EC, macrophages and smooth muscle cells (SMC) (Pirillo et al., 2013). The main receptors to be identified to have a role in oxLDL uptake by cells are scavenger receptor-A (SRA) and CD36 (Kunjathoor et al., 2002; Steinberg, 1997). Both of these receptors have been identified to have a role in the innate immune response (Kunjathoor et al., 2002). $APOE^{-/-}$ KO (knock-out) mice (a commonly used atherosclerosis disease model) coupled with either $SRA^{-/-}$ or $CD36^{-/-}$ KO were shown to have a decrease in atherosclerotic plaque sizes, compared to $APOE^{-/-}$ alone (Suzuki et al., 1997; Febbraio et al., 2000). This suggests that both of these receptors have an important role in the uptake of oxLDL during atherosclerotic plaque development. Cells also uptake oxLDL through receptor mediated endocytosis using lectin like oxidised low-density lipoprotein receptor-1 (LOX-1 or OLR1) (Murphy et al., 2008). LOX-1 is expressed at very low levels by healthy EC however in response to inflammatory signals (such as TNFα) an increase in LOX-1 has been detected (Kume et al., 1998). LOX-1 has also been shown to be expressed by EC in early in atherosclerosis and by SMC and macrophages in more advanced plaques (Kataoka et al., 1999).

Endothelial cells at branch points in arteries, where the blood flow is turbulent rather than laminar, are subjected to decreased shear stress, which is thought to make them susceptible to phenotypic changes (Passerini et al., 2004). Changes such as a decrease in NO production, a vasodilator, which also inhibits platelet and leukocyte activation and an increase in

endothilin-1 (ET-1) and angiotensin II both known vasoconstrictors (Thorin and Webb, 2010; Ziegler et al., 1998). These findings have also been demonstrated to be common amongst atherosclerosis patients (Oemar et al., 1998; Lerman et al., 1995; Schieffer et al., 2000). Dysfunctional EC also begin to constitutively express inflammatory markers such as selectins, ICAM-1, VCAM-1 and PECAM-1 on their surface (Iiyama et al., 1999; Eriksson et al., 2001; Zibara et al., 2000). The chemokine CCL2 has also been documented to be highly expressed in atherosclerotic plaques (Ikeda and Matsui, 2002).

However, EC are not the only cells to have an altered phenotype in this disease. Vascular SMC have been shown to undergo phenotypic changes and infiltrate the developing atherosclerotic plaque. Under normal healthy conditions SMC can be found in the medial layer of the artery wall where their main function is to maintain vascular tone as well as produce collagen, elastin and proteoglycans, which constitute part of the surrounding extracellular matrix (Owens et al., 2004). SMC retain their plasticity and respond to phenotypic changes in the surrounding environment, although ordinarily in health, they proliferate at an extremely low rate within the vessel wall (Rzucidlo et al., 2007). In response to vascular injury, SMC proliferate and migrate at an increased rate, they also adopted a more secretory phenotype (Gorski and Walsh, 1995). One of the first physical signs of phenotypic changes of SMC is a loss of vascular tone, resulting in stiffening of the arteries (arteriosclerosis) and the onset of hypertension, which is often associated with atherosclerosis (Rzucidlo et al., 2007).

Cross talk between SMC and EC has been well documented during the development of atherosclerosis (Libby 2012). SMC differentiate into a more secretory phenotype in response to the cytokines and chemokines produced by the activated EC and leukocytes (Wang et al., 1991). Conversely SMC secrete inflammatory cytokines and chemokines, which will activate the EC

aiding in platelet and leukocyte capture (Rainger et al., 2001; Barath et al., 1990). TGF-β released by SMC has been demonstrated to activate EC and aid in platelet capture to intact endothelium (**Figure 1-16**) (Rainger and Nash, 2001; Tull et al., 2006). Platelet capture by dysfunctional EC during early atherosclerotic plaque development has been well documented and is thought to be one of the key steps in plaque development (Burger and Wagner, 2003; Huo and Ley, 2004; Schober et al., 2002; Totani and Evangelista, 2010; von Hundelshausen et al., 2001). Once activated, platelets will release chemokines and aid in the inflammatory response (**Figure 1-16**), (von Hundelshausen et al., 2001). Activated platelets are also known to express P-selectin on their surface, it has been demonstrated that early platelet adhesion could play a role in leukocyte capture through P-selectin bridges (**Figure 1-16**), (Schober et al., 2002). Kuckleburg et al, (2011) demonstrated preferential recruitment of monocytes by platelet P-selectin bridges, both in vitro and in vivo (**Figure 1-16**).

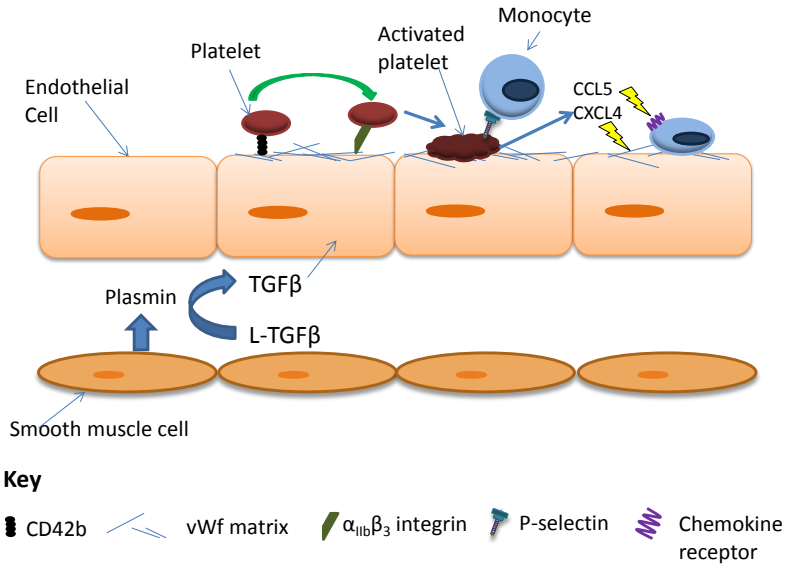


**Figure 1-16: Platelets aid in monocyte capture to the endothelium through P-selectin bridges**

During the atherosclerosis disease process secretory phenotype smooth muscle cells secrete plasmin. Plasmin (a serine protease) cleaves TGF-β into its active form. TGF-β stimulates EC which release vWf from Weibel Palade bodies so it can be trafficked to the surface. vWf captures platelets through interaction with CD42b, these interactions are short lived and are able to break and reform resulting in the platelet rolling along the vWf matrix (indicated by the green arrow). Platelets become activated and $\alpha_{IIb}\beta_3$ integrin undergoes a conformational change allowing it to bind to vWf, this results in the platelet becoming firmly adherent. Activated platelets secrete CCL5 which activate monocytes through CCR1 or CCR5, resulting in monocyte activation and arrest. CXCL4 activates EC through CXCR3b, and is thought to aid in monocyte transmigration (although this signal alone is insufficient to induce transmigration). (Figure adapted from Kuckleburg et al., 2011).

As well as recruiting platelets, dysfunctional EC are also able to recruit leukocytes due to the inflammatory molecules they express. Eriksson et al, (2001) demonstrated leukocyte recruitment to atherosclerotic plaques in 5-18 month $APOE^{-/-}$ KO mice was dependent on selectin expression. However monocytes have been shown to be the key leukocyte subset to be recruited at the onset of this disease. The chemokine CCL2, highly chemotactic for monocytes has been shown to be present in the atherosclerotic plaque. Absence of either the CCL2 or CCR2 using CCL2-/- or CCR2-/- mice fed a high fat diet showed reduced monocyte infiltration into the atherosclerotic plaque and a reduction in the burden of disease (Gu et al., 1998; Boring et al.,

1998). Once inside the intima, monocytes differentiate to form dendritic cells and macrophages which up regulate scavenger receptors such as LOX-1, CD36 and SRA (Woollard, 2013). An increase in these receptors leads to increased uptake of oxLDL. The lipid laden cell forms a foam cell, which is thought to be intrinsically inflammatory in nature (Libby, 2012). This process is responsible for the characteristic fatty streaks seen at the beginning of this disease process (Libby, 2012), although foam cells are evident at all stages of plaque development.

As the disease progresses antigen presenting cells (monocytes, macrophages and dendritic cells) will display peptides on MHC-II receptors allowing recruitment of helper T-lymphocytes and a role for the adaptive immune response (Woollard, 2013). However it is unclear whether the T-cell response is protective or detrimental to disease progression (Zhou et al., 2000; Ait-Oufella et al., 2006).

### 1.4.2 Role of leukocyte-platelet aggregates in atherosclerosis

Monocyte recruitment to the endothelium is an important step in atherosclerotic disease progression. The role platelets play in aiding in this process may also be a key step. It has been well documented that monocyte-platelet aggregates (MPA) and neutrophil-platelet aggregates (NPA) form in circulating blood, with increased incidence observed in patients suffering from diseases including DM, RA and atherosclerosis (Htun et al., 2006; Joseph et al., 2001; Furman et al., 1998; Harding et al., 2004). This implies a potential role for these aggregates in disease progression.

Atherosclerosis patients have been shown to have increased circulating activated platelets, which are identified through the expression of surface P-selectin. It is thought that the main mechanism through which leukocyte-platelet aggregates form is through platelet P-selectin and monocyte PSGL-1 interaction (Gkaliagkousi et al., 2009). Platelet P-selectin is therefore able

to interact with any leukocyte. However evidence suggests that neutrophil-platelet and lymphocyte-platelet aggregates (LPA) form with a lower propensity than monocyte-platelet aggregates (Joseph et al., 2001; Gkaliagkousi et al., 2009; Michelson et al., 2001).

Once MPA form, activated platelets release chemokines such as CCL5 which has been shown to activate monocytes, leading to increased CCL2 expression (Weyrich et al., 1996). As well as increased activation of monocytes, there is also increased potential for heterotypic aggregates to be recruited to the endothelium, as platelets may be captured through additional pathways (other than the leukocyte adhesion cascade) such as through interactions with vWf expressed on the surface of activated EC.

Upon platelet activation platelet microvesicles are generated. These are known to express P-selectin, CD41 and CD42b (Shai et al., 2012). Platelet microvesicles have also been documented to interact with monocytes and neutrophils (Forlow et al., 2000; Scholz et al., 2002). Expression of CD41 and CD42b may also allow for interactions and potential recruitment of leukocytes to surface expressed vWf on EC, although this remains speculative and is an experimental target of this thesis.

We hypothesise that platelets or microvesicles generated upon their activation play a role in the recruitment of leukocytes in inflammation and inflammatory disease. Our overall aim is to find out whether platelet or platelet derived microvesicles aggregate with leukocytes and whether platelet microvesicles have a potential role in aiding in monocyte recruitment in a chronic inflammatory disease environment.

The specific aims of this thesis are:

1) To identify whether platelets can be captured by endothelial cells, using glomerular endothelial cells for the disease model.
2) To identify if leukocyte-platelet or leukocyte-platelet microvesicle aggregates are generated upon platelet activation, using a variety of platelet agonists, also to find if differences occur in the rate or efficiency of aggregate formation depending on the agonist used.
3) To identify a way of potentially blocking the interaction between leukocytes and platelets or leukocytes and platelet microvesicles.
4) To identify a role for monocyte-platelet microvesicle aggregates in recruitment to vWf.

# 2. Chapter 2- METHODS

### 2.1.0 Protocols for cell culture and platelet adhesion to GEnC

### 2.1.1 Establishing cell line cultures

Immortalized cell line glomerular endothelial cells (GEnC), a kind gift from Simon Satchell, University of Bristol, have been created by transducing primary GEnC with a temperature sensitive simian virus 40 large tumour antigen (SV40LT) and telomerase using retroviral vectors (Satchell et al., 2006). When incubated at 33°C (5% $CO_2$) cell line GEnC proliferate and can be sub-cultured (Satchell et al., 2006). However incubating GEnC at 37°C (5% $CO_2$) causes SV40LT to be 'switched off', as the temperature sensitive virus is removed and the cells growth is arrested. Cell line GEnCs were cultured in complete endothelial cell growth medium (EGM2-MV) (Lonza).

Immortalized cell line podocytes (a gift from Moin Saleem, University of Bristol), were also created using SV40LT and telomerase using retroviral vectors (Saleem et al., 2002). When incubated at 33°C (5% $CO_2$) podocytes proliferate and appear to form a monolayer. However when incubated at 37°C (5% $CO_2$) for 1-2 weeks they differentiate and form the classic foot like projections, associated with podocytes. Podocytes were cultured in Roswell Park Memorial Institute (RPMI) medium (with L-glutamine and sodium bicarbonate) (Sigma) with supplements added as follows; 100U/ml penicillin, 0.1mg/ml streptomycin both components of penicillin streptomycin solution (Sigma), 2mM L-glutamine (Sigma), ITS (Sigma) containing recombinant human insulin 1µg/ml, human transferrin 1.1µg/ml and sodium selenite 1ng/ml and 10% (v/v) foetal Calf Serum (FCS) (Gibco).

Both cell line GEnC and cell line podocytes were sub-cultured using the following method: Culture medium was removed from the flask by aspiration. 2mls 0.02% (w/v) ethylenediaminetetraacetic acid (EDTA) (Sigma) was added to the flask and left for 1 minute to

chelate cations, necessary for adhesion receptor function. After 0.02% (w/v) EDTA was removed, 0.005g trypsin (Sigma) prepared in 0.02% (w/v) EDTA and was added to the flask. Cells became rounded and detached from the culture substrate. The trypsin was neutralized by adding twice the volume of complete medium. The cell suspension was removed from the flask and centrifuged at 500g for five minutes. Cells were suspended in their appropriate medium and seeded into either a $25cm^2$ or $75cm^2$ flask.

For long term storage of cell line GEnC or podocytes they were sub-cultured as above, however, instead of seeding a fresh flask, cells were suspended in 90% FCS (gibco) 10% (v/v) dimethyl sulphoxide hybri-max (DMSO) (Sigma). Cells were stored as 1ml aliquots frozen down in cool cell (Biocision), which is placed in a -80°C freezer, before being transferred to liquid nitrogen tanks for long term storage. Cell line GEnC or podocytes were taken out of nitrogen storage and defrosted in luke warm water. The 1ml contents was then added to 6ml of appropriate fresh medium and put straight into a $25cm^2$ culture flask, or a $75cm^2$ culture flask containing 10mls of fresh medium. The flask was incubated at 33°C until confluent.

**2.1.2 Sub-culturing primary GEnC (HRGEC)**

1mg/ml fibronectin (Sigma) (isolated from human plasma) was prepared in sterile water. $25cm^2$ flasks were coated with 50µg of fibronectin for 1 hour. Fibronectin was the recommended substrate for these cells. A vial containing $5x10^5$ primary GEnC (HRGEC ScienCell) was thawed at 37°C and cells were added to the previously coated $25cm^2$ flask along with 6ml of complete EGM2-MV. The cells were sub-cultured using the following method. Culture medium was removed from the flask by aspiration. 3mls 0.02% (w/v) EDTA was added to the flask for 1 minute. After 0.02% (w/v) EDTA was removed, 0.05% (w/v) trypsin (trypsin-EDTA Solution 10X - SAFC biosciences) prepared in 0.02% (w/v) EDTA and was added to the flask. Cells became

rounded and detached from the culture substrate. Trypsin was neutralized by adding 2mls FCS and 2mls complete EGM2-MV. The cell suspension was removed from the flask and centrifuged at 300g for 5 minutes. Cells were suspended in EGM2-MV medium and seeded into a $25cm^2$ flask previously coated with 1mg/ml fibronectin (as described above). Primary GEnC (HRGEC) were not sub-cultured for use in experiments beyond passage 3.

**2.1.3 Isolating and maintaining HUVEC primary cultures**

Full ethical approval and written consent was obtained before human umbilical cords were obtained from the Women's Hospital, Birmingham. Endothelial cells were isolated using collagenase digestion as described previously (Cooke et al., 1993). Briefly, undamaged cord sections of about 3-4 inches, were sprayed with ethanol 70% (V/V). The vein was cannulated and washed twice with PBS, incubated with collagenase (1X) (Worthington) at 37°C for 15 minutes. Cords were then massaged for one minute and flushed with PBS. Cells were centrifuged at 500g for five minutes and suspended in 5 ml of complete M199 medium (Gibco) (penicillin-streptomycin 0.1mg/ml; amphotericin (Sigma), 2.5µg/ml; gentamycin (Sigma), 35µg/ml; 1/500 human epidermal growth factor (Sigma), 10ng/ml; hydrocortisone (Sigma), 1µg/ml and 20% heat inactivated FCS). Human umbilical vein endothelial cells (HUVEC) were cultured in 4ml of M199 complete media in $25cm^2$ flasks pre-coated with 2% (w/v) gelatine.

**2.1.4 Assay for detection of vWf using fluorescence microscopy**

Cell line GEnC (batch 1) were seeded in a chamber slide with between $1x10^4$ and $4.8x10^4$ cells/well they were left overnight at 37°C. GEnC were either untreated for internal vWF detection or treated with 100U/ml TNFα (Sigma) and 10ng/ml TGFβ (R&D Systems) for 24 hrs for surface vWf detection. GEnC were washed twice with Dulbecco's phosphate buffered saline (PBS) (Sigma), then, fixed with either (i) 2% (w/v) formaldehyde (FA) for 10 minutes (for surface

detection) or (ii) 2% (w/v) FA for 5 min followed by 1% (w/v) triton for 10 minutes. Triton was used to puncture the membrane allowing the antibody to enter the cell. GEnCs were washed twice with PBS. A 2% (w/v) BSA (Sigma) blocking solution (made using PBS with $Ca^{2+}$ and $Mg^{2+}$) was then left on the cells for 30 minutes. 10µg/100µl of either FITC labelled, sheep antihuman vWf antibody (AbD serotec cat. no. AHP 062F, polyclonal) or FITC labelled sheep IgG isotype control (polyclonal) antibody, (The Binding Site) was added in 1% (w/v) BSA, 2% (v/v) FCS in PBS. GEnC were then incubated with either vWf or isotype control antibody for 1 hour. They were then incubated with 1µg/ml Hoechst 33342 component trihydrochloride (Invitrogen) to stain the nucleus. GEnC were then washed five times with PBS. Images were taken using a fluorescent invert microscope (Olympus IX71) and Image Pro version 6.3 (Media Cybernetics) was used to add pseudo colour.

For detection of internal vWf for cell line GEnC batch (2), these cells were incubated for 5 days at 37°C (5% $CO_2$) to ensure complete removal of the SV40LT virus. Cell line podocytes were used as a negative control and were incubated at 37°C for one week, to differentiate and to allow for complete removal of SV40LT. Primary HUVEC were used as a positive control and were cultured at 37°C (5% $CO_2$). These cells were seeded into separate wells of a chamber slide at $1x10^4$ cells/well. These were left overnight at 37°C (5% $CO_2$). The protocol for detection of internal vWf was then followed as stated in paragraph above.

**2.1.5 Platelet isolation**

The protocol has been adapted from Tull *et al* (2006). Blood from healthy volunteers was collected into a tube containing 10% (w/v) citrate phosphate dextrose solution (CPDA) (Sigma). It was centrifuged at 200g for 10 minutes. The platelet rich plasma (PRP) was collected and 0.013g theophylline (Sigma) was added to it, this was then centrifuged for 10 minutes at

1000g. The pellet was then suspended in theophylline buffer; 0.15% (w/v) BSA, 1.3mg/ml theophylline, Dulbecco's phosphate buffered saline (PBS) - without calcium chloride and magnesium chloride and washed for 10 minutes at 1000g. Platelets could then be suspended at desired concentration in appropriate buffer for use in experiments.

### 2.1.6 Optimising calcein staining of platelets

This technique was based on previous experiments, which were designed to detect platelet adhesion to HUVEC. The protocol has been adapted from Tull *et al* (2006). Platelets need to be stained with a fluorescent marker for use in assays designed to detect platelet surface adhesion to EC, in this case GEnC. However it is important that the fluorescent stain is bright enough to be detected but does not increase platelet activation as this would cause the data to be misleading. We tested the effect of staining platelets with 1µg/ml and 5µg/ml of calcein.

Blood from a healthy volunteer was collected into a tube containing 5U/ml heparin (Sigma). The heparinised blood was centrifuged at 1000g for 5 minutes and the platelet poor plasma (PPP) was collected. Platelets (from the same donor) were isolated as described above (**2.1.5 Platelet Isolation**). However, the platelet pellet was suspended in theophylline buffer at a concentration of $2x10^8$ platelets/ml, and before continuing with the protocol, platelets were stained with either 1µg/ml or 5ug/ml of calcein (Sigma) for 20 minutes at room temperature (RT) in the dark. The platelets were washed twice in 10mls theophylline buffer for 10 minutes at 1000g. $2x10^8$platelets/ml were then suspended in 80% PBS (with $Ca^{2+}$ and $Mg^{2+}$) (containing 0.15% w/v BSA) and 20% PPP or instead suspended in theophylline buffer, 20µl of each was pipetted on to a glass slide. Images were taken using a fluorescent invert microscope (Olympus IX71) and Image Pro version 6.3 (Media Cybernetics).

Platelets suspended in 80% (v/v) PBSA, 20% (v/v) autologous PPP (PBS buffer), in the presence of calcium, become activated and spread on a glass substrate (**Figure 2-1A**). However, when incubated with 5µg/ml calcein in theophylline buffer fewer are activated, indicating that up to 5µg/ml calcein does not cause further platelet activation (**Figure 2-1B**). Platelets suspended in PBS buffer on a glass substrate following incubation with both 1µg/ml and 5µg/ml calcein is demonstrated by figures 2-1C and D, respectively. 5µg/ml calcein shows a clearly visible stain (**Figure 2-1D**) and does not cause further platelet activation (**Figure 2-1B**). We therefore chose to use this concentration when assessing platelet adhesion to GEnC.

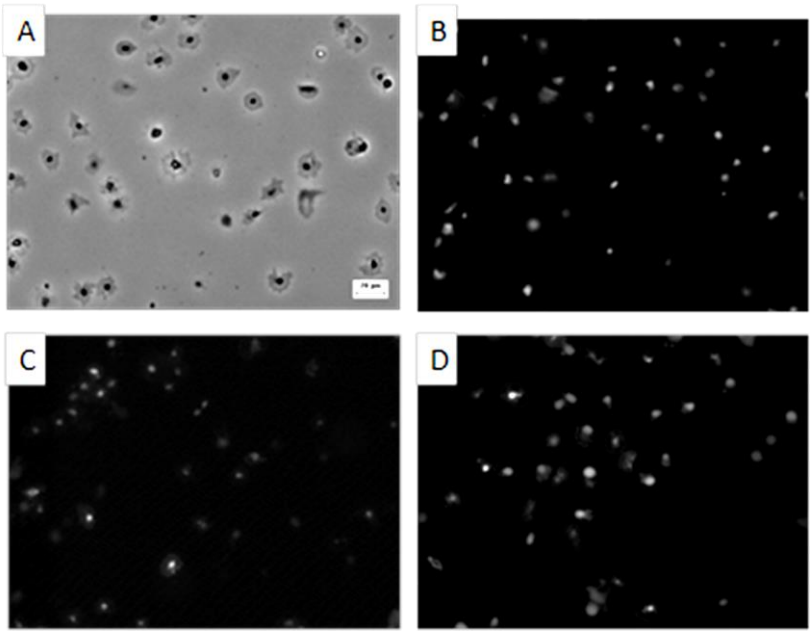


**Figure 2-1: Calcein staining platelets**

Platelets were isolated from whole blood and pipetted onto a glass substrate, images taken using Olympus IX71 x64 magnification. A) shows isolated, unstained platelets suspended in 80% (v/v) PBS 20% (v/v) platelet poor plasma on a glass substrate. Platelets are activated and the characteristic spreading is clearly demonstrated. B) shows platelets suspended in theophylline buffer stained with 5µg/ml calcein most of the platelets are not activated as they remain small and round, showing that calcein stain is not causing further platelet activation. C) shows platelets isolated and suspended in PBS buffer (containing PPP), stained with 1µg/ml calcein, these platelets appear dim and are difficult for the software to detect. D) shows platelets isolated and suspended in PBS buffer (containing PPP), stained with 5µg/ml calcein these appear bright and can easily be detected by the image pro software. Scale bar represents 20µm.

**2.1.7 Platelet adhesion to GEnC**

A 24 well plate was coated with 1% (w/v) gelatine diluted using PBS. (GEnC batch 1) were sub- cultured (**2.1.1 Establishing Cell Line Cultures**). They were seeded at a concentration of $1x10^5$ cells per well. They were left at 33°C (5% $CO_2$) until confluent, then at 37°C overnight to ensure removal of SVLT40 virus, before 24 hour treatment with TNFα (100U/ml) or TGFβ (10ng/ml) or both cytokines in combination (at the same concentrations) in EGM2-MV media. Control wells had EGM2-MV medium change, each treatment was done in duplicate (**Figure 2-2A**).

Platelets were isolated as previously descibed. $2x10^8$ platelets/ml were stained with 5µg/ml of calcein in theophylline buffer for 20 minutes at RT in the dark. The platelets were washed twice in 10mls theophylline buffer for 10 minutes at 1000g, an extra wash step was added to the standard protocol to ensure the removal of excess calcein, as this is a fluorescent live cell stain any excess would stain the GEnC monolayers leading to false detection of platelet adhesion. $2x10^8$platelets/ml were then suspended in 80% (v/v) M199 -without phenol red (Gibco) containing 0.15% (w/v) BSA and 20% (v/v) PPP (from the heparinised blood). When appropriate 5U/ml heparin was added at this point. A small aliquot was treated with 10µM ADP (Sigma). Either 300µl untreated or ADP stimulated platelet suspension containing $6x10^7$ platelets was added to the plate, which was incubated at 37°C for 1hr in the dark (**Figure 2-2B**).

At the end of the incubation period the cells were fixed with 1% (w/v) FA for 10 minutes. Monolayers were then washed four times with PBS, before images were taken using fluorescent invert microscope (Olympus IX71) and Image Pro version 6.3 (Media Cybernetics) at x32 magnification. Using Image Pro version 5.0 (Media Cybernetics) the percentage coverage of the GEnC monolayer by platelets, was calculated, as well as the average size of the platelets/platelet

aggregates and the number of platelets/platelet aggregates adhering to the GEnC monolayer (**Figure 2-3**). Unpaired one way or two way ANOVA analysis was carried out, using prism version 5.01 (GraphPad Software). The data was only included if the monolayer of the well was intact, as it is well known that platelets will adhere to the subendothelial matrix (**Figure 2-4**).


**Figure 2-2A: Cytokine treatment of GEnC in a 24 well plate**

Figure 2-2 shows the wells of a 24 well plate containing GEnC monolayers treated either with 100U/ml TNF or 10ng/ml TGFβ, or a combination of both cytokines in EGM2-MV medium. Control wells contained only EGM2-MV medium.

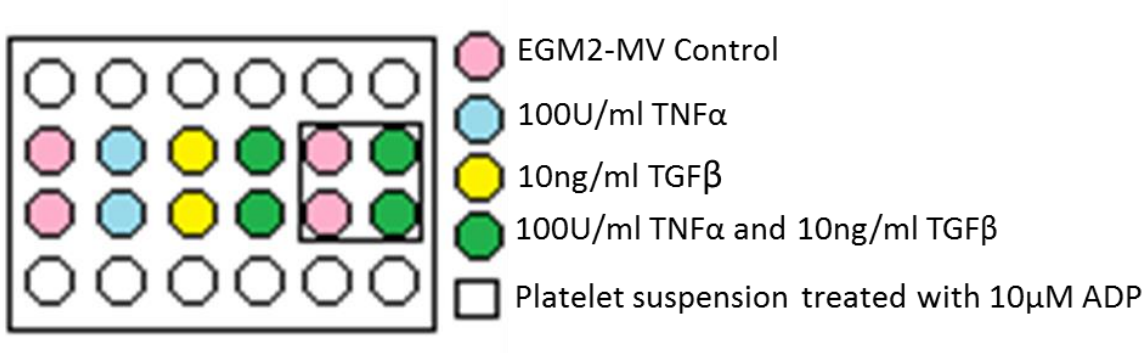


**Figure 2-2B: Incubation of GEnC monolayers with untreated or 10µM ADP stimulated platelets**

Suspensions of $6x10^7$ platelets in 20% (v/v) PPP 80% (v/v) medium 199 (without phenol red) either unstimulated, or treated with 10µM ADP were added to cytokine stimulated or untreated GEnC monolayers and incubated for 1 hour at 37°C (5% $CO_2$).

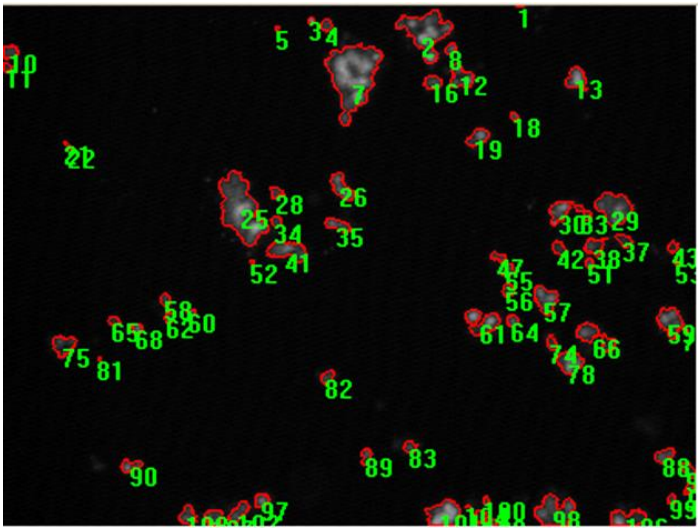

**Figure 2-3: Platelet adhesion analysis.**

Figure 2-3 demonstrates Image pro version 5.0 (Media Cybernetics) depicting fluorescent platelets compared to the black background. The software is able to determine the number and size of the aggregates forming.

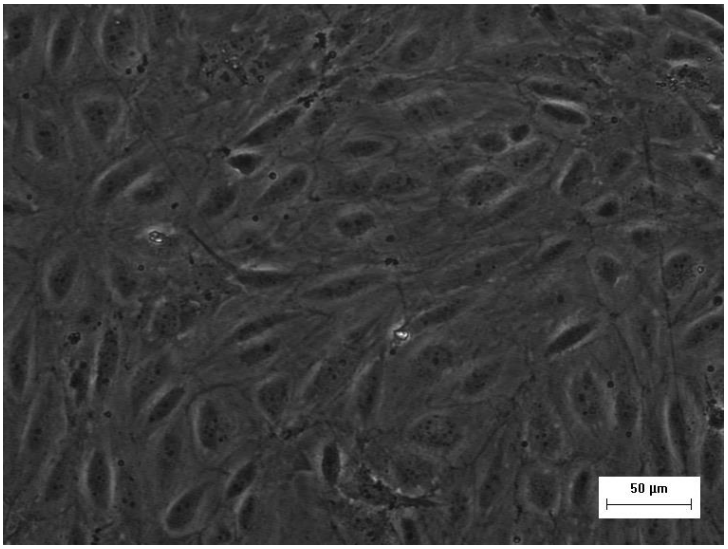


**Figure 2-4: Intact GEnC monolayer**

Figure 2-4 demonstrates an intact GEnC monolayer used in platelet adhesion assay. Image taken using Olympus IX71 fluorescent invert microscope and Image pro version 6.3. Scale bar represents 50µm.

### 2.1.8 Assay for detecting cell surface markers using flow cytometry

| Antibody | Company | Catalogue number | Clone | Working concentration |
|---|---|---|---|---|
| **Primary antibodies** | | | | |
| CD54 (ICAM-1) – allophycocyanin (APC) | BD pharmingen | 559771 | HA58 | 1/50 |
| CD31 (PECAM-1 ) - PE (Phycoerythrin) | R&D Systems | FAB2567P | Clone 9G11 | 1/50 |
| VWf-FITC (Fluorescein isothiocyanate) | ABD Serotec | AHP062F | Polyclonal | 1/100 |
| Mouse Anti-CD62E | Sigma | S9555 | 1.2B6 | 1/200 |
| **Secondary antibodies** | | | | |
| Goat-anti mouse-FITC | DAKO | F0479 | Polyclonal | 1/200 |
| **Isotype antibodies** | | | | |
| Mouse IgG1 | DAK-GO1 | | DAK-GO1 | 1/200 |
| Mouse IgG1-PE | Immuno tool | 21275514 | PPV-06 | 1/50 |
| Sheep IgG1-FITC | The Binding Site | | | 1/100 |
| Mouse IgG- APC | Biolegend | 400122 | MOPC-21 | 1/50 |

**Table 2-1: Antibodies for detection of cell markers, relevant isotypes and secondary antibodies**

As GEnC batch 2 appeared to have lost its characteristic cobblestone appearance this prompted us to test for EC markers, HUVEC were used as a positive control and the epithelial, podocyte cell line were used as a negative control. A 25cm$^2$ flask containing cell line GEnC (batch 2) were left at 37$^o$C (5% $CO_2$) for at least 5 days, for growth arrest to take place and to ensure complete removal of the SV40LT. A 25cm$^2$ flask containing cell line podocytes was left at 37$^o$C

(5% $CO_2$) for at least 7 days to differentiate and for removal of SV40LT virus. The cells were then sub-cultured as previously described and seeded into a 24 well plate ($1x10^5$ cells/well) along with primary HUVEC (which had been cultured at 37°C (5% $CO_2$) throughout. The cells were left at 37°C (5% $CO_2$) overnight to allow them to adhere. Each cell type was cultured in its own appropriate medium throughout. For ICAM-1 and PECAM-1 detection wells containing each cell type were treated with 100U/TNFα for 4 hours prior to removal from the plate. For E-selectin detection, cells were treated with 1000U/TNFα for 4 hours prior to removal from the plate. This is because these markers are part of the leukocyte adhesion cascade and are only expressed as part of the inflammatory response.

For detection of either ICAM-1 or PECAM-1 cells were removed from each well of the plate as previously described, cells were transferred into flow cytometry tubes. 2mls ice-cold 2% (w/v) BSA in PBS was added to increase wash volume and for non-specific blocking. As cells were live they were washed at 4°C, 500g for 5 mins. The supernatant was removed and the cell pellet was suspended in either 50µl 2% (w/v) BSA in PBS containing allophycocyanin (APC) labelled mouse anti-human ICAM-1 (CD54) antibody or relevant concentration of APC labelled mouse IgG isotype control antibody, or PE labelled mouse anti human PECAM-1 antibody or relevant concentration of PE labelled mouse IgG antibody (**Table 2.1**). The cells were incubated with antibody on ice for 40 minutes, in the dark. 2ml ice-cold 2% (w/v) BSA in PBS was added to increase wash volume and the cells were centrifuged at 4°C, 500g for 5mins. The cells were then suspend and stored in 300µl of 2% (w/v) FA. Before running flow cytometry the cells were centrifuged at 500g and suspended in 300µl PBS for data acquisition.

For detection of E-selectin cells were washed with 2% (w/v) BSA in PBS. Then incubated for 30 minutes on ice, with 200µl/well of 2% (w/v) BSA in PBS containing either mouse

monoclonal anti- human E-selectin (CD62E) antibody or mouse IgG1 isotype antibody (**Table 2-1**). Each well was then washed with 0.5mls 2% (w/v) BSA in PBS, 3 times. Before incubating on ice, in the dark with 200µl/well of 2% (w/v) BSA in PBS, containing FITC labelled polyclonal goat anti-mouse antibody (**Table 2-1**). The cells were then washed, once, with 0.5mls 2% (w/v) BSA in PBS and then with 0.5mls of 0.02% (w/v) EDTA per well. 0.5mls of cell dissociation buffer (Gibco) (an isotonic and enzyme free solution of salts and chelating agents and cell conditioning agents in PBS) was then added to each well and the plate was incubated at 37 $^{o}$C, for 15 minutes, until cells rounded up and detached. The cells were then transferred to flow cytometry tubes. Washes were preformed in 2% (w/v) BSA as before. The pelleted cells were then suspended in 300µl of 2% (w/v) FA to fix them ready for analysis. Before running flow cytometry the cells were centrifuged at 500g and suspended in 300µl PBS for data acquisition.

For detection of internal vWf cells were removed from the plate as previously described once cells had rounded and detached from the flask, they were transferred to flow cytometry tubes, containing 2mls ice-cold 5% (v/v) FCS in PBS to neutralize trypsin. Cells were then washed at 4°C 500g for 5 minutes. The supernatant was removed and the cells were suspended in 50µl medium A (Invitrogen fix and perm kit) and incubated in the dark for 15 minutes at RT. 2ml of 5% (v/v) FCS in PBS was added to each tube to increase wash volume and then centrifuged at 500g for 5 minutes and the supernatant removed. The cell pellet was suspended in 50µl of medium B (Invitrogen fix and perm kit) containing either FITC labelled sheep anti-human vWf antibody (AbD serotec) or FITC labelled sheep IgG isotype control antibody, (The Binding Site) at a 1/100 dilution. This was then incubated at 37$^{o}$C in the dark for 40 minutes. Cells were then washed in 2mls of 5% (v/v) FCS in PBS, 500g for 5 minutes. The cells were suspended in 300µl of PBS ready for flow cytometry.

Data was acquired using a DAKO Cyan flow cytometer 1.5x$10^3$ events for each cell type were collected based on the size and granularity of the cells this is demonstrated by figure 2-5, gates G1 (HUVEC), G3 (Podocytes) and G5 (GEnC batch 2). Analysis was carried out using Dako Summit 4.3 software. A gate was set to include 5% of the isotype control for each cell type, (**Figure 2-5**), gates G2 (HUVEC), G4 (Podocytes) and G6 (GEnC batch 2), the median fluorescent intensity (MFI) of ICAM-1 in each gate was recorded. The MFI of the isotype for each cell type was also recorded and could be subtracted to calculate the change in MFI. This analysis was repeated for PECAM-1, E-selectin and vWf.

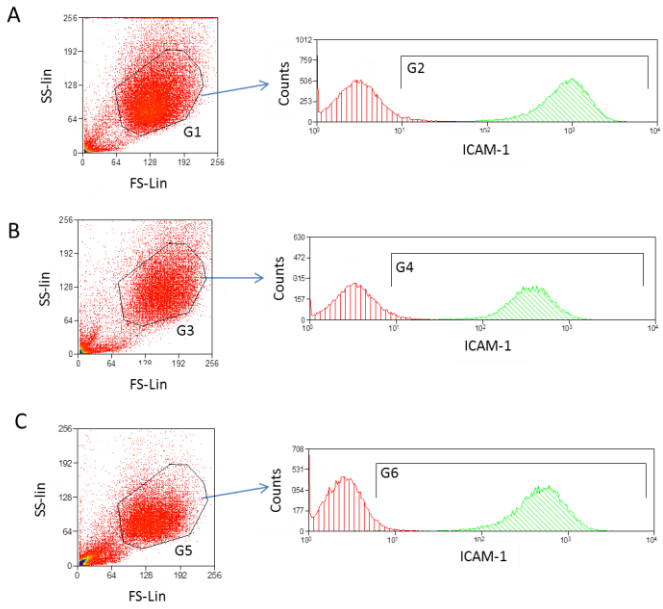


**Figure 2-5: Gating strategy to assess cell markers on HUVEC, podocytes and batch 2 GEnC**

Figure 2-5 demonstrates the gating strategy for collecting 1.5x$10^4$ events based on size and granularity for A) HUVEC (G1), B) podocytes (G3) and C) GEnC batch 2 (G5). A gate was then set, which included 5% of the isotype control and the MFI for surface ICAM-1 expression found in this gate was recorded. This was repeated for each cell type A) HUVEC gate (G2), B) podocyte gate (G4) and C) GEnC batch 2 gate (G6). This method was adopted for analysis of surface PECAM-1 and E-selectin and internal vWf.

### 2.2.0 Method development for detection of leukocyte-platelet aggregates in whole blood

For experiments to determine leukocyte-platelet aggregate formation, blood was collected from a healthy volunteer and immediately transferred to a tube containing 10% citrate phosphate dextrose solution (CPDA). Cells were fixed with 1% (w/v) FA for 10 minutes followed by two wash steps at 500g for 5 minutes in 3mls PBS, unless stated otherwise. In order for flow cytometry data to be acquired, red cells were lysed using ACK lysis buffer (Gibco) according to manufacturer's instructions. ACK was added at x10 starting volume of whole blood, this was mixed gently 3 times and incubated for 10 minutes at RT. ACK was diluted using PBS ~ x10 volume added, to prevent further lysis and damage to leukocytes, and samples were centrifuged at 500g for 5 minutes. To remove any residual ACK this wash step was repeated using 5-10mls PBS, before samples were suspended in 300µL PBS ready for flow cytometry.

| Antibody | Company | Catalogue number | Clone | Working concentration | Cells identified |
|---|---|---|---|---|---|
| CD3-PerCP | BD bioscience | 345766 | SK7 | 10/100 | T-Lymphocytes |
| CD14-PE | Immuno Tools | 21270144 | MEM-18 | 1/100 | Monocytes |
| CD14- APC | e-Bioscience | 17-0149-42 | 61D3 | 0.1µg/100µl | Monocytes |
| CD16-FITC | DAKO/Alere | YYF701101 | | 2/100 | Monocytes/ Neutrophils |
| CD16-PEcyanine7 (PEcy7) | e-Bioscience | 25-0168-42 | eBioCB16 | 0.012µg/100µl | Monocytes /Neutrophils |
| CD20-PEcy7 | AbCam | Ab82002 | B-Ly1 | 5/100 | B-Lymphocytes |
| CD42b- APC | BD-Pharmingen | 551061 | HIP1 | 7/100 | Platelets |
| P-selectin CD62P-FITC | BD-Pharmingen | 555523 | AK-4 | 1/50 | Platelets |
| CD162 PE | e-Bioscience | 12-1629-42 | FLEG | 0.024µg/100µl | Leukocytes |
| **Isotype** | | | | | |
| Mouse IgG1-PE | Immuno Tools | 21275514 | PPV-06 | 1/100 or 0.012µg/100µl | |
| Mouse IgG1-FITC | DAKO(Alere) | YYX092701 | | 2/100 or 0.025µg/100 | |
| Mouse IgG- APC | Biolegend | 400122 | MOPC-21 | 0.1-0.2µg/100µl | |
| Mouse IgG-PEcy7 | e-Bioscience | 25-4714-41 | P3.6.2.8.1 | 0.012µg-0.25/ml | |

**Table 2-2: Flow cytometry antibodies**

### 2.2.1 Lysing red blood cells with ACK lysis buffer

Blood from a healthy volunteer was collected into 10% (w/v) CPDA and aliquoted into 0.3ml volumes. Blood aliquots were either fixed or left untreated. ACK lysis buffer was used to lyse red blood cells following manufactures instructions. The remaining live cells were fixed. Cells were suspended in 100µL PBS with CD14 (Immuno Tools) and CD3 antibodies (BD bioscience) for 30 minutes (**Table 2-2**), cells were washed twice in 5mls PBS at 500g for five minutes. Cells were then suspended in 300µl PBS for analysis by flow cytometry.

Data was acquired using a Dako Cyan flow cytometer, a total of $2.5x10^5$ events were collected (including all leukocyte cell types) based on the size and granularity of the cells, analysis was carried out using Dako Summit 4.3 software. Figure 2-6A and B demonstrate that lysis of live RBC with ACK lysis buffer is not successful as the leukocyte populations can't be distinguished from each other. However Figure 2-6C and D demonstrate that fixing with 1% FA prior to treatment with ACK, allows effective lysis to occur, without damaging leukocytes. As leukocyte subpopulations can clearly be identified based on differences in their size and granularity. This is further confirmed by the use of antibodies against the monocyte marker CD14 and the T-cell marker CD3 (**Figure 2-6D**).

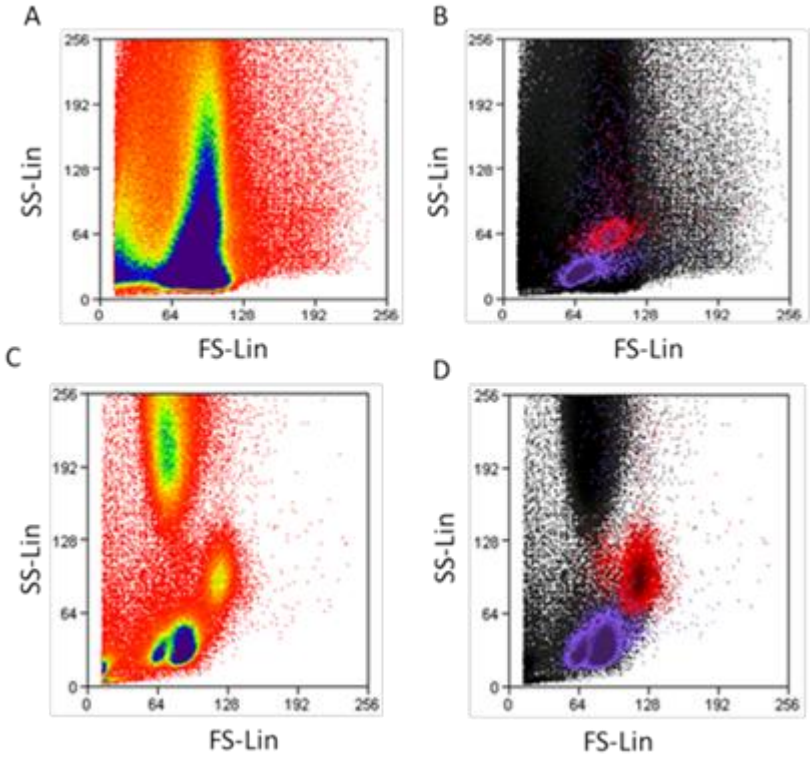


**Figure 2-6: Red blood cell lysis with ACK lysis buffer**

A and B) both show live blood cells treated with ACK lysis buffer based on size and granularity, however the lysis method has not been effective as there appears to be red cell contamination. B) Shows that damage to leukocytes has occurred, based on the change in size and granularity of CD3 positive lymphocytes (purple) and CD14 positive monocytes (red). C) and D) both show previously fixed blood where red blood cells have been lysed with ACK lysis buffer. D) The CD3 positive lymphocyte (purple), CD14 positive monocyte (red) and neutrophil subpopulations can clearly be identified.

### 2.2.2 Using fixed or live cells for antibody staining

When used for detection of leukocyte-platelet aggregates in whole blood, samples would need to be fixed at the end of a time course, to prevent any further leukocyte-platelet aggregate formation from occurring. However, we wanted to make sure that antibodies could recognise their receptor once cells were fixed. Blood from a healthy volunteer was collected into 10% (v/v) CPDA and aliquoted into 0.3ml aliquots. Aliquots were either fixed immediately or cells were left

live. One fixed and one live aliquot was incubated for 30 minutes at RT or on ice with the following antibodies; PE labelled CD14 antibody, FITC labelled CD16 and APC labelled CD42b, (**Table 2-2**). The remaining live cell aliquots were fixed. RBC were lysed. Samples were suspended in 300µl PBS for analysis by flow cytometry, data was acquired using a Dako Cyan flow cytometer, a total of $2x10^4$ events were collected in the monocyte gate based on the size and granularity (**Figure 2-7**). Analysis was carried out using Dako Summit 4.3 software.

The data revealed that incubating live whole blood samples at either RT or on ice with CD14 and CD16 antibody resulted in the activation of monocytes and both receptors being shed (**Figure 2-7 D and E**). However, when cells are fixed prior to incubation with CD14 and CD16 antibody the monocyte populations ($CD14^+CD16^-$ and $CD14^+CD16^+$) can clearly be identified (**Figure 2-7 A-C**).

### 2.2.3 Measuring MPA formation at a defined shear rate

Ideally, it would have been better to carry out experiments to look at MPA formation at a defined shear rate. 1ml of blood collected into 10% (v/v) CPDA, from a healthy volunteer was added to a cone and plate viscometer and blood was sheared at a known rate of either $46S^{-1}$, $115S^{-1}$ or $230^{-1}$ for 30 minutes. At 5, 15 and 30 minutes a 200µL aliquot of blood was taken and fixed. An aliquot of blood was also fixed shortly after phlebotomy as a control. The samples were then suspended in 300uL PBS and incubated with PE labelled CD14, FITC labelled CD16 and APC labelled CD42b antibodies for 30 minutes (**Table 2-2**). Red cells were lysed and cells were suspended in 300uL PBS ready for flow cytometry. Analysis was carried out using Dako Summit 4.3 software. However, following incubation in the cone and plate viscometer the auto fluorescence of the cells was altered and they produced a strong FITC signal. An example of unstained samples which were sheared at $115S^{-1}$ and $230^{-1}$ are shown below (**Figure 2-8**).

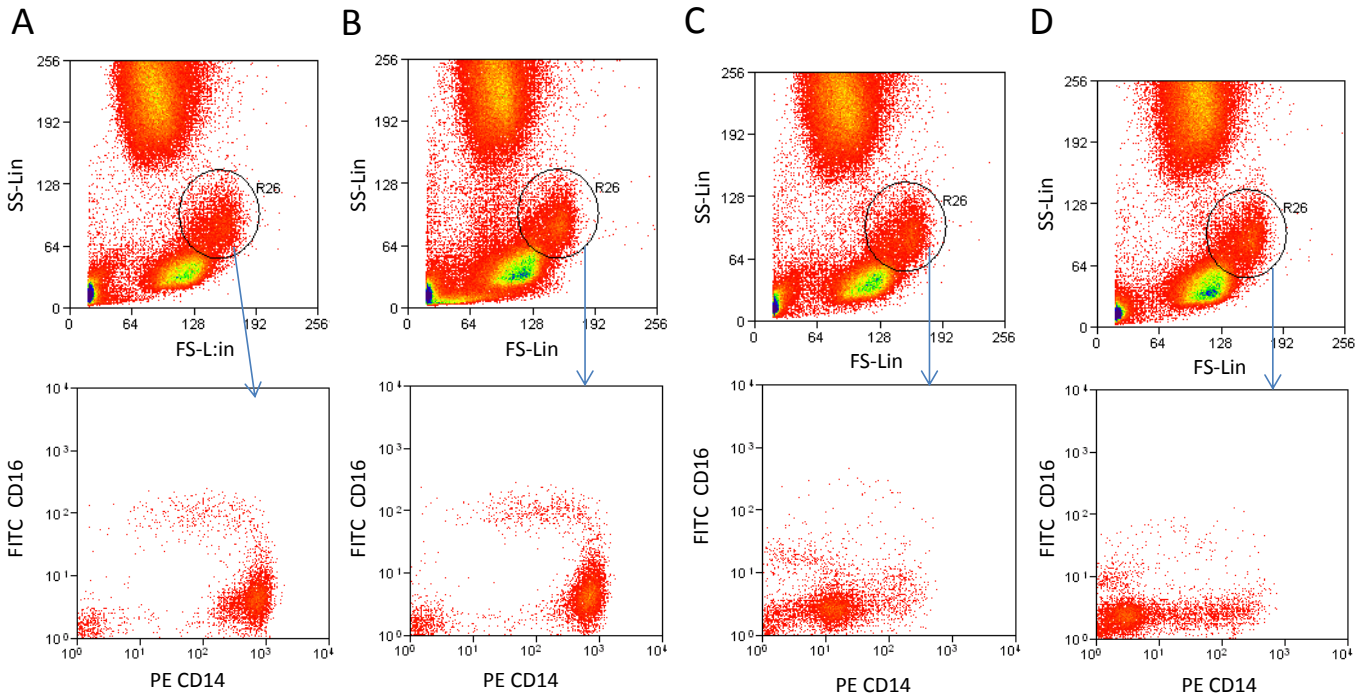


**Figure 2-7: Fixed or live antibody stain**

A) shows whole blood which has been fixed with 1% (w/v) FA, then incubated at room temperature (RT) for 30 minutes or B) on ice for 30 minutes, with CD14 and CD16 antibodies before lysis with ACK. C) demonstrates whole blood which has been in incubated at RT for 30 minutes or D) on ice for 30 minutes with antibodies, before fixing with 1% (w/v) FA and red blood cell lysis with ACK lysis buffer. Gate R26, which includes the monocyte population based on their size and granularity has been applied (demonstrated by blue arrow) to a CD14 vs CD16 plot. A and B demonstrate that when cells are fixed prior to incubation with antibodies the monocyte population based on CD14 and CD16 expression can clearly be distinguished. However C and D demonstrate that incubation with antibodies at either 4°C or RT before cells are fixed results in the loss of CD16 expression by monocytes in whole blood.

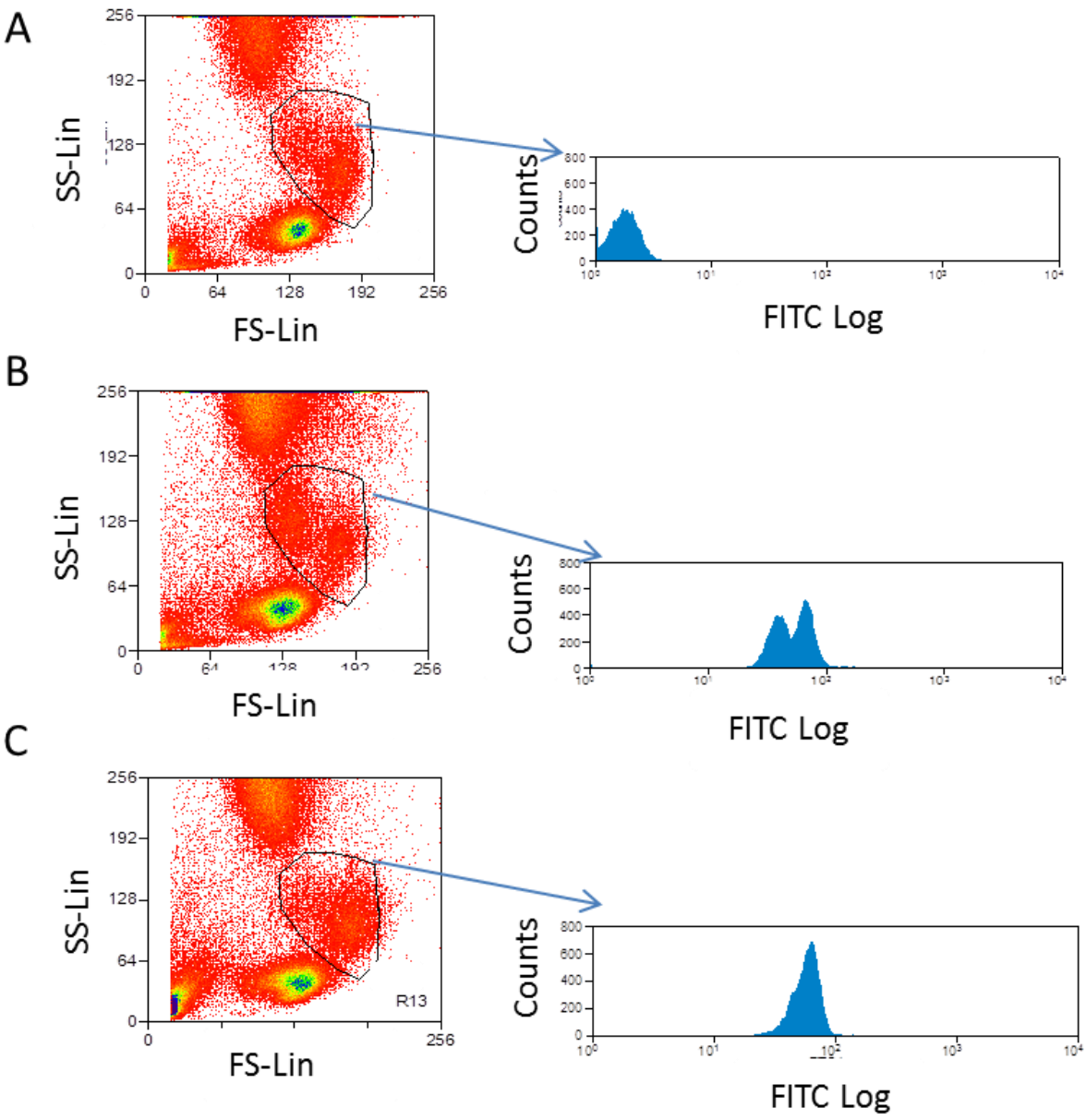


**Figure 2-8: Auto fluorescence of leukocytes is altered after incubation in the cone and plate viscometer**

Whole blood was A) fixed prior to any treatment, or incubated in the cone and plate viscometer for 30 minutes at B) $115S^{-1}$ or C) $230S^{-1}$ before fixing. Data were acquired using flow cytometry. A) demonstrates that fixed blood has low auto fluorescence. B) and C) indicate that following incubation in the cone and plate viscometer the auto fluorescence of unstained monocytes is increased.

### 2.3.0 Final protocol for detection of leukocyte-platelet aggregates in whole blood

### 2.3.1 Detection of leukocyte-platelet aggregates in whole blood using flow cytometry

Blood was collected from a healthy volunteer and immediately transferred to a tube containing 10% (v/v) CPDA. 300µL of blood was aliquoted into 5ml tubes. Some aliquots were fixed immediately for a control (0 minute) and also to calibrate the flow cytometer. Remaining aliquots were incubated with a platelet agonist, at either a high or low concentration (**Table 2-3**) at 37°C on a roller mixer for 5 minute intervals, ranging between 5-30 minutes and 60 minutes. A high concentration of platelet agonist can be defined as; causing full aggregation of washed platelets. A low concentration is the lowest concentration of agonist shown to cause full aggregation of washed platelets of highly responsive donors. Untreated samples were incubated on a roller mixer at 37°C for 30 minutes and 60 minutes. At the end of the incubation period samples were fixed. Samples were suspended in 300µL PBS. The following antibodies, from a previously prepared master mix, were added; PE labelled CD14 antibody, FITC labelled CD16 and APC labelled CD42b (GPIb) (**Table 2-2**). Of the immediately fixed aliquots one was left unstained, another was used to prepare an isotype (**Table 2-2**) another had FITC CD16, PE CD14 and APC isotype control (**Table 2-2** and **Figure 2-12**). Single colours were added to individual aliquots for compensation of the flow cytometer. After 30 minutes incubation with antibody, RBC were lysed. Each sample was suspended in 300µl of PBS. Data were acquired using a Dako Cyan flow cytometer, a total of $2x10^4$ events were collected in the monocyte gate based on the size and granularity of the cells.

| Platelet receptor(s) | Platelet Agonist | Company | Concentration |
|---|---|---|---|
| P2Y1 P2Y12 | ADP | Sigma | 30µM |
| P2Y1 P2Y12 | ADP | | 3µM |
| PAR1 | TRAP* | Alta Biosciences | 100µM |
| PAR1 | TRAP* | | 10µM |
| TP | U46619 | Cayman Chemical Company | 10µM |
| TP | U46619 | | 3µM |
| CLEC2 | Rhodocytin | Gift from Johannes Eble (University of Münster) | 100nM |
| CLEC2 | Rhodocytin | | 30nM |
| GPVI | CRP-XL | University of Cambridge | 1µg/ml |
| Charge dependent/TLR2 and TLR4 | Calf thymus histones | Worthington | 1mg/ml |
| CD36 | Oxidised LDL | Intracell (USA) Cat no. RP-047 | 50µg/ml |

**Table 2-3: Table of agonists used and the receptor, through which they are known to activate platelets**

*Trap peptide: H-Ser-Phe-Leu-Leu-Arg-Asn-OH

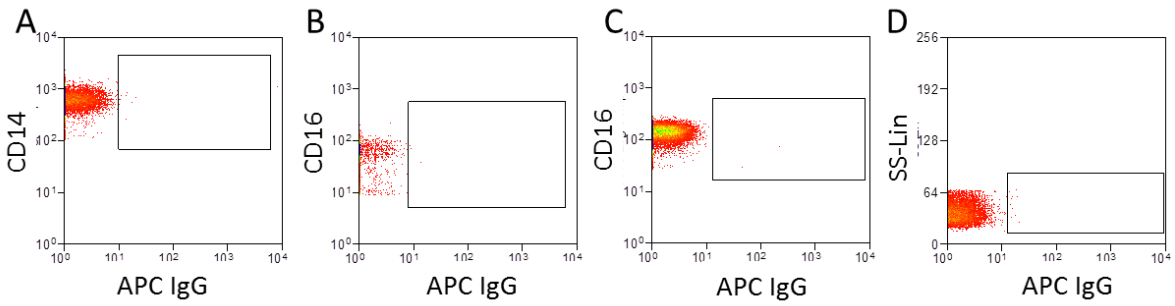


**Figure 2-9: Allophycocyanin isotype control**

Whole blood was fixed with 1% (w/v) FA and incubated with CD14 (PE), CD16 (FITC) and APC IgG for 30 minutes before red blood cells were lysed. Leukocytes were suspended in PBS and data were acquired using flow cytometry. Gating is set using 0 minute time point. There is little to no, non specific binding of APC Isotype to A) $CD14^{+}CD16^{-}$ monocyte subset, B) $CD14^{+}CD16^{+}$ monocyte subset, C) neutrophils or D) lymphocytes.

### 2.3.2 Leukocyte-platelet aggregate detection; analysis using Summit software

Summit version 4.3 was used to analyse the flow cytometry data acquired. The same gating strategy was used for analysing data from each experiment. The monocyte population was defined by size and granularity (**Figure 2-10**), as well as by CD14 and CD16 expression. The gating strategy ensured minimal contamination by other blood cells. Monocytes could then be split into two populations $CD14^{+}CD16^{-}$ (~90% population) and $CD14^{+}CD16^{+}$ (~10% population), (**Figure 2-10**). CD42b and CD14 dual positive staining indicated $CD14^{+}CD16^{-}$ monocyte-platelet aggregate formation (MPA). CD42b and CD16 dual positive staining indicated MPA formation for the $CD14^{+}CD16^{+}$ subset of monocytes. 0 minute (control) was used for applying gates to define dual positive events for both monocyte populations (**Figure 2-10**). The gates were not changed between samples and the percentage MPA for each time point was recorded.

The neutrophil population was defined by size and granularity (**Figure 2-11**). The gating strategy was set to minimise contamination by other leukocytes (**Figure 2-11**). CD42b and CD16

dual positive staining indicated neutrophil-platelet aggregate (NPA) formation. The 0 minute (control) was used for gating on dual positive events (**Figure 2-11**). The gates were not changed between samples and the percentage NPA were recorded for each time point.

The lymphocyte population was defined by size and granularity (**Figure 2-12**). CD42b positive events with the same granularity as lymphocytes indicated lymphocyte-platelet aggregate (LPA) formation. The 0 minute time point was used for gating on CD42b positive events (**Figure 2-12**). The gates were not changed between samples and the LPA were recorded for each time point.

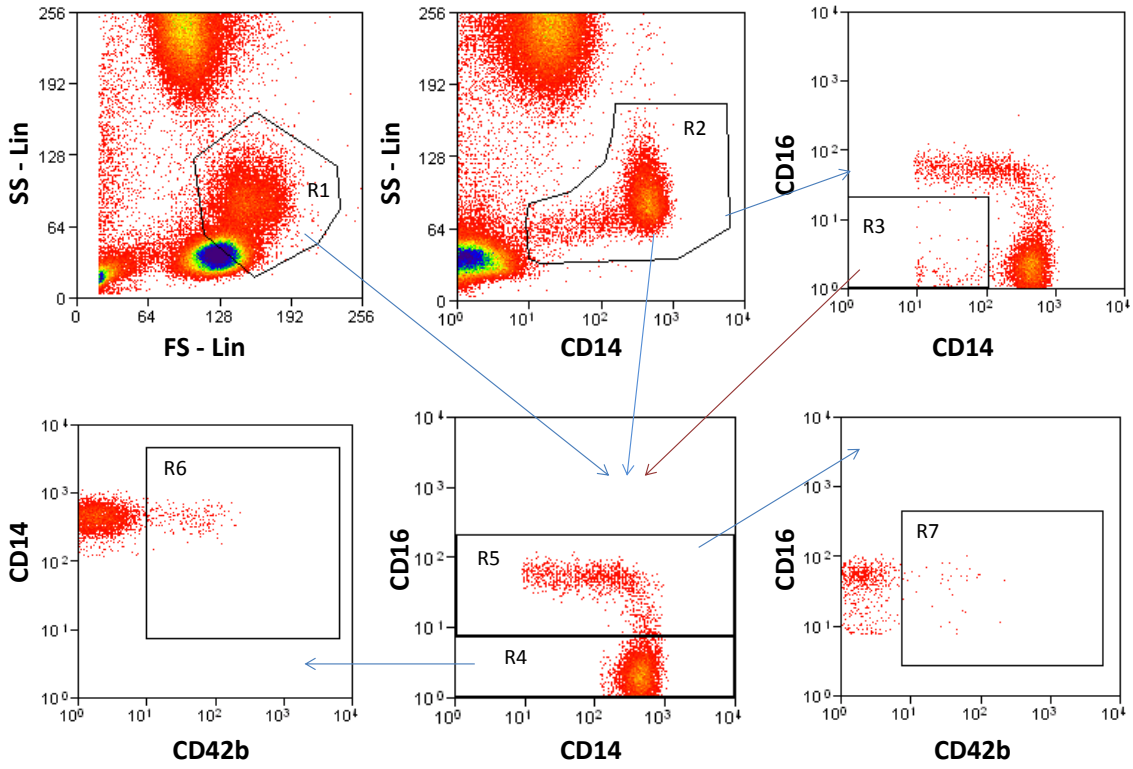


**Figure 2-10: Gating strategy for detecting MPA in lysed whole blood**

Gate R1 defines monocytes by size and granularity (some $CD14^{+}CD16^{+}$ monocytes can be found in the lymphocyte region). Gate R2, monocytes defined by CD14 expression and granularity. Gate R2 is then applied to a CD14 vs CD16 plot (indicated by blue arrow) and gate R3 is set to include events expressing low levels of CD14 and CD16. A combination of gate R1 and R2 and not R3 is used to define the monocyte population (a 'not' gate is indicated by brown arrow). This can subsequently be split into two populations ~90% $CD14^{+}CD16^{-}$ (gate R4) and ~10% $CD14^{+}CD16^{+}$ (gate R5). Gate R4 is then applied to CD42b vs CD14 plot, dual positive expression of both platelet CD42b and monocyte CD14 markers (gate R6) defines a $CD14^{+}CD16^{-}$ monocyte platelet aggregate. Gate R5 is then applied to CD42b vs CD16 plot, expression of both platelet CD42b and monocyte CD16 markers (gate R7) defines a $CD14^{+}CD16^{+}$ monocyte platelet aggregate. (Gating strategy adapted from Shantsila et al., 2011.)

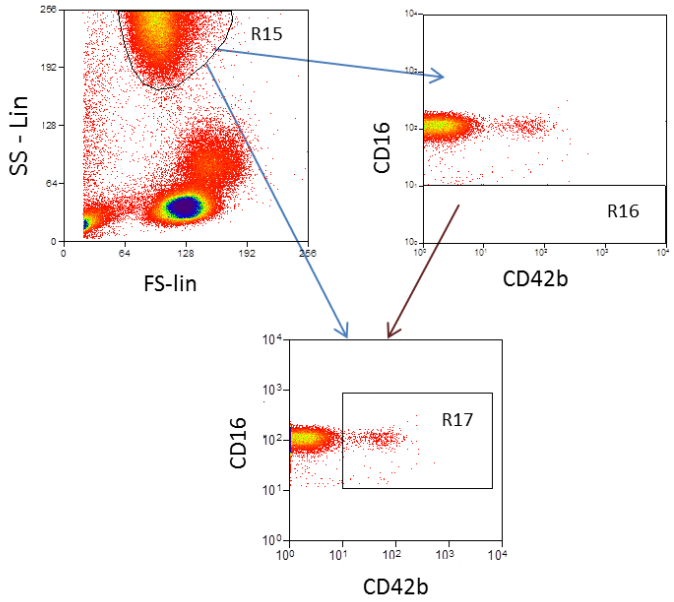


**Figure 2-11: Gating strategy for detecting NPA in lysed whole blood**

Gate R15 defines neutrophils by size and granularity. Gate R15 is then applied to a CD42b vs CD16 plot (indicated by blue arrow) and gate R16 is set to include events expressing low levels of CD16. A combination of gate R15 and not R16 is used to define the neutrophil population (a 'not' gate is indicated by brown arrow). Gate R17 incudes dual positive expression of both platelet CD42b and neutrophil CD16 markers and defines neutrophil-platelet aggregates.

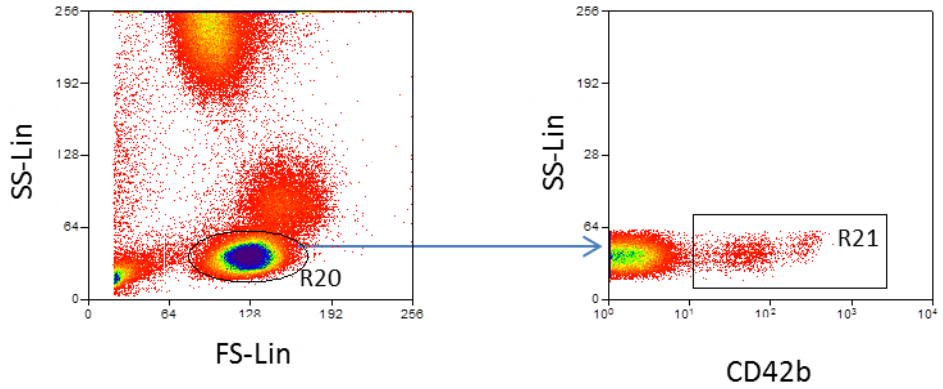


**Figure 2-12: Gating strategy for detecting LPA in lysed whole blood**

Gate R20 defines lymphocytes by size and granularity. Gate R20 is then applied to a CD42b vs ss plot (indicated by blue arrow). Gate R21 includes events which have the same granularity as the lymphocyte population but are positive for the expression of platelet specific CD42b this defines a lymphocyte-platelet aggregate.

### 2.3.3 Determining the level of platelet specific CD42b present on monocytes and neutrophils following treatment of whole blood with a platelet agonist

It was important to establish the MFI of the CD42b being expressed in each leukocyte subpopulation region. This will suggest whether the increase in leukocyte-platelet aggregate formation is likely to be due to leukocytes binding to platelets, or leukocytes adhering to platelet derived microvesicles (PMV). Summit version 4.3 was used to analyse the flow cytometry data acquired. The same gating strategy was used for analysing data from each experiment. Untreated platelets (0 minute) were defined by size and granularity. A gate was set to include 95% of the total platelets expressing CD42b, this was defined as the 'platelet' gate (gate R9 **Figure 2-13D**). A gate was set to include the remaining events this was defined as the 'microvesicle' gate (gate R10 **Figure 2-13D**).

Monocytes were defined using the same gating strategy as before (**Figure 2-10 and Figure 2-14**). To find the CD42b MFI on the $CD14^{+}CD16^{-}$ monocyte population gate R4 (**Figure 2-14**) can now be applied to CD42b histogram with the 'platelet' and 'microvesicle' gates (**Figure 2-14**). (These gates were previously defined in **figure 2-13**.) An increase in events in gate R11 suggests microvesicle accumulation by the $CD14^{+}CD16^{-}$ monocyte subpopulation, whereas events, which occur in gate R12 suggest platelet adhesion to this monocyte subpopulation (**Figure 2-14**). For the $CD14^{+}CD16^{+}$ monocyte subset (gate R5 **Figure 2-14**) can now be applied to the CD42b histogram. An increase in events in gate R13 suggest microvesicle accumulation by the $CD14^{+}CD16^{+}$ monocyte subpopulation, whereas events in gate R14 suggest platelet adhesion to this monocyte subpopulation (**Figure 2-14**). The MFI and percentage events in these gates can be recorded for each subpopulation at each time point. The neutrophil population (defined

by size and granularity as well as CD16 expression) can be analysed using a similar method (**Figure 2-15**).

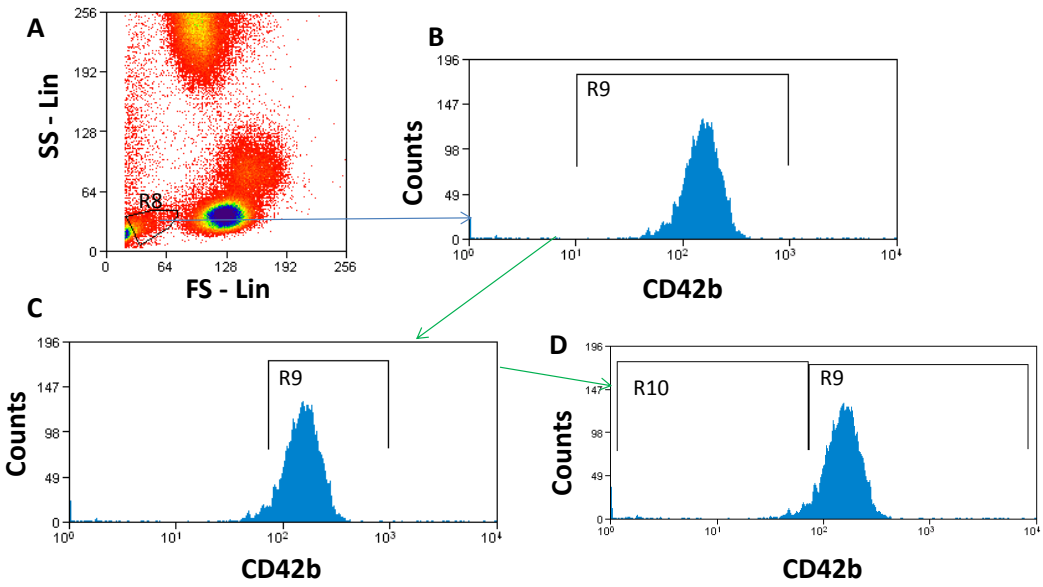


**Figure 2-13: Gating Strategy for Defining 'Platelet' and 'PMV' Gates**

A) Gate R8 defines platelets by size and granularity. B) Gate R8 is applied to a CD42b histogram (indicated by the blue arrow) gate R9 is set to include 100% of the platelet peak. C) Shows the gate moved (indicated by the green arrow) and set to include 95% of the events shown in the original platelet peak. D) shows gate R9 which can now be defined as the platelet gate (95% confidence intervals) and R10 the microvesicle gate.

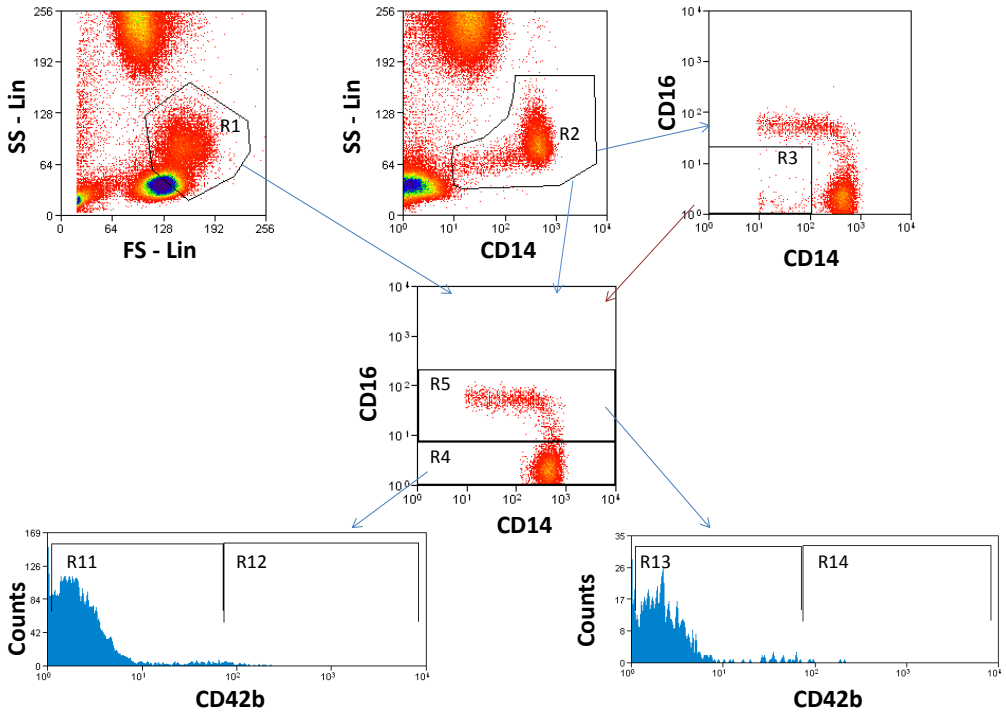


**Figure 2-14: Gating strategy for comparing CD42b MFI in the platelet and PMV gates, for monocyte subsets, following treatment with a platelet agonist**

Gate R1 defines monocytes by size and granularity (some $CD14^{+}CD16^{+}$ monocytes can be found in the lymphocyte region). Gate R2 defines monocytes by their expression of CD14 and granularity, this gate is then applied to a CD14 vs CD16 plot (indicated by the blue arrow). Gate R3 removes events expressing low levels of CD14 and CD16. A combination of gate R1 and R2 and not R3 is used to define the monocyte population (a brown arrow is used to indicate a 'not' gate). Monocytes can be further divided into two subpopulations ~90% $CD14^{+}CD16^{-}$ (gate R4) and ~10% $CD14^{+}CD16^{+}$ (gate R5). Gate R4 can then be applied to a CD42b histogram to show CD42b expression in $CD14^{+}CD16^{-}$ monocyte gate. An increase in CD42b MFI in gate R11 suggests platelet microvesicle accumulation by $CD14^{+}CD16^{-}$ monocytes. An increase in CD42b MFI in gate R12 suggests platelet adhesion to $CD14^{+}C16^{-}$monocytes. Gate R5 can be applied to a CD42b histogram, increases in CD42b MFI in R13 will suggest $CD14^{+}CD16^{+}$ monocytes accumulating platelet microvesicles. Increases in CD42b in gate R14 will suggest platelet adhesion to $CD14^{+}CD16^{+}$ monocytes.

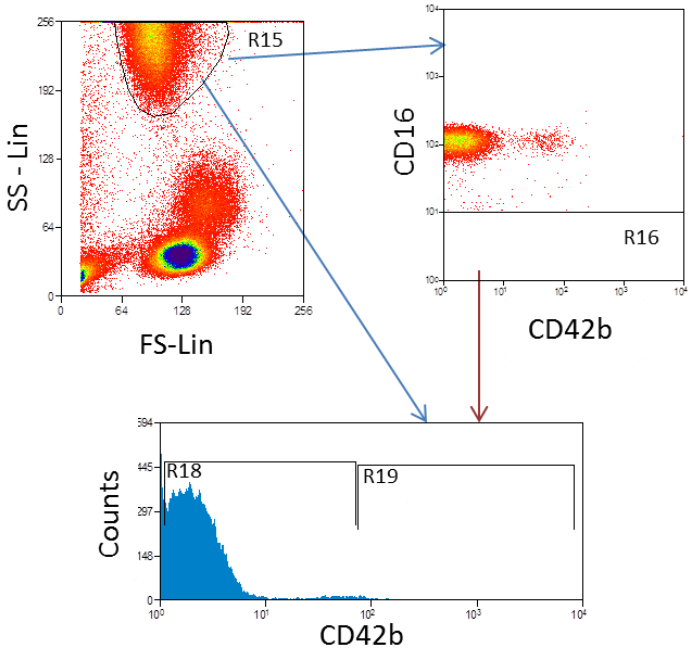


**Figure 2-15: Gating strategy for comparing CD42b MFI in the platelet and PMV gates, for neutrophils, following Treatment with a Platelet Agonist**

Gate R15 defines neutrophils by size and granularity. Gate R15 is then applied to a CD42b vs CD16 plot (indicated by blue arrow) and gate R16 is set to include events expressing low levels of CD16. A combination of gate R15 and not R16 is used to define the neutrophil population (a 'not' gate is indicated by brown arrow). Gate R16 can then be applied to a CD42b histogram to show CD42b expression in the neutrophil gate. An increase in CD42b MFI in gate R18 suggests platelet microvesicle accumulation by neutrophils. An increase in CD42b MFI in gate R19 suggests platelet adhesion to neutrophils.

### 2.3.4 Five minute time course with calf thymus histones to assess the effects on leukocyte-platelet aggregate formation

Samples were processed as previously described except, samples were incubated for between 5s, and 5 minutes at 37°C on a roller mixer following treatment with 1mg/ml calf thymus histones (CTH). For controls a sample was fixed shortly after phlebotomy and an untreated sample was incubated for 5 minutes. Samples were analysed as previously described.

### 2.3.5 Titration of calf thymus histones and histone H4 to assess the effects on leukocyte-platelet aggregate formation

Whole blood samples from healthy volunteers, collected into 10% (v/v) CPDA were incubated for 30 mins at 37°C on a roller mixer with 0.25, 1, 5, 10, 25 100, and 1000µg/ml CTH. Or 1, 5, 10, 25, 100µg/ml recombinant histone H4 (New England Bio Labs). Untreated blood (control) was also incubated for 30 minutes or fixed immediately after phlebotomy. Samples were then processed and analysed as described previously.

### 2.3.6 Identifying leukocyte-platelet aggregates based on P-Selectin expression

Whole blood samples from healthy volunteers, collected into 10% (v/v) CPDA were incubated for 30 mins at 37°C on a roller mixer, either untreated or with 30µM ADP, 100µM TRAP or 1µg/ml CRP-XL. As a control a sample was fixed shortly after phlebotomy (0 minute). However, the master mix of antibodies added on this occasion included PE labelled CD14 antibody, PE-Cy7 labelled CD16, APC labelled CD42b (GPIb) and FITC labelled mouse anti-human P-selectin antibody (**Table 2-2**). An isotype control was prepared at the relevant concentrations (**Table 2-2**). Samples were processed as described previously. On this occasion analysis also included leukocyte-platelet aggregate expression based on P-selectin expression, which used a similar gating strategy to those described in figure 2-12, 2-13 and 2-15, except flow cytometry plots showed (P-selectin instead of CD42b) P-selectin vs CD14, P-selectin vs CD16 and P-selectin vs side scatter for determining $CD14^{+}CD16^{-}$ MPA, $CD14^{+}CD16^{+}$ MPA/NPA and LPA respectively. FITC IgG for each leukocyte is shown in Figure 2-16 (APC IgG is used at the same concentration as previously-figure 2-9).

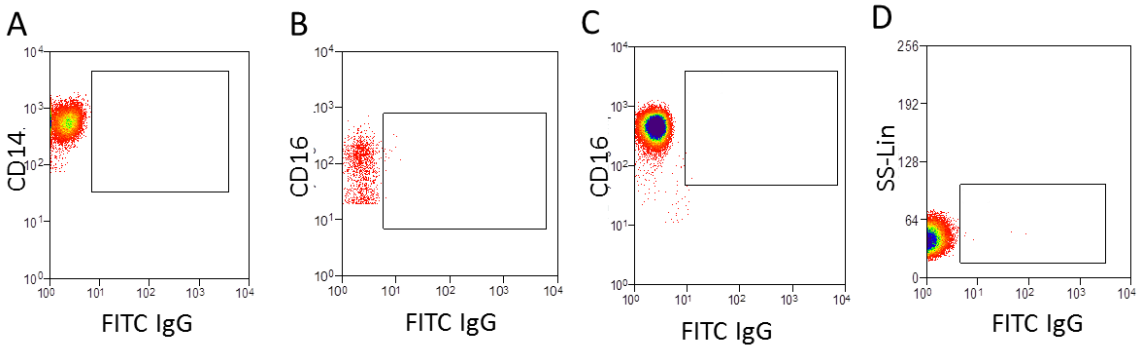


**Figure 2-16: FITC-IgG isotype control**

Whole blood was fixed with 1% (w/v) FA and incubated with CD14 (PE), CD16 (PEcy7) and FITC IgG for 30 minutes before red blood cells were lysed. Leukocytes were suspended in PBS and data were acquired using flow cytometry. Gating is set using 0 minute time point. There is little to no, non specific binding of FITC Isotype to A) $CD14^{+}CD16^{-}$ monocyte subset, B) $CD14^{+}CD16^{+}$ monocyte subset, C) neutrophils or D) lymphocytes.

### 2.3.7 Surface PSGL-1 expression by leukocyte subsets

Whole blood samples from healthy volunteers, collected in 10% (v/v) CPDA were aliquoted into 300µl volumes and incubated for 30 mins at 37°C on a roller mixer either untreated or with, 100µM TRAP or 1µg/ml CRP-XL. As a control a sample was fixed shortly after phlebotomy (0 minute). Samples were processed as described previously. However on this occasion each sample was split in two and a different master mix of antibodies was added to each; 1) APC labelled CD14, FITC labelled CD16 and PE labelled PSGL-1 (**Table 2-2**). 2) PerCP labelled CD3, PEcy7 labelled CD20 and PE labelled PSGL-1 (**Table 2-2**). Data was acquired using a Dako Cyan flow cytometer, a total of $2x10^4$ events were collected in the monocyte gate, lymphocyte gate or neutrophil gate based on the size and granularity of the cells. Summit version 4.3 was used to analyse the flow cytometry data acquired. The same gating strategy was used for analysing data from each experiment (**Figure 2-18-2-20**). Isotype control for each leukocyte subset is shown in figure 2-17.

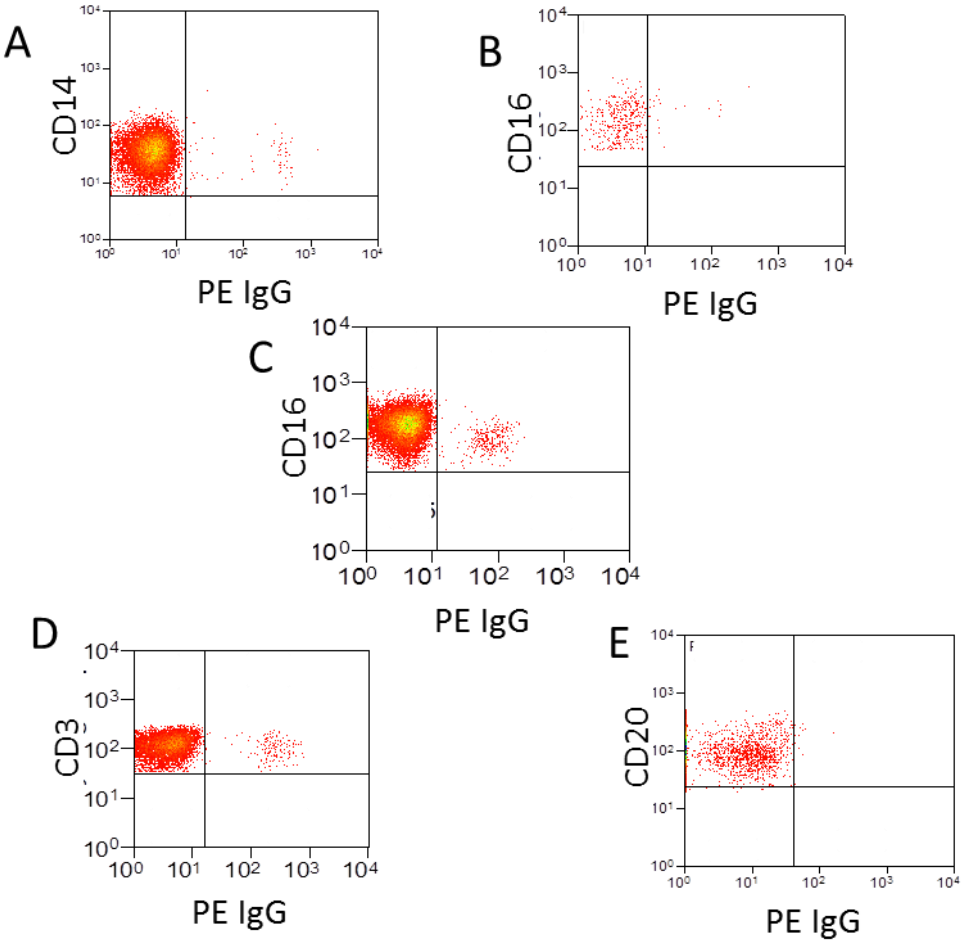


**Figure 2-17: PE IgG isotype for each leukocyte subset**

Whole blood was fixed with 1% (w/v) FA and incubated with; A),B) and C) CD14 (APC), CD16 (PECy7) and PE IgG or D) and E) CD3 (PerCP) CD20 (PECy7) and PE IgG for 30 minutes before red blood cells were lysed. Leukocytes were suspended in PBS and data were acquired using flow cytometry. Gating is set using 0 minute time point. There is little (<2%) to no, non specific binding of PE IgG Isotype to A) $CD14^{+}CD16^{-}$ monocyte subset, B) $CD14^{+}CD16^{+}$ monocyte subset, C) neutrophils, D) T- lymphocytes or E) B-lymphocytes.

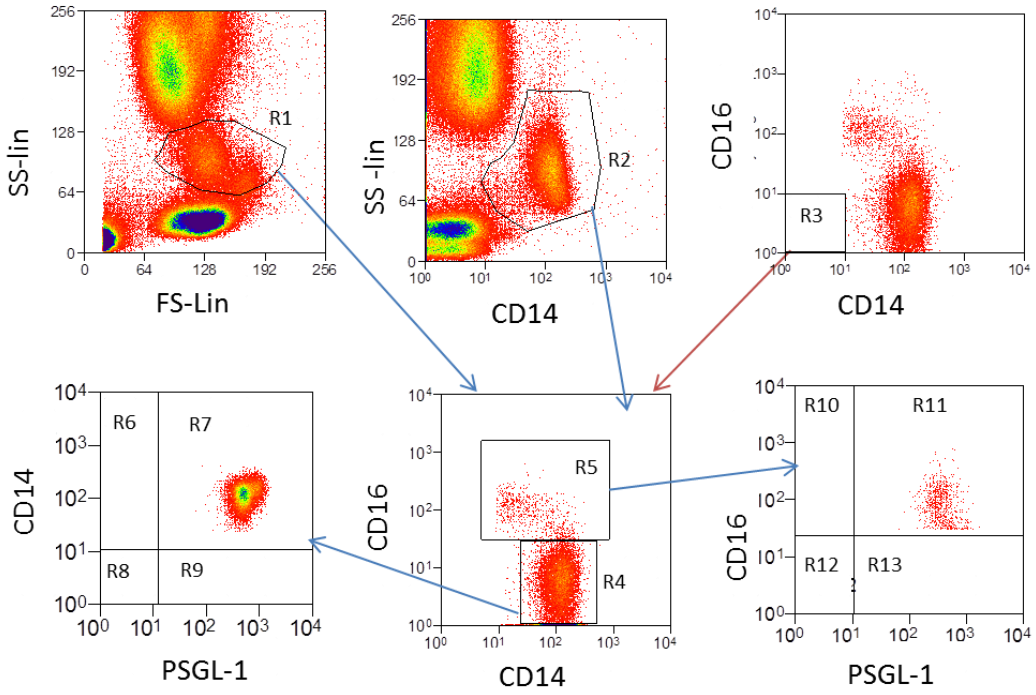


**Figure 2-18: PSGL-1 expression on monocyte subsets**

Gate R1 defines monocytes by size and granularity (some $CD14^{+}CD16^{+}$ monocytes can be found in the lymphocyte region). Gate R2, monocytes defined by CD14 expression and granularity. Gate R2 is then applied to a CD14 vs CD16 plot (indicated by blue arrow) and gate R3 is set to include events expressing low levels of CD14 and CD16. A combination of gate R1 and R2 and not R3 is used to define the monocyte population (a 'not' gate is indicated by brown arrow). This can subsequently be split into two populations ~90% $CD14^{+}CD16^{-}$ (gate R4) and ~10% $CD14^{+}CD16^{+}$ (gate R5). Gate R4 is then applied to PSGL-1 vs CD14 plot the MFI of PSGL-1 and percent positive (gate R7) can be recorded. Gate R5 is then applied to PSGL-1 vs CD16 plot, the MFI of PSGL-1 and percent positive (gate R11) can be recorded for the CD14-CD16+ population.

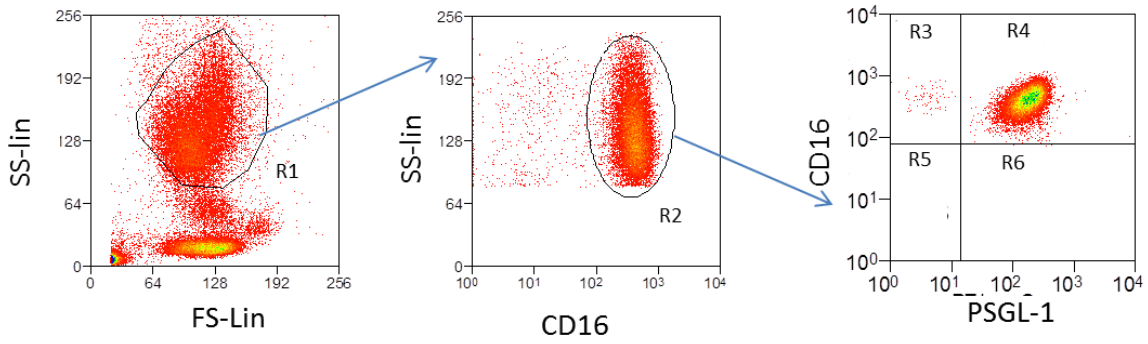


**Figure 2-19: PSGL-1 expression on neutrophils**

Gate R1 defines neutrophils by size and granularity. Gate R2 is then applied to a CD16 vs granularity plot (indicated by blue arrow) and gate R2 is set to include events expressing high levels of CD16. Gate R1 and R2 define the neutrophil population which can be applied to a PSGL-1 vs CD16 plot. The MFI of PSGL-1 and percentage of PSGL-1 positive neutrophils can be recorded (Gate R4)

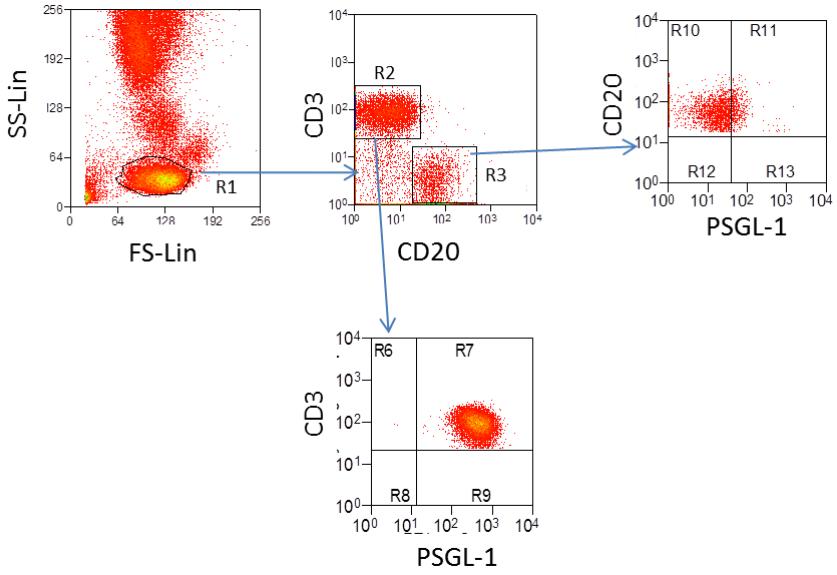


**Figure 2-20: PSGL-1 expression on lymphocyte subsets**

Gate R1 defines lymphocytes by size and granularity. Gate R2 is then applied to a CD3 positive T-cells. Gate R3 is set to include the CD20 positive B-cells. Gate R2 can be set on PSGL-1 vs CD3 and the MFI of PSGL-1 and percentage of PSGL-1 positive T-cells can be recorded (Gate R7). Gate R3 can be set on PSGL-1 vs CD20 and the MFI of PSGL-1 and percentage of PSGL-1 positive B-cells can be recorded (Gate R11).

### 2.3.8 Titration of P-selectin blocking antibody (G1) in whole blood

2.5µg/ml, 5µg/ml, 10µg/ml and 20µg/ml of P-selectin blocking (Cat. No. 252-020 clone G1) antibody (Ancell, USA) was added to 0.3mls blood (collected into 10% v/v CPDA from healthy volunteers). 100µM TRAP was added and samples were incubated at 37°C for 30 minutes. Samples were washed in ice cold 1.7mg/ml EDTA in PBS (to prevent platelet -aggregates forming). Samples were incubated at RT for 20 minutes in the dark, with 1/200 dilution of FITC labelled goat anti-mouse secondary antibody (DAKO cat. no. F0479). Samples were fixed and incubated with APC labelled CD42b antibody for 30 minutes. Red cells were lysed. Data were acquired using Dako Cyan flow cytometer, Summit version 4.3 was used to analyse the data acquired. A gate was set on the platelet population based on size and granularity. A gate was then set to include all CD42b positive events (platelets) the percentage of the CD42b positive platelets expressing P-selectin was recorded and plotted (**Figure 2-21**). ~95% of CD42b positive platelets were P-selectin positive. We decided to use this concentration for blocking experiments.

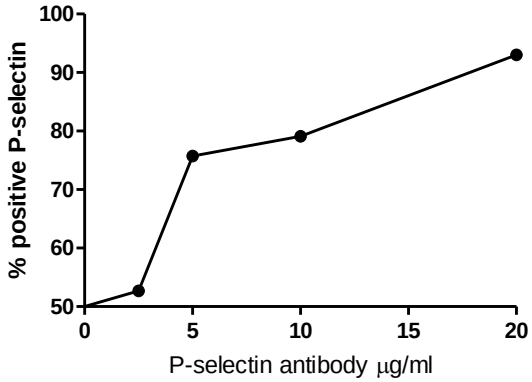


**Figure 2-21: P-selectin blocking antibody (G1) titration**

P-selectin blocking antibody (G1) was titrated on platelets in whole blood. Up to ~95% platelets based on size and granularity and CD42b expression have P-selectin antibody bound.

### 2.3.9 Leukocyte-platelet aggregate formation in the presence of P-Selectin blocking antibody

20µg/ml of mouse anti-human P-selectin blocking antibody (G1) or the same concentration of unlabelled mouse IgG1 (eBiosience Cat. no. 14-4714-82, clone P3.6.2.8.1) was added to 300µL of whole blood (collected into 10% v/v CPDA from healthy volunteers). Other aliquots were left untreated at this point. Following the addition of 30µM ADP, 100µM TRAP, 1µg/ml CRP-XL, or 100µg/ml human recombinant H4 histone, samples were incubated for 30 minutes at 37°C on a roller mixer. An untreated control was fixed shortly after phlebotomy. Samples were then processed and leukocyte-platelet aggregates were analysed as described previously (**Figure 2-10 - 2-12**).

### 2.4.0 Generating monocyte-microvesicle aggregates

### 2.4.1 Isolation of platelet microvesicles.

Platelets were isolated as described previously. Platelets were suspended at a required concentration in 0.15% (w/v) PBSA. 2.5ml of each platelet suspension was incubated with platelet agonists at 37°C for 30 minutes. Samples were split into 2 x 1.25ml aliquots and centrifuged at 2000g for 20 minutes and 13000g for 2 minutes. Supernatants were collected each time. 1ml was stored at -80°C (for further experiments). The remaining 1ml was analysed using Nanosight LM10 version C (Nanosight Ltd) and Nanosight NTA version 2.2 software (Nanosight Ltd). Nanosight software is able to track PMV and calculate the size distribution and concentration of the vesicles present (**Figure 2-22**). To give an accurate measurement the Nanosight must track a minimum of 200 PMV. So this could be achieved the minimum track length was set to 10. This allowed 200 particles to be tracked and caused the least change in mean diameter and concentration/ml compered to auto settings (**Figure 2-23**)

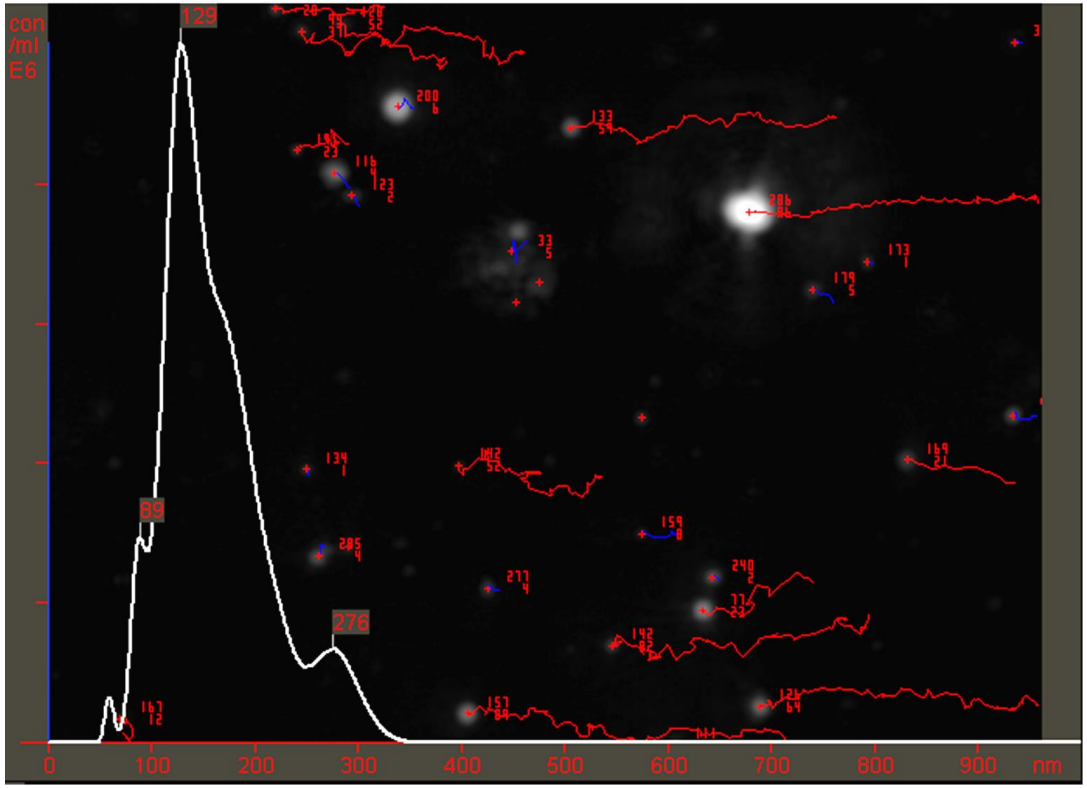


**Figure 2-22: Nanosight tracking**

Demonstrates Nanosight background settings to identify as many microvesicles as possible, with as little background detected as possible, the Nanosight tracks the particles, which allows the number and size of the microvesicles to be determined

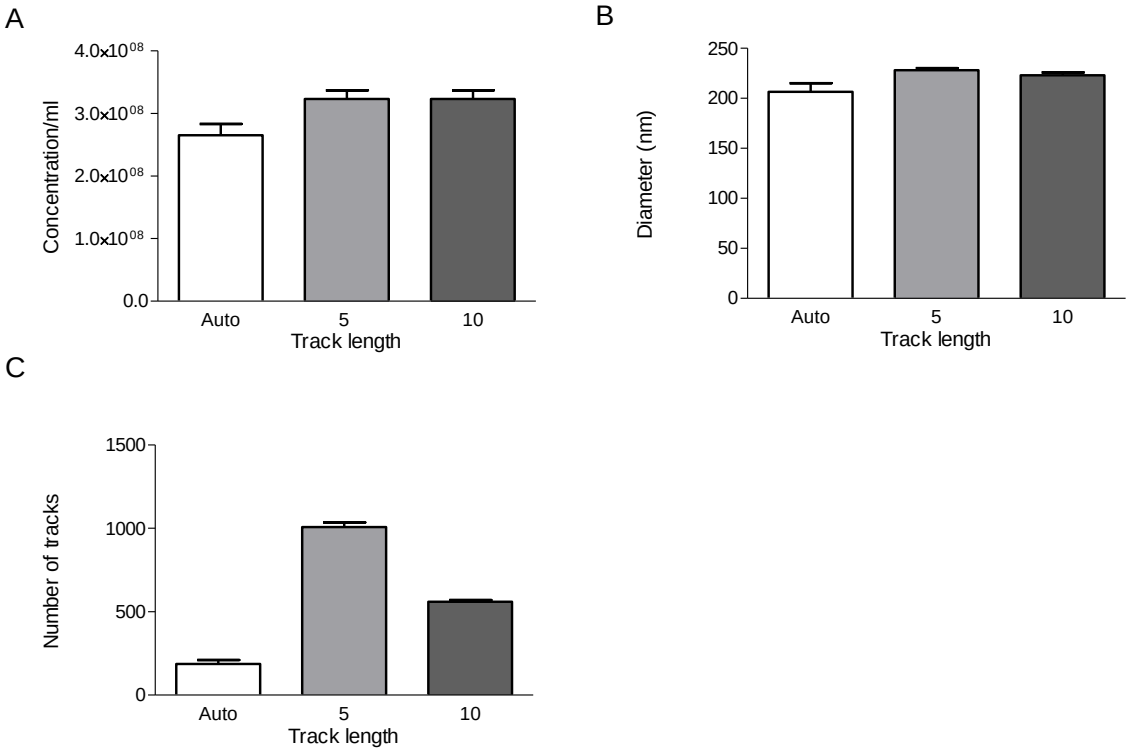


**Figure 2-23: Comparing selected track length for Nanosight analysis**

Microvesicles generated by incubating untreated platelets ($8x10^8$/ml) at 37°C for 30 minutes. A) Demonstrates concentration of PMV detected by Nanosight. B) shows the mean diameter detected by the Nanosight and C) shows the number of tracks detected by the Nanosight. Over 200 tracks need to be detected for Nanosight analysis to be considered accurate. C) shows that less than 200 tracks are detected when the track length is left at auto, when the track length is set to 10 enough tracks are detected and A) and B) show the smallest change in the data compared to auto.

### 2.4.2 Titration of number of platelets for generating microvesicles

Platelets were isolated as previously described. Platelets were suspended in 0.15% (w/v) PBSA (with $Ca^{2+}$ and $Mg^{2+}$) at concentrations of $2x10^8$, $4x10^8$, and $8x10^8$ platelets/ml. PMV were generated as described previously, using 100µM TRAP as the platelet agonist. TRAP was chosen as it appeared to be the strongest agonist in the context of microvesicle generation in whole blood. Data from the Nanosight analysis using $2x10^8$ platelets/ml did not have a high enough

track number for an accurate PMV concentration to be determined. However a higher concentration of platelets appears to lead to a higher number of PMV being generated (**Figure 2-24**).

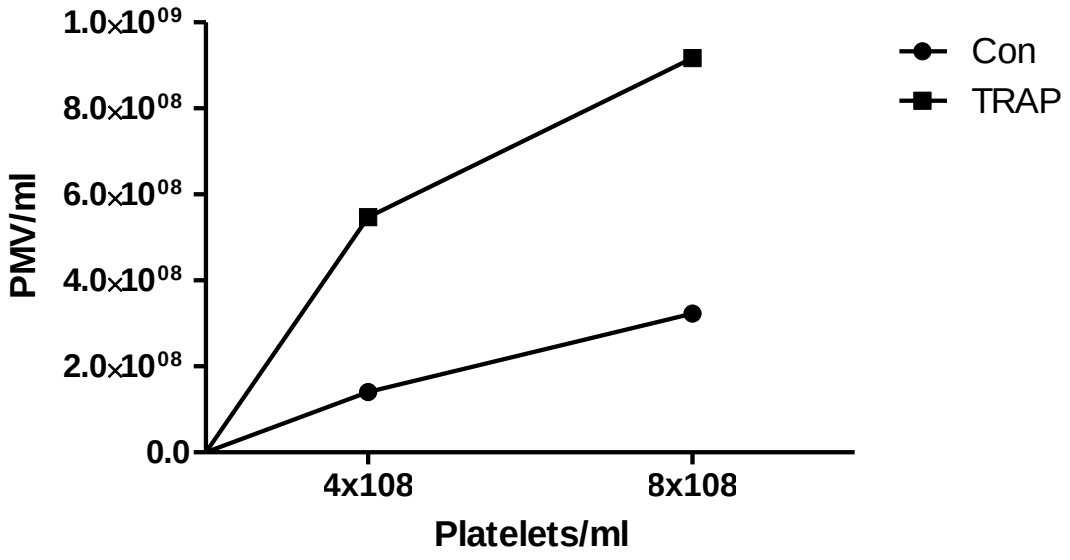


**Figure 2-24: Increasing platelet number and the effect on PMV generation**

Microvesicles generated by incubating isolated washed platelets with 100µM TRAP for 30 minutes at 37°C. An increase in concentration of platelets results in an increase in PMV generation.

### 2.4.3 Comparing platelet agonists in their ability to cause microvesicle generation in washed isolated platelets

Previous data suggested that a higher concentration of platelets lead to more PMV being generated. We decided to use a concentration of $8x10^8$ platelets/ml as this would enable us to generate the most microvesicles. Platelets were isolated as described previously. Platelets were suspended in 0.15% (w/v) PBSA (with $Ca^{2+}$ and $Mg^{2+}$) at a concentration of $8x10^8$ platelets/ml. PMV were generated as previously described using either 100µM TRAP, 1µg/ml CRP-XL, or 10µM

U46619 as platelet agonists. 10µM U46619 and 1µg/ml CRP-XL were used in combination to see if stimulating platelets through two different pathways lead to an increase in the number of platelet microvesicles.

**2.4.4 Monocyte isolation**

Blood from healthy volunteers was collected into EDTA. MACS buffer 2mM EDTA, 0.5% BSA in PBS was prepared. 2.5mls of Histopaque 1077 (Sigma) was layered on top of 2.5mls Histopaque 1119 (Sigma) in a 10ml tube the reconstituted blood was layered on top, this was centrifuged at 1000g for 40 minutes. The histopaque creates a density gradient so that when the blood is centrifuged the RBC (which are heaviest) will collect at the bottom of the tube, the leukocytes will also be separated into two bands. Polymorphic nuclear cells (PMN), the heavier cells, form a band above the red blood cells and the lighter cells which form a band higher up the density gradient which contains peripheral blood mononuclear cells (PBMC). The cells in the top band were collected and suspended in 10 ml MACS buffer. Cells were centrifuged at 200g for 6 minutes at RT (this would allow PBMC cells to pellet but not platelets.) This wash step was repeated. PBMC were then suspended in 1ml of ice cold MACS buffer and washed at 200g at 4°C for 6 minutes.

PMBC were suspended in MACS buffer at a concentration of $10^8$/ml in a total volume of 100µL, containing 20µL of $CD14^+$ beads (MACS Miltenyi). This was incubated on ice for 20 minutes. The wash volume was increased to 1ml with ice cold MACS buffer and PBMC were centrifuged at 500g for 6 minutes at 4°C. PBMC were suspended in 500µL of MACS buffer and put through a prewashed (MACS buffer) MS column (MACS Miltenyi), which is contained within a magnet. The column was washed three times with 500µL of MACS buffer each time. The monocytes will be attached to the $CD14^+$ magnetic beads and remain in the column, the

lymphocytes (and any remaining contaminating platelets) will be washed out of the column. Column was removed from the magnet and flushed with 1ml MACS buffer to isolate monocytes with >95% purity. Monocytes were suspended in 1ml ice cold MACS buffer and centrifuged at 500g for 6 minutes. Monocytes were suspended at desired concentration in 0.15% (w/v) PBSA.

### 2.4.5 Generating monocyte-PMV aggregates

Platelet microvesicles (from healthy volunteers) were generated as previously described. Monocytes (from healthy volunteers) were isolated as previously described. 1ml of PMV (in 0.15% w/v PBSA) were defrosted at RT after storage in -80°C. $1x10^6$ monocytes were suspended in 0.15% w/v PBSA (control) or 1ml of platelet microvesicles, samples were incubated at 37°C for 30 minutes on a roller mixer. Remaining monocytes were fixed for unstained control and single staining to calibrate the flow cytometer. At the end of the incubation period samples were fixed. The following antibodies were added; PE labelled CD14 antibody, FITC labelled CD16, APC labelled CD42b from a previously prepared master mix (**Table 2-2**). Of the immediately fixed aliquots one was left unstained, another was used to prepare an isotype (**Table 2-2**). Samples were incubated for 30 minutes on ice. At the end of the incubation period samples were washed twice in 0.15% (w/v) PBSA at 500g for 5 minutes. Each sample was suspended in 300µl of PBS ready for analysis. Data were acquired using a Dako Cyan flow cytometer, a total of $2x10^4$ events were collected in the monocyte gate based on the size and granularity of the cells. Analysis was carried out as previously described. Figure 2-25 demonstrates there is little to no, nonspecific binding of the Isotype controls to monocytes.

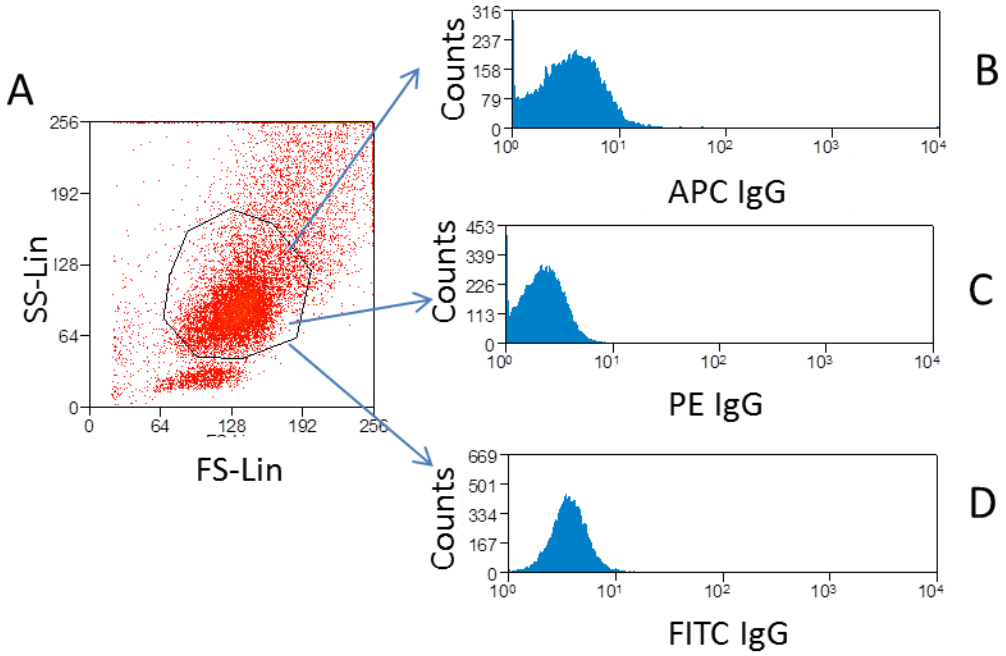


**Figure 2-25: Allophycocyanin IgG isotype with isolated monocytes**

Washed isolated monocytes were incubated with previously isolated platelet microvesicles for 30 minutes at 37°C. Samples were fixed and incubated with IgG isotype antibodies labelled with PE, FITC or APC. A) monocytes defined by size and granularity, B) APC IgG, C)PE IgG and D) FITC IgG.

### 2.4.6 New Nanosight prism

The Nanosight prism was replaced due to the occurrence of unforeseen damage. However, the new prism appeared to have better resolution, which lead to an increase in the number of particles being tracked, and a higher concentration/ml being detected. A sample from the same donor which had been stored at -80°C was analysed using the new Nanosight prism. This was compared to data previously obtained from the old prism. ~4x more particles could now be detected compared to previous data (**Figure 2-26**).

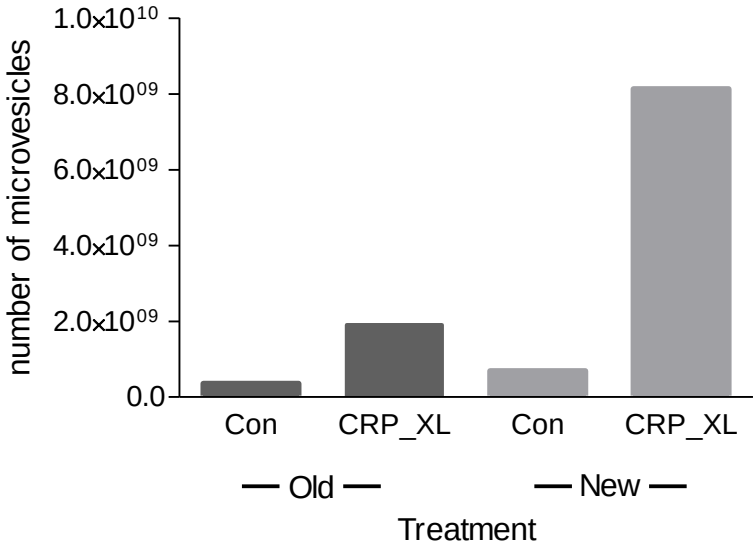


**Figure 2-26: Differences between the new Nanosight prism and the old Nanosight prism**

Microvesicles generated by incubating 2.5ml isolated, washed platelets ($8x10^8$/ml) with 1µg/ml CRP-XL for 30 minutes at 37°C. Each 1ml aliquot was measured using the Nanosight, with the old prism and the new. An increase (~x4) in PMV can be detected with the new prism.

### 2.4.7 APES coating microslides

A small piece of 1mm (diameter) tubing was attached to the end of a glass microslide (1mm x 50mm x 0.1mm W x L x D) this allowed it to be attached to the end of a pipette. The microslide was filled with acetone (Fisher Scientific) which was then expelled. This was done twice. The microslide was filled with 1% (w/v) (3-aminopropyl)triethoxysilane (APES) (Sigma) in acetone and left for 10 minutes, before washing with 1% (w/v) APES and then acetone. Microslides were filled with deonised water and then autoclaved.

### 2.4.8 Flow assay protocol

Previously prepared APES coated microslides were incubated with 100µg/ml human vWf (HTI) at 37°C for 2 hours. At the end of the incubation period slides were incubated for a

minimum of 1 hour with 1% (w/v) BSA (for blocking) or for controls slides were incubated with 1% (w/v) BSA at 37°C for a minimum of 1 hour. In some experiments, slides were incubated with P-selectin blocking antibody (G1) or IgG control for 30 minutes immediately before use.

The glass slide was connected to a Harvard syringe pump, which perfused wash or sample at a wall shear stress of 0.1Pa (**Figure 2-27**). At the other end, the channel was connected to an electronic switching valve (Lee Products, Gerards Cross, UK), which allowed selection from two reservoirs containing sample; monocytes (in some instances monocyte/microvesicle) or wash 0.15% (w/v) PBSA (**Figure 2-27**). Monocytes were perfused for a total of 3.5 minutes. After 1 minute of initiating perfusion, digital images of the experiment were collected every 340ms over a 17s period, for 6 different fields of view on the slide (**Figure 2-27**).

The recordings were analysed with Image-Pro 5.0 software (Media Cybernetics). Phase bright monocytes, which made interactions with vWf of at least 340ms in duration were classed as 'rolling'. Any phase bright monocytes, which were stationary throughout the duration of the 17s recording, were classed as 'adherent' (**Figure 2-28**). Both populations were counted and averaged for 6 fields of view and the percentage of rolling monocytes was calculated. The number of adherent cells/$mm^2$ was calculated using the calibrated microscope field dimensions, to find the surface area of the image of the vWf coated microslides and multiplying by the number of cells counted.

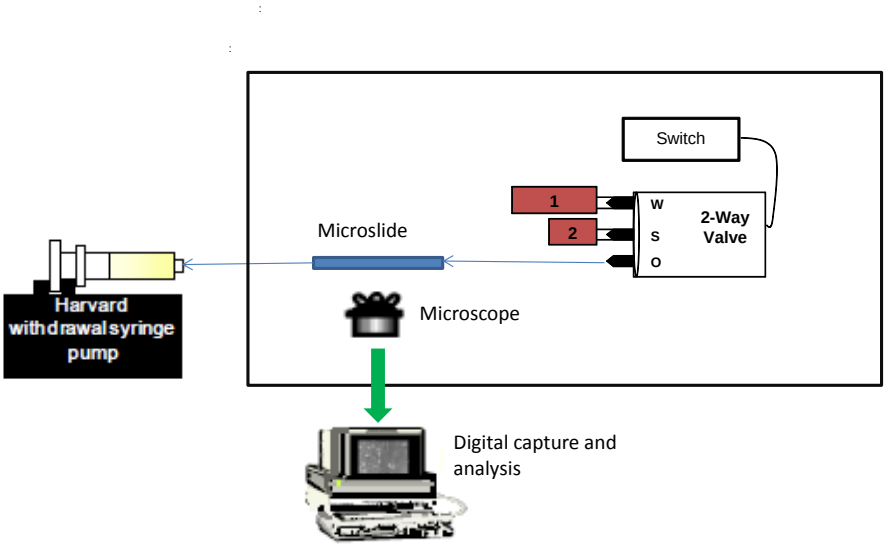


**Figure 2-27: Flow assay setup**

Flow assay was set up as above. The vwf or BSA coated microslide (1mm x50mm x0.1mm, W x L x H) was within a temperature controlled heat box (37°C). Wash buffer (0.15% w/v BSA) was placed in a syringe cut off (1) and sample in syringe cut off (2) both were connected to a two way valve. The appropriate buffer or sample could be perfused by selecting using the two way valve. The outlet of the two way valve was connected to the microslide and the Harvard syringe pump was used to draw the liquid through at a sheer rate of (14.3µL/min). Data was acquired using digital capture.

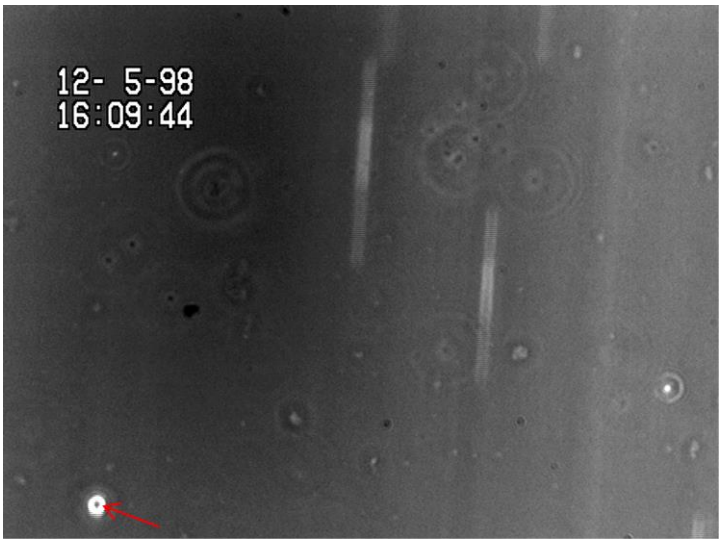


**Figure 2-28: Monocyte interacting with vWf coated slide**

Any phase bright monocytes (indicated by the red arrow), which made interactions with vWf for a minimum of 340ms were classed as 'rolling'.

### 2.4.9 Monocyte adhesion to vWf coated slides

Early experiments indicated that monocytes may be interacting with vWf coated slides. We therefore thought it important to test which flow rate gave minimal, but measurable, interactions. Previously prepared APES coated microslides were incubated with 100µg/ml human vWf (HTI) at 37°C for 2 hours. At the end of the incubation period slides were incubated for a minimum of 1 hour with 1% (w/v) BSA (for blocking).

Monocytes were isolated (from healthy volunteers) as previously described and suspended at $1x10^6$ cells/ml. Using the Harvard syringe pump to control the flow rate monocytes were perfused at a wall shear stress of either 0.05Pa, 0.1Pa, 0.2Pa for a total of 3.5 minutes. 0.1Pa was chosen for as a low level of measurable interactions between monocytes and vWf coated microslides were observed at this shear stress (**Figure 2-29**). Data was acquired and analysed as stated previously.

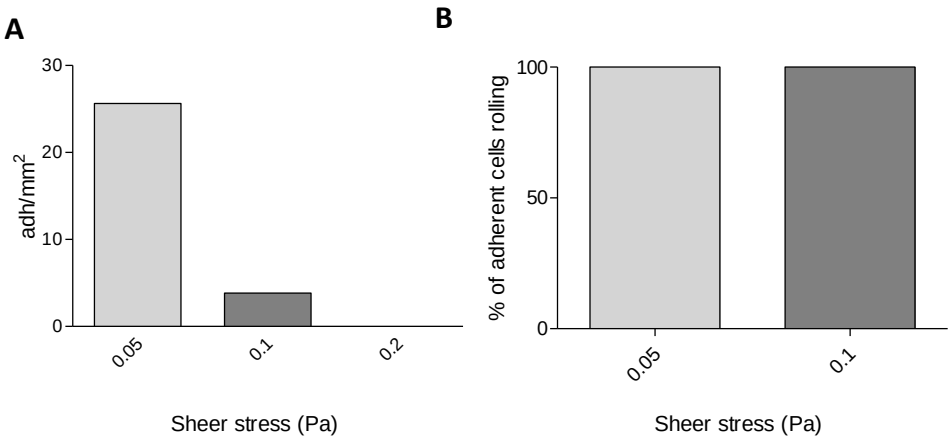


**Figure 2-29: Monocytes perfused over vWf coated microslides at different shear stresses**

Isolated monocytes (mixed subsets) incubated for 30 minutes at 37°C (in the absence of PMV) were perfused across 100µg/ml vWf substrate at wall shear stresses of 0.05Pa, 0.1Pa and 0.2Pa. A) There was a decrease in monocyte capture as shear stress increased. B) 'Rolling' was defined as interaction with the substrate for at least 1 frame (340ms). The majority (>95%) of monocytes that interacted with Vwf 'rolled' along the substrate at either a shear stress of 0.05Pa or 0.1Pa.

### 2.4.10 Monocyte-microvesicle aggregates adhesion to vwf coated microslides

Monocyte-PMV aggregates were generated as previously described. Immediately after the 30 minute incubation period samples were added to the appropriate reservoir. During the 30 minute incubation period vWf coated slides were simultaneously incubated with P-selectin blocking antibody (G1) 20µg/ml or IgG control antibody (eBioscience Cat. no. 14-4714-82, clone P3.6.2.8.1) at the same concentration. Data were acquired and analysed as previously described.

### 2.5.0 Western blot for detection of P-Selectin contamination of vWf

An 8% separating gel was prepared (10ml); deionised Water 4.6ml; 1.5M TRIS (Sigma) pH 8.8 2.5ml; 10% (w/v) SDS (Sigma) 100µl; acrylamide/bis (30%/0.8% w/v) (Geneflow) 2.7ml; 10% (w/v) APS (Sigma) 90µl and TEMED (Sigma) 10µl. Once set, a stacking gel was prepared; deionised water 2.94ml; 0.5M TRIS HCL (Sigma) pH6.8 (1.25ml); 10% (w/v) SDS 50µl; acrylamide/bis (30%/0.8%); 10% (w/v) APS 50µl; and TEMED 10µl. This was layered on top of the separating gel and allowed to set. Two gels were prepared in parallel.

Once set the gels were placed into an electrophoresis rig (Biorad) which was filled with 25mM Tris base and 190mM glyceine (Geneflow), 0.1% SDS dissolved in deonised water. 2x Laemmli buffer was prepared; 20% (v/v) glycerol (Sigma), 10% (v/v) 2-mecaptoethanol (Sigma), 4%(w/v) SDS, 0.004%(w/v) bromophenol blue (Sigma) and 125mM Tris base pH 6.8 (adjusted with HCL). Samples containing 100µg recombinant human P-selectin (R&D systems) or 250µg human vWf were added to an equal volume of Laemmli buffer (40µL: 40µL) and heated to 70°C for 10 minutes. Heating the sample in the presence of 2-mecaptoethanol will break disulphide bonds and denature the protein.

20μL of each sample was loaded on to the gel. Ladder was added to one lane. The gel was left to electrophorese at 200V for 45 minutes. Gels were removed from the tank. One gel was stained with coomassie blue (G250) for 1 hour at RT. This was later left in destain 40% (v/v) methanol (Sigma), 10% (v/v) acetic acid (Sigma) in deoinised water, for 2 hours before being incubated with 25ml instant blue (expedion) for ~1 hour.

The other gel was used for western blotting. Polyvinylidene fluoride (PVDF) membrane (Immobilon) was soaked in methanol for 5s before rinsing in deoinised water for 2 minutes. Stacking gel was removed with a scalpel, before, gel, membrane, filter paper and sponges were equilibrated in pre chilled (4°C) transfer buffer for 15 minutes. (Transfer buffer; 20% v/v methanol, 190mM glycine (Sigma) and 25mM TRIS base.) The gel and membrane were assembled between filter paper and sponges. The protein is negatively charged (due to the SDS) and will move towards the positive electrode, the membrane must be positioned towards the positive electrode to ensure proper transfer of bands. Electrophorese was carried out at 4°C for 1 hour at 100V.

PBS-t was prepared; 0.1% (w/v) tween-20 (Sigma) in PBS. The membrane was removed from the tank and incubated for 1 hour with 20% (w/v) powdered milk (marvel) dissolved in PBS-t. The membrane was washed three times with PBS-t. The membrane was cut in half (each had identical amounts of protein and ladder) one was incubated with 0.1μg/ml sheep anti human P-selectin antibody (R&D systems) in 5ml PBS-t, the other in 5ml PBS-t, at 4°C on a roller mixer. The following day membranes were washed in PBS-t for 10 minutes at RT and rinsed twice in PBS-t. Membranes were then incubated with 20mls PBS-t containing 0.1μg/ml donkey anti-sheep horseradish peroxidase (HRP) conjugated secondary antibody (Abcam) for 1 hour at RT.

Membranes were rinsed three times in PBS-t and then washed for 10 minutes in PBS-t. Following on from this, membranes were incubated with ECL detection mix (GE healthcare) for 5 minutes at RT. ECL is the susbstrate for HRP and allows for its detection on photographic film (Amersham). Membranes were detected on photographic film following a 10s exposure.

**2.6.0 Statistics**

Data are expressed as mean ± standard deviation (SD) or standard error of the mean (SEM). Data have been analysed using Prism software, using one or two-way ANOVA followed by Dunnett's, Bonferroni's or Tukey's multiple comparisons, post-test; and t-test for normal Gaussian distributions.

# 3. Chapter 3- PLATELET ADHESION TO GLOMELULAR ENDOTHELIAL CELLS UNDER PROINFLAMMATORY CONDITIONS

### 3.1.0 Introduction

The kidneys have several functions, which include blood pressure regulation and retaining electrolyte balance. However, the role they are best known for is within the urinary system, where they filter the blood to remove waste products and produce urine. The main apparatus involved in filtration of the blood, the glomerulus, requires a specialised structure to be able to carry out this role (White, 2012).

A specialised ball of capillaries forms the glomerular filter (White, 2012). It consists of glomerular endothelial cells (GEnC) surrounded by epithelial cells, known as podocytes (White, 2012). Between these cells is a glomerular basement membrane (GBM), synthesised by both cell types. Together these make up the glomerular filtration barrier (GFB) (St John and Abrahamson, 2001). The glomerulus is surrounded by the Bowman's capsule (space), which collects the waste products, which pass through the GFB (Miner, 2011). The waste, which eventually forms urine, then passes into the proximal convoluted tubule and towards the ureters and into the bladder, from where it is later excreted from the body (White, 2012).

GEnCs are a specialised type of endothelial cell, which contain fenestrations, 60-80nm wide (Satchell, 2004). These fenestrations are wide enough to allow water and waste products such as urea to pass through. However, they are covered in a negatively charged glycocalyx, 200-400nm thick, which helps to prevent large proteins passing through the vessel wall (Satchell, 2004). Specialised epithelial podocytes, wrap around the glomerular vessel, protruding foot like projections, which make contact with the GBM (Miner, 2011). The spaces between these projections form slit diaphragms, which allow the passage of waste products into the Bowman's capsule (Welsh and Saleem, 2010). Podocytes are known to produce angiopoietin (ang1) and vascular endothelial growth factor (VEGF), (Satchell, 2004). Glomerular endothelial cells express

the corresponding receptors for these agents, Tie2 and VEGFR2, suggesting that podocytes are able to regulate the functional phenotype of GEnCs. When GEnC monolayers were treated with ang1 an increase in transepithelial electrical resistance (TEER) of up to 11.4$\Omega cm^2$ was observed (Satchell, 2004). *In vivo* a reduction in permeability would prevent proteins passing across the GBM (Satchell, 2004). This demonstrates evidence of cross talk between the two cell types.

If damage occurs to the GFB then it may become 'leaky' allowing larger proteins to pass into the urine (Menon and Valentini, 2010). Over time, the worsening damage will result in complete loss of function of the GFB so it is no longer able to filter the blood (White, 2012). This will have severe effects on health and will lead to a patient needing kidney dialysis for the remainder of their life, unless a suitable kidney donor becomes available. The glomerulus is a specialised microvascular capillary bed, which has a large volume of blood pass through it and the structure of the glomerulus makes it particularly vulnerable to inflammatory disease (White, 2012; Passerini et al., 2004). Inflammation of the glomerulus is known as glomerulonephritis, of which there are many causes. It is thought that platelet adhesion to GEnC could have an important role early in disease development. Mouse models have shown that platelets are recruited to GEnC after mice have been administered with anti-GBM antibody (Devi et al., 2010). P-selectin expressed by activated platelets has been shown to aid leukocyte recruitment in this model (Devi et al., 2010).

Earlier work carried out by Tull et al., (2006) using a co-culture system, involving secretory phenotype SMC and HUVEC demonstrated that these SMC, associated with the inflammatory disease atherosclerosis, could prime EC to capture platelets. SMC signalling through TGF-β leads to the release of vWf from EC, so it can be expressed on the surface of the EC and form a matrix. Platelets are known to be able to bind to vWf through interactions firstly

with CD42b, allowing platelet capture from flow and platelet rolling. Then upon platelet activation, through $\alpha_{IIb}\beta_3$ integrin firm adhesion can occur. Platelets have also been shown to play an important role in leukocyte capture in this model (Kuckleburg et al., 2011). This implies they may have an important role in early development of an inflammatory disease more generally. The co-culture methods previously used to study the interaction between SMC and HUVEC, can be used to replicate the renal glomerular environment, as GEnC and podocytes can be co-cultured in the same way. This would allow investigation into how the cells of the glomerulus interact during inflammatory episodes.

The hypothesis for this project is that GEnC will capture platelets using a mechanism involving a vWf matrix forming on the cell surface. Platelets adherent to GEnC will aid in leukocyte capture, through surface P-selectin expression. Cross talk with podocytes will down regulate platelet adhesion and therefore leukocyte capture. The aims for this study were to investigate:

1) If cell line GEnC retained endothelial cell properties and markers

2) If platelets can adhere to GEnC under proinflammatory conditions

3) If antibodies against platelet receptors CD42b and $\alpha_{IIb}\beta_3$ inhibit platelet adhesion to GEnC

4) If inhibiting platelet activation through ADP receptors depletes platelet adhesion to GEnC

5) If GEnC are able to capture platelets under flow conditions

6) If podocytes regulate platelet adhesion to GEnC.

### 3.2.0 Methods

### 3.2.1 Immunocytochemistry to detect the presence of vWf

Cell line GEnC, cell line podocytes or HUVEC were seeded in a chamber slide with between $1x10^4$ and $4.8x10^4$ cells/well, they were left overnight at 37°C. GEnC were either untreated or treated with 100U TNFα and 10ng/ml TGFβ for 24 hours. Cells were fixed with either (i) 2% (w/v) FA for 10min (for surface detection of vWF) or (ii) 2% (w/v) FA for 5 min followed by 1% (w/v) triton for 10mins. This was followed by incubation with 2% (w/v) PBSA blocking solution for 30 minutes. Then incubation with either FITC labelled, sheep antihuman vWf antibody or FITC labelled sheep IgG isotype control antibody in 2% (v/v) FCS, 1% (w/v) PBSA for 1 hour. After, cells were treated with 1μg/ml Hoechst component trihydrochloride to stain the nucleus. Images were taken using a fluorescent invert microscope (Olympus IX71) and Image Pro software. For further details see methods section 2.1.1 and 2.1.4.

### 3.2.2 Platelet adhesion to GEnC monolayers under static conditions

A 24 well plate was coated with 1% (w/v) gelatine diluted using PBS. GEnC were seeded at a concentration of $1x10^5$ cells per well and left at 33°C until confluent. They were then left at 37°C overnight before 24 hour treatment with TNF (100U) or TGF (10ng/ml) in EGM2-MV media or both cytokines in combination (at the same concentrations). Control wells had EGM2-MV media changed.

Platelets were isolated and suspended at a concentration of $2x10^8$/ml in theophylline buffer and stained with 5μg/ml calcein. Platelets were washed twice before being suspended at a concentration of $2x10^8$/ml in 20% (v/v) autologous platelet poor plasma 80%(v/v) M199 (without phenol red) containing 0.15% (w/v) BSA. Platelets were either left untreated or treated

with 10μM ADP. 300μL of platelet suspension containing $6x10^7$ platelets were added to each well, GEnC were incubated for 1 hour at 37°C. Cells were fixed by the addition of 1% (w/v) FA. Cells were washed and images were taken using fluorescent invert microscope (Olympus IX71). Analysis was carried out using Image Pro (Image Pro Express software) and graphpad prism version 5.0. For further details see methods 2.1.5-2.1.7.

### 3.2.3 Flow cytometry for detection of GEnC cell markers

Cell line podocytes were differentiated for one week at 37°C, and cell line GEnC batch 2 were left at 37°C for five days to ensure complete removal of the temperature sensitive SV40LT virus. These cells, along with primary HUVEC, were seeded into 24 well plates and grown to confluence. For detection of ICAM-1 or PECAM-1 cells were treated with 100U TNFα for 4 hours. For detection of E-selectin cells were treated with 1000U TNFα for 4 hours. For detection of internal vWf cells were left untreated.

For ICAM-1 and PECAM-1 detection, cells were removed from the plate using 0.005g trypsin in 0.02% (w/v) EDTA and washed in ice cold 2% (w/v) PBSA. Cells were incubated on ice with APC labelled ICAM-1 or PE-labelled PECAM-1 or relevant isotype controls for 40 minutes before fixing with 2% (w/v) FA. For E-selectin detection, cells in a 24 well plate were incubated on ice with unlabelled anti human E-selectin for 30 minutes, wells were washed and cells were incubated with FITC labelled polyclonal goat anti-mouse antibody. Following this incubation, cells were removed from the plate using cell dissociation buffer and transferred to flow cytometry tubes. Cells were fixed using 2% (w/v) FA and washed in PBSA before data were acquired using flow cytometry.

For detection of internal vWf, cells were removed from the plate using 0.005g trypsin in 0.02% (w/v) EDTA and washed in PBS containing 5% (v/v) FCS. Cells were suspended in

Invitrogen fix and perm medium A for 15 minutes in the dark. Cells were then washed again, before being suspended in medium B, containing either FITC labelled vWf antibody or relevant isotype control. After a 40 minute incubation, cells were washed in PBS containing 5% (v/v) FCS, suspended in PBS and data were acquired using flow cytometry. For further details see methods section 2.1.8.

### 3.3.0 Results

#### 3.3.1 Batch 1 cell line GEnC retain endothelial morphology

Before assays studying platelet adhesion to GEnC could be carried out, it was important to confirm that GEnC (batch 1) expressed vWf, as previous data from our lab indicates that this is an important part of the mechanism involved in EC capture of platelets (Tull et al., 2006). Figure 3-1A, shows the characteristic string like appearance of vWf on the cell surface after 24 hour treatment, with 100U TNFα and 10ng/ml TGFβ. Figure 3-1B, demonstrates total vWf expression of GEnC, including both the vWf present in Weibel Palade bodies; the GEnC internal stores, as well as the string like surface vWf. Figure 3-1C and 3-1D confirm there is minimal nonspecific binding to either the surface or internal stores of vWf by an appropriate isotype control. This demonstrates that cell line GEnC (batch 1) express vWf, confirming they are endothelial cells and retain this EC property.

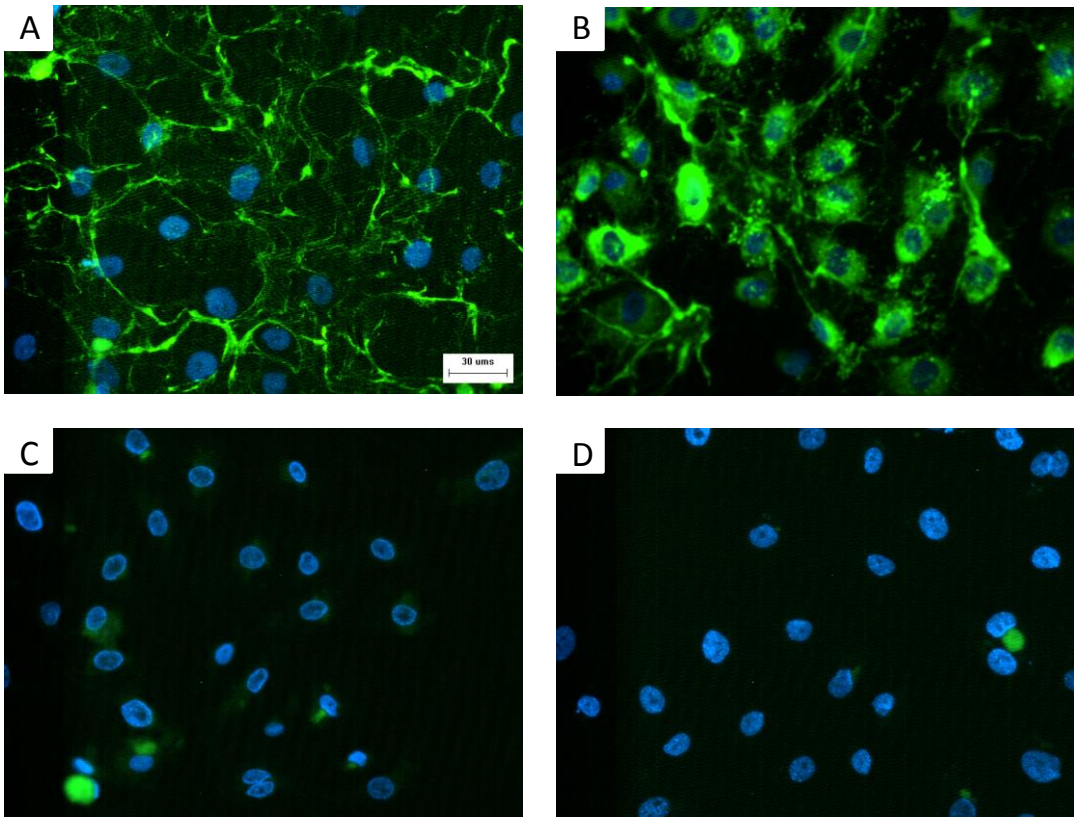


**Figure 3-1: Expression of endothelial cell marker vWF by batch 1 GEnC**

GEnC were cultured at 33°C until confluent monolayers formed, the cells were then incubated at 37°C overnight to remove the temperature sensitive simian virus 40 large tumour antigen and prevent further growth. For surface detection of vWf A) and C) GEnC were treated for 24 hours with 100U/ml TNFα and 10ng/ml TGFβ before fixing with 2% (w/v) formaldehyde. For detection of total von Willebrand factor (vWf), B) and D) cells were left untreated before fixing with 2% (w/v) formaldehyde, followed by 1% (w/v) triton. A) and B) have been incubated for 30 minutes with FITC labelled sheep anti-human vWf antibody, C) and D) with sheep anti-human Isotype control (green). All have been treated with 0.1% (v/v) Hoescht nuclear stain (blue). A) demonstrates the characteristic sting like surface expression of vWf associated with inflammation. B) shows GEnC total vWf including both surface expressed and within internal stores (Weibel Palade bodies). C) and D) confirm there is minimal nonspecific binding of isotype control to either the surface or internal stores of vWf. Scale bar represents 30µm.

### 3.3.2 Platelet adhesion to batch 1 GEnC in the presence of coagulation

Calcein stained platelets can be detect using fluorescent microscopy. This staining technique can be applied to detect platelet adhesion to confluent (unstained) GEnC monolayers. The size of the aggregates and the number of (individual) platelets or platelet aggregates adhering can also be determined. No additional heparin was added to the final platelet suspension for experiments represented by figures 3-2 - 3-8, meaning that these experiments have been done in the presence of coagulation. A significant increase in percentage platelet coverage (~12%) is observed after GEnC treatment with TNFα & TGFβ, but not with TGFβ alone (**Figure 3-2, 3-3 and 3-4**). Treatment of platelets with ADP had no significant effect on percentage platelet coverage, for both untreated GEnC and TNFα and TGFβ treated GEnC (**Figure 3-4**). This data demonstrates that treatment of the endothelium is responsible for an increase in platelet adhesion, rather than platelet activation.

As platelets may adhere to GEnC as individual platelets or platelet aggregates, in order to count the number of either of these adhering to the GEnC monolayer we have used the term 'particles' throughout this chapter to describe this. Neither GEnC treatment with TGFα, TNFα & TGFβ, or platelet treatment with ADP had a significant effect on the number of particles adhering to GEnC (**Figure 3-5 and 3-6**). However, there is a significant increase in the size of the platelet aggregates forming after treatment with TNFα and TGFβ (~40μm) but not TGFβ alone (**Figure 3-7**). There is also a significant increase in the size of the platelet aggregates forming after platelet treatment with ADP (**Figure 3-8**). GEnC treatment and platelet treatment combined leads to aggregates ~100μm, together figure 3-5, 3-6, 3-7 and 3-8 indicate that the increase in percentage platelet coverage of GEnC is due to larger aggregates forming rather than an increase in the number of individual platelets.

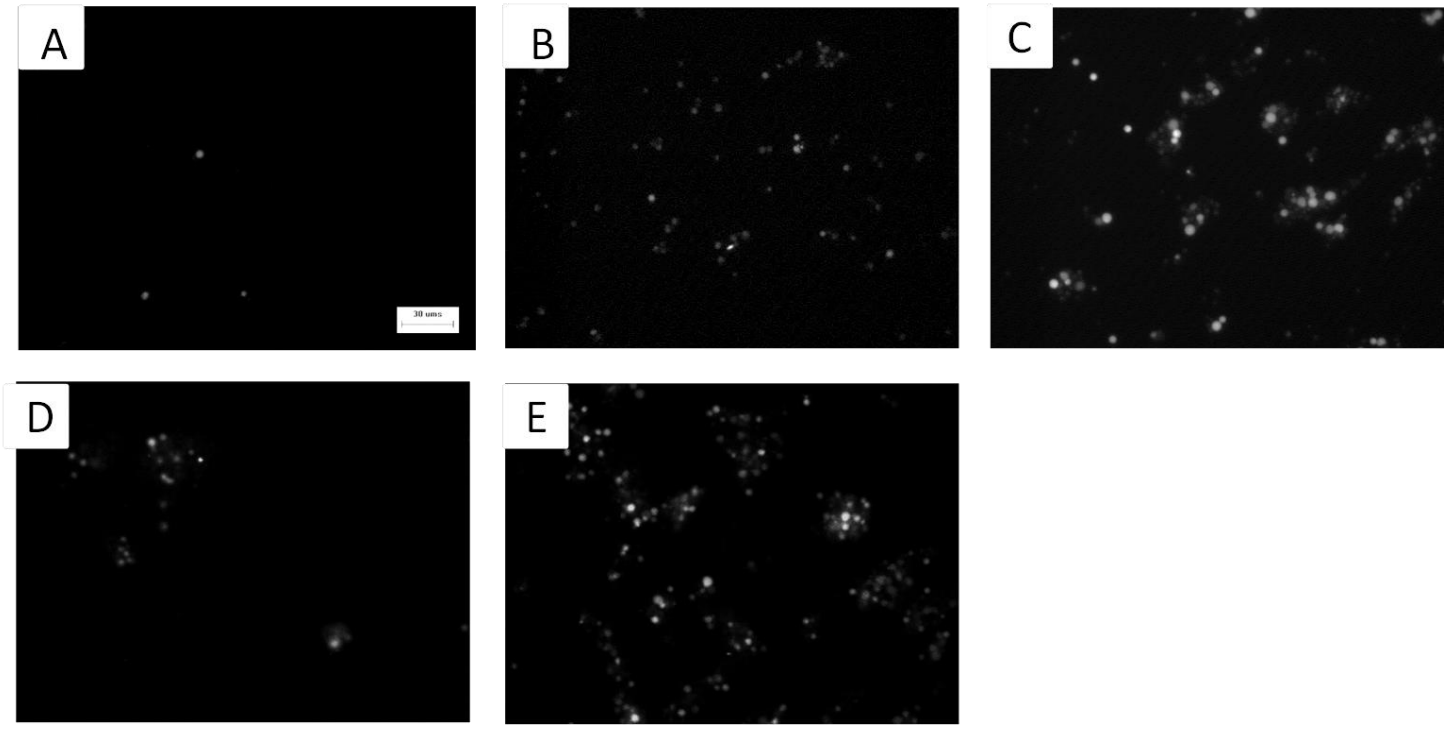


**Figure 3-2: Platelet adhesion to GEnC in the presence of fibrin deposition**

Confluent monolayers of GEnC were incubated at 37°C overnight to remove the temperature sensitive simian virus 40 large tumour antigen and prevent further growth. GEnC were then treated with 10ng/ml TGFβ, both 100U/ml TNFα and 10ng/ml TGβ or left untreated overnight at 37°C. GEnC were then incubated with washed, isolated platelets stained with 5µg/ml calcein (suspended in 20% v/v PPP, 80% v/v M199 medium), which were either untreated or treated with 10µM ADP, for 1 hr. Cells were fixed with 1% (w/v) formaldehyde and washed three times with PBS before images were acquired with Olympus IX71 fluorescent invert microscope and image pro 6.3. Figure 3-2 demonstrates an example of platelet adhesion to GEnC monolayers, A) untreated (control), B) TGFβ C) TNFα & TGFβ, D) untreated EC and ADP treated platelets and E) TNFα and TGFβ treated GEC and ADP treated platelets. Scale bar represents 30µm.

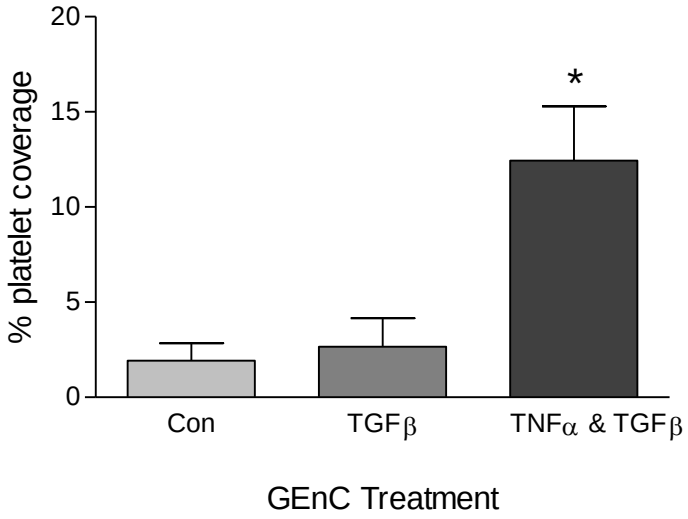


**Figure 3-3: The effects of TNFα and TGFβ on platelet adhesion to GEnC**

Confluent monolayers of GEnC were incubated at 37°C overnight to remove the temperature sensitive simian virus 40 large tumour antigen and prevent further growth. GEnC were then treated with 10ng/ml TGFβ, both 100U/ml TNFα and 10ng/ml TGβ or left untreated overnight at 37°C. GEnC were then incubated with washed, isolated, platelets (suspended in 20% v/v PPP, 80% v/v M199 medium), which had been stained with 5μg/ml calcein, for 1 hr. Cells were fixed with 1% (w/v) formaldehyde and washed three times with PBS before images were taken using Olympus IX71 fluorescent invert microscope. Data were analysed using image pro-software. One way ANOVA ($P<0.05$) indicates that EC treatment has an effect on platelet adhesion. There is a significant increase in platelet adhesion to GEnC following GEnC treatment with TNFα & TGFβ compared to untreated control. *,** and *** indicate $P<0.05$, $P<0.01$ and $P<0.001$ respectively, post hoc test Dunnett's. Data are mean +/- SEM of 2-3 experiments.

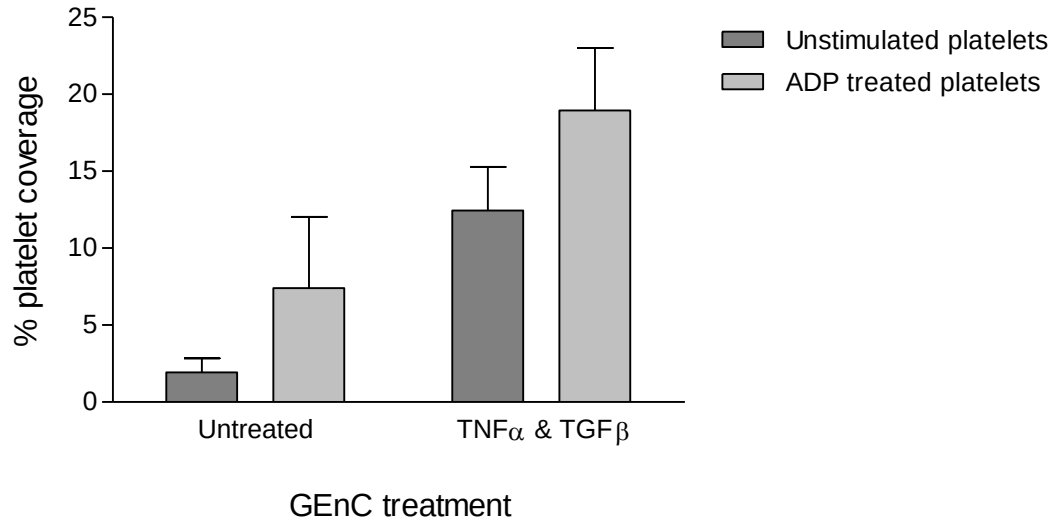


**Figure 3-4: The effects of ADP treatment of platelets on their adhesion to GEnC**

Confluent monolayers of GEnC were incubated at 37°C overnight to remove the temperature sensitive simian virus 40 large tumour antigen and prevent further growth. GEnC were then treated with both 100U/ml TNFα and 10ng/ml TGβ or left untreated overnight at 37°C. GEnC were then incubated with washed, isolated platelets (suspended in 20% v/v PPP, 80% v/v M199 medium), stained with 5µg/ml calcein, which, were either not activated or incubated with 10µM ADP for 1 hr. Cells were then fixed with 1% (w/v) formaldehyde and washed three times with PBS, before images were taken using Olympus IX71 fluorescent invert microscope. Data were analysed using image pro-software. Two-way ANOVA indicates that GEnC treatment with TNFα & TGFβ has a significant effect on increasing percentage platelet coverage ($P<0.05$) post hoc test Bonferroni not significant. However platelet treatment with ADP has no effect (ANOVA ns). Data are mean +/- SEM of 2-3 experiments.

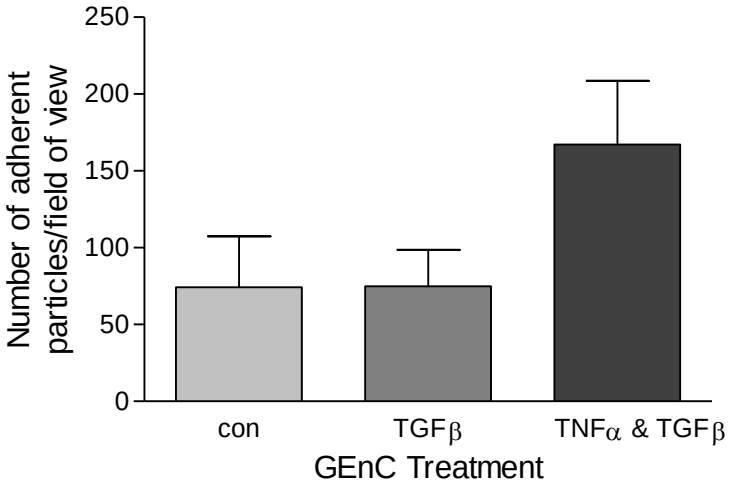


**Figure 3-5: The effects of TNFα and TGFβ on the number of fluorescent particles detected on GEnC**

Confluent monolayers of GEnC were incubated at 37°C overnight to remove the temperature sensitive simian virus 40 large tumour antigen and prevent further growth. GEnC were then treated with 10ng/ml TGFβ, both 100U/ml TNFα and 10ng/ml TGβ or left untreated overnight at 37°C. GEnC were then incubated with washed, isolated, platelets (suspended in 20% v/v PPP, 80% v/v M199 medium), stained with 5μg/ml calcein, for 1 hr. Cells were fixed with 1% (w/v) formaldehyde and washed three times with PBS, before images were taken using Olympus IX71 fluorescent invert microscope. Data were analysed using image pro-software. ANOVA (ns) indicates that GEnC treatment does not affect the number of platelets or platelet aggregates (particles) adhering. Data are mean +/- SEM of 2-3 experiments.

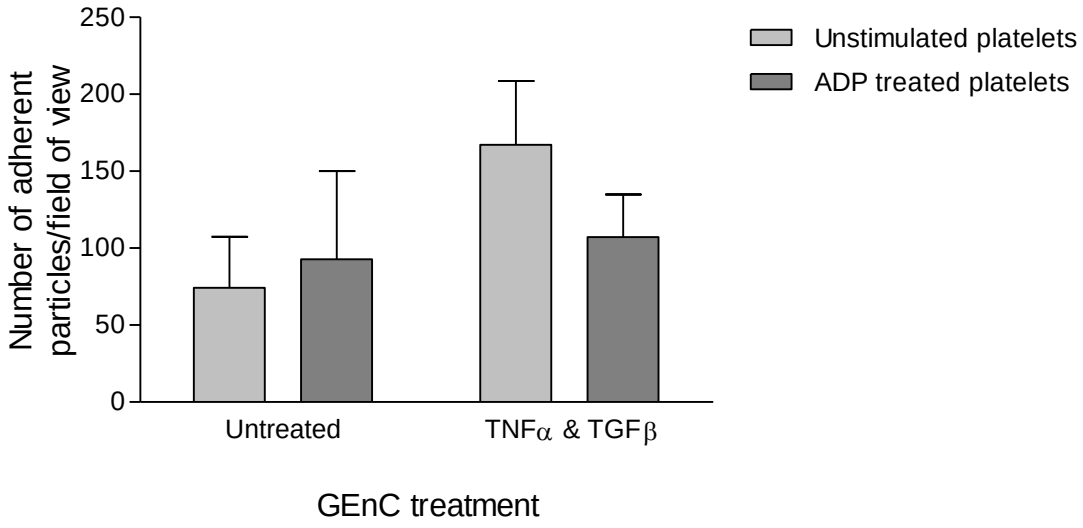


**Figure 3-6: The effects of ADP on the number of fluorescent particles detected on GEnC**

Confluent monolayers of GEnC were incubated at 37°C overnight to remove the temperature sensitive simian virus 40 large tumour antigen and prevent further growth. GEnC were then treated with both 100U/ml TNFα and 10ng/ml TGβ or left untreated overnight at 37°C. GEnC were then incubated with washed, isolated platelets, (suspended in 20% v/v PPP, 80% v/v M199 medium), stained with 5µg/ml calcein, which, were either not activated or incubated with 10µM ADP for 1 hr. Cells were then fixed with 1% (w/v) formaldehyde and washed three times with PBS, before images were taken using Olympus IX71 fluorescent invert microscope. Data were analysed using image pro-software. Two-way ANOVA indicates that neither GEnC treatment with TNFα & TGFβ or platelet treatment with ADP has any effect on the number of adherent platelets or platelet aggregates (particles) to the GEnC monolayer (ANOVA ns). Data are mean +/- SEM of 2-3 experiments.

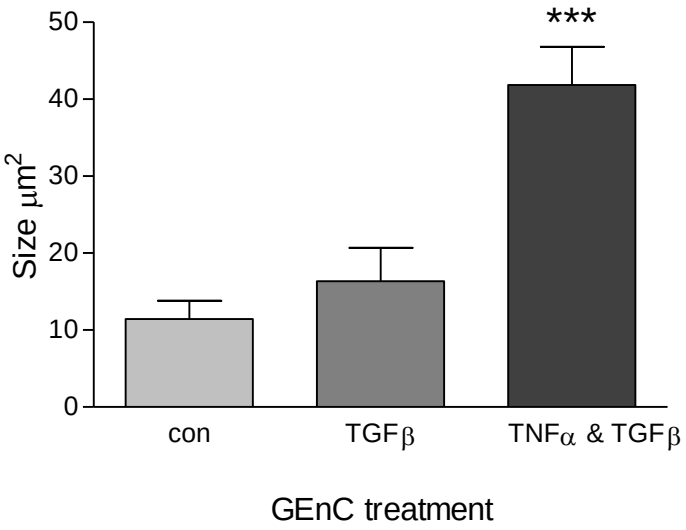


**Figure 3-7: The effects of TNFα and TGFβ on the size of fluorescent particles detected on GEnC**

Confluent monolayers of GEnC were incubated at 37°C overnight to remove the temperature sensitive simian virus 40 large tumour antigen and prevent further growth. GEnC were then treated with 10ng/ml TGFβ, both 100U/ml TNFα and 10ng/ml TGβ or left untreated overnight at 37°C. GEnC were then incubated with washed, isolated, platelets (suspended in 20% v/v PPP, 80% v/v M199 medium), stained with 5µg/ml calcein, for 1 hr. Cells were fixed with 1% (w/v) formaldehyde and washed three times with PBS, before images were taken using Olympus IX71 fluorescent invert microscope. Data were analysed using image pro-software. ANOVA ($P<0.01$) confirms that GEnC treatment has a significant effect on the size of the platelet aggregates adhering. *,** and *** indicate $P<0.05$, $P<0.01$ and $P<0.001$ respectively, post hoc test Dunnett's. Data are mean +/- SEM of 2-3 experiments.

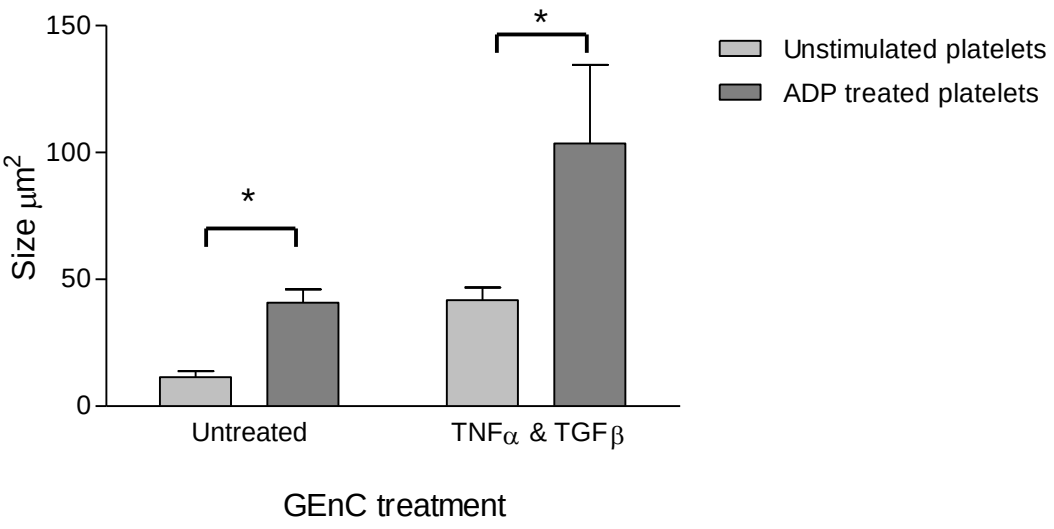


**Figure 3-8: The effect of ADP treatment on the size of fluorescent particles detected on GEnC**

Confluent monolayers of GEnC were incubated at 37°C overnight to remove the temperature sensitive simian virus 40 large tumour antigen and prevent further growth. GEnC were then treated with both 100U/ml TNFα and 10ng/ml TGβ or left untreated overnight at 37°C. GEnC were then incubated with washed, isolated platelets, (suspended in 20% v/v PPP, 80% v/v M199 medium), stained with 5μg/ml calcein, which, were either not activated or incubated with 10μM ADP for 1 hr. Cells were then fixed with 1% (w/v) formaldehyde and washed three times with PBS, before images were taken using Olympus IX71 fluorescent invert microscope. Data were analysed using image pro-software. Two-way ANOVA indicates that both GEnC treatment with TNFα & TGFβ ($P<0.05$) and platelet treatment with ADP ($P<0.05$) has an effect on the size of the platelet aggregates adhering to the GEnC monolayer. However, both treatments act independently to each other (ANOVA ns). *,** and *** indicate $P<0.05$, $P<0.01$ and $P<0.001$ respectively, post hoc test Bonferroni. Data are mean +/- SEM of 2-3 experiments.

### 3.3.3 Platelet adhesion to batch 1 GEnC in the absence of fibrin

To inhibit the fibrin deposition 5U/ml of heparin was added to the final platelet suspension. This allowed the assay to be repeated when coagulation was inhibited (**Figure 3-9**). Percentage platelet coverage of GEnC monolayers was significantly increased (~2%) after GEnC treatment with TNFα and TGFβ (**Figure 3-10**). There was no significant increase detected following treatment of GEnC with either of these cytokines alone (**Figure 3-10 and 3-11**). A combination of GEnC cytokine treatment and platelet treatment with ADP led to a further increase in the percentage platelet coverage (~10%), (**Figure 3-10**). In this instance, platelet treatment with ADP was able to significantly increase percentage platelet coverage of untreated GEnC monolayers, demonstrating that platelet activation alone could have an effect (**Figure 3-11**).

The number of adherent particles on GEnC monolayers was significantly increased after GEnC treatment with TNFα and TGFβ (**Figure 3-12 and 3-13**). However, platelet treatment with ADP had no effect on the overall numbers of adherent particles (**Figure 3-13**). The size of the platelet aggregates which formed was significantly increased, after cytokine treatment of GEnC or after platelet treatment with ADP (**Figure 3-14 and 3-15**). Together, this data indicates that GEnC treatment with TNFα and TGFβ increases both the number of platelets adhering and the overall size of the aggregates which form, but platelet treatment with ADP only affects the size of the aggregates which form (**Figure 3-12, 3-13, 3-14 and 3-15**).

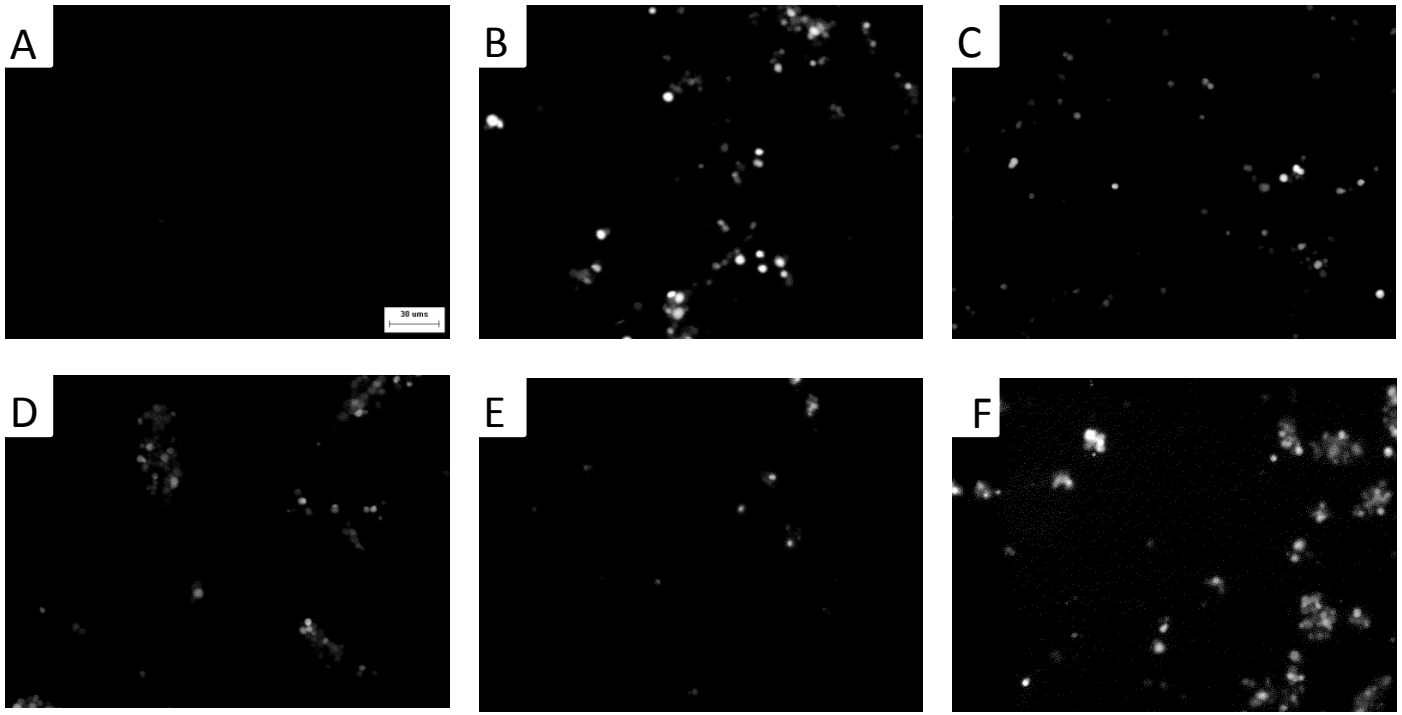


**Figure 3-9: Platelet adhesion to GEnC when coagulation is inhibited**

Confluent monolayers of GEnC were incubated at 37°C overnight to remove the temperature sensitive simian virus 40 large tumour antigen and prevent further growth. GEnC were then treated with 100U/ml TNFα, 10ng/ml TGFβ, both 100U/ml TNFα and 10ng/ml TGβ or left untreated overnight at 37°C. GEnC were then incubated with washed, isolated platelets stained with 5µg/ml calcein (suspended in 20% v/v PPP, 80% v/v M199 medium), which were either untreated or treated with 10µM ADP, for 1 hr. Cells were fixed with 1% (w/v) formaldehyde and washed three times with PBS before images were taken using Olympus IX71 fluorescent invert microscope. Figure demonstrates an example of platelet adhesion to GEnC monolayers, A) untreated (control), B) TNFα, C) TGFβ D) TNFα & TGFβ, E) untreated EC and ADP treated platelets and F) TNFα and TGFβ treated GEC and ADP treated platelets. Scale bar represents 30µm.

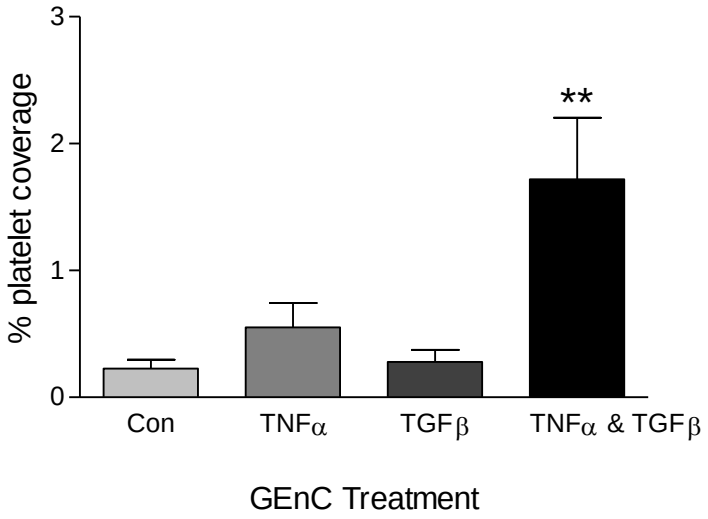


**Figure 3-10: The effect of TNFα and TGFβ on platelet adhesion to GEnC when coagulation is inhibited**

Confluent monolayers of GEnC were incubated at 37°C overnight to remove the temperature sensitive simian virus 40 large tumour antigen and prevent further growth. GEnC were then treated with 100U/ml TNFα, 10ng/ml TGFβ, both 100U/ml TNFα and 10ng/ml TGβ or left untreated overnight at 37°C. GEnC were then incubated with washed, isolated platelets (suspended in 20% v/v PPP, 80% v/v M199 medium), stained with 5μg/ml calcein, for 1 hr. Cells were fixed with 1% (w/v) formaldehyde and washed three times with PBS before images were taken using Olympus IX71 fluorescent invert microscope. Data were analysed using image pro-software. One way ANOVA ($P<0.01$) indicates that EC treatment has an effect on platelet adhesion. There is a significant increase in platelet adhesion to GEnC following GEnC treatment with TNFα & TGFβ compared to untreated control. *,** and *** indicate $P<0.05$, $P<0.01$ and $P<0.001$ respectively, post hoc test Dunnett's. Data are mean +/- SEM of 5 experiments.

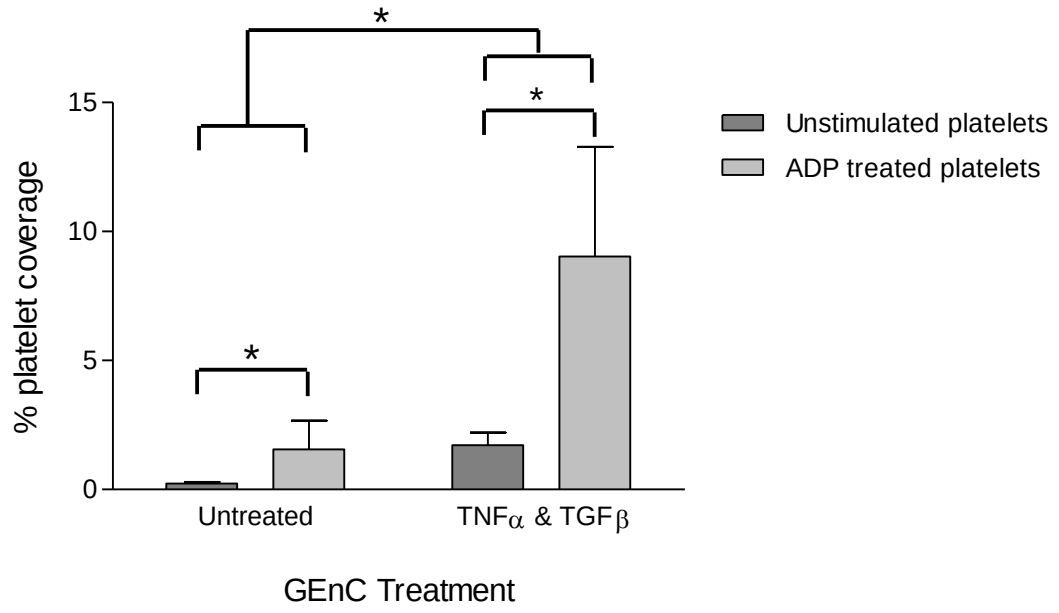


**Figure 3-11: The effect of ADP treatment of platelets on their adhesion to GEnC when coagulation is inhibited**

Confluent monolayers of GEnC were incubated at 37°C overnight to remove the temperature sensitive simian virus 40 large tumour antigen and prevent further growth. GEnC were then treated with both 100U/ml TNFα and 10ng/ml TGβ or left untreated overnight at 37°C. GEnC were then incubated with washed, isolated platelets, (suspended in 20% v/v PPP, 80% v/v M199 medium), stained with 5μg/ml calcein, which, were either not activated or incubated with 10μM ADP for 1 hr. Cells were then fixed with 1% (w/v) formaldehyde and washed three times with PBS before images were taken using Olympus IX71 fluorescent invert microscope. Data were analysed using image pro-software. Two-way ANOVA ($P<0.05$) indicates that both GEnC treatment with TNFα & TGFβ and platelet treatment with ADP has a significant effect on increasing percentage platelet coverage. However ANOVA (ns) indicates that these two treatments show no interaction with each other. Bonferroni indicates there is a significant increase in percentage platelet coverage after GEnC treatment with TNFα and TGFβ or after platelet treatment with ADP. *,** and *** indicate $P<0.05$, $P<0.01$ and $P<0.001$ respectively, post hoc test Bonferroni. Data are mean +/- SEM of 4-5 experiments.

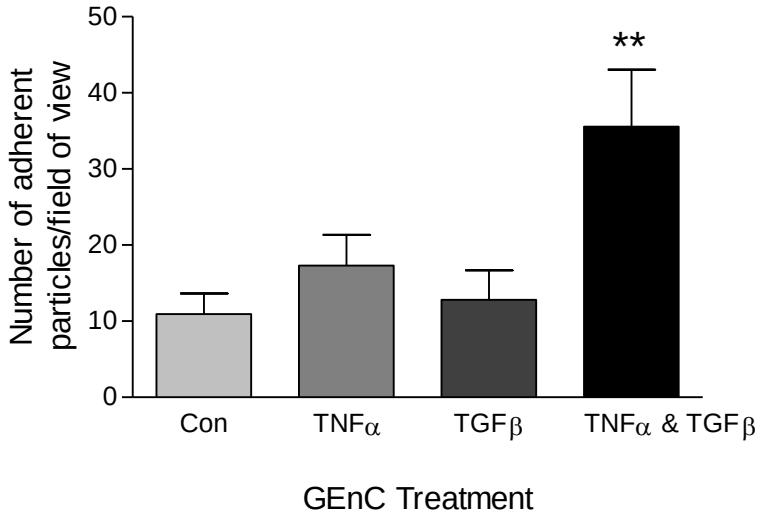


**Figure 3-12: The effect of TNFα and TGFβ on the number of fluorescent particles detected on GEnC when coagulation is inhibited**

Confluent monolayers of GEnC were incubated at 37°C overnight to remove the temperature sensitive simian virus 40 large tumour antigen and prevent further growth. GEnC were then treated with 100U/ml TNFα, 10ng/ml TGFβ, both 100U/ml TNFα and 10ng/ml TGβ or left untreated overnight at 37°C. GEnC were then incubated with washed, isolated, platelets, (suspended in 20% v/v PPP, 80% v/v M199 medium), stained with 5μg/ml calcein, for 1 hr. Cells were fixed with 1% (w/v) formaldehyde and washed three times with PBS before images were taken using Olympus IX71 fluorescent invert microscope. Data were analysed using image pro-software. ANOVA ($P<0.01$) indicates that GEnC treatment significantly increases the number of particles adhering. *,** and *** indicate $P<0.05$, $P<0.01$ and $P<0.001$ respectively, post hoc test Dunnett's. Data are mean +/- SEM of 5 experiments.

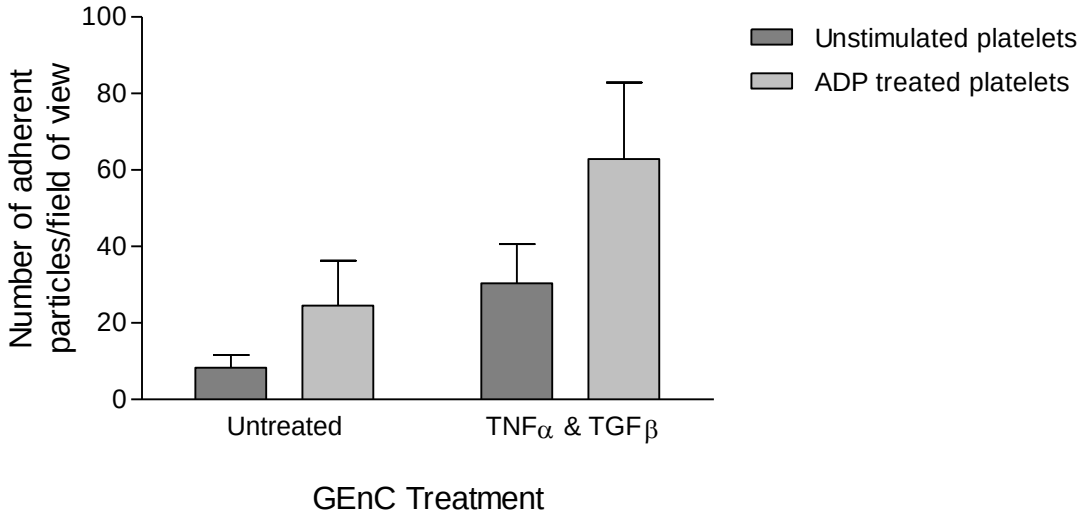


**Figure 3-13: The effect of platelet treatment with ADP on the number of fluorescent particles detected on GEnC when coagulation is inhibited**

Confluent monolayers of GEnC were incubated at 37°C overnight to remove the temperature sensitive simian virus 40 large tumour antigen and prevent further growth. GEnC were then treated with both 100U/ml TNFα and 10ng/ml TGβ or left untreated overnight at 37°C. GEnC were then incubated with washed, isolated platelets, (suspended in 20% v/v PPP, 80% v/v M199 medium), stained with 5µg/ml calcein, which, were either not activated or incubated with 10µM ADP for 1 hr. Cells were then fixed with 1% (w/v) formaldehyde and washed three times with PBS before images were taken using Olympus IX71 fluorescent invert microscope. Data was analysed using image pro-software. Two-way ANOVA ($P<0.05$) indicates that GEnC treatment with TNFα & TGFβ causes a significant increase in the number of adherent platelets or platelet aggregates (particles) adhering to the GEnC monolayer (post hoc test Bonferroni not significant). However platelet treatment with ADP has no effect (ANOVA ns). Data are mean +/- SEM of 4-5 experiments.

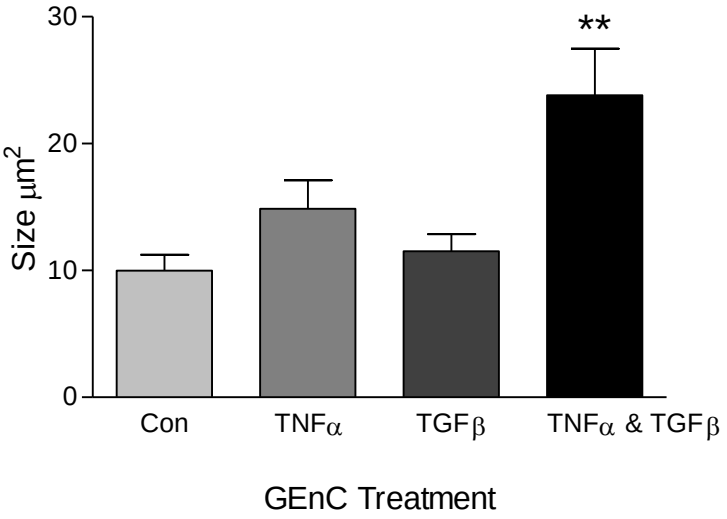


**Figure 3-14: The effect of TNFα and TGFβ on the size of fluorescent particles detected on GEnC when coagulation is inhibited**

Confluent monolayers of GEnC were incubated at 37°C overnight to remove the temperature sensitive simian virus 40 large tumour antigen and prevent further growth. GEnC were then treated with 100U/ml TNFα, 10ng/ml TGFβ, both 100U/ml TNFα and 10ng/ml TGβ or left untreated overnight at 37°C. GEnC were then incubated with washed, isolated, platelets (suspended in 20% v/v PPP, 80% v/v M199 medium), stained with 5µg/ml calcein, for 1 hr. Cells were fixed with 1% (w/v) formaldehyde and washed three times with PBS before images were taken using Olympus IX71 fluorescent invert microscope. Data were analysed using image pro-software. ANOVA ($P<0.01$) confirms that GEnC treatment has a significant effect on the size of the platelet aggregates adhering. *,** and *** indicate $P<0.05$, $P<0.01$ and $P<0.001$ respectively, post hoc test Dunnett's. Data are mean +/- SEM of 5 experiments.

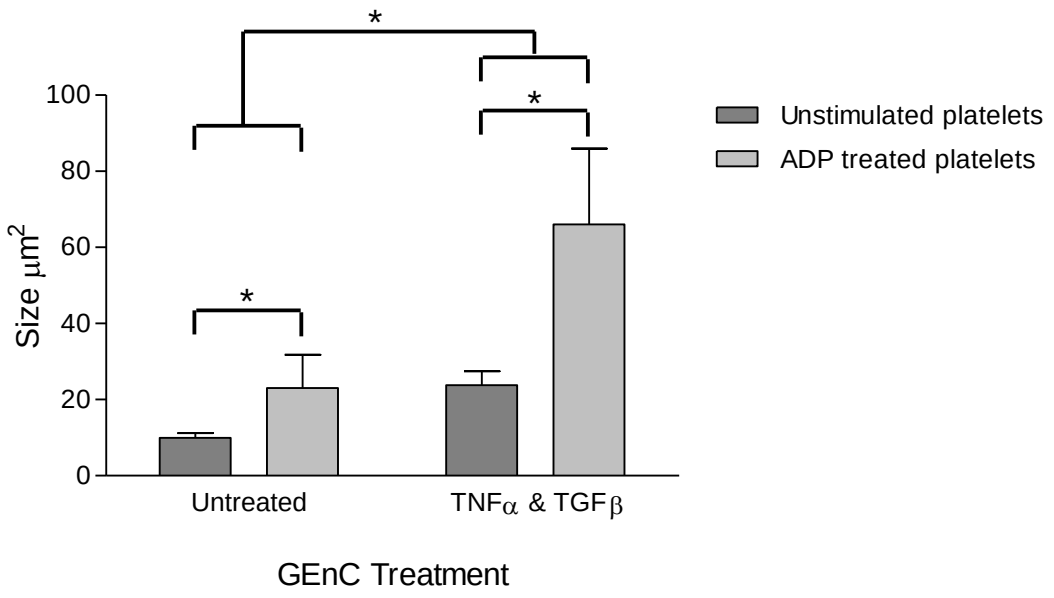


**Figure 3-15: The Effect of ADP treatment on size of fluorescent particles detected on GEnC when coagulation is inhibited**

Confluent monolayers of GEnC were incubated at 37°C overnight to remove the temperature sensitive simian virus 40 large tumour antigen and prevent further growth. GEnC were then treated with both 100U/ml TNFα and 10ng/ml TGβ or left untreated overnight at 37°C. GEnC were then incubated with washed, isolated platelets (suspended in 20% v/v PPP, 80% v/v M199 medium), stained with 5µg/ml calcein, which, were either not activated or incubated with 10µM ADP for 1 hr. Cells were then fixed with 1% (w/v) formaldehyde and washed three times with PBS before images were taken using Olympus IX71 fluorescent invert microscope. Data were analysed using image pro-software. Two-way ANOVA indicates that both GEnC treatment with TNFα & TGFβ ($P<0.05$) and platelet treatment with ADP ($P<0.05$) has any effect on the size of the platelet aggregates adhering to the GEnC monolayer. However both treatments act independently to each other (ANOVA ns). Bonferroni indicates a significant increase in size of platelet aggregates adhering to GEnC monolayers after GEnC treatment with TNFβ and TGFβ or platelet treatment with ADP. *,** and *** indicate $P<0.05$, $P<0.01$ and $P<0.001$ respectively, post hoc test Bonferroni. Data are mean +/- SEM 4-5 experiments.

### 3.3.4 Characterising the phenotype of batch 2 cell line GEnC

Our collaborators in Bristol who produced the cell line GEnC, do not recommend its use after passage 41 (P41) as it has not been proven to retain endothelial cell properties past this point. Therefore, to continue the study earlier passage GEnC were required. When culturing cell line GEnC (batch 2) there appeared to be a change in the phenotype of these cells, they lost their classic cobblestone appearance and began to appear longer and thinner (**Figure 3-16**). This prompted tests for EC markers. Primary HUVEC, cell line GEnC batch 2 and cell line podocytes all expressed surface ICAM-1 in response to 4 hour treatment with TNFα (**Table 3-1**).

The epithelial podocytes cell line did not express PECAM-1 (change in MFI compared to isotype 0.62 which is negligible), (**Table 3-2**). GEnC (batch 2) however, did express this marker (change in MFI compared to isotype ~80.69) but at lower levels than HUVEC (change in MFI compared to isotype ~245) (**Table 3-2**). Table 3-3 demonstrates that the epithelial cell line podocytes did not express E-selectin in response to treatment with 1000U TNFα. However, and surprisingly, cell line GEnC (batch 2) did not express E-selectin either (**Table 3-3**). HUVEC expressed high levels of E-selectin in response to 1000U TNFα (**Table 3-3**). Moreover, Table 3-4 clearly demonstrates that cell line GEnC (batch 2) and podocytes did not express vWf (either on the surface or internal stores), (**Table 3-4**). However, HUVEC express high total levels of vWf (change in MFI ~256 compared to the isotype control), (**Table 3-4**).

### 3.3.5 Immunocytochemistry to detect vWf in batch 2 cell line GEnC

To further confirm the flow cytometry data which demonstrated there was no vWf expression by the GEnC cell line (batch 2) and to check that podocytes were indeed negative for this marker, we used immunocytochemistry. Figure 3-17 clearly demonstrates that both cell line

GEnC (batch 2) and cell line podocytes do not express any internal or surface vWf. However, in accordance with the flow cytometry data HUVEC again demonstrated express high levels of internal and surface vWf expression (**Figure 3-17**). There is no nonspecific binding of the isotype control to any of the cell types (**Figure 3-17**).

### 3.3.6 Primary GEnC do not express vWf

A possible short term solution to the problem of obtaining GEnC, which was suitable for use in platelet adhesion assay experiments, was using primary GEnC. As human tissue is not readily available, this had to be bought from an external source, making it too expensive to make it a viable source to continue the project long term. However figure 3-18 demonstrates that primary GEnC (HRGEC) were unable to form a proper monolayer. Figure 3-19C demonstrates that cell line GEnC expressed high levels of both internal and surface vWf. Primary GEnC (HRGEC) may have expressed very low levels of vWf, although as classic punctate staining of the Weible Palade bodies can't be detected, the small amount of staining observed may be due to nonspecific binding of the vWf antibody to these particular cells (**Figure 3-19A**). Figure 3-19C and D show primary GEnC (HRGEC) and cell line GEnC (batch 1) do not bind sheep anti-human isotype control. The little to no vWf expressed by primary GEnC (HRGEC) meant that we were unable to use them for platelet adhesion assays as vWf is an important part of the mechanism for platelet capture by EC.

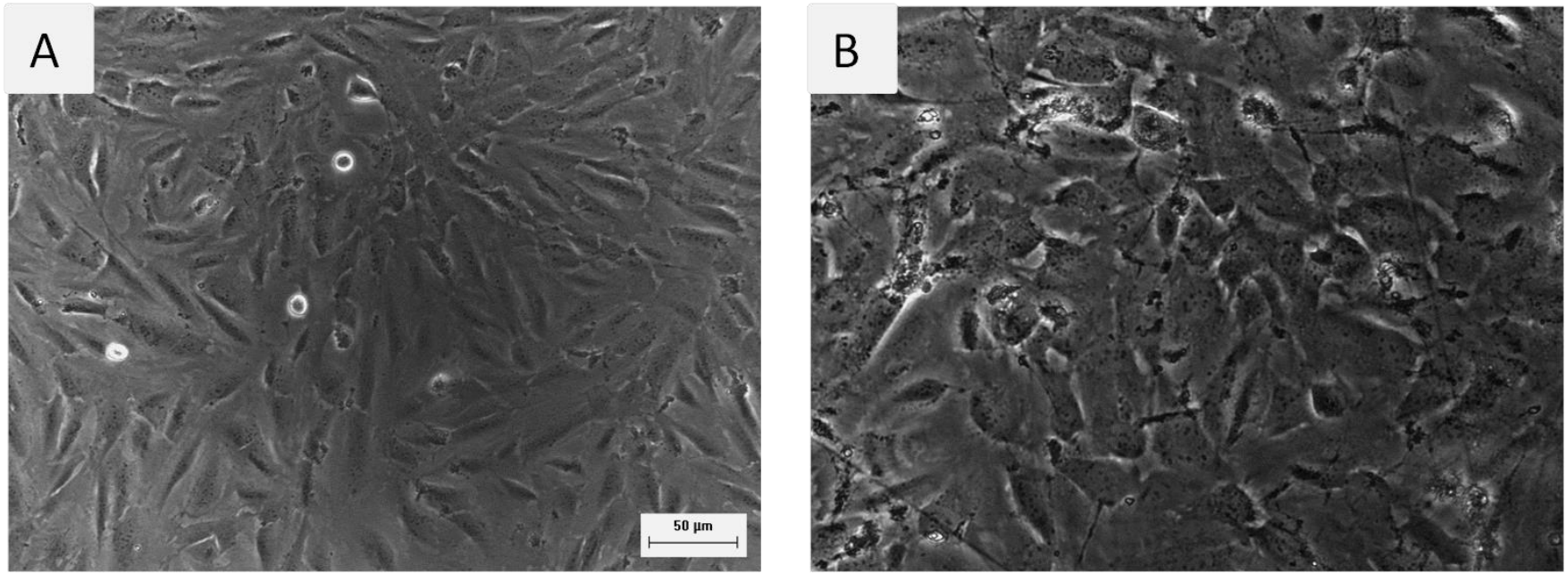


**Figure 3-16: Batch 2 cell line GEnC morphology**

A) GEnC cell line (batch 2) below P41, grown at 33°C and 5% $CO_2$. The cells have not yet reached confluence but they are irregular shapes and sizes. They don't display classic cobble stone appearance. B) shows GEnC cell line (batch 2) after 24hrs at 37°C and 5% $CO_2$. Some of the cells appear to have lost contact inhibition and have grown over each other. Other cells have started to die. This destroys the monolayer, so it is no longer suitable for platelet adhesion experiments. Images acquired using Olympus IX70 invert microscope and Image pro 6.2 (Media Cybernetics). Scale bar represents 50µm.

| | Isotype MFI | ICAM-1 MFI | Change in MFI |
|---|---|---|---|
| HUVEC | **14.48** | **857.70** | **843.22** |
| Podocytes | **10.85** | **360.46** | **349.61** |
| GEnC | **7.29** | **498.93** | **491.64** |

**Table 3-1: Surface ICAM-1 expression by HUVEC, podocytes and GEnC**

Confluent monolayers of each cell type primary HUVEC, podocyte cell line and GEnC cell line (batch 2) were cultured in 24 well plates. One well of each was treated with 100U TNFα for 4 hours before being removed from plates and incubated with APC labelled ICAM-1 or relevant isotype control on ice. Data were acquired using flow cytometry. A gate was set to contain 5% of the isotype control and the MFI for ICAM-1 was recorded in this gate. Table 3-1 demonstrates that all three cell types express ICAM-1. HUVEC express the highest levels and podocytes the lowest. Data are MFI from one experiment.

| | Isotype MFI | PECAM-1 MFI | Change in MFI |
|---|---|---|---|
| HUVEC | **16.14** | **260.43** | **244.29** |
| Podocytes | **16.73** | **17.35** | **0.62** |
| GEnC | **28.76** | **109.45** | **80.69** |

**Table 3-2: Surface PECAM-1 Expression by HUVEC and GEnC but not podocytes**

Confluent monolayers of each cell type primary HUVEC, podocyte cell line and GEnC cell line (batch 2) were cultured in 24 well plates. One well of each was treated with 100U TNFα for 4 hours before being removed from plates and incubated with PE labelled PECAM-1 or relevant isotype control on ice. Data were acquired using flow cytometry. A gate was set to contain 5% of the isotype control and the MFI for PECAM-1 was recorded in this gate. Table 3-1 demonstrates that HUVEC and GEnC express PECAM-1, with HUVEC expressing the highest levels. Podocytes do not express this marker. Data are MFI from one experiment.

| | Isotype MFI | E-selectin MFI | Change in MFI |
|---|---|---|---|
| HUVEC | **12.99** | **209.69** | **196.7** |
| Podocytes | **19.33** | **15.57** | **-3.76** |
| GEnC | **20.78** | **20.78** | **0** |

**Table 3-3: Surface E-selectin expression by HUVEC but not podocytes or GEnC**

Confluent monolayers of each cell type primary HUVEC, podocyte cell line and GEnC cell line (batch 2) were cultured in 24 well plates. One well of each was treated with 1000U TNFα for 4 hours before incubation with unlabelled mouse anti-human E-selectin antibody or relevant isotype control for 30 minutes in the dark, followed by incubation with FITC-labelled polyclonal goat anti-mouse secondary antibody. Cells were removed from the plate. Data were acquired using flow cytometry. Data suggests that only HUVEC express surface E-selectin after treatment with TNFα. Data are MFI from one experiment.

| | Isotype MFI | vWf MFI | Change in MFI |
|---|---|---|---|
| HUVEC | **13.97** | **270.01** | **256.04** |
| Podocytes | **13.97** | **17.35** | **3.38** |
| GEnC | **24.98** | **24.98** | **0** |

**Table 3-4: Total vWf expression by HUVEC, podocytes and GEnC**

Confluent monolayers of each cell type HUVEC, podocyte cell line and GEnC cell line (batch 2) were cultured in 24 well plates. Cells were removed from plates and incubated with Invitrogen fix and perm kit (according to the manufacturers instructions). Cells were then incubated with FITC labelled vWf antibody or relevant isotype control. Data were acquired using flow cytometry. HUVEC express vWf, podocytes may express very low levels but GEnC do not express any. Data are MFI from one experiment.

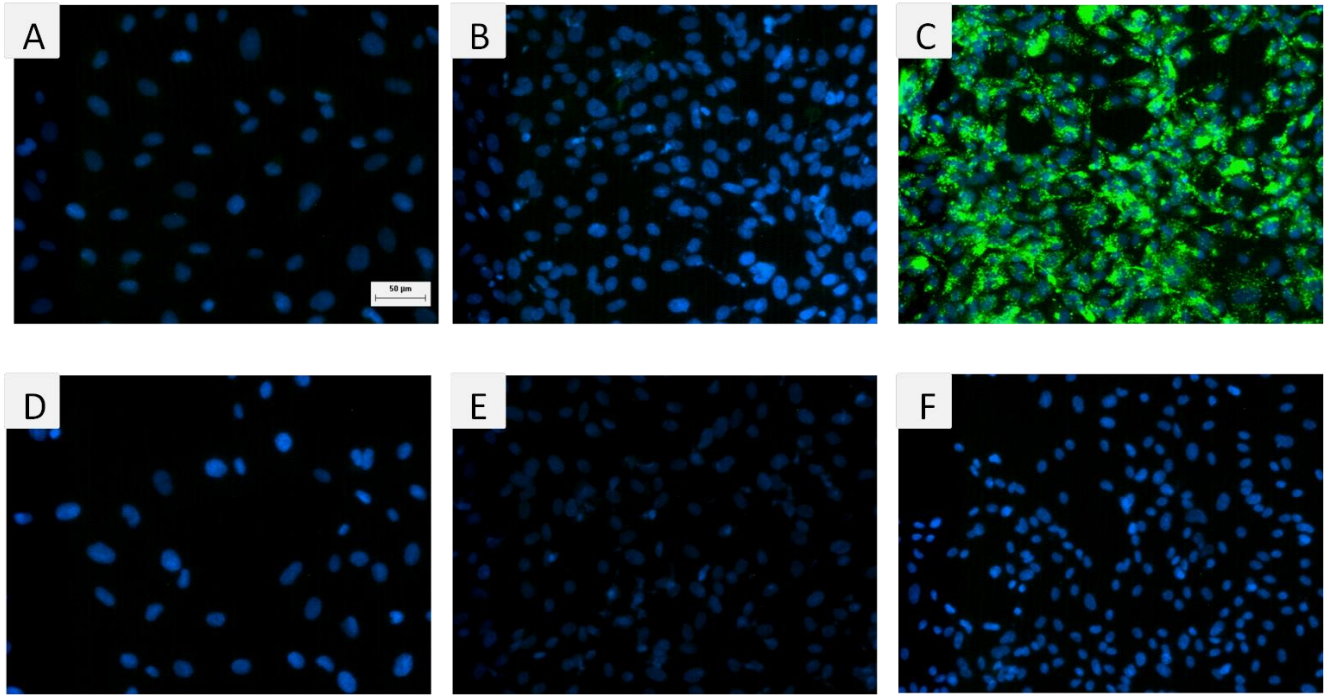


**Figure 3-17: Immunocytochemistry for detection of vWf on Batch 2 GEnC**

Cell line GEnC (batch 2) and cell line podocytes were cultured at 33°C until confluent monolayers formed, the cells were then incubated at 37°C overnight to remove the temperature sensitive simian virus 40 large tumour antigen and prevent further growth. (Primary) HUVEC have been grown to confluence at 37°C. Cells were fixed with 2% (w/v) formaldehyde, followed by 1% (w/v) triton. A) B) and C) have been incubated for 30 minutes with FITC labelled sheep anti-human vWf antibody, D) E) and F) with sheep anti-human Isotype control (green). All have been treated with 0.1% (v/v) Hoescht nuclear stain (blue). A) Podocyte cell line do not express vWf D) there is no nonspecific binding of relevant isotype control to cell line podocytes. B) shows cell line GEnC (batch 2) do not express vWf and E) demonstrates there is no nonspecific binding of relevant isotype control to GEnC cell line (batch 2) C) shows total von Willebrand factor expression by HUVEC, (F) HUVEC does not bind isotype control. Scale bar represents 50µm.

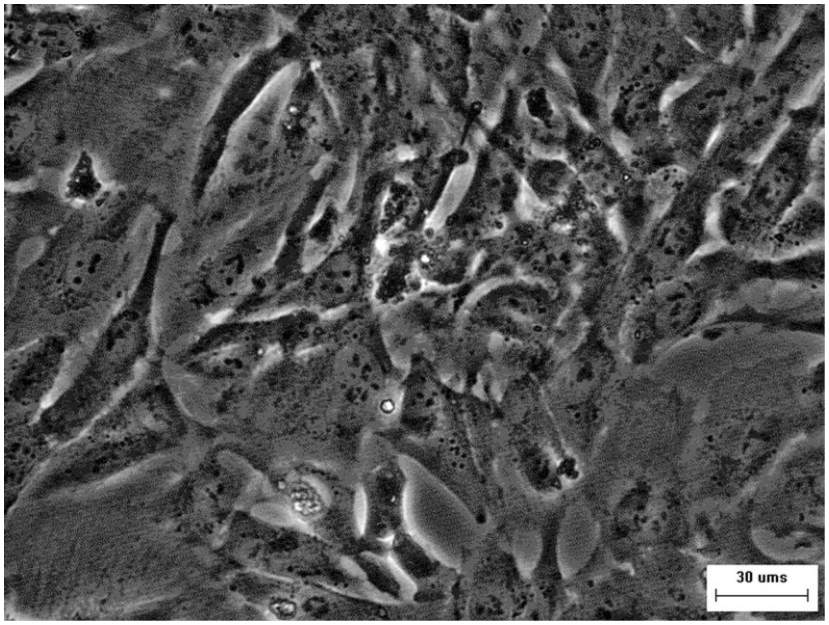


**Figure 3-18: Primary GEnC (HRGEC) morphology**

Passage 1 primary GEnC (HRGEC) a monolayer has not formed. There are places where the cells have lost contact inhibition and are growing over each other and spaces where the cells have retracted. Image obtained using Olympus IX71. Scale bar represents 30µm.

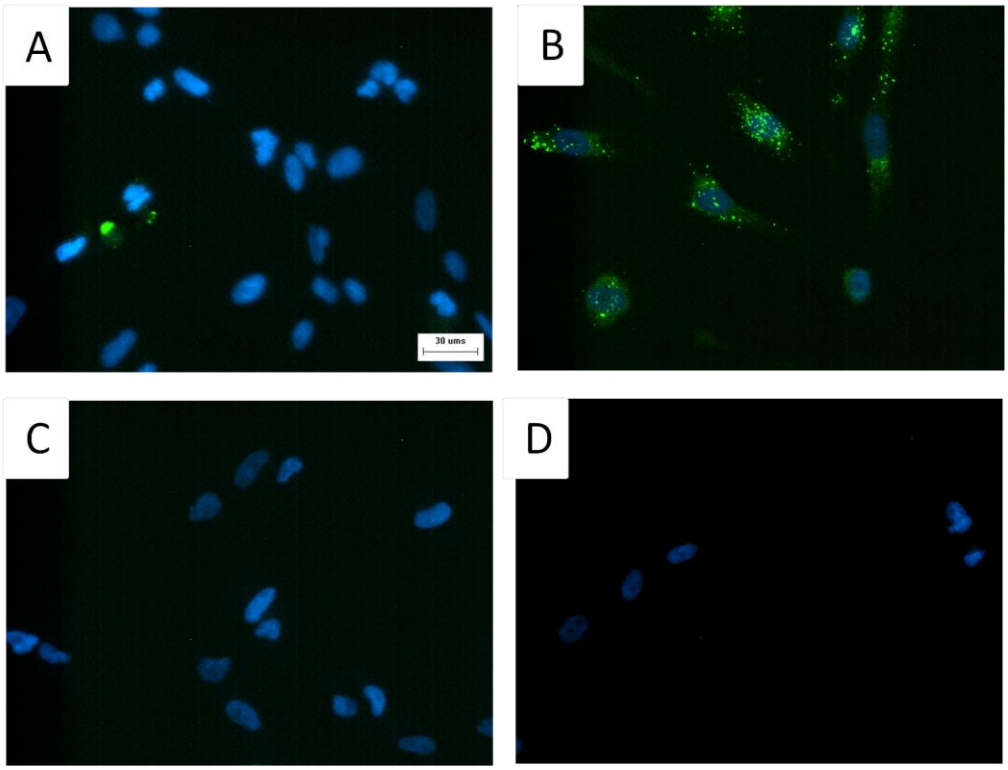


**Figure 3-19: Immunocytochemistry for detection of vWf in primary GEnC**

Cell line GEnC (batch 1) and were cultured at 33°C, the cells were then incubated at 37°C overnight to remove the temperature sensitive simian virus 40 large tumour antigen and prevent further growth. Primary GEnC (HRGEC) were cultured at 37°C. Cells were fixed with 2% (w/v) formaldehyde, followed by 1% (w/v) triton. A) and B) have been incubated for 30 minutes with FITC labelled sheep anti-human vWf antibody, C) and D) with sheep anti-human Isotype control (green). All have been treated with 0.1% (v/v) Hoescht nuclear stain (blue). A) total von Willebrand factor expression primary GEnC, (C) primary GEnC isotype control C) total von Willebrand factor expression by cell line GEnC (batch 1). D) Cell line GEnC isotype control showing no nonspecific binding to these cells. Scale bar represents 30µm.

**3.4.0 Discussion**

Here, immortalized Cell line GEnC were chosen instead of primary GEnC as human kidney tissue is not readily available and could not be used as a reliable source. Cell line GEnC and cell line podocytes were created by transducing primary cells with a temperature sensitive simian virus 40 large tumour antigen (SV40LT) and telomerase using retroviral vectors (Saleem et al., 2002; Satchell et al., 2006). When they are incubated at 33°C (5% $CO_2$) they proliferate and should have a cobble stone appearance forming a confluent monolayer, they can also be sub-cultured (Saleem et al., 2002; Satchell et al., 2006). However, at 37°C SV40LT can be 'switched off' as the temperature sensitive virus is removed and the cells growth is arrested (Saleem et al., 2002; Satchell et al., 2006).

Under normal conditions EC produce NO, which, prevents platelet activation. This is through a mechanism which inhibits the release of platelet intracellular calcium, thus preventing the release of α and δ granule contents as well as conformational change occurring to $\alpha_{IIb}\beta_{III}$ integrin (Gkaliagkousi et al., 2007). However, upon activation EC reduce NO production. For studying the effects of platelet adhesion to GEnC, monolayers of GEnC have been treated with the cytokines TNFα and TGFβ.

*In vivo* TNFα is released from activated cells (such as macrophages) and it stimulates surrounding EC leading to the upregulation of inflammatory markers such as E-selectin, ICAM-1 and PECAM-1, all key players in the leukocyte adhesion cascade (Ley et al., 2007). TGFβ is thought to be released from secretory phenotype SMC, a phenotypic change associated with atherosclerosis (Tull et al., 2006). TGFβ activates EC to release vWf to the surface, this enables EC to capture platelets, which in turn aid in leukocyte capture through the formation of P-selectin bridges (Tull et al., 2006; Kuckleburg et al., 2011). As previous evidence suggests that

vWf is crucial for platelet capture by EC, before any platelet adhesion assays were carried out we confirmed that the GEnC (batch 1) used in our experiments expressed vWf.

The platelet adhesion assays were carried out in the presence of coagulation (more widely associated with venous thrombosis) and repeated when coagulation was inhibited by the addition of extra heparin. There are two main coagulation pathways the extrinsic pathway and the contact activation pathway, these merge to form the common pathway and both result in fibrin deposition. During inflammation, TNFα stimulates tissue factor (TF) expression on endothelial cells (Petäjä, 2011). This starts the extrinsic pathway of the coagulation cascade in which serine proteases are converted from their zymogen form into their active form (Levi et al., 2004). The contact activation pathway is the lesser important of the two coagulation pathways, which is initiated following endothelial damage and exposure of collagen (Davie et al., 1991). This pathway should not play any role in these experiments where EC monolayers are intact. Thrombin, a well known and potent platelet activator, is produced as a by product of the coagulation cascade, which ultimately results in fibrin deposition (Coughlin, 2000). Fibrin allows platelet crosslinking to occur through binding to $\alpha_{IIb}\beta_3$ integrin, resulting in stable clot formation (Levi et al., 2004).

Under static conditions where coagulation was able to occur, we have demonstrated that there is an increase in percentage platelet coverage of GEnC monolayers after GEnC treatment with TNFα and TGFβ, this is higher in the presence of coagulation (~12%), than in the presence of heparin (~2%). Coagulation results in increased levels of fibrin being available, allowing platelets to aggregate more readily, increasing the size of the platelet aggregates forming and therefore increasing the platelet percentage coverage of GEnC. In the presence of coagulation, activation of platelets with ADP did not significantly increase platelet adhesion to

GEnC. This could be due to the effects of ADP being masked by the coagulation cascade and the presence of thrombin a more powerful platelet activator.

Combined cytokine treatment results in the expression of vWf on the surface of the GEnC, allowing platelet adhesion to occur to these cells. This adhesion is first supported by CD42b but this interaction will lead to transient increases in cytosolic $Ca^{2+}$ levels, platelet activation and release of ADP from δ granules. ADP is known to play a role in a positive feedback loop during platelet activation, encouraging platelet aggregates to form. The data suggests there is no interaction between cytokine treatment of GEnC and ADP treatment of platelets when platelets adhere to GEnC under static conditions. This is not surprising as these two treatments act through two different mechanisms in order to increase platelet adhesion.

Data from this study clearly demonstrates that treatment of GEnC with either TNFα or TGFβ alone is not enough to significantly increase platelet adhesion to GEnC. In line with this Tull et al, (2006) also found that cytokine treatment of EC (in this case HUVEC) with TNFα did not lead to an increase in platelet adhesion. This is expected as TNFα increases E-selectin, PECAM-1 and ICAM-2, which play important roles in leukocyte adhesion rather than platelet adhesion. However Tull et al, (2006) clearly demonstrated that TGFβ signalling alone was able to significantly increase platelet adhesion to EC through interactions with surface vWf.

Primary GEnC are known to express the serine/threonine kinase receptors TGFβR1 and TGFβR2, which form heterodimers in response to TGFβ binding, allowing TGFβ signalling to occur (Choi and Ballermann, 1995). Podocytes are known to produce TGFβ in response to oxLDL or high glucose (Ding et al., 1997; Pavenstädt et al., 2003). TGFβ signalling can lead to apoptosis in both cell types (Choi and Ballermann, 1995; Pavenstädt et al., 2003). It has also been implicated in glomerosclerosis, leading to damage to the GFB (Soon Lee, 2013; Mozes et al., 1999). This

implies a role for TGFβ signalling in disease and implies that cross-talk between EC and podocytes can occur through this signalling pathway. However, it has not yet been demonstrated if TGFβ signalling in GEnC leads to the release of vWf from internal stores and its expression on the cell surface.

The data from this study shows no significant increase in platelet adhesion after treatment with TGFβ alone, suggesting that in this case TGFβ signalling is not enough to cause the release of vWf from internal stores and expression on the surface. However, had more GEnC (batch 1) been available it would have been interesting to confirm whether this was the case using immunocytochemistry to detect surface vWf. It would also have been interesting to find out if treatment of primary GEnC with TGFβ was enough to significantly increase platelet adhesion (had a reliable source of primary GEnC been available). It could be that cell line GEnC loose receptors over time or due to immortalisation and are less responsive than primary cells.

Our collaborators at Bristol have demonstrated that cell line GEnC retain primary GEnC properties until passage 41 (Satchell et al., 2006). They should express endothelial cell markers such as E-selectin, PECAM-1 (CD31), ICAM-2 (CD102), VEGFR-2 and von Willebrand factor (vWf) (Satchell et al., 2006). They do not recommend the use of GEnC past P41. Unfortunately on completion of the first objectives, earlier passage GEnC were required. On receiving new GEnC (batch 2) there was an obvious change in phenotype, these cells did not form the characteristic 'cobblestone' EC monolayer. Data in this study demonstrates that after 4 hour treatment of GEnC (batch 2) with TNFα these cells do not express high levels of PECAM-1, or any E-selectin. E-selectin expression on primary HUVEC has previously been shown to peak after 4 hour treatment with TNFα, which is why this time point was chosen (Rainger and Nash, 2001). We

also demonstrate GEnC (batch 2) do not express any vWf. This implies the loss of EC markers from these cells.

The lack of vWf, a crucial part of the mechanism for platelet adhesion to EC in our model, makes them unsuitable for use in further experiments. The use of this cell line therefore had to be discontinued. Primary GEnC (HRGEC) were purchased to try to continue the study, however, due to expense this would not have been a viable long term plan. Unfortunately these cells also failed to express vWf and were also not useful for these experiments.

**Conclusions**

We have demonstrated that GEnC monolayers treated with TNFα and TGFβ express a matrix of vWf on the surface. We have also demonstrated that under static conditions, after treatment of GEnC with these cytokines platelet adhesion is significantly increased compared to the untreated control. Platelet treatment with ADP further increased platelet adhesion to GEnC in the presence of heparin. However, if coagulation was able to occur ADP had no effect, probably due to its behaviour being masked by the presence of the more potent platelet agonist thrombin.

# 4. Chapter 4- MONOCYTE-PLATELET AGGREGATE FORMATION IN RESPONSE TO TREATMENT WITH TRAP OR HISTONES

### 4.1.0 Introduction

Elevated levels of monocyte-platelet aggregates (MPA) have been detected in conjunction with several inflammatory diseases including, SLA, RA, DM, cerebrovascular ischemia, ischaemic stroke as well as atherosclerosis (Furman et al., 2001; Harding et al., 2004; Htun et al., 2006; Ishikawa et al., 2012; Joseph et al., 2001; Shantsila and Lip, 2009). This indicates a potential role for MPA in inflammatory diseases. Of particular interest to us is the possibility that MPA contribute to disease progression in atherosclerosis.

There are several mechanisms through which leukocyte-platelet aggregate formation could play a role in disease progression. The formation of these heterotypic aggregates allows for cross-talk to occur between the two cell types, forming a potentially important link between inflammation and thrombosis. Platelet recruitment to dysfunctional endothelial cells is also thought to occur early in inflammatory diseases such as atherosclerosis (Ross, 1999). Platelets adherent to dysfunctional EC both *in vitro* and *in vivo* have been demonstrated to aid in leukocyte recruitment. Indeed, preferential recruitment of monocytes by adherent platelets was observed in some models (e.g. Kuckleburg et al., 2011). This mechanism could have an important role in disease progression. It is also possible that MPA, which form in the circulation could have an increased chance of recruitment to damaged or dysfunctional endothelial cells.

Platelet activation has been shown to be important in MPA formation (Michelson et al., 2001). There are several routes through which platelets can become activated (Rivera et al., 2009). One important pathway which results in irreversible platelet activation is through PAR-1 and PAR-4 signalling induced by thrombin. PAR-1 is thought to be the most responsive of these receptors and therefore most important receptor at lower concentrations of thrombin (Kahn et al., 1999). Thrombin is generated as part of the coagulation cascade, of which the end product,

fibrin, has an important role in platelet crosslinking and clot formation (Coughlin, 2000). Thus, thrombin generation is an example of crosstalk between coagulation and thrombosis (Coughlin, 2000). End stage atherosclerosis can result in plaque rupture, which triggers thrombus formation, leading to localised increase in thrombin (Coughlin, 2000; Libby, 2012; Ross, 1999). The clinical outcome may potentially be fatal for the patient as it can result in myocardial infarction (MI) or stoke (Ross, 1999). However, patients who have survived have been shown to have increased levels of circulating MPA, following MI (Mickelson et al., 1996). As platelet activation plays an important role in MPA formation, and as thrombin is known to be active in this phase of disease, it is not unreasonable to assume that the PAR-1 pathway plays some role in MPA formation.

Histones are proteins which are used to package DNA into chromatin. There are four histones H2A, H2B, H3 and H4 which associate to form an octomer which DNA is able to wrap around (Peterson and Laniel, 2004). Upon cellular death or severe damage histones will be released from the cell into the circulation or tissue fluids, where they are thought to have antimicrobial properties (Fuchs et al., 2011, 2010). However, they are also known to be extremely damaging to surrounding host cells, with histone H3 and H4 being most damaging (Xu et al., 2009). Both of these histones have been shown to activate platelets, with H4 being the most potent platelet activator (Semeraro et al., 2011). It was first thought histones activated platelets through a charge based interaction. However, it has now been demonstrated that histone H4 stimulates platelets, at least in part, through the TLR-2 and TLR-4 receptors (Fuchs et al., 2011; Semeraro et al., 2011). Following MI which results in tissue necrosis, it is likely that histones will be released into the circulation where they may potentially activate platelets. This suggests that histones may also have an important role in MPA formation.

Activated platelets are known to shed platelet microvesicles (PMV) from their plasma membrane, which can be identified by positivity for platelet specific markers such as CD42b, CD41 and P-selectin (CD62P) (Hargett & Bauer 2013; Flaumenhaft et al. 2009). Elevated levels of microvesicles have been identified in patients suffering from chronic inflammatory diseases such as atherosclerosis and following trauma (Beyer and Pisetsky, 2010). PMV adhesion to isolated neutrophils, another leukocyte subset, has indeed been demonstrated to occur *in vitro* (Forlow et al., 2000). It is therefore possible that PMV could also interact with monocytes in a similar manner. We hypothesized that after treatment of whole blood with a platelet agonist, generation of PMV would occur and that these PMV, along with platelets, would have the ability to bind to monocytes and form MPA.

It is also well known that monocytes are a heterogeneous cell type, of which there are two main subsets including the $CD14^{+}CD16^{-}$ (90% population) and the $CD14^{+}CD16^{+}$ (10% population) (Shantsila et al., 2011). Following MI in a mouse model, the healing myocardium has been shown to be dominated by different monocyte subsets during the repair process (Nahrendorf et al., 2007). The more pro-inflammatory (equivalent $CD14^{+}CD16^{-}$ monocyte subset) Ly6-$C^{hi}$ were shown to be recruited at high levels during the early response. As recruitment of this subset decreased, Ly6-$C^{lo}$ (equivalent $CD14^{+}CD16^{+}$ monocyte subset) recruitment increased, this subset is able to produce inflammation resolving and growth repair signals (Nahrendorf et al., 2007). It is possible that differences occur in the ability of these monocyte subsets to form heterotypic aggregates with platelets.

Our aims for this chapter therefore were to determine;

1) If activation of platelets in whole blood with TRAP or histones would lead to the formation of MPA and to specifically assess the level of CD42b accumulation by monocytes following this treatment.
2) If platelet activation through these two different routes had any effect on the rate, or efficiency of MPA formation.
3) If there was preferential binding of platelets to a subset of monocytes following treatment with either agonist.

### 4.2.0 Methods

#### 4.2.1 MPA Formation in Whole Blood Following Treatment with TRAP, CTH or Human Recombinant Histone H4

Briefly CPDA anti-coagulated whole blood (from a healthy volunteer) was gently stirred and incubated at 37°C for up to 1 hour, either untreated or with 100µM or 10µM thrombin receptor activating peptide (TRAP) a protease receptor 1 (PAR1) signalling peptide (SLFFRN), between 0.25-1mg/ml calf thymus histones (CTH) or between 1-100µg/ml human recombinant histone H4. Analysis of MPA formation was determined using flow cytometry for the monocyte markers CD14, CD16 and the platelet marker CD42b (**Figure 4.1**). Statistical analysis was carried out using Graph Pad Prism version 5.0. (For further detail see methods section 2.3.1-2.3.5.)

### 4.3.0 Results

### 4.3.1 The Effect of Platelet Activation through PAR-1 Signalling on MPA Formation in Whole Blood

Our first aim was to determine if activation of platelets in whole blood could lead to MPA formation and specifically assess the CD42b accumulation by the monocyte population. We therefore used a high concentration of a well known and potent platelet agonist; TRAP. This (SLFFRN) peptide version of TRAP causes platelet activation by signalling through PAR-1. Following treatment of stirred whole blood at 37°C with 100µM TRAP and measurement of aggregation by dual coloured flow cytometry, there was a significant increase in MPA formation for both $CD14^{+}CD16^{-}$ and $CD14^{+}CD16^{+}$ monocyte subsets after 15 minute incubation compared to the 0 minute control (**Figures 4-2A and B**). A maximum of ~70% $CD14^{+}CD16^{-}$ monocytes were positive for the platelet marker CD42b after 60 minutes (**Figures 4-2A**). Whereas ~55% of $CD14^{+}CD16^{+}$ subset were positive for CD42b at this time point (**Figure 4-2B**). Figures 4-1A, B, 4-2A and B, show no significant increase in monocyte associated platelet markers are detected in samples incubated and stirred at 37°C for up to 60 minutes, without the addition of TRAP.

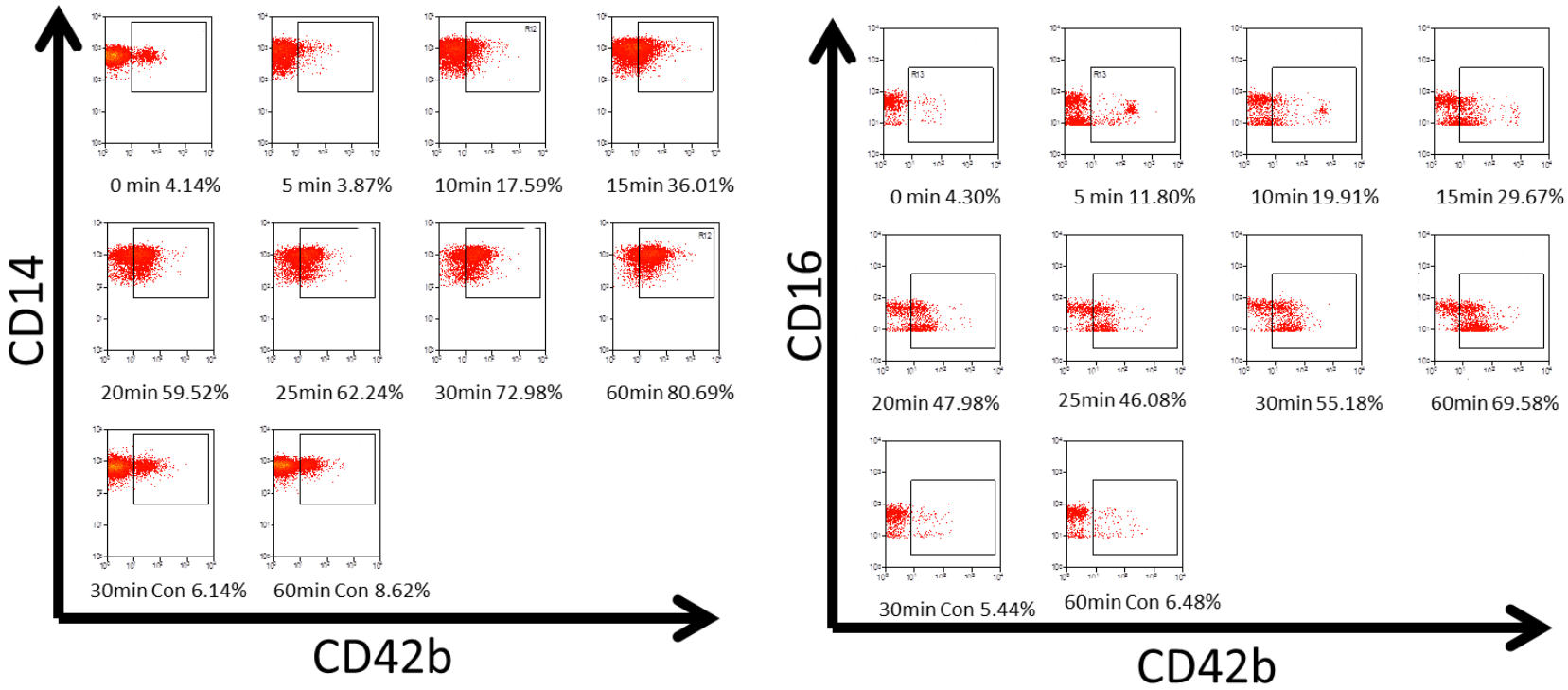


**Figure 4-1: MPA Formation in the Presence of 100µM TRAP**

Whole blood was fixed prior to treatment (0 minute) or incubated for up to 60 minutes at 37°C with or without 100µM TRAP. Monocyte-platelet aggregates (MPA) were detected using flow cytometry with antibodies against the platelet marker CD42b and monocyte markers CD14 and CD16. The flow cytometry plots in A) show the increase in percentage MPA over time for the $CD14^{+}CD16^{-}$ monocyte subset and B) $CD14^{+}16^{+}$ monocyte subset. (Representative experiment from data set of 3).

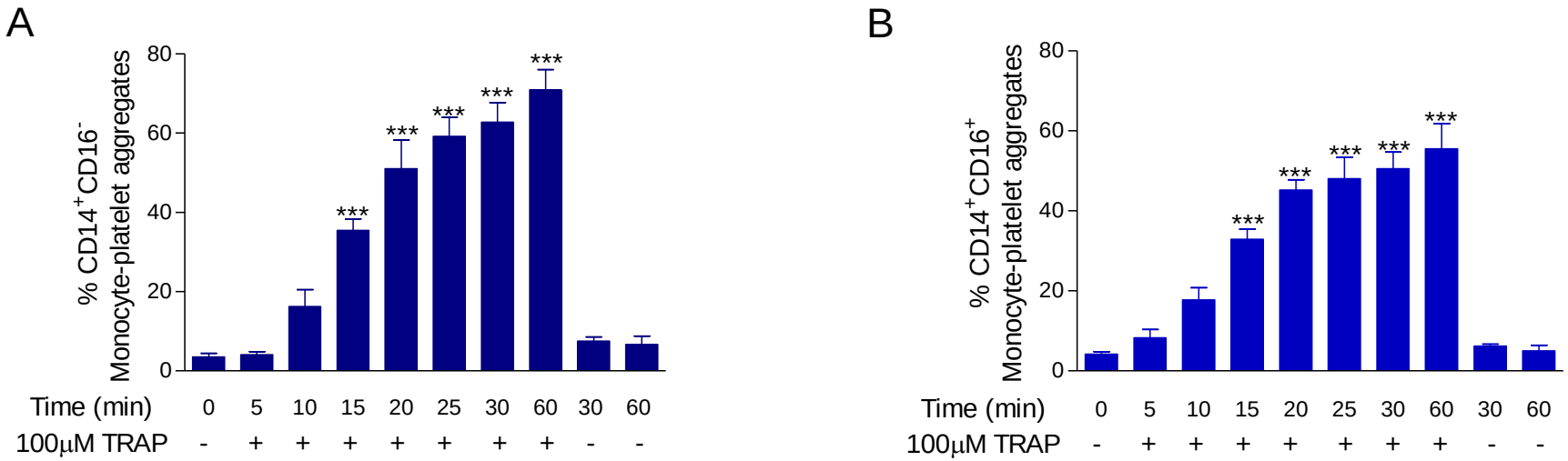


**Figure 4-2: MPA formation in whole blood after addition of 100µM TRAP**

Whole blood incubated with or without the addition of 100µM TRAP, at 37°C and mixed. The control (0) was fixed prior to any treatment. Data were acquired using flow cytometry. A significant increase in MPA formation after 15 minute incubation with TRAP was observed for A) the $CD14^{+}CD16^{-}$ monocyte population and B) the $CD14^{+}CD16^{+}$ monocyte population. Both monocyte subsets showed a significant increase in MPA formation over time (ANOVA $P<0.001$). *,** and *** indicate $P<0.05$, $P<0.01$ and $P<0.001$ respectively, post hoc test Dunnett's. Data are mean +/- SEM of 3 experiments.

### 4.3.2 Determining the level of CD42b accumulation by monocytes in response to platelet activation through PAR1

Having measured the efficiency of MPA formation (as a percentage of positive monocytes) in response to addition of TRAP to whole blood, we wanted to determine the accumulation of CD42b by monocytes. Figure 4-3 shows an example of the accumulation of platelet marker CD42b by the $CD14^{+}CD16^{-}$ monocyte population, over time, following treatment with TRAP. The increase in CD42b median fluorescent intensity (MFI) was surprisingly low, even at the 30 minute time point. Indeed, compared to the mean MFI of whole platelets from the same experiment, which have been included in this plot, the MFI for CD42b on TRAP induced MPA did not approach that of a single activated platelet (**Figure 4-3**). The effects of TRAP when visualised as a time course was even more surprising. This analysis showed that over time monocytes were accumulating CD42b in quanta, which were lower than individual platelets, but cumulative over the duration of the experiment (**Figure 4-4 and 4-5**). One possible explanation for this is that monocytes may be accumulating platelet derived microvesicles produced upon platelet activation, rather than binding whole platelets. Notably, on the $CD14^{+}CD16^{+}$ (but not the $CD14^{+}CD16^{-}$) monocytes there was an indication that low levels of monocytes were associated with a single or multiple platelets (small peaks with an MFI ≈ that of single platelets were observed on this subset at early time points). This response was transient and was lost after 15 minutes and was representative of rare interactions (**Figure 4-5**).

To further investigate the level of CD42b accumulation by monocytes over time we developed a gating strategy that would show CD42b accumulation (MFI) by monocytes following treatment with platelet agonists (see Methods chapter 2.3.3 for details). We termed the gate containing the low MFI the microvesicle gate and the gate containing high MFI the platelet gate.

After treatment with 100µM TRAP the MFI of CD42b on the $CD14^{+}CD16^{-}$ monocyte subset in the microvesicle gate increased over time reaching a maximum at 60 minutes (**Figure 4-4 and 4-6B**). The percentage of events in this gate also increased over time (**Figure 4-6D**). There was no change in MFI or percentage positive cells in the untreated controls (**Figure 4-6 B and D**). The MFI shown in the platelet-monocyte gate never reached that of a resting platelet (**Figure 4-6C**). Indeed, the increase in percentage events, which is detected over time is due to the tail of the low MFI peak drifting into this gate (**Figure 4-6E**). There was no change in the MFI or percentage of events in any untreated samples (**Figure 4-6C and E**). The data suggests that $CD14^{+}CD16^{-}$ monocytes may possibly accumulate PMV in this instance.

The formation of MPA on $CD14^{+}CD16^{+}$ monocytes was qualitatively different for the $CD14^{+}CD16^{-}$ subset. Here, after treatment with 100µM TRAP the MFI of CD42b in the microvesicle gate reached a maximum at 60 minutes (**Figure 4-7B**). The percentage of events in the microvesicle gate also showed an increase over time (**Figure 4-7D**). The MFI in the platelet gate was higher than that of a resting platelet between 5-15 minutes although the percentage of events in this gate remained low (**Figure 4-7C and 4-7E**). This indicates that a small number of the $CD14^{+}CD16^{+}$ monocytes may be binding one or more whole platelets during this part of the time course. There was no change in MFI or percentage events for any of the untreated controls (**Figure 4-7B, C,D and E**).

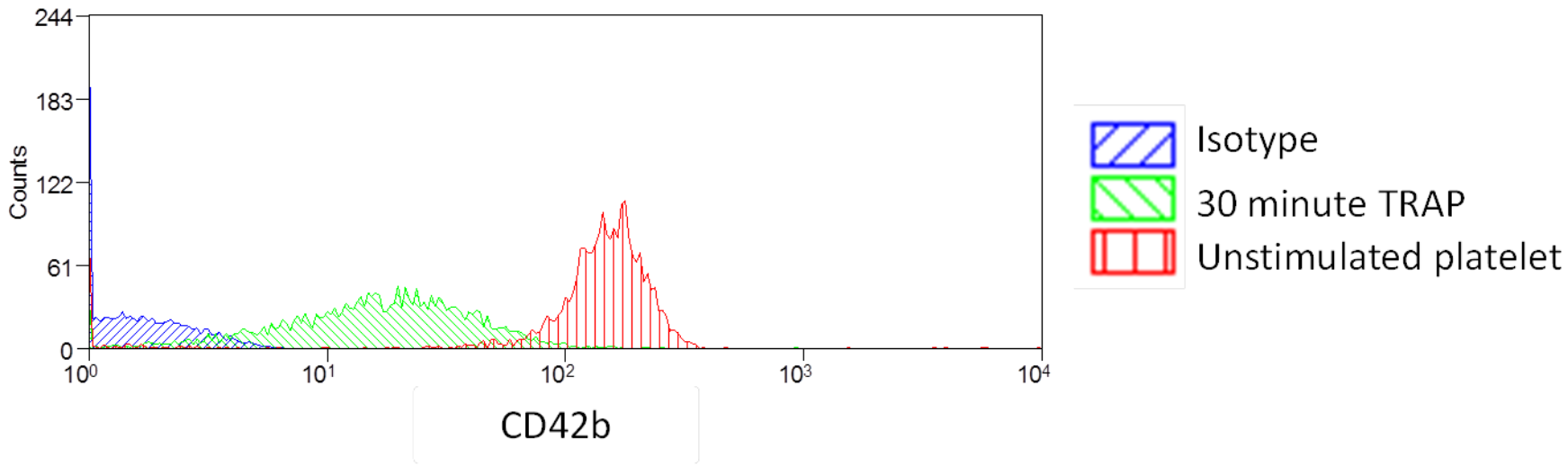


**Figure 4-3: Flow cytometry overlay showing CD42b MFI of resting platelet and MPA formed after treatment with 100µM TRAP**

Whole blood was fixed prior to any treatment and the CD42b MFI of resting platelets was determined. Whole blood was incubated at 37°C for 30 minutes with 100µM TRAP. Monocytes were identified by CD14, CD16 expression and CD42b MFI of monocyte-platelet aggregates was detected. The overlay demonstrates the CD42b MFI of $CD14^{+}CD16^{-}$ monocyte subset does not reach that of a resting platelet.

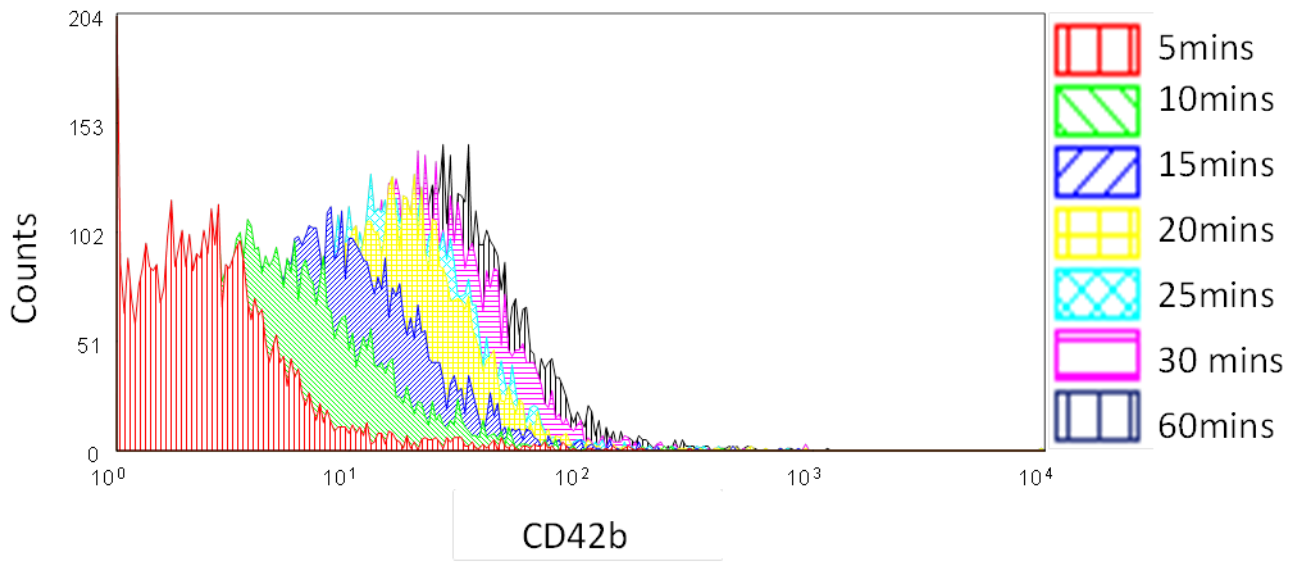


**Figure 4-4: Flow cytometry overlay indicating CD42b expression on the $CD14^+CD16^-$ monocyte population after treatment with 100µM TRAP**

Whole blood was incubated at 37°C for up to 60 minutes with 100µM TRAP. Monocytes were identified by CD14, CD16 expression and CD42b on monocyte-platelet aggregates was detected. The overlay demonstrates the CD42b on the $CD14^+CD16^-$ monocyte subset increases over time but remains low. (Data shows 1 representative experiment from 3).

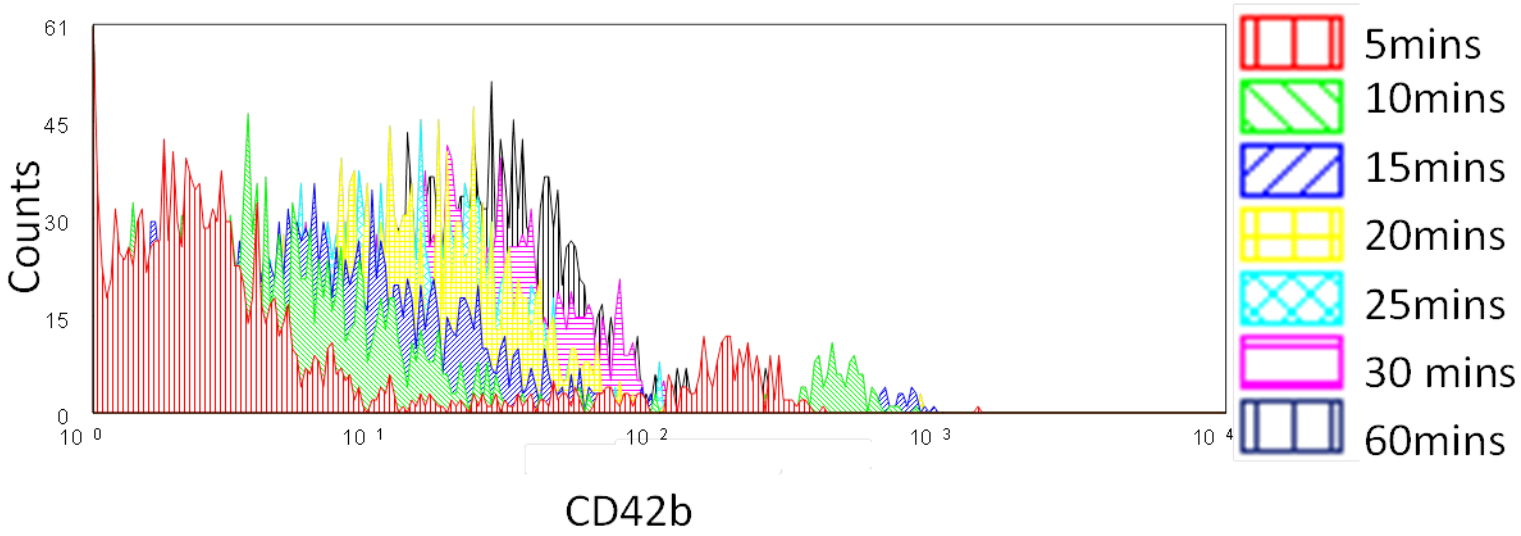


**Figure 4-5: Flow cytometry overlay indicating CD42b expression on the $CD14^{+}CD16^{+}$ monocyte population after treatment with 100µM TRAP**

Whole blood was incubated at 37°C for up to 60 minutes with 100µM TRAP. Monocytes were identified by CD14 and CD16 expression and CD42b on monocyte-platelet aggregates was detected. The overlay demonstrates the CD42b on $CD14^{+}CD16^{+}$ monocytes increases over time but remains low. However, smaller peaks with a high MFI at 5mins, 10mins and 15mins were observed. (Data shows 1 representative experiment from 3).

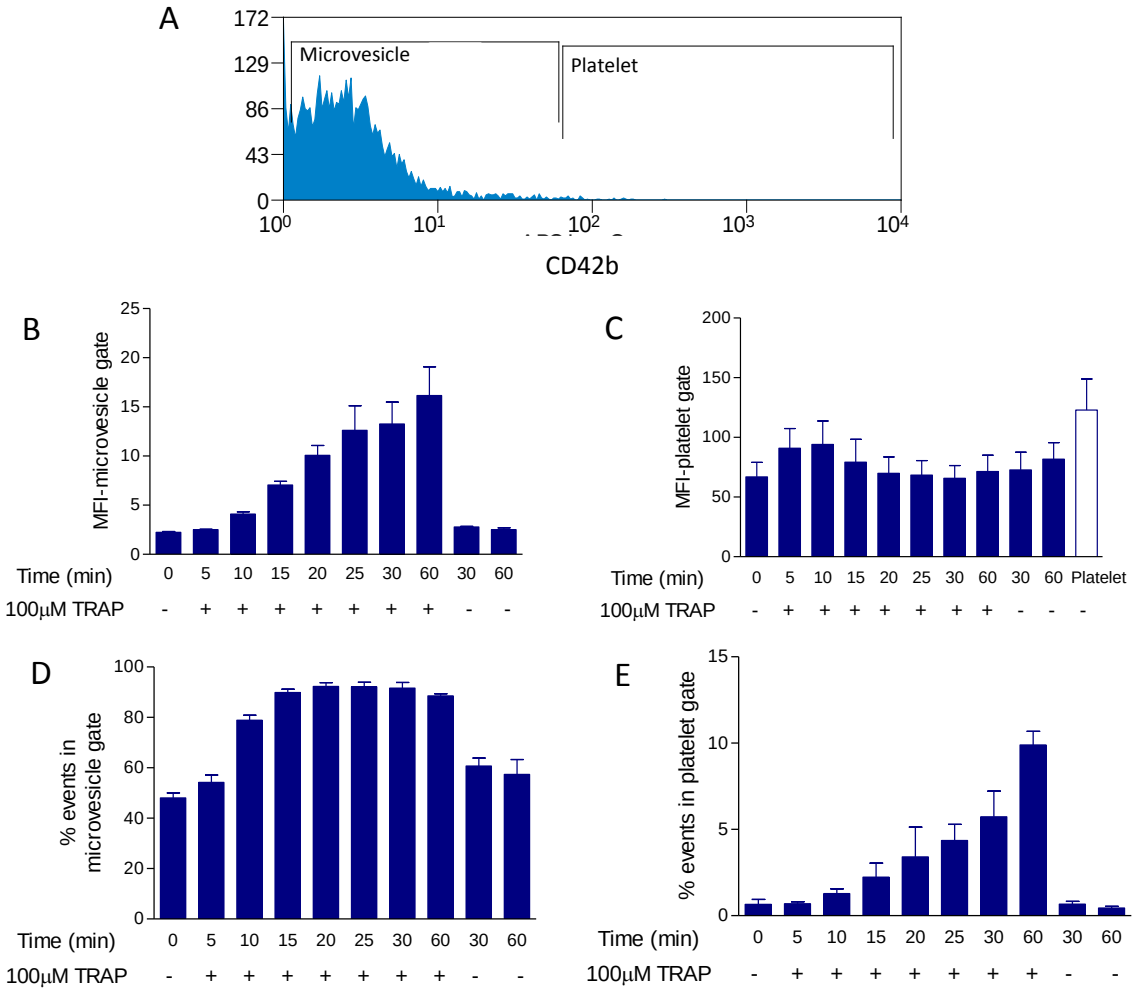


**Figure 4-6: CD42b expression on the CD14$^+$CD16$^-$ monocyte population after treatment with 100μM TRAP**

Whole blood was incubated with or without the addition of 100μM TRAP at 37°C and mixed. Control (0) was fixed prior to any treatment. Data were acquired using flow cytometry. A) Demonstrates the gating strategy at the 5 minute time point. B) and D) show an increase in the CD42b MFI and percent positive cells respectively, in the microvesicle gate, over time, for the CD14$^+$CD16$^-$ monocyte population. C) Shows the CD42b MFI in the platelet gate, E) demonstrates the increase in percent positive cells in the platelet gate over time. Data are mean +/- SEM of 3 experiments.

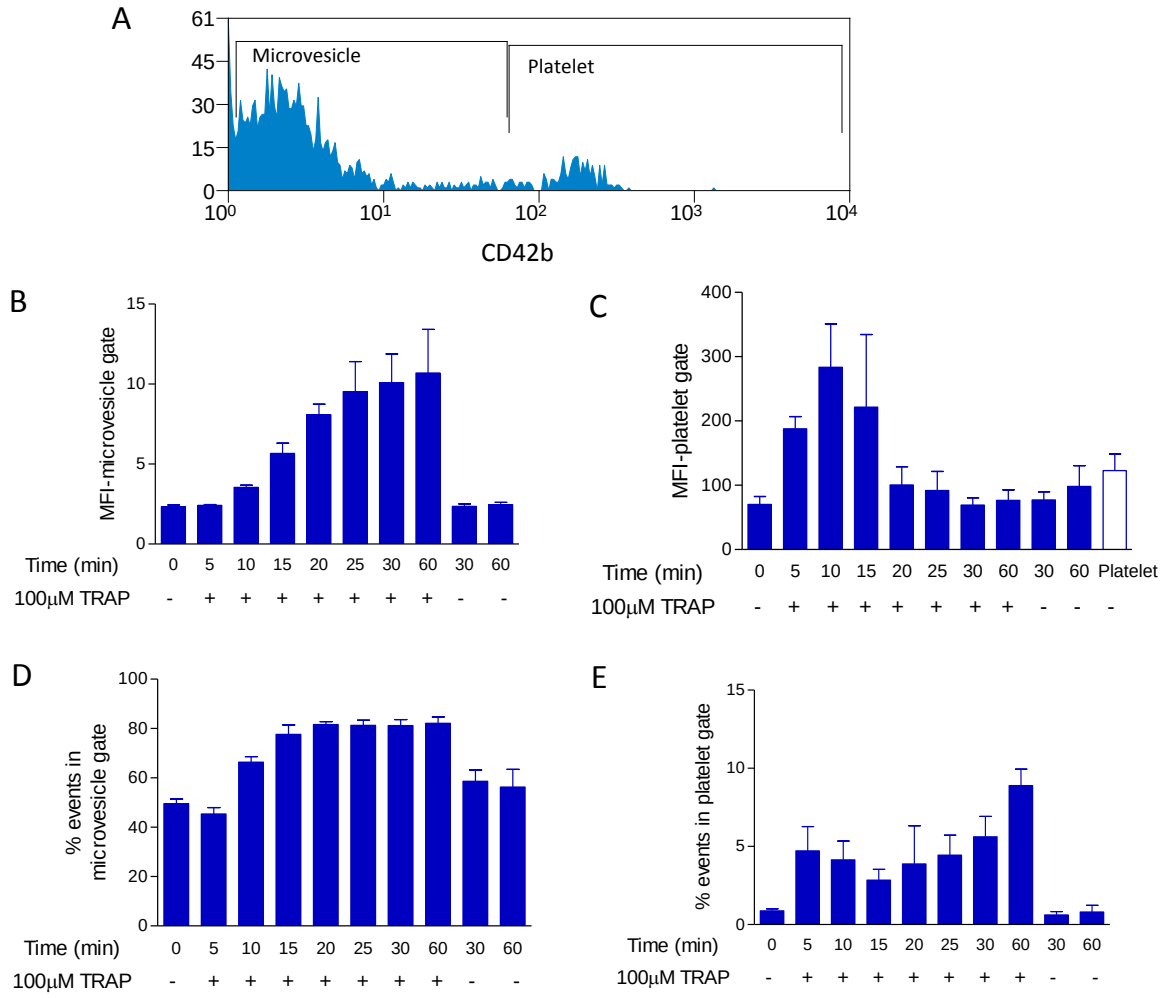


**Figure 4-7: CD42b expression on the $CD14^{+}CD16^{+}$ monocyte population after treatment with 100μM TRAP**

Whole blood was incubated with or without the addition of 100μM TRAP at 37°C and mixed. Control (0) was fixed prior to any treatment. Data were acquired using flow cytometry. A) Shows the gating strategy at the 5 minute time point. B) and D) show the increase in the CD42b MFI and percentage of positive events, respectively, in the microvesicle gate, over time, for the $CD14^{+}CD16^{+}$ monocyte subset. C) Shows that a small number of $CD14^{+}CD16^{+}$ MPA have a CD42b MFI higher than that of a resting platelet following 5-15 minutes treatment. E) Shows an increase in percent positive cells in the platelet gate over time. Data are mean +/- SEM of 3 experiments.

### 4.3.3 The effect of a lower concentration of TRAP on MPA formation in whole blood

Having demonstrated that activation of platelets in whole blood through the PAR-1 pathway leads to an increase in MPA formation over time and that monocyte accumulation of CD42b is lower than that of a resting platelet in most instances. We now wanted to find out if a lower concentration of PAR-1 agonist, TRAP (10µM) would have a similar effect. A significant increase in MPA formation compared to 0 minute control was detected for both monocyte subsets after 10 minute incubation with TRAP (**Figure 4-8 A and B**).

We now wanted to assess the accumulation of the platelet specific marker, CD42b, by both monocyte populations. Firstly, the $CD14^{+}CD16^{-}$ subset showed an increase in CD42b MFI in the microvesicle gate (**Figure 4-9A**). This suggests potential accumulation of PMV over time. At 30-60 minutes the MFI reaches that of a resting platelet (**Figure 4-9B**). However, this should be interpreted with caution as the MFI of a resting platelet is surprisingly low in this instance (**Figure 4-9B**).

The $CD14^{+}CD16^{+}$ monocyte subset again shows an increase in CD42b MFI over time (**Figure 4-10B**). Again, suggesting potential accumulation of PMV over time. After 5-10 minute treatment with 10µM TRAP the CD42b MFI is far greater than that of a resting platelet indicating that at these early time points, platelets may in fact be adhering to monocytes (**Figure 4-10B**). The CD42b MFI remains close to that of a resting platelet throughout the time course. However, the data should be interpreted with caution as the resting platelet MFI is low in this instance (**Figure 4-10B**).

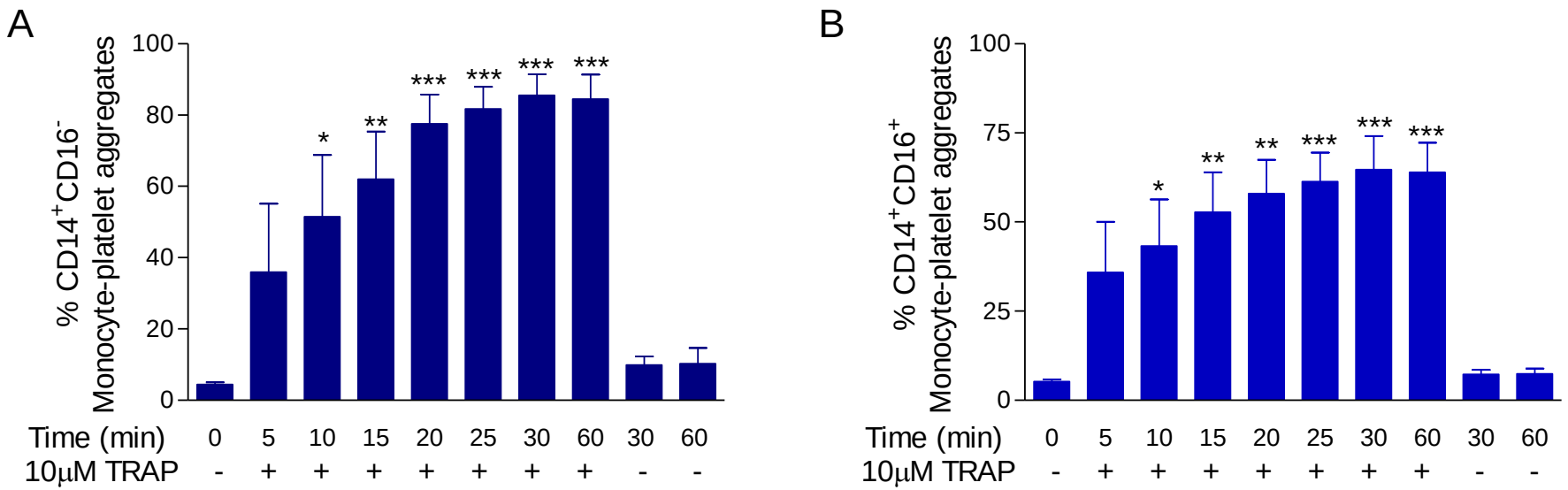


**Figure 4-8: MPA formation in whole blood after addition of 10μM TRAP**

Whole blood was incubated with or without the addition of 10μM TRAP at 37°C and mixed. Control (0) blood was fixed prior to any treatment. Data were acquired using flow cytometry. A significant increase in MPA formation after 10 minute incubation with TRAP compared to (0) control was demonstrated for A) the $CD14^+CD16^-$ monocyte population and B) the $CD14^+CD16^+$ monocyte population. Both monocyte subsets showed a significant increase in MPA formation over time (ANOVA $P<0.001$). *,** and *** indicate $P<0.05$, $P<0.01$ and $P<0.001$ respectively, post hoc test Dunnett's. Data are mean +/- SEM of 4 experiments.

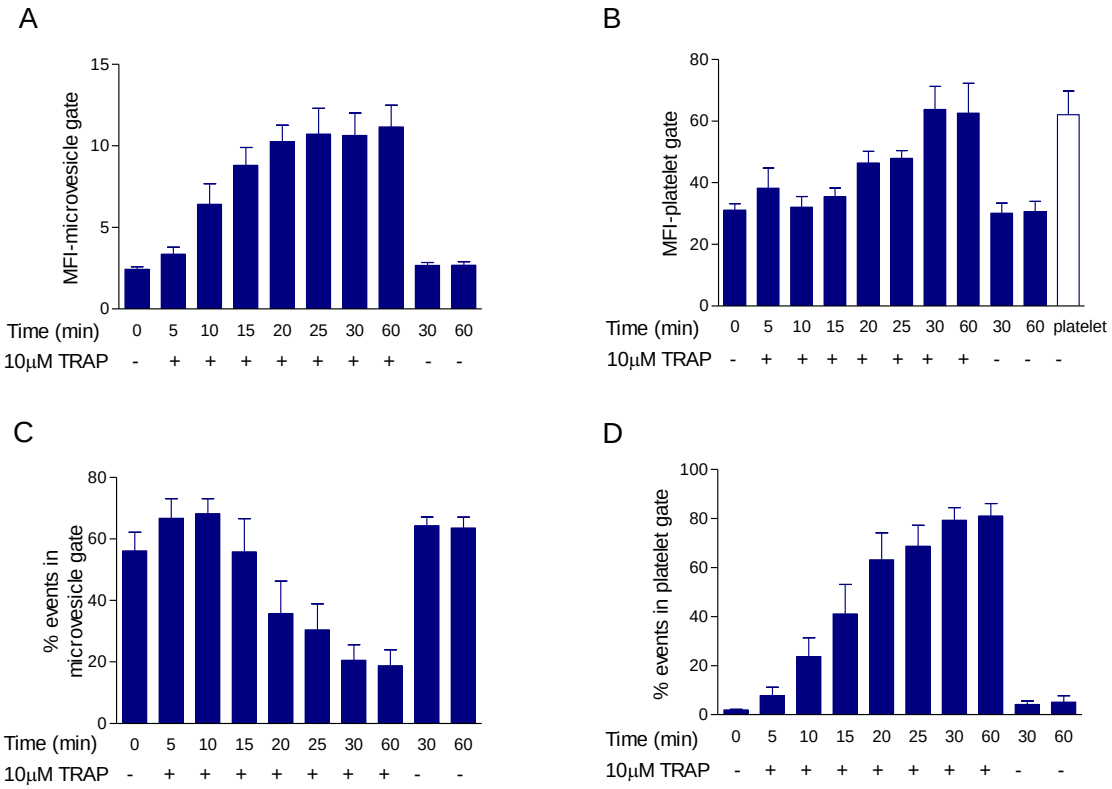


**Figure 4-9: CD42b expression on the $CD14^{+}CD16^{-}$ monocyte population after treatment with 10μM TRAP**

Whole blood was incubated with or without the addition of 10μM TRAP at 37°C and mixed. Control (0) was fixed prior to any treatment. Data were acquired using flow cytometry. A) Shows the increase in the CD42b MFI in the microvesicle gate for the $CD14^{+}CD16^{-}$ monocyte population, over time. B) Shows the CD42b MFI of the $CD14^{+}CD16^{-}$ MPA is equal to that of a resting platelet following 30-60 minutes treatment with TRAP. C) Shows a decrease in CD42b positive events in the microvesicle gate over time and D) shows an increase in the percent positive events in the platelet gate over time. Data are mean +/- SEM of 4 experiments.

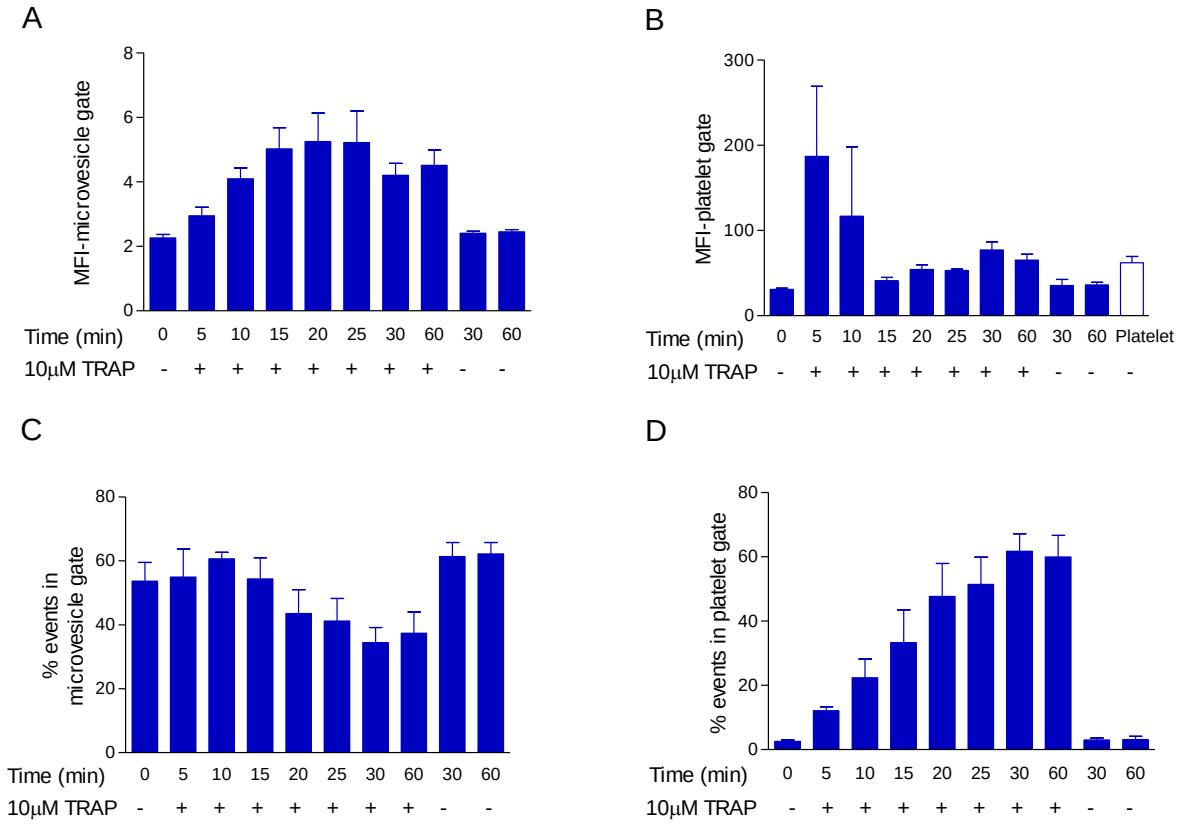


**Figure 4-10: CD42b expression on the CD14$^+$CD16$^+$ monocyte population after treatment with 10μM TRAP**

Whole blood was incubated with or without the addition of 10μM TRAP at 37°C and mixed. Control (0) fixed prior to any treatment. Data were acquired using flow cytometry. A) Shows the increase in the CD42b MFI in the microvesicle gate for the CD14$^+$CD16$^+$ monocyte population over time. B) Shows the CD42b MFI on the CD14$^+$CD16$^+$ monocyte population is higher than a resting platelet following 5-10 minute treatment and remains roughly equal to that of a resting platelet throughout the remainder of the time course. C) Shows a decrease in percentage of CD42b positive events in the microvesicle gate over time and D) shows an increase in the percentage of CD42b positive events in the platelet gate over time. Data are mean +/- SEM of 4 experiments.

### 4.3.4 Determining the level of MPA formation in whole blood in response to treatment with calf thymus histones

Having determined that MPA form in whole blood in response to platelet activation through a well known signalling pathway (PAR-1), we now wanted to find out if activating platelets using a very different signalling pathway would lead to an increase in MPA formation. It is thought that histones activate platelets through charge based interactions and through TLR-2 and TLR-4 receptors (Semeraro et al., 2011), thus we used histones derived from calf thymus (CTH) to stimulate whole blood.

After 60 minutes of incubation of whole blood with CTH no significant increase in MPA can be detected compared to the 0 minute control for the $CD14^{+}CD16^{-}$ monocyte subset (**Figure 4-11A**). However, in contrast to this, a significant increase in MPA formation can be detected for the $CD14^{+}CD16^{+}$ subset as early in the time course as 5 minutes (**Figure 4-11B**). This increase remains fairly constant, between 25-35% MPA formation throughout (**Figure 4-11B**). Again, there is no significant increase in MPA in blood which has been incubated for up to 60 minutes, without the addition of any CTH (**Figure 4-11A and B**).

We now wanted to assess the level of CD42b accumulation by monocytes following treatment with CTH. Figure 4-12 demonstrates that there is no change in the platelet marker, CD42b MFI of the $CD14^{+}CD16^{-}$ subset over time after treatment with CTH. However, figure 4-13 indicates that after treatment with CTH a separate CD42b positive peak can be detected between 5-60 minutes for the $CD14^{+}CD16^{+}$ subset. Further analysis revealed that the CD42b MFI of this subset equalled the CD42b MFI of a resting platelet, after 10 minute treatment with CTH (**Figure 4-14B**). The percentage of events appearing in this gate remains above 8% throughout the time course (**Figure 4-14 D**). This suggests that the $CD14^{+}CD16^{+}$ monocyte subset are most

likely binding platelets. This time there is very little change in the CD42b MFI in the microvesicle gate and very little change in the percentage of the events occurring in this gate (**Figure 4-14A and C**). This suggests that in this instance PMV adhesion to monocytes has very little, to no role in MPA formation upon platelet activation with CTH.

### 4.3.5 MPA formation after five minute treatment with calf thymus histones

After demonstrating that five minute (300s) treatment of whole blood incubated and stirred at 37°C with CTH leads to an almost maximum response in $CD14^{+}CD16^{+}$ monocyte-platelet aggregate formation, we decided to further study the effect CTH had on MPA formation within five minutes. Blood incubated for 300s without the addition of CTH showed no significant increase in MPA formation compared to 0 minute control, for both monocyte subsets (**Figure 4-15A and B**).

After 5s incubation with CTH (agonist added at room temperature and fixed after 5s) a significant increase can be seen compared to 0 minute control for the $CD14^{+}CD16^{-}$ monocyte subset (**Figure 4-15A**). A significant increase can also be detected after 30s treatment with CTH for both monocyte subsets (**Figure 4-15A and B**). This is the maximum response observed for both subsets. $CD14^{+}CD16^{-}$ showed ~15% MPA formation and $CD14^{+}CD16^{+}$ ~50% MPA formation (**Figure 4-15A and B**). A similar result to that observed in a previous time course was again seen after 300s (5 minutes) treatment with CTH, ~25% MPA formation for the $CD14^{+}CD16^{+}$ monocyte subset but no effect on the $CD14^{+}CD16^{-}$ monocyte subset (**Figure 4-11 A, B and 4-15A and B**).

Having demonstrated that MPA form (for both monocyte subsets) after 5-30s treatment with CTH, we wanted to determine the accumulation of CD42b by monocytes. Figure 4-16A and C demonstrate an increase in the CD42b MFI and the percentage of events occurring in this gate after 5 and 30s treatment with CTH. It could be that the $CD14^{+}CD16^{-}$ monocyte subset may be

accumulating platelet derived microvesicles at these early time points. Figure 4-16 B and D suggests that it is unlikely that whole platelets are binding to this monocyte subset, as the MFI never reaches that of a resting platelet, despite the small increase in the percentage of events occurring in that gate after 5 and 30s. In this instance a similar pattern is seen with the $CD14^{+}CD16^{+}$ monocyte subset (**Figure 4-17A-D**).

### 4.3.6 Titration of CTH and the effect on MPA formation in whole blood

After finding 30 minutes incubation with 1mg/ml CTH caused a significant increase in MPA formation for the $CD14^{+}CD16^{+}$ monocyte subset, which appeared to be mainly due to platelet adhesion, in this instance. We now wanted to find out if a lower concentration of CTH could have a significant effect on heterotypic aggregate formation at this time point. We could not detect significant increases in the formation of MPA at concentrations below 1mg/ml, for either subset of monocytes (**Figure 4-18A and B**).

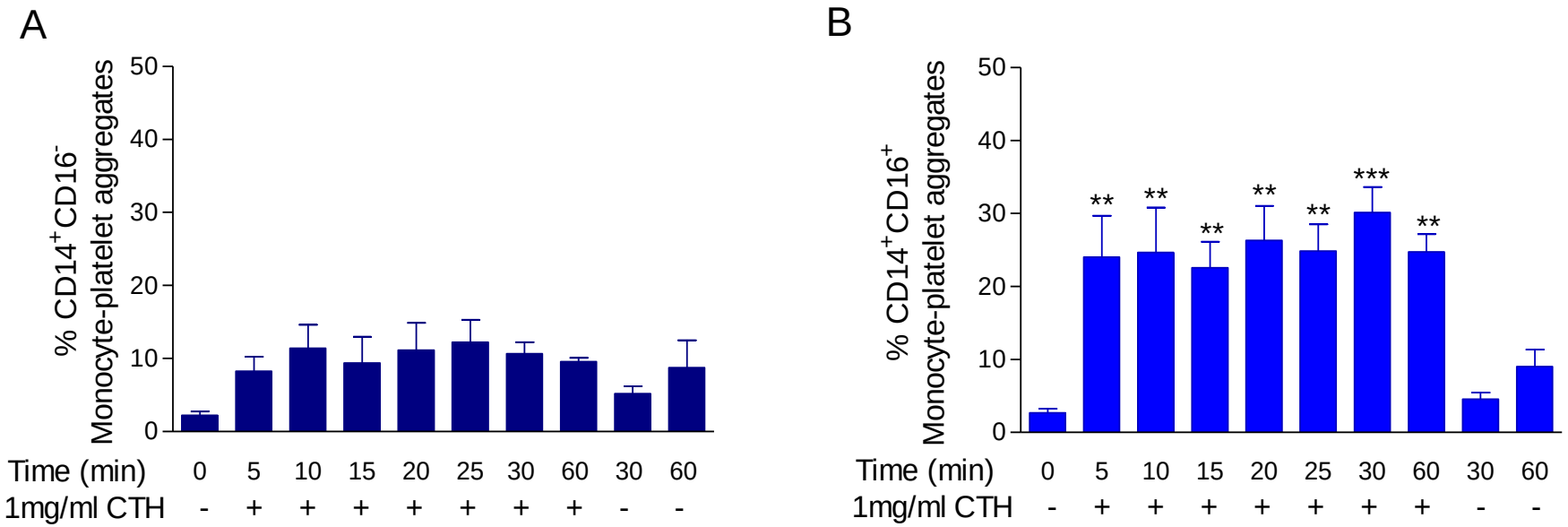


**Figure 4-11: MPA formation in whole blood after addition of 1mg/ml CTH**

Whole blood was incubated with or without the addition of 1mg/ml CTH, at 37°C and mixed. The control (0) was fixed prior to any treatment. Data were acquired using flow cytometry. A) No significant increase in MPA formation can be seen compared to 0 minute (untreated) control for the $CD14^+CD16^-$ monocyte population. B) A significant increase in MPA formation can be detected after 5 minute treatment with CTH for the $CD14^+CD16^+$ monocyte population. Treatment of the $CD14^+CD16^+$ monocyte subset with CTH showed a significant effect on MPA formation over time (ANOVA $P<0.001$). *,** and *** indicate $P<0.05$, $P<0.01$ and $P<0.001$ respectively, post hoc test Dunnett's. Data are mean +/- SEM of 3-4 experiments.

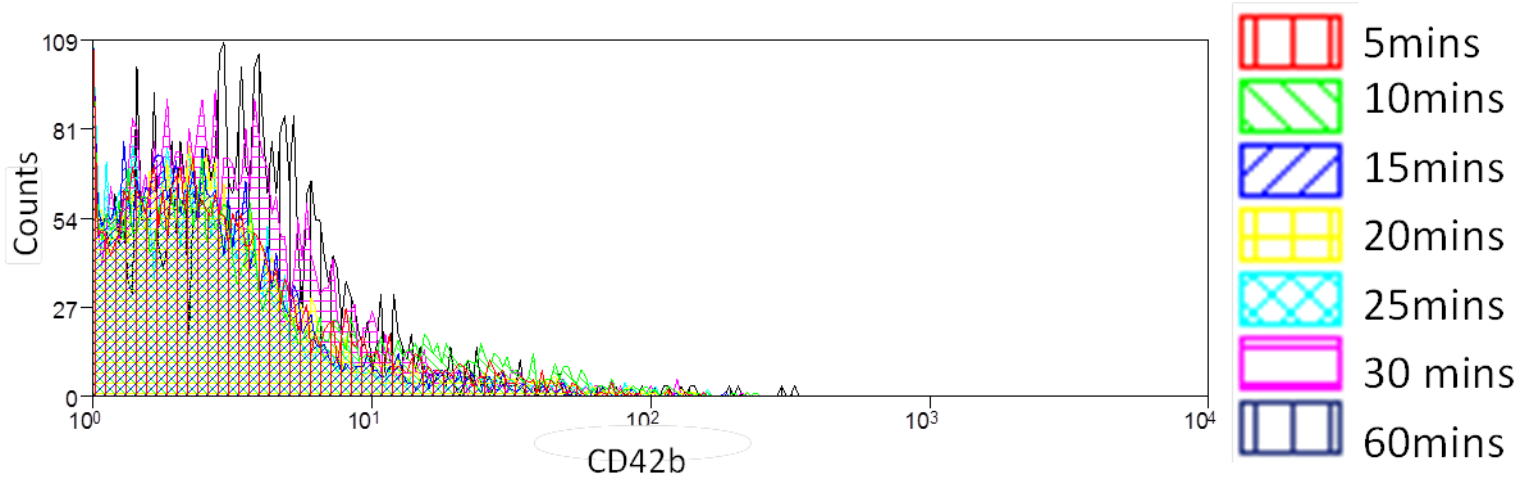


**Figure 4-12: Flow cytometry overlay indicating CD42b expression on the $CD14^+CD16^-$ monocyte population after treatment with 1mg/ml CTH**

Whole blood was incubated at 37°C for up to 60 minutes with 1mg/ml CTH. Monocytes were identified by CD14, CD16 expression and CD42b MFI on monocyte-platelet aggregates was detected using flow cytometry. The overlay demonstrates the CD42b MFI on $CD14^+CD16^-$ monocyte subset does not change over time. (Data shows 1 representative experiment from 4).

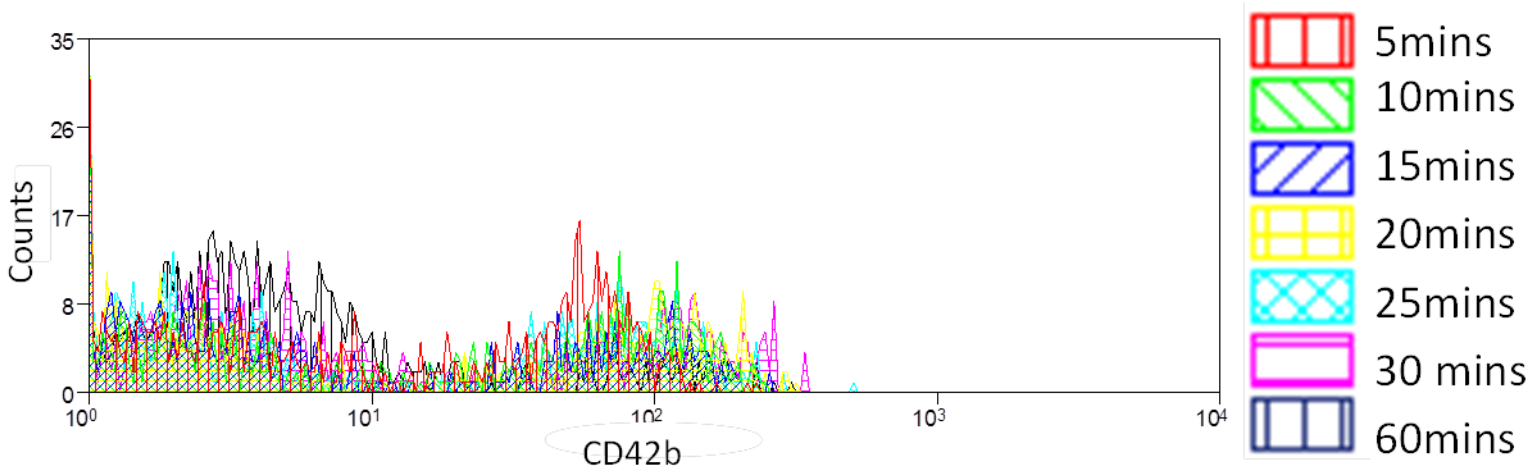


**Figure 4-13: Flow cytometry overlay indicating CD42b expression on the $CD14^+CD16^+$ monocyte population after treatment with 1mg/ml CTH**

Whole blood was incubated at 37°C for up to 60 minutes with 1mg/ml CTH. Monocytes were identified by CD14, CD16 expression and CD42b MFI on monocyte-platelet aggregates was detected using flow cytometry. The overlay demonstrates the CD42b MFI on $CD14^+CD16^+$ monocyte subset is increased after treatment with CTH and remains the same throughout the time course. (Data shows 1 representative experiment from 4).

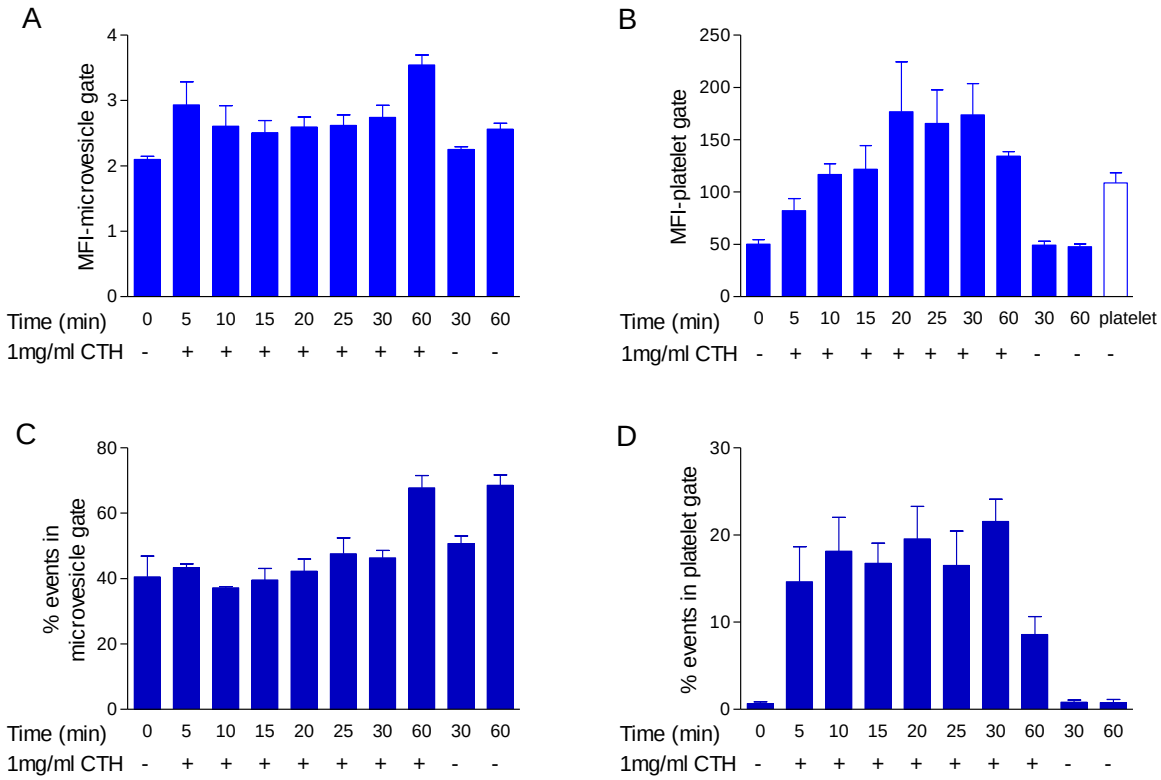


**Figure 4-14: CD42b expression on the CD14$^{+}$CD16$^{+}$ monocyte population after treatment with 1mg/ml CTH**

Whole blood was incubated at 37°C with or without 1mg/ml CTH, control (0) fixed prior to treatment, data were acquired using flow cytometry. A) and C) shows no change in the CD42b MFI or events occurring in the microvesicle gate, respectively, for the CD14$^{+}$CD16$^{+}$ monocyte population. B) Shows the CD42b MFI is higher than a resting platelet following 10-60 minute treatment with CTH D) shows an increase in the percentage of events occurring in the platelet gate compared to untreated blood.

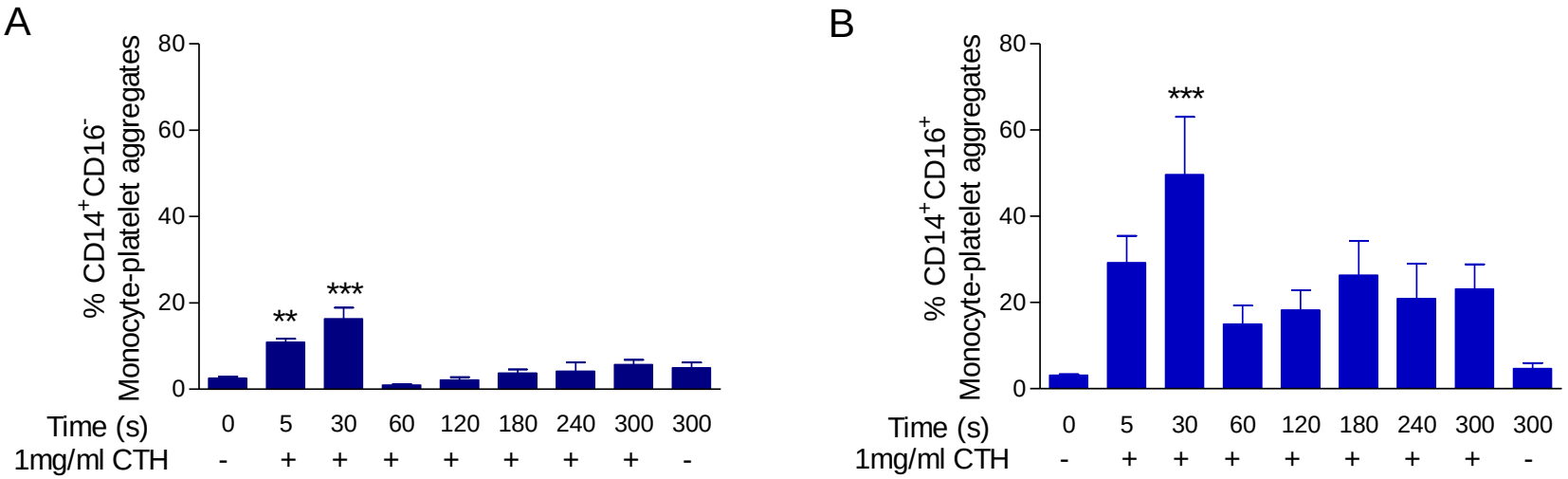


**Figure 4-15: MPA formation in whole blood after addition of 1mg/ml CTH**

Whole blood was incubated at 37°C with or without 1mg/ml CTH, control (0) fixed prior to treatment, MPA were detected using flow cytometry. A) $CD14^{+}CD16^{-}$ monocyte population and B) $CD14^{+}CD16^{+}$ monocyte population both show a significant change in MPA formation over time, ANOVA $P<0.001$ and ANOVA $P<0.01$, respectively. (*,** and *** indicate $P<0.05$, $P<0.01$ and $P<0.001$ respectively, compared to 0 minute, blood fixed prior to any treatment, post hoc test Dunnett's.) Data are mean +/- SEM of 3 experiments.

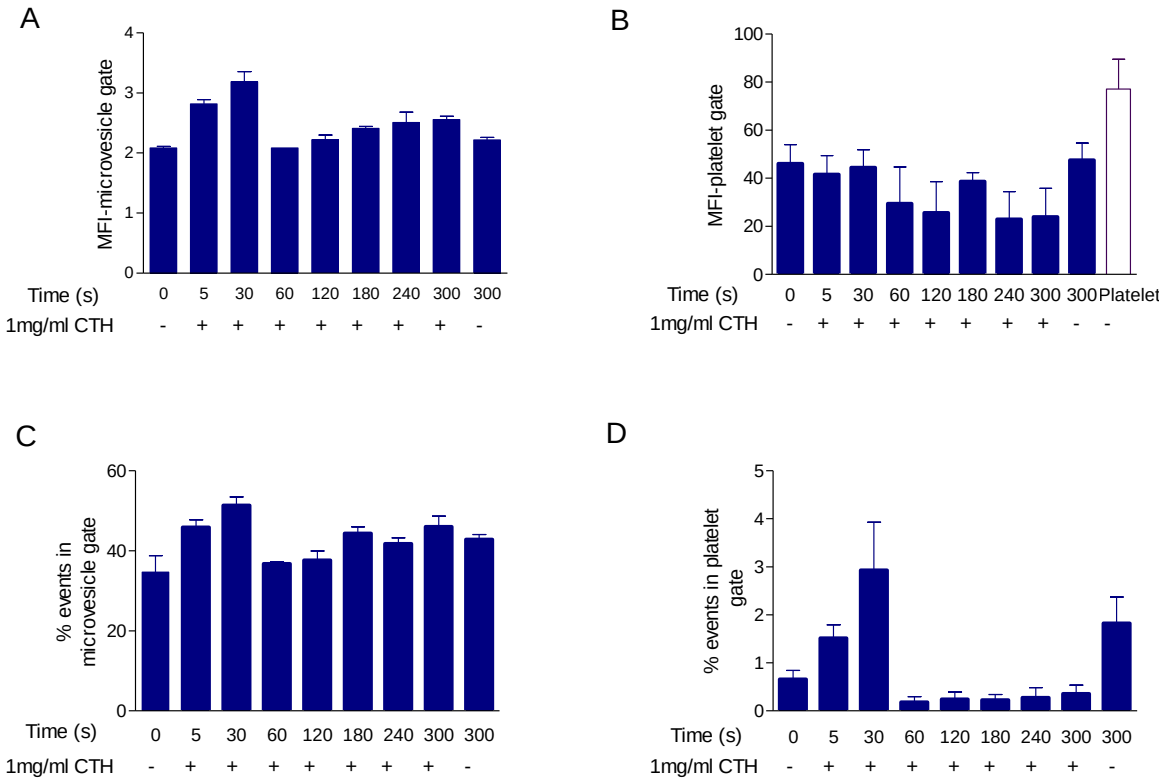


**Figure 4-16: CD42b expression on $CD14^{+}CD16^{-}$ monocyte population after treatment with CTH**

Whole blood was incubated at 37°C with or without 1mg/ml CTH. Control (0) was fixed prior to treatment. Data were acquired using flow cytometry. A) and C) demonstrate a small increase in CD42b MFI and percent positive cells, respectively, in the microvesicle gate, after 5-30s treatment with CTH, for the $CD14^{+}CD16^{-}$ monocytes. B) Demonstrates that the MFI of $CD14^{+}CD16^{-}$ MPA never reaches that of a resting platelet, D) demonstrates an increase in percent CD42b positive $CD14^{+}CD16^{-}$ MPA in the platelet gate at 5s and 30s. Data are mean +/- SEM of 3 experiments.

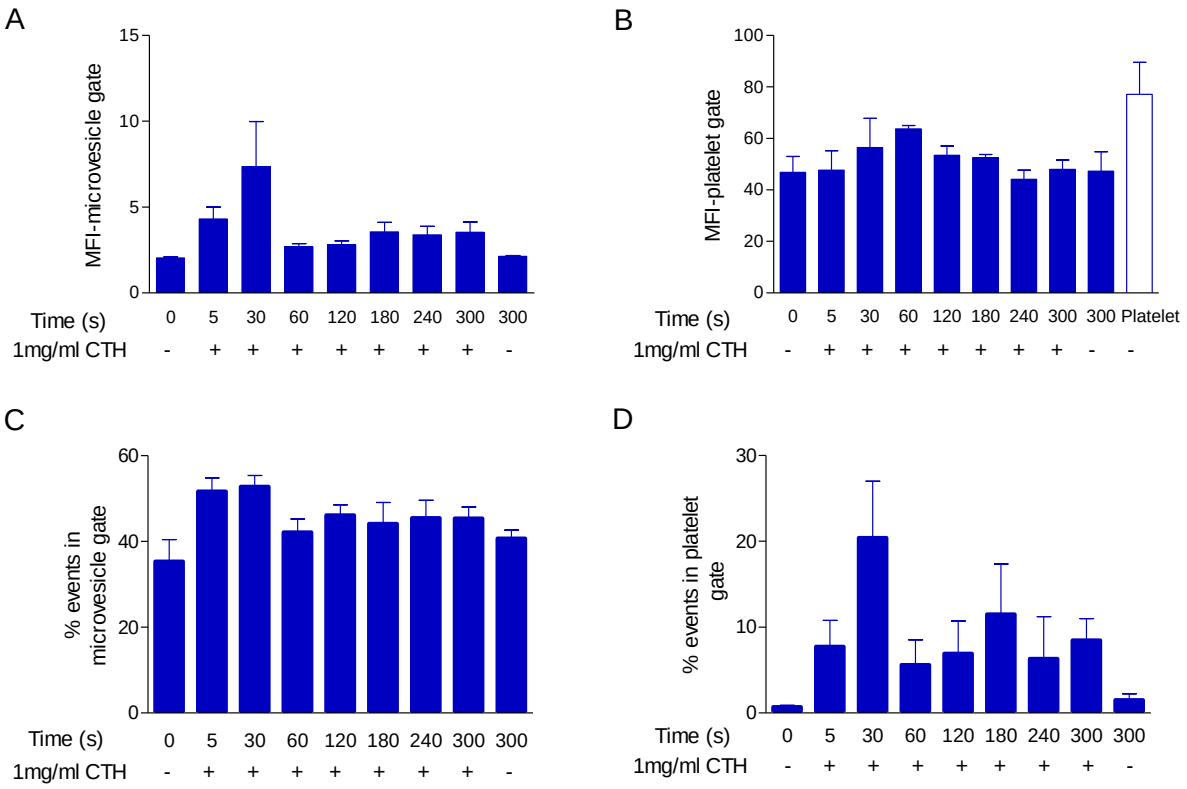


**Figure 4-17: CD42b expression on $CD14^+CD16^+$ monocyte population after treatment with CTH**

Whole blood was incubated at 37°C with or without 1mg/ml CTH. Control (0) was fixed prior to treatment. Data were acquired using flow cytometry. A) indicates that the $CD14^+CD16^+$ MPA have a small increase in CD42b MFI in the microvesicle gate following 5-30s treatment with CTH, C) shows an increase in percent positive cells in this gate, at 5 and 30s time points. B) Shows that the CD42b MFI of $CD14^+CD16^+$ MPA never reaches that of a resting platelet, although D) demonstrates a large increase in CD42b percent positive cells in this gate at 5s and 30s. Data are mean +/- SEM of 3 experiments.

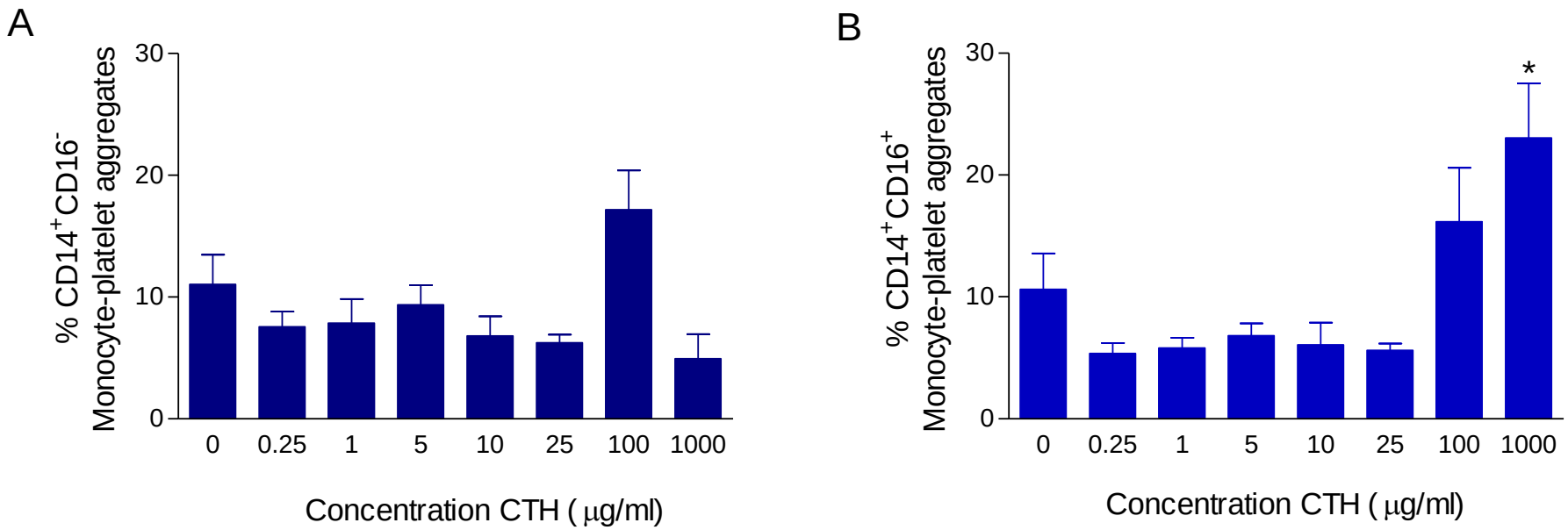


**Figure 4-18: Titration of calf thymus histones and their effect on MPA formation**

Whole blood was incubated and stirred at 37°C for 30 minutes with varying concentrations of calf thymus histones. The control (0) indicates untreated whole blood also incubated for 30 minutes. Data were acquired using flow cytometry for monocyte markers CD14, CD16 and the platelet marker CD42b. A) $CD14^{+}CD16^{-}$ monocyte population, (ANOVA $P<0.01$) demonstrates a significant effect of increasing concentration of CTH on MPA formation. B) $CD14^{+}CD16^{+}$ monocyte population, ANOVA ($P<0.001$) indicates a significant effect of increasing CTH concentration on MPA formation. (*,** and *** indicate $P<0.05$, $P<0.01$ and $P<0.001$ respectively, compared to 0μg/ml, post hoc test Dunnett's.) Data are mean +/- SEM of 5-6 experiments.

### 4.3.7 MPA formation after treatment with recombinant human histone H4

Having demonstrated (using CTH) that histones are able to induce MPA formation in whole blood we decided to use a more biologically relevant version of histones for a human system, recombinant human histone H4. H4 was chosen as it has been previously demonstrated to activate platelets (Semeraro et al., 2011). Treatment with 100µg/ml H4 was shown to significantly increase percentage MPA formation for both monocyte subsets after 30 minutes compared to untreated controls (**Figure 4-19 A and B**). There was no significant increase in MPA formation for either subset after treatment with a lower concentration of H4 (**Figure 4-19A and B).**

After finding a significant increase in percentage MPA formation after treatment of whole blood with 100µg/ml H4 histones, we wanted to assess the CD42b accumulation by the monocyte subsets. After treatment with 100µg/ml H4, figure 4-20 and 4-21 show that in this instance, MPA appear to have a CD42b MFI similar to that of a resting platelet. Interestingly, we observed a similar pattern of response for the $CD14^{+}CD16^{+}$ monocyte subset and the $CD14^{+}CD16^{-}$ monocytes. This is of interest, as it indicates that there is a qualitative difference in the response of human cells to histones derived from different species.

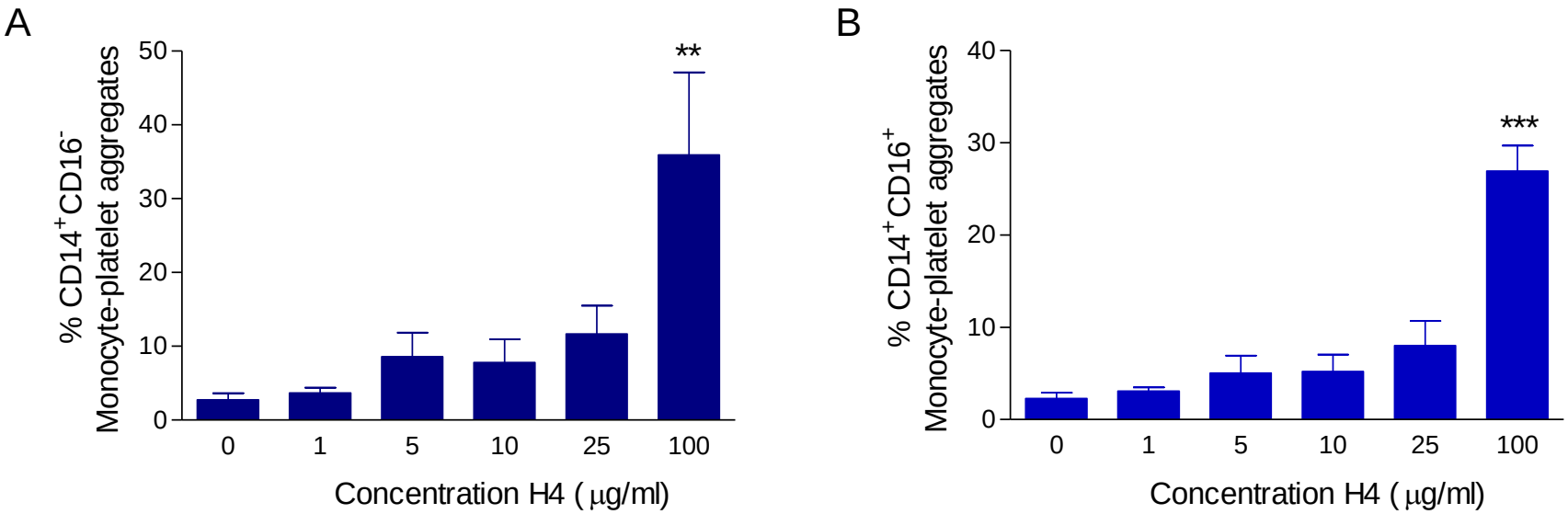


**Figure 4-19: Titration of recombinant histone H4 and its effect on MPA formation in whole blood**

Whole blood was incubated and stirred at 37°C for 30 minutes with between 1-100μg/ml human recombinant H4 histone. The control (0μg/ml) also incubated for 30 minutes without the addition of any agonist. Data were acquired using flow cytometry. A) Shows percentage MPA formation $CD14^+CD16^-$ monocyte subset, ANOVA ($P<0.01$), indicates an increase in MPA formation in response to increasing H4 concentration. B) Shows percentage MPA formation for the $CD14^+CD16^+$ monocyte subset, ANOVA ($P<0.001$), indicates an increase in MPA formation in response to increasing H4 concentration. (*,** and *** indicate $P<0.05$, $P<0.01$ and $P<0.001$ respectively, compared to 0μg/ml, post hoc test Dunnett's). Data are mean +/- SEM of 4 experiments.

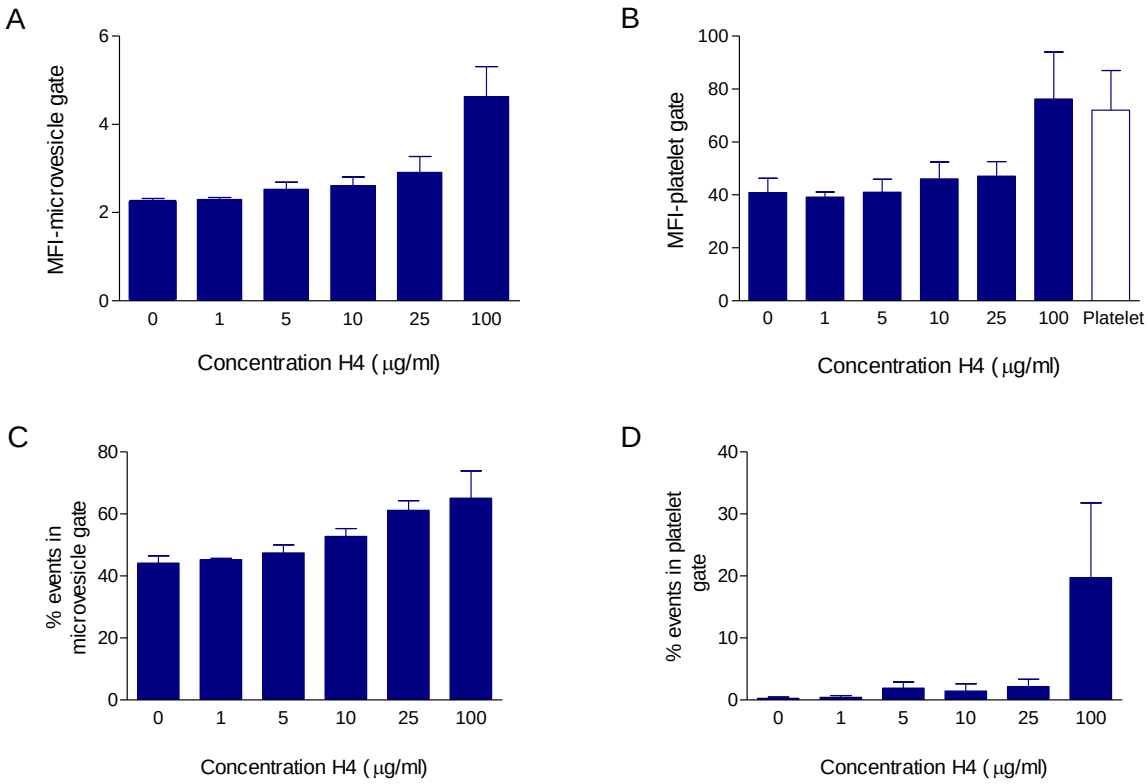


**Figure 4-20: CD42b expression on the CD14$^{+}$CD16$^{-}$ monocyte population after treatment with human recombinant histone H4**

Whole blood was incubated and stirred at 37°C for 30 minutes with between 1-100μg/ml human recombinant H4 histone. Control (0μg/ml) has been incubated for 30 minutes without the addition of any agonist. Data were acquired using flow cytometry. A) Shows a small increase in CD42b MFI in the microvesicle gate, after treatment with 100μg/ml H4. While C) shows an increase in the percent of CD42b positive cells in this gate. B) Demonstrates that the CD42b MFI of MPA formed after treatment with 100μg/ml H4 histones reaches that of a resting platelet. D) Demonstrates a large increase in the percent CD42b positive cells in this gate after treatment with 100μg/ml H4. Data are mean +/- SEM of 4 experiments.

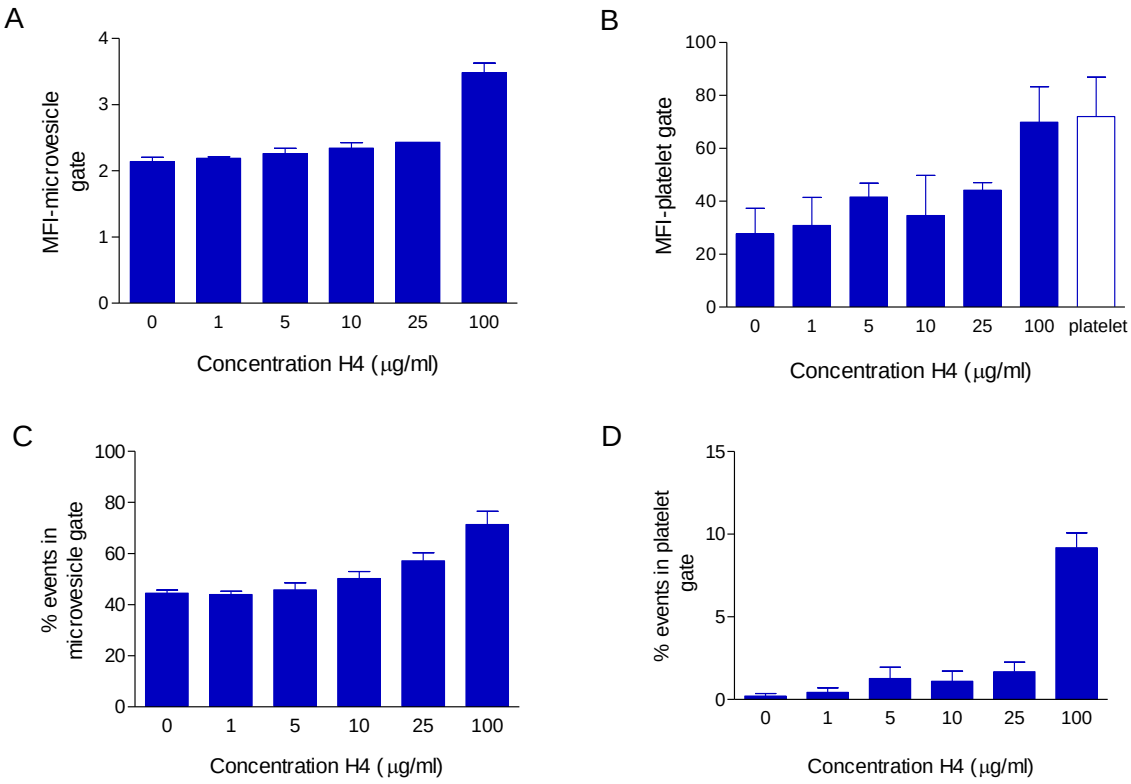


**Figure 4-21: CD42b expression on the $CD14^{+}CD16^{+}$ monocyte population after treatment with human recombinant histone H4**

Whole blood was incubated and stirred at 37°C for 30 minutes with between 1-100μg/ml human recombinant H4 histone. Control (0μg/ml) has been incubated for 30 minutes without the addition of any agonist. Data were acquired using flow cytometry. A) Shows a small increase in CD42b MFI in the microvesicle gate after treatment with 100μg/ml H4, C) also shows an increase in the CD42b positive cells in this gate. B) Demonstrates that the CD42b MFI of MPA formed after treatment with 100μg/ml H4 histones reaches that of a resting platelet. D) Demonstrates a large increase in percent CD42b positive in this gate after treatment with 100μg/ml H4. Data are mean +/- SEM of 4 experiments.

**4.4.0 Discussion**

An interesting point of contention arises from our observations using unstimulated blood in regard to the true level of circulating monocytes that are positive for platelet markers. Our own data from fixed whole blood (0 minute control- fixed within 10 minutes of venepuncture) showed on average that 4% of circulating monocytes were positive for the platelet marker CD42b. This is in contrast to data from other laboratories, e.g. Passacquale et al, (2011). These authors showed a baseline of ~25% monocytes forming aggregates with platelets in fixed untreated blood. However, in the latter study the blood was not fixed immediately after phlebotomy, being incubated with antibodies against CD14, CD16 and CD42b, followed by a period during which RBC were lysed before fixing (Passacquale et al., 2011). Moreover, Passacquale used a less stringent gating strategy, than that currently adopted to identify monocyte populations during flow cytometry analysis. These differences in sample processing and measurement could explain discrepancies between the data.

However, it is important to highlight that these may not be the only confounding parameters when measuring the baseline levels MPA in healthy, circulating, whole blood. Thus, we found that stirred, unstimulated whole blood samples (on a roller mixer) for up to 60 minutes, at 37°C showed no significant increase in MPA formation compared to blood which had been rapidly fixed. This data is important for 2 reasons. Firstly, it shows that platelet activation is necessary, for a significant number of MPA to form under the conditions used in our experiments, under stringent conditions of stirring. Secondly, it strongly indicates that monocyte-platelet interactions are readily formed in whole blood under static conditions (i.e. without shear). However, these do not represent true levels of monocyte-platelet interaction, being an artefact of post phlebotomy treatment. Interestingly, Harding et al, (2007), tested the

effect of a time delay on monocyte-platelet aggregate formation in whole blood at room temperature. They observed an average of ≈2% increase in MPA formation every 10 minutes in citrated whole blood samples. Together, these data imply that caution is required in interpreting data on the levels of MPA formation in the circulation using anticoagulated whole blood to make measurements, as there is a propensity for platelets and monocytes to aggregate under static conditions, within minutes of blood withdrawal. Importantly, these interactions may be labile, as imposition of shear forces disrupts this process.

The anticoagulant itself can also have an effect on MPA formation, EDTA chelates calcium and inhibits platelet activation, this is not a sensible anticoagulant to use when studying MPA formation as its use will lead to a reduction in the numbers of MPA detected (Basavaraj et al., 2012). However, there is an increase in MPA formation at baseline in whole blood collected in heparin compared to blood collected in citrate (Basavaraj et al., 2012). This means that heparinised blood would have increased MPA formation as an artefact of the anticoagulant. Throughout this study, blood has been collected into CPDA to avoid increased or decreased MPA formation being detected as a result of the anticoagulant used.

Our data clearly demonstrates that treatment of whole blood with a known platelet agonist, in this case TRAP or CTH, results in an increase in MPA formation over time. This is in agreement with previous studies, which have also indicated that activation of platelets through the PAR1 pathway increases MPA formation in whole blood (Jensen et al., 2001; Xiao and Théroux, 2004). In the current study a lower concentration of TRAP (10µM) was found to be just as effective as a higher one (100µM). Previous aggregometry data using washed isolated platelets stimulated with 10µM TRAP has shown that maximal platelet activation can be achieved using this concentration of agonist (Stephens et al., 2005). If maximal response to the

platelet agonist is also achieved in whole blood, then it is likely that there will be no difference in MPA formation between these concentrations. However, the data showed an increase in donor variability at lower concentrations of TRAP, with some donors clearly more responsive than others at these marginal concentrations. Future work should determine the sensitivity of MPA formation to platelet agonists, as the concentrations used currently represent robust stimulation, and our data indicates that this may not be required to induce interactions between platelets and monocytes.

It has been well documented that upon platelet activation CD42b positive platelet microvesicles are generated (Flaumenhaft et al., 2009; Hargett and Bauer, 2013). Indeed, previous studies using activation of platelets through the PAR-1 pathway, resulted in robust microvesicle generation (Heijnen et al., 1999; Nygaard et al., 2014). TRAP peptide has also previously been reported to increase microvesicle shedding in sheared ($10,000S^{-1}$) samples of whole blood (Chow et al., 2000). Our time course data demonstrate that monocytes accumulate CD42b in quanta that are significantly less than whole platelets, implying that monocytes could be accumulating PMV over time rather than binding to whole platelets. Interestingly, most studies report MPA formation as the percentage increase in monocytes which become positive for platelet markers in response to platelet activation. Very few have determined the number of platelets adhering per monocyte, or have reported the MFI of flow cytometry experiments. One exception is work by Xiao and Théroux, (2004), who showed that blood from acute coronary syndrome (ACS) patients had a baseline of 45% MPA formation with 4 platelets adhering per monocyte, this was increased upon TRAP treatment to 95% MPA formation with 10 platelets adhering per monocyte. (Unstimulated whole blood from healthy controls was shown to have 15% MPA formation with 3 platelets adhering to each monocyte.) This is in contrast to data from the current study, which suggests that PMV generated upon platelet activation, may

adhere to monocytes, with whole platelets occasionally binding to $CD14^{+}CD16^{+}$ monocytes within the first 15 minutes of the time course. However, the study by Xiao et al (2004) involves blood incubated under static conditions for 15 minutes before detection of MPA formed by a heterogeneous monocyte population using flow cytometry, with CD42a as a platelet marker. Static conditions could encourage whole platelet binding and we would interpret this study as measuring artifactual interactions between monocytes and platelets. Indeed, the concept that 15% of monocytes in healthy individuals are circulating with on average 3 adherent platelets would seem to make little physiological sense.

In this study we measured formation of MPA using CD42b as a platelet marker on monocytes. Upon platelet activation with thrombin surface expression of CD42b has been shown to decrease (Hourdillé et al., 1992; Schmitz et al., 1998; Hourdillé et al., 1990). CD42b is believed to be expressed on the platelet surface in lipid rafts, which upon activation become incorporated into the actin cytoskeleton (Hourdillé et al., 1990; Munday et al., 2010). Other studies have indicated that this translocation may be reversible, although surface expression decreased after 10 minute treatment with thrombin, it was found to recover over time, peaking at 60 minutes (Michelson et al., 1994). If a low concentration of thrombin was used to activate platelets (less than 0.1U/ml), CD42b surface expression was found to be fully recoverable however, at higher concentrations (2U/ml), only partially recoverable (Michelson et al., 1994). This may be indicative of shedding of the receptor on MV after activation, with lost molecules being replenished to some extent from internal stores. Future studies of MPA formation in whole blood should optimise the use of other markers such as CD41 and/or P-selectin in conjunction with CD42b to determine, which is the most robust marker of MPA formation.

In contrast to the data which suggests PMV adhere to monocytes, observed during a 60 minute time course, following treatment with TRAP, further analysis of MPA formed after treatment with 1mg/ml CTH revealed that whole platelets were most likely binding to monocytes in response to this agonist. Lower concentrations of this agonist were shown to have no significant effect on MPA formation. Platelet adhesion occurred after 10 minute treatment with 1mg/ml CTH and continued throughout the 60 minute time course. Specifically, platelets adhered only to the $CD14^{+}CD16^{+}$ monocyte subset and no effect was seen on the larger $CD14^{+}CD16^{-}$ subset. Although the behaviour after treatment with CTH is very different to that observed after treatment with TRAP, in both instances the adhesion of whole platelets only occurred on the $CD14^{+}CD16^{+}$ monocyte subset. It is unclear as to why this should be, but this observation certainly merits further scrutiny.

As an almost maximum amount of MPA could be detected after 5 minute treatment with CTH we felt it was important to look at earlier time points with this agonist. There was some indication that at early time points (< 1 minute) very few cells accumulated low numbers of microvesicles in this assay, although whether these were generated by CTH stimulated platelets or represent the constitutive population of platelet marker positive microvesicles, ordinarily resident in the plasma is not known. With respect to the binding of whole platelets, analysis suggested a biphasic response, with a very small number of monocytes rapidly (i.e. within 5-30s) binding platelets which were then shed. This was then followed by a slower but more sustained accumulation of platelets by a more substantial proportion of monocytes (≈20%). We did not ascertain whether very early and transient responses were evident after TRAP stimulation, but further work could include repeating this short time course with this agonist to find out if the levels of CD42b expression follow similar patterns.

The data generated with CTH was interesting, especially as it highlighted a monocyte subset specific accumulation of platelets. However, we felt it was important to use a more biologically relevant version of histones in human blood and opted to treat samples with recombinant human histone H4. This has previously been shown to be the most potent histone in the context of platelet activation (Semeraro et al., 2011). A titration revealed that this histone was effective at concentrations an order of magnitude lower than CTH, significantly increasing MPA formation. Interestingly, a significant increase in MPA formation was detected for both monocyte subsets, implying that there is a differential response of platelets to bovine and human histones. Further analysis revealed that this was likely to be due to whole platelet binding to monocytes. The fact that H4 was effective at a lower concentration than CTH is not surprising, as H4 would only account for a small proportion of the CTH mixture, and as other histones have been shown to have minimal effects on platelet activation it is probably safe to assume that the H4 in CTH was largely responsible for the response to this agonist (Semeraro et al., 2011).

**Conclusions**

We have demonstrated that platelet activation is required for MPA formation. Upon platelet activation through the PAR-1 signalling pathway there is a significant increase in MPA formation over time. The data suggests that this could be due to PMV being generated upon platelet activation and subsequently adhering to monocytes. In contrast to this, treatment with CTH leads to a significant increase in $CD14^{+}CD16^{+}$ monocytes forming MPA and this appears to be mainly due to platelet adhesion to this monocyte subset. However, use of recombinant human histone H4 resulted in MPA formation for both monocyte subsets, which appeared to be mainly due to whole platelet adhesion to both monocyte subsets.

# 5. Chapter-5 MONOCYTE-PLATELET AGGREGATE FORMATION IN RESPONSE TO TREATMENT WITH OTHER PLATELET AGONISTS

### 5.1.0 Introduction

Formation of MPA has been reported to increase in patients with chronic inflammatory diseases, including those with atherosclerosis (Furman et al., 1998; Harding et al., 2007; Htun et al., 2006; Joseph et al., 2001; Shantsila et al., 2011). An increase in platelet activation is often reported alongside these observations and it is thought to have an important role in MPA formation (Xiao and Théroux, 2004). However, there are several signalling pathways through which platelet activation can occur (Rivera et al., 2009).

These include platelet activation through glycoprotein VI (GPVI) (Nieswandt and Watson, 2003). If damage occurs to the endothelium, the subendothelial matrix will be exposed. Unlike the endothelium, which works to prevent platelet activation (through NO production amongst other mechanisms), the subendothelial matrix contains collagen, a potent platelet activator (Rivera et al., 2009). Localised platelet activation under these circumstances is necessary to prevent haemorrhage. Under conditions of high shear stress platelets will be captured through weak interactions between platelet CD42b and vWf (Rivera et al., 2009). These weak interactions will allow platelets to roll until platelet GPVI binds to collagen, which results in platelet activation and firm adhesion (Nieswandt and Watson, 2003). Unstable atherosclerotic plaque rupture can lead to exposure of collagen and platelet activation through this mechanism (Libby, 2012). However, upon activation platelets themselves will generate ADP and thromboxane, which further enhances platelet activation, in an autocrine or paracrine fashion through positive feedback loops (Rivera et al., 2009). As MPA have been found at increased levels following atherosclerotic plaque rupture, (Sarma, 2002) this suggests a potential role for platelet activation by collagen, ADP and thromboxane.

Oxidised LDL plays a significant role in the development of atherosclerosis. It is thought to be a potential platelet activator acting through LOX-1 or CD36, scavenger receptors expressed on the platelet cell surface (Chen et al., 2001; Korporaal et al., 2007). Upon plaque rupture there is also a chance platelets could come into contact with oxLDL, and low levels of oxLDL have been measured in the circulation of patients with atherosclerosis

Podoplanin is the only known endogenous ligand for platelet CLEC-2 (Hughes et al., 2010). Podoplanin is expressed by kidney podocytes, lung type I alveolar cells and lymphatic endothelial cells (Hughes et al., 2010). Activation through this receptor can also occur upon binding of rhodocytin, produced by the Malayan pit viper, *Calloselasma rhodostoma.* Now a commonly used agent for activating platelets through this signalling pathway (Suzuki-Inoue et al., 2006). To our knowledge the effect of platelet activation through the CLEC-2 pathway on MPA formation has not yet been investigated.

Platelet activation often leads to PMV generation and it has been suggested that the resulting PMV are able to interact with monocytes (Beyer and Pisetsky, 2010; Mause et al., 2005). Formation of MPA (or indeed monocyte-microvesicle aggregates) could have important implications for disease progression as this would provide a mechanism for cross talk between inflammation and thrombosis. Previous data has also suggested increased recruitment of MPA to EC (Kuckleburg et al., 2011). This could potentially occur through either leukocyte recruitment to selectins or through platelet recruitment to vWf. Data from the previous chapter has demonstrated that differences occur in the ability of MPA to form upon the route of platelet activation, we therefore believed it was necessary to screen more agonists.

Our aims for this chapter therefore were to determine;

1) If the route of platelet activation had any effect on the rate, or total percentage increase in MPA formation.
2) To assess the accumulation of the platelet specific marker CD42b, by monocytes over time.
3) If there was any difference in the ability of monocyte subsets to form MPA or if there were any differences in the levels of CD42b accumulated by each subset over time.

**5.2.0 Methods**

**5.2.1 MPA formation in whole blood following treatment with platelet agonist reagents**

Briefly CPDA anti-coagulated whole blood was gently stirred and incubated at 37°C with platelet agonists including 10µM and 3µM thromboxane mimetic U46619, 100nM and 30nM rhodocytin, 30µM and 3µMADP, 1µg/ml collagen related peptide (cross linked form) CRP-XL, 1mg/ml calf thymus histones or 50µg/ml oxLDL. Analysis of MPA formation was determined using flow cytometry for the monocyte markers CD14, CD16 and the platelet marker CD42b. Statistical analysis was carried out using Graph Pad Prism version 5.0. (For further detail see methods section 2.3.1-2.3.3.)

### 5.3.0 Results

### 5.3.1 The effect of platelet activation through different signalling pathways on MPA formation in whole blood

We wished to determine if the route of platelet activation causes any difference in the rate, or extent of heterotypic aggregate formation. To do this whole blood was incubated and stirred with a range of platelet agonists including thromboxane mimetic U46619, snake venom toxin rhodocytin, ADP, CRP-XL as well as oxLDL.

Differences between agonists were indeed observed. Thus, dealing with the $CD14^{+}CD16^{-}$ monocyte subset first; we observed a difference in the dynamics of MPA formation, with ADP inducing significant MPA formation within 15 minutes (**Table 5-1**). However, by 30 minutes all of the agents that delivered an increase in MPA formation had done so, with the exception of oxLDL (**Table 5-1**). Using the 60 minute time point as an exemplar, most agonists delivered MPA with ≈ 40% efficiency (**Table 5-1**). Rhodocytin however, appeared the more potent of the agonists delivering MPAs with an efficiency of ≈ 70% (**Table 5-1**). MPA formation with the $CD14^{+}CD16^{+}$ subset of monocytes showed broadly similar patterns (**Table 5-2**).

| Agonist | Time point 0 | 5 Minutes | 10 Minutes | 15 Minutes | 20 Minutes | 25 Minutes | 30 Minutes | 60 Minutes | 30 Minutes con | 60 Minutes con | ANOVA |
|---|---|---|---|---|---|---|---|---|---|---|---|
| **30µM ADP** | 2.1± 0.4 | 8.3±2.3 | 8.1±0.8 | 24.6±4.3 * | 33.5± 7.8 *** | 37.2±6.4 *** | 42.9±4.2 *** | 41.7±7.6 *** | 12.0±4.8 | 15.6±7.0 | P<0.0001 |
| **1µg/ml CRP-XL** | 2.5± 0.4 | 4.8±0.5 | 5.3±0.5 | 6.7±2.2 | 14.1±6.5 | 18.5±5.1 | 29.1±9.0 ** | 33.6±8.2 *** | 9.8±1.8 | 12.2±4.4 | P< 0.001 |
| **10µM U46619** | 3.3±1.0 | 4.6±1.2 | 6.1±1.4 | 12.6±3.0 | 18.5±2.8 * | 32.1±4.2 *** | 38.1±7.1 *** | 39.4±2.6 *** | 7.7±1.1 | 9.5±1.5 | P<0.0001 |
| **100nM Rhodocytin** | 2.1±0.3 | 4.4±0.7 | 4±0.2 | 10.8±1.5 | 21.0±5.4 *** | 47.6±4.2 *** | 58.8±2.5 *** | 67.9±2.4 *** | 3.3±0.8 | 5.0±1.8 | P<0.0001 |
| **50µg/ml oxLDL** | 2.8±0.6 | 5.8±1.1 | 6±1.0 | 6.9±1.2 | 6.8±1.9 | 6.8±1.8 | 6.5±1.9 | 12.8±5.5 | 6.9±2.4 | 7.8±2.3 | ns |

**Table 5-1: MPA formation for the $CD14^{+}CD16^{-}$ monocyte subset after treatment with various platelet agonists**

Table 5-1 shows the mean percentage monocyte-platelet aggregate formation ($CD14^{+}CD16^{-}$ monocyte subset), in stirred whole blood, incubated at 37°C in response to different agonists over time. 30 Con and 60 Con are stirred and incubated at 37°C without the addition of any agonist. *,** and *** indicate P<0.05, P<0.01 and P<0.001 respectively post hoc test (Dunnett's) following a One-way ANOVA. (Data are mean +/- SEM; ADP 4-7 experiments, CRP-XL 4 experiments, U46619 3 experiments, rhodocytin 3 experiments and oxLDL 5-6 experiments.)

| Agonist | Time point 0 | 5 Minutes | 10 Minutes | 15 Minutes | 20 Minutes | 25 Minutes | 30 Minutes | 60 Minutes | 30 Minutes con | 60 Minutes con | ANOVA |
|---|---|---|---|---|---|---|---|---|---|---|---|
| **30µM ADP** | 3.0±0.5 | 8.4±3.1 | 8.0±1.1 | 21.3±3.8* | 27.2±7.2 *** | 32.7±5.3 *** | 38.3±2.7 *** | 31.5±6.5 *** | 7.9±1.9 | 10.4±3.4 | P<0.0001 |
| **1µg/ml CRP-XL** | 3.0±0.5 | 14.2±3.4 | 13.5±2.7 | 14.9±3.1 | 20.5±7.2 * | 26.6±5.9 ** | 36.2±4.7 *** | 42.8±5.2 *** | 6.0±0.5 | 10.2±3.9 | P<0.0001 |
| **10µM U46619** | 3.9±1.0 | 7.2±1.6 | 8.0±1.7 | 12.7±1.4 | 15.1±1.9 | 23.7±5.8 * | 27.5±4.6 ** | 33.3±10.8 *** | 6.8±2.2 | 7.1±0.5 | P<0.001 |
| **100nM Rhodocytin** | 2.5±0.2 | 8.2±1.4 | 10.1±3.0 | 19.8±3.1 * | 24.8±8.2 ** | 42.9±5.4 *** | 53.4±2.7 *** | 58.0±2.6 *** | 4.0±1.1 | 4.2±1.8 | P<0.0001 |
| **50µg/ml oxLDL** | 3.7±5.1 | 7.7±1.6 | 8.7±2.2 | 9.0±2.3 | 9.2±2.7 | 10.2±3.0 | 10.1±2.2 | 19.9±10.7 | 6.6±1.5 | 8.8±1.9 | ns |

**Table 5-2: MPA formation for the $CD14^{+}CD16^{+}$ monocyte subset after treatment with various platelet agonists**

Table 5-2 shows the mean percentage monocyte-platelet aggregate formation ($CD14^{+}CD16^{+}$ monocyte subset), in stirred whole blood, incubated at 37°C in response to different agonists over time. 30 Con and 60 Con are stirred and incubated at 37°C without the addition of any agonist. *,** and *** indicate P<0.05, P<0.01 and P<0.001 respectively post hoc test (Dunnett's) following a One-way ANOVA. (Data are mean +/-SEM ADP 4-7 experiments, CRP-XL 4 experiments, U46619 3 experiments, rhodocytin 3 experiments and oxLDL 5-6 experiments.)

### 5.3.2 Determining the level of accumulation of CD42b by monocytes in response to treatment with agonist reagents

Having determined the accumulation of platelet specific CD42b by monocytes after treatment with TRAP and CTH previously, we wanted to repeat this analysis for other platelet agonists. After treatment of whole blood with 30µM ADP and 100nM Rhodocytin followed by mixing at 37°C, the $CD14^{+}CD16^{-}$ monocyte subset showed an increase in CD42b MFI in the microvesicle gate (**Table 5-3**). Treatment with rhodocytin showed the greatest increase, followed by U46619 and then CRP-XL (**Table 5-3**). An increase in percentage of events in the microvesicle gate over time was observed, following treatment with any of the agonists (**Table 5-4**). However, no change in CD42b MFI or percentage was detected for any of the untreated samples (**Table 5-3, 5-4 ,5-5 and 5-6**). A possible explanation for the low level of accumulation of CD42b, by $CD14^{+}CD16^{-}$ monocytes, is that following treatment with any of these platelet agonists they are accumulating PMV, generated upon platelet activation. However, when the CD42b MFI of resting platelets was surprisingly low then data should be interpreted with caution (**Table 5-5 and 5-6**).

After treatment of whole blood with any of the agonists the $CD14^{+}CD16^{+}$ monocyte subset also showed an increase in CD42b MFI and percentage of events, over time, in the microvesicle gate (**Table 5-7 and Table 5-8**). Treatment with rhodocytin produced the greatest increase in CD42b MFI, followed by ADP, U46619 and CRP-XL (**Table 5-7**). Again indicating that under these conditions PMV may potentially be adhering to $CD14^{+}CD16^{+}$ monocytes.

The data from the $CD14^{+}CD16^{+}$ monocyte subset suggested platelet adhesion may also be occurring after treatment with most platelet agonists. After treatment with 1µg/ml CRP-XL the CD42b MFI in the platelet gate was higher than that of a resting platelet throughout the time

course (**Table 5-9**). Treatment with U46619 produced the highest CD42b MFI (421.2) at 15 minutes.

This suggests that more than one platelet may be binding to the monocyte, however, the MFI reduced over time to lower than that of a platelet at 60 minutes (**Table 5-9**). After treatment with 100nM rhodocytin the CD42b MFI in the platelet gate was roughly that of a resting platelet between 5-25mins (**Table 5-9**). The percentage of events, which would be consistent with whole platelet binding, remained low for most agonists. 30µM ADP showed an increase in percentage, but data should be interpreted with caution, as the CD42b MFI of a resting platelet was surprisingly low (**Table 5-10**).

### 5.3.3 The effect on MPA formation following treatment with lower concentrations of agonist reagents

After finding that treatment with high concentrations of platelet agonists possibly leads to microvesicle generation by platelets, which in turn adhere to monocytes, we wanted to find out, what effect lower concentrations of ADP, U46619 and rhodocytin would have. In order to achieve this whole blood was incubated and stirred at 37°C for up to 60 minutes after treatment with 3µM ADP, 3µM U46619 and 30nM rhodocytin.

Of these three agonists rhodocytin was found to be the most effective with a maximum of ~65% and 60% MPA for the $CD14^{+}CD16^{-}$ and $CD14^{+}CD16^{+}$ monocyte subsets respectively (**Table 5-11 and 5-12**). The weaker agonists were 3µM U46619 and 3µM ADP both giving a maximum of roughly 30% MPA formation for the $CD14^{+}CD16^{-}$ monocyte subset (**Table 5-11**). U46619 showed a maximum of 35% MPA on the $CD14^{+}CD16^{+}$ subset whereas ADP showed a maximum of 30% (**Table 5-12**).

| Agonist | Time point 0 | 5 Minutes | 10 Minutes | 15 Minutes | 20 Minutes | 25 Minutes | 30 Minutes | 60 Minutes | 30 Minutes con | 60 Minutes Con |
|---|---|---|---|---|---|---|---|---|---|---|
| **30µM ADP** | 3.1 | 4.6 | 4.9 | 7.5 | 10.9 | 10.3 | 10.7 | 11.1 | 4.7 | 4.5 |
| **1µg/ml CRP-XL** | 2.2 | 2.8 | 3.0 | 3.1 | 4.0 | 4.4 | 5.4 | 6.1 | 2.5 | 2.9 |
| **10µM U46619** | 2.6 | 3.0 | 3.3 | 4.5 | 5.6 | 7.6 | 8.7 | 8.9 | 3.2 | 3.4 |
| **100nM Rhodocytin** | 2.1 | 2.5 | 2.8 | 4.4 | 5.7 | 10.0 | 12.1 | 14.0 | 2.2 | 2.3 |

**Table 5-3: CD42b MFI on the $CD14^{+}CD16^{-}$ monocyte subset in the microvesicle gate after treatment with high concentrations of agonist**

CD42b MFI in the microvesicle gate for the $CD14^{+}CD16^{-}$ monocyte subset, following treatment of stirred whole blood, incubated at 37°C with different agonists over time. 30 Con and 60 Con are stirred and incubated at 37°C without the addition of any agonist. 0 min control is untreated and fixed instantly prior to any incubation period. (Data are mean; ADP 4-7 experiments, CRP-XL 4 experiments, U46619 3 experiments and rhodocytin 3 experiments.)

| Agonist | Time point 0 | 5 Minutes | 10 Minutes | 15 Minutes | 20 Minutes | 25 Minutes | 30 Minutes | 60 Minutes | 30 Minutes con | 60 Minutes Con |
|---|---|---|---|---|---|---|---|---|---|---|
| **30µM ADP** | 56.9 | 74.1 | 80.0 | 78.6 | 83.1 | 79.0 | 77.1 | 82.4 | 71.1 | 69.5 |
| **1µg/ml CRP-XL** | 49.1 | 69.3 | 72.8 | 74.5 | 80.7 | 83.4 | 84.2 | 85.9 | 61.0 | 71.4 |
| **10µM U46619** | 48.6 | 61.0 | 77.0 | 79.8 | 85.2 | 90.3 | 91.3 | 93.4 | 69.9 | 76.9 |
| **100nM Rhodocytin** | 43.6 | 56.6 | 69.2 | 86.9 | 91.7 | 94.9 | 91.7 | 92.1 | 50.3 | 52.6 |

**Table 5-4: Percentage of the $CD14^{+}CD16^{-}$ monocyte subset in the microvesicle gate after treatment with high concentrations of agonist**

CD42b positive percentage of events in the microvesicle gate for the $CD14^{+}CD16^{-}$ monocyte subset, following treatment of stirred whole blood, incubated at 37°C with different agonists over time. 30 Con and 60 Con are stirred and incubated at 37°C without the addition of any agonist. 0 min control is untreated and fixed instantly prior to any incubation period. (Data are mean; ADP 4-7 experiments, CRP-XL 4 experiments, U46619 3 experiments and rhodocytin 3 experiments.)

| Agonist | Time point 0 | 5 Minutes | 10 Minutes | 15 Minutes | 20 Minutes | 25 Minutes | 30 Minutes | 60 Minutes | 30 Minutes con | 60 Minutes Con | Platelet |
|---|---|---|---|---|---|---|---|---|---|---|---|
| **30µM ADP** | 92.1 | 84.6 | 94.4 | 79.2 | 68.6 | 66.6 | 70.0 | 71.6 | 68.1 | 52.2 | 194.0 |
| **1µg/ml CRP-XL** | 42.3 | 50.8 | 64.0 | 40.9 | 54.0 | 34.9 | 33.6 | 35.9 | 35.5 | 34.5 | 77.6 |
| **10µM U46619** | 75.8 | 121.2 | 107.7 | 112.2 | 124.2 | 84.1 | 81.4 | 72.7 | 75.1 | 76.3 | 157.7 |
| **100nM Rhodocytin** | 61.9 | 99.8 | 86.4 | 88.8 | 137.0 | 88.5 | 69.5 | 62.0 | 69.6 | 63.2 | 110.3 |

**Table 5-5: CD42b MFI on the $CD14^{+}CD16^{-}$ monocyte subset in the platelet gate after treatment with high concentrations of agonist**

CD42b MFI in the platelet gate for the $CD14^{+}CD16^{-}$ monocyte subset, following treatment of stirred whole blood, incubated at 37°C with different agonists over time. 30 Con and 60 Con are stirred and incubated at 37°C without the addition of any agonist. 0 min control is untreated and fixed instantly prior to any incubation period. (Data are mean; ADP 4-7 experiments, CRP-XL 4 experiments, U46619 3 experiments and rhodocytin 3 experiments.)

| Agonist | Time point 0 | 5 Minutes | 10 Minutes | 15 Minutes | 20 Minutes | 25 Minutes | 30 Minutes | 60 Minutes | 30 Minutes con | 60 Minutes Con |
|---|---|---|---|---|---|---|---|---|---|---|
| **30µM ADP** | 1.5 | 2.9 | 3.2 | 8.7 | 10.5 | 15.8 | 19.0 | 13.1 | 6.3 | 8.2 |
| **1µg/ml CRP-XL** | 1.0 | 1.2 | 0.7 | 0.8 | 1.7 | 2.3 | 5.9 | 6.4 | 3.8 | 3.2 |
| **10µM U46619** | 1.3 | 1.2 | 1.1 | 1.2 | 1.2 | 1.8 | 2.5 | 2.2 | 1.8 | 1.0 |
| **100nM Rhodocytin** | 0.6 | 1.8 | 0.7 | 0.7 | 1.0 | 2.1 | 6.3 | 7.0 | 0.7 | 0.4 |

**Table 5-6: Percentage of the $CD14^{+}CD16^{-}$ monocyte subset in the platelet gate after treatment with high concentrations of agonist**

CD42b positive percentage of events in the platelet gate for the $CD14^{+}CD16^{-}$ monocyte subset, following treatment of stirred whole blood, incubated at 37°C with different agonists over time. 30 Con and 60 Con are stirred and incubated at 37°C without the addition of any agonist. 0 min control is untreated and fixed instantly prior to any incubation period. (Data are mean; ADP 4-7 experiments, CRP-XL 4 experiments, U46619 3 experiments, rhodocytin 3 experiments.)

| Agonist | Time point 0 | 5 Minutes | 10 Minutes | 15 Minutes | 20 Minutes | 25 Minutes | 30 Minutes | 60 Minutes | 30 Minutes con | 60 Minutes Con |
|---|---|---|---|---|---|---|---|---|---|---|
| **30µM ADP** | 3.2 | 4.1 | 4.3 | 5.7 | 8.8 | 8.2 | 8.5 | 8.8 | 4.0 | 3.8 |
| **1µg/ml CRP-XL** | 2.2 | 2.8 | 3.0 | 3.2 | 4.0 | 4.6 | 5.6 | 6.5 | 2.4 | 2.7 |
| **10µM U46619** | 2.7 | 3.0 | 3.0 | 3.9 | 4.6 | 5.7 | 6.0 | 7.8 | 3.1 | 3.3 |
| **100nM Rhodocytin** | 2.1 | 2.4 | 2.7 | 4.2 | 5.0 | 8.9 | 10.6 | 12.6 | 2.3 | 2.3 |

**Table 5-7: CD42b MFI on the $CD14^{+}CD16^{+}$ monocyte subset in the microvesicle gate after treatment with high concentrations of agonist**

CD42b MFI in the microvesicle gate for the $CD14^{+}CD16^{+}$ monocyte subset, following treatment of stirred whole blood, incubated at 37°C with different agonists over time. 30 Con and 60 Con are stirred and incubated at 37°C without the addition of any agonist. 0 min control is untreated and fixed instantly prior to any incubation period. (Data are mean; ADP 4-7 experiments, CRP-XL 4 experiments, U46619 3 experiments and rhodocytin 3 experiments.)

| Agonist | Time point 0 | 5 Minutes | 10 Minutes | 15 Minutes | 20 Minutes | 25 Minutes | 30 Minutes | 60 Minutes | 30 Minutes con | 60 Minutes Con |
|---|---|---|---|---|---|---|---|---|---|---|
| **30µM ADP** | 61.8 | 67.0 | 73.2 | 77.1 | 77.4 | 75.7 | 74.6 | 78.3 | 69.9 | 69.4 |
| **1µg/ml CRP-XL** | 50.6 | 60.8 | 66.2 | 68.1 | 74.7 | 78.7 | 80.1 | 82.2 | 59.0 | 67.6 |
| **10µM U46619** | 48.6 | 54.6 | 54.1 | 62.2 | 69.7 | 76.3 | 77.6 | 83.5 | 67.3 | 75.3 |
| **100nM Rhodocytin** | 45.2 | 53.4 | 64.0 | 77.1 | 82.8 | 88.3 | 87.2 | 87.6 | 50.8 | 52.0 |

**Table 5-8: Percentage of the $CD14^{+}CD16^{+}$ monocyte subset in the microvesicle gate after treatment with high concentrations of agonist**

CD42b positive percentage of events in the microvesicle gate for the $CD14^{+}CD16^{+}$ monocyte subset, following treatment of stirred whole blood, incubated at 37°C with different agonists over time. 30 Con and 60 Con are stirred and incubated at 37°C without the addition of any agonist. 0 min control is untreated and fixed instantly prior to any incubation period. (Data are mean; ADP 4-7 experiments, CRP-XL 4 experiments, U46619 3 experiments and rhodocytin 3 experiments.)

| Agonist | Time point 0 | 5 Minutes | 10 Minutes | 15 Minutes | 20 Minutes | 25 Minutes | 30 Minutes | 60 Minutes | 30 Minutes con | 60 Minutes Con | Platelet |
|---|---|---|---|---|---|---|---|---|---|---|---|
| **30µM ADP** | 84.8 | 85.4 | 95.7 | 78.2 | 67.8 | 70.0 | 71.2 | 72.7 | 78.8 | 73.5 | 194.0 |
| **1µg/ml CRP-XL** | 41.8 | 149.9 | 156.5 | 210.3 | 169.8 | 175.9 | 91.6 | 46.1 | 39.6 | 35.4 | 77.6 |
| **10µM U46619** | 76.8 | 284.9 | 317.3 | 421.2 | 234.4 | 285.3 | 155.4 | 83.2 | 82.9 | 83.2 | 157.7 |
| **100nM Rhodocytin** | 59.1 | 116.8 | 135.5 | 144.4 | 167.4 | 101.6 | 63.5 | 75.3 | 76.4 | 59.6 | 110.3 |

**Table 5-9: CD42b MFI on the $CD14^+CD16^+$ monocyte subset in the platelet gate after treatment with high concentrations of agonist**

CD42b MFI in the platelet gate for the $CD14^+CD16^+$ monocyte subset, following treatment of stirred whole blood, incubated at 37°C with different agonists over time. 30 Con and 60 Con are stirred and incubated at 37°C without the addition of any agonist. 0 min control is untreated and fixed instantly prior to any incubation period. (Data are mean; ADP 4-7 experiments, CRP-XL 4 experiments, U46619 3 experiments and rhodocytin 3 experiments.)

| Agonist | Time point 0 | 5 Minutes | 10 Minutes | 15 Minutes | 20 Minutes | 25 Minutes | 30 Minutes | 60 Minutes | 30 Minutes con | 60 Minutes Con |
|---|---|---|---|---|---|---|---|---|---|---|
| **30µM ADP** | 1.8 | 2.7 | 2.6 | 7.6 | 8.4 | 12.8 | 16.2 | 12.9 | 3.9 | 8.0 |
| **1µg/ml CRP-XL** | 1.5 | 8.1 | 5.4 | 5.0 | 5.2 | 4.8 | 7.7 | 8.8 | 2.7 | 3.0 |
| **10µM U46619** | 1.6 | 3.9 | 4.7 | 4.7 | 1.8 | 2.1 | 2.4 | 2.0 | 1.6 | 1.2 |
| **100nM Rhodocytin** | 0.7 | 1.9 | 2.3 | 2.5 | 2.8 | 3.1 | 6.7 | 7.2 | 1.1 | 0.4 |

**5-10: Percentage of the $CD14^+CD16^+$ monocyte subset in the platelet gate after treatment with high concentrations of agonist**

CD42b positive percentage of events in the platelet gate for the $CD14^+CD16^+$ monocyte subset, following treatment of stirred whole blood, incubated at 37°C with different agonists over time. 30 Con and 60 Con are stirred and incubated at 37°C without the addition of any agonist. 0 min control is untreated and fixed instantly prior to any incubation period. (Data are mean; ADP 4-7 experiments, CRP-XL 4 experiments, U46619 3 experiments and rhodocytin 3 experiments.)

| Agonist | Time point 0 | 5 Minutes | 10 Minutes | 15 Minutes | 20 Minutes | 25 Minutes | 30 Minutes | 60 Minutes | 30 Minutes con | 60 Minutes con | ANOVA |
|---|---|---|---|---|---|---|---|---|---|---|---|
| **3µM ADP** | 4.9±1.1 | 17.0±5.6 | 14.6±2.0 | 17.2±2.8 | 27.5±4.9 * | 31.7±7.6 ** | 31.2±8.2 ** | 29.7±5.0 ** | 6.5±1.8 | 6.67±1.8 | P<0.0001 |
| **3µM U46619** | 5.3±0.9 | 12.1±6.2 | 13.3±4.8 | 20.6±3.9 | 37.3±3.8 *** | 39.4±4.8 *** | 43.3±5.9 *** | 28.8±6.4 ** | 7.2±2.7 | 10.1±2.7 | P<0.0001 |
| **30nM Rhodocytin** | 4.9±0.9 | 8.9±1.5 | 6.3±1.9 | 7.8±2.5 | 16.3±1.3 | 44.5±1.7 *** | 53.8±6.2 *** | 65.8±7.5 *** | 5.4±0.8 | 6.9±0.4 | P<0.0001 |

**Table 5-11: MPA formation for the $CD14^{+}CD16^{-}$ monocyte subset after treatment with low concentrations of various agonists**

Table 5-11 shows the mean percentage monocyte-platelet aggregate formation ($CD14^{+}CD16^{-}$ monocyte subset) in stirred whole blood incubated at 37°C in response to different agonists over time. 30 Con and 60 Con are stirred and incubated at 37°C without the addition of any agonist. *,** and *** indicate P<0.05, P<0.01 and P<0.001 respectively post hoc test (Dunnett's) following a One-way ANOVA. (Data are mean +/-SEM; ADP 5-6 experiments, U46619 6-7 experiments and rhodocytin 4-5 experiments.)

| Agonist | Time point 0 | 5 Minutes | 10 Minutes | 15 Minutes | 20 Minutes | 25 Minutes | 30 Minutes | 60 Minutes | 30 Minutes con | 60 Minutes con | ANOVA |
|---|---|---|---|---|---|---|---|---|---|---|---|
| **3µM ADP** | 5.3±1.2 | 13.7±3.9 | 13.3±2.0 | 16.2±4.3 | 23.2±5.2 | 27.5±9.3 | 27.3±10.5 | 26.9±7.0 | 6.4±2.1 | 7.4±2.0 | P<0.05 |
| **3µM U46619** | 6.1±1.1 | 10.7±2.9 | 13.8±3.1 | 19.8±3.0 | 32.0±4.9 *** | 32.9±5.3 *** | 35.9±5.7 *** | 28.6±6.0 ** | 7.1±2.5 | 10.4±3.3 | P<0.0001 |
| **30nM Rhodocytin** | 5.5±0.7 | 13.1±2.6 | 11.3±1.7 | 12.6±1.1 | 29.3±3.3 *** | 51.0±4.0 *** | 55.5±5.7 *** | 60.1±5.8 *** | 4.9±0.8 | 6.8±0.6 | P<0.0001 |

**Table 5-12: MPA formation for the $CD14^{+}CD16^{+}$ monocyte subset after treatment with low concentrations of various agonists**

Table 5.12 shows the mean percentage monocyte-platelet aggregate formation ($CD14^{+}CD16^{+}$ monocyte subset) in stirred whole blood incubated at 37°C in response to different agonists over time. 30 Con and 60 Con are stirred and incubated at 37°C without the addition of any agonist. *,** and *** indicate P<0.05, P<0.01 and P<0.001 respectively post hoc test (Dunnett's) following a One-way ANOVA. (Data are mean+/-SEM; ADP 5-6 experiments, U46619 6-7 experiments and rhodocytin 4-5 experiments.)

### 5.3.4 Determining the level of platelet or PMV adhesion to monocytes in response to treatment with low concentrations of agonist reagents

Having demonstrated that lower concentrations of platelet agonists are able to significantly increase the percentage of MPA, which formed in stirred whole blood. We now wanted to assess the accumulation of CD42b, by monocytes, over time following treatment with a platelet agonist. The $CD14^{+}CD16^{-}$ monocyte subset had the highest CD42b MFI in the microvesicle gate after treatment with U46619 or rhodocytin (**Table 5-13**). It was lower after treatment with ADP (**Table 5-13**). There was an increase in the percentage of events in this gate over time (**Table 5-14**). The data suggests that platelet derived microvesicles may possibly be adhering to monocytes upon activation with these agonists. This monocyte subset never reached the MFI of a resting platelet after treatment with any of the agonists, this together with the percentage of events in this gate suggests that $CD14^{+}CD16^{-}$ monocytes probably don't bind to whole platelets (**Table 5-15 and 5-16**).

Again an increase in CD42b MFI can be detected in the microvesicle gate for the $CD14^{+}CD16^{+}$ monocyte subset. The highest CD42b MFI detected was again after treatment with rhodocytin, followed by treatment with U46619 and then 3µM ADP (**Table 5-17**). There is an increase in percentage of events in the CD42b microvesicle gate over time except after treatment with 3µM ADP where it remains stable (**Table 5-18**).

The CD42b in the platelet gate again suggests that in some instances whole platelets may be adhering to $CD14^{+}CD16^{+}$ monocytes. After treatment with U46619 or rhodocytin the MFI of CD42b in the platelet gate is higher than that of a resting platelet (**Table 5-19**). However, the low percentage of CD42b positive events in the platelet gate indicates that following U46619 treatment this is only the case for a small number of monocytes (**Table 5-20**).

| Agonist | Time point 0 | 5 Minutes | 10 Minutes | 15 Minutes | 20 Minutes | 25 Minutes | 30 Minutes | 60 Minutes | 30 Minutes con | 60 Minutes Con |
|---|---|---|---|---|---|---|---|---|---|---|
| **3µM ADP** | 2.9 | 4.2 | 4.7 | 4.7 | 5.7 | 5.9 | 5.5 | 6.2 | 3.5 | 3.6 |
| **3µM U46619** | 2.7 | 3.3 | 3.8 | 4.7 | 8.1 | 7.9 | 8.6 | 6.5 | 2.9 | 3.3 |
| **30nM Rhodocytin** | 2.4 | 2.9 | 2.7 | 3.1 | 4.8 | 7.9 | 8.9 | 10.4 | 2.4 | 2.6 |

**Table 5-13: CD42b MFI on the $CD14^{+}CD16^{-}$ monocyte subset in the microvesicle gate after treatment with low concentrations of agonist**

CD42b MFI in the microvesicle gate for the $CD14^{+}CD16^{-}$ monocyte subset, following treatment of stirred whole blood, incubated at 37°C with different agonists over time. 30 Con and 60 Con are stirred and incubated at 37°C without the addition of any agonist. 0 min control is untreated and fixed instantly prior to any incubation period. (Data are mean; ADP 5-6 experiments, U46619 6-7 experiments and rhodocytin 4-5 experiments.)

| Agonist | Time point 0 | 5 Minutes | 10 Minutes | 15 Minutes | 20 Minutes | 25 Minutes | 30 Minutes | 60 Minutes | 30 Minutes con | 60 Minutes Con |
|---|---|---|---|---|---|---|---|---|---|---|
| **3µM ADP** | 59.1 | 75.7 | 82.5 | 72.7 | 68.0 | 65.5 | 62.6 | 71.3 | 70.2 | 77.0 |
| **3µM U46619** | 58.3 | 65.7 | 72.9 | 82.3 | 85.7 | 85.5 | 82.7 | 86.5 | 66.9 | 74.4 |
| **30nM Rhodocytin** | 56.3 | 71.6 | 66.4 | 76.6 | 89.8 | 88.1 | 82.7 | 75.1 | 55.1 | 61.0 |

**Table 5-14: Percentage of the $CD14^{+}CD16^{-}$ monocyte subset in the microvesicle gate after treatment with low concentrations of agonist**

CD42b positive percentage of events in the microvesicle gate for the $CD14^{+}CD16^{-}$ monocyte subset, following treatment of stirred whole blood, incubated at 37°C with different agonists over time. 30 Con and 60 Con are stirred and incubated at 37°C without the addition of any agonist. 0 min control is untreated and fixed instantly prior to any incubation period. (Data are mean; ADP 5-6 experiments, U46619 6-7 experiments and rhodocytin 4-5 experiments.)

| Agonist | Time point 0 | 5 Minutes | 10 Minutes | 15 Minutes | 20 Minutes | 25 Minutes | 30 Minutes | 60 Minutes | 30 Minutes con | 60 Minutes Con | Platelet |
|---|---|---|---|---|---|---|---|---|---|---|---|
| **3µM ADP** | 55.3 | 55.3 | 47.7 | 43.0 | 44.4 | 46.8 | 49.6 | 42.1 | 45.1 | 39.9 | 115.9 |
| **3µM U46619** | 63.8 | 111.9 | 105.9 | 77.5 | 69.9 | 69.1 | 73.9 | 75.5 | 68.9 | 64.2 | 146.6 |
| **30nM Rhodocytin** | 40.3 | 78.0 | 57.6 | 43.6 | 66.5 | 45.9 | 40.5 | 42.4 | 38.1 | 38.3 | 75.9 |

**Table 5-15: CD42b MFI on the $CD14^{+}CD16^{-}$ monocyte subset in the platelet gate after treatment with low concentrations of agonist**

CD42b MFI in the platelet gate for the $CD14^{+}CD16^{-}$ monocyte subset, following treatment of stirred whole blood, incubated at 37°C with different agonists over time. 30 Con and 60 Con are stirred and incubated at 37°C without the addition of any agonist. 0 min control is untreated and fixed instantly prior to any incubation period. (Data are mean; ADP 5-6 experiments, U46619 6-7 experiments and rhodocytin 4-5 experiments.)

| Agonist | Time point 0 | 5 Minutes | 10 Minutes | 15 Minutes | 20 Minutes | 25 Minutes | 30 Minutes | 60 Minutes | 30 Minutes con | 60 Minutes Con |
|---|---|---|---|---|---|---|---|---|---|---|
| **3µM ADP** | 4.2 | 9.9 | 8.1 | 10.0 | 17.1 | 21.2 | 21.9 | 17.6 | 4.7 | 5.0 |
| **3µM U46619** | 1.9 | 5.5 | 4.9 | 5.7 | 7.7 | 8.4 | 11.3 | 5.4 | 1.3 | 1.2 |
| **30nM Rhodocytin** | 2.1 | 3.3 | 1.8 | 1.4 | 2.1 | 8.3 | 14.5 | 23.3 | 2.1 | 1.8 |

**Table 5-16: Percentage of the $CD14^{+}CD16^{-}$ monocyte subset in the platelet gate after treatment with low concentrations of agonist**

CD42b positive percentage of events in the platelet gate for the $CD14^{+}CD16^{-}$ monocyte subset, following treatment of stirred whole blood, incubated at 37°C with different agonists over time. 30 Con and 60 Con are stirred and incubated at 37°C without the addition of any agonist. 0 min control is untreated and fixed instantly prior to any incubation period. (Data are mean; ADP 5-6 experiments, U46619 6-7 experiments and rhodocytin 4-5 experiments.)

| Agonist | Time point 0 | 5 Minutes | 10 Minutes | 15 Minutes | 20 Minutes | 25 Minutes | 30 Minutes | 60 Minutes | 30 Minutes con | 60 Minutes Con |
|---|---|---|---|---|---|---|---|---|---|---|
| **3µM ADP** | 3.0 | 3.9 | 4.3 | 4.4 | 4.8 | 5.1 | 4.9 | 5.1 | 3.6 | 3.6 |
| **3µM U46619** | 2.7 | 2.8 | 3.1 | 3.7 | 5.8 | 5.6 | 6.2 | 5.5 | 2.7 | 3.1 |
| **30nM Rhodocytin** | 2.2 | 2.6 | 2.5 | 2.8 | 4.2 | 6.1 | 6.7 | 7.4 | 2.2 | 2.4 |

**Table 5-17: CD42b MFI on the $CD14^{+}CD16^{+}$ monocyte subset in the microvesicle gate after treatment with low concentrations of agonist**

CD42b MFI in the microvesicle gate for the $CD14^{+}CD16^{+}$ monocyte subset, following treatment of stirred whole blood, incubated at 37°C with different agonists over time. 30 Con and 60 Con are stirred and incubated at 37°C without the addition of any agonist. 0 min control is untreated and fixed instantly prior to any incubation period. (Data are mean; ADP 5-6 experiments, U46619 6-7 experiments and rhodocytin 4-5 experiments.)

| Agonist | Time point 0 | 5 Minutes | 10 Minutes | 15 Minutes | 20 Minutes | 25 Minutes | 30 Minutes | 60 Minutes | 30 Minutes con | 60 Minutes Con |
|---|---|---|---|---|---|---|---|---|---|---|
| **3µM ADP** | 61.5 | 76.4 | 79.9 | 69.3 | 67.3 | 63.5 | 60.4 | 68.0 | 70.7 | 77.7 |
| **3µM U46619** | 59.2 | 58.0 | 62.0 | 73.3 | 76.8 | 77.1 | 76.8 | 80.6 | 66.5 | 72.8 |
| **30nM Rhodocytin** | 54.2 | 63.4 | 58.2 | 68.0 | 77.1 | 76.8 | 71.8 | 72.7 | 52.8 | 58.7 |

**Table 5-18: Percentage of the $CD14^{+}CD16^{+}$ monocyte subset in the microvesicle gate after treatment with low concentrations of agonist**

CD42b positive percentage of events in the microvesicle gate for the $CD14^{+}CD16^{+}$ monocyte subset, following treatment of stirred whole blood, incubated at 37°C with different agonists over time. 30 Con and 60 Con are stirred and incubated at 37°C without the addition of any agonist. 0 min control is untreated and fixed instantly prior to any incubation period. (Data are mean; ADP 5-6 experiments, U46619 6-7 experiments, rhodocytin 4-5 experiments.)

| Agonist | Time point 0 | 5 Minutes | 10 Minutes | 15 Minutes | 20 Minutes | 25 Minutes | 30 Minutes | 60 Minutes | 30 Minutes con | 60 Minutes Con | Platelet |
|---|---|---|---|---|---|---|---|---|---|---|---|
| **3µM ADP** | 60.5 | 57.1 | 49.3 | 44.8 | 45.7 | 51.5 | 60.0 | 45.5 | 47.6 | 42.7 | 107.0 |
| **3µM U46619** | 68.3 | 183.9 | 171.3 | 129.6 | 125.2 | 103.2 | 91.4 | 85.4 | 82.3 | 84.9 | 146.6 |
| **30nM Rhodocytin** | 52.2 | 124.0 | 124.5 | 146.0 | 165.3 | 71.5 | 72.3 | 50.9 | 41.5 | 45.0 | 75.9 |

**Table 5-19: CD42b MFI on the $CD14^{+}CD16^{+}$ monocyte subset in the platelet gate after treatment with low concentrations of agonist**

CD42b MFI in the platelet gate for the $CD14^{+}CD16^{+}$ monocyte subset, following treatment of stirred whole blood, incubated at 37°C with different agonists over time. 30 Con and 60 Con are stirred and incubated at 37°C without the addition of any agonist. 0 min control is untreated and fixed instantly prior to any incubation period. (Data are mean; ADP 5-6 experiments, U46619 6-7 experiments and rhodocytin 4-5 experiments.)

| Agonist | Time point 0 | 5 Minutes | 10 Minutes | 15 Minutes | 20 Minutes | 25 Minutes | 30 Minutes | 60 Minutes | 30 Minutes con | 60 Minutes Con |
|---|---|---|---|---|---|---|---|---|---|---|
| **3µM ADP** | 4.3 | 7.0 | 6.8 | 9.4 | 14.7 | 19.6 | 20.9 | 17.2 | 4.4 | 4.7 |
| **3µM U46619** | 2.1 | 6.3 | 7.6 | 6.5 | 6.4 | 6.5 | 7.5 | 3.7 | 1.5 | 1.5 |
| **30nM Rhodocytin** | 3.4 | 7.4 | 7.2 | 4.5 | 6.8 | 12.5 | 16.8 | 19.2 | 2.0 | 2.2 |

**Table 5-20: Percentage of the $CD14^{+}CD16^{+}$ monocyte subset in the platelet gate after treatment with low concentrations of agonist**

CD42b positive percentage of events in the platelet gate for the $CD14^{+}CD16^{+}$ monocyte subset, following treatment of stirred whole blood, incubated at 37°C with different agonists over time. 30 Con and 60 Con are stirred and incubated at 37°C without the addition of any agonist. 0 min control is untreated and fixed instantly prior to any incubation period. (Data are mean; ADP 5-6 experiments, U46619 6-7 experiments and rhodocytin 4-5 experiments.)

**5.4.0 Discussion**

Upon addition of a known platelet agonist, either ADP, rhodocytin, U46619 or CRP-XL, to stirred whole blood incubated at 37°C, there was a significant increase in MPA formation. However, the data suggests no differences were observed between monocyte subsets in their ability to form MPA. A previous study, has shown that blood from patients with coronary artery disease had increased MPA compared to controls, they also report that $CD14^{+}CD16^{+}$ monocyte subset showed no significant increase in MPA formation compared to the $CD14^{+}CD16^{-}$ subset (Czepluch et al., 2014).

The degree of MPA formation was time dependent and increased with the duration of incubation. An increase in aggregate formation after treatment with a platelet agonist is to be expected, as previous data demonstrates that MPA formation increases upon platelet activation (Michelson et al., 2001; Jensen et al., 2001; Gkaliagkousi et al., 2007). Interestingly, Xiao & Théroux, (2004), showed patients suffering from ACS have an increased propensity to form MPA after blood was treated with either ADP or TRAP *ex vivo*.

However, addition of 50µg/ml oxLDL appeared to have little effect on MPA formation over time, with the exception of a small non significant increase seen after 60 minutes. Others have shown that oxLDL can activate platelets, although the agonistic effect is not as dynamic as the classical routes of platelet activation (Chen et al., 2001; Korporaal et al., 2007). It would be interesting in future experiments to determine whether increasing the incubation period, to more than 60 minutes results in a time dependent increase in MPA formation in response to this agonist, albeit with very different dynamics from the other agents tested.

Here we observed no differences in maximum response for percentage MPA formation using lower concentrations of rhodocytin, ADP or U46619 compared to the higher

concentrations, indicating that these agonists are just as effective at lower concentrations. Previous aggregometry data using washed isolated platelets, stimulated with 30nM rhodocytin has shown that maximal platelet activation can be achieved with this concentration of agonist (Pollitt et al. 2010). It has also been demonstrated that 1µM U46619 can cause platelet aggregation in PRP (Moraes et al., 2007). If maximal response to the platelet agonist is also achieved in whole blood then it is likely that there will be no difference in MPA formation between concentrations. The data showed an increase in donor variability at lower concentrations of all agonists, with some donors clearly more responsive than others at these marginal concentrations. Future work should determine the sensitivity of MPA formation to platelet agonists, as the concentrations used currently represent robust stimulation and our data indicates that this may not be required to induce interactions between platelets and monocytes.

Subtle differences between platelet agonists were observed; rhodocytin appeared to be the most potent agonist, whereas ADP, U46619 and CRP-XL showed a much lower maximum response. The difference in maximum response of MPA formation between agonists may be due primarily to the agonists ability to activate platelets. For example, ADP is recognised as a relatively weak platelet agonist (released by platelets themselves), which must signal through both P2Y1 and P2Y12 receptors in order to fully activate platelets, usually in a positive feedback loop to reinforce activation through other receptors. Thromboxane, also synthesised by platelets is able to cause further activation through a positive feedback loop, in this instance by signalling through TP receptor (Paul et al., 1999). It would be of interest to determine how much of the MPA formation in response to agonists such as CRP-XL were dependent upon these feedback loops, experiments could be readily conducted in the presence of specific receptor antagonists.

Further analysis revealed that the levels of CD42b on MPA rarely equalled that of a single resting platelet. Indeed, our time course data suggested that monocytes accumulate CD42b in quanta that are significantly less than whole platelets. It has been well documented that upon platelet activation CD42b positive PMV are generated (Flaumenhaft et al., 2009; Hargett and Bauer, 2013). Increased levels of microvesicles have been found alongside increased levels of soluble P-selectin (a well known marker for inflammation) in patients with chronic inflammatory disease (Burton et al., 2013; Joseph et al., 2001). Christersson et al, (2010) also demonstrated that the number of microvesicles in whole blood increased after treatment with ADP. One explanation for MPA accumulation of CD42b in quanta less than a platelet, which was observed in this study, could be that monocytes may be accumulating platelet derived microvesicles over time, rather than binding to whole platelets. A potential confounding issue with this analysis is the fact that CD42b is a 'shedable' marker (Michelson et al., 1994). It is therefore possible that after platelet activation CD42b is shed, reducing the MFI of an activated platelet compared to a resting one. Future studies should optimise the use of other markers such as CD41 or P-selectin.

As well as appearing to possibly accumulate CD42b positive microvesicles, the $CD14^{+}CD16^{+}$ monocyte subset appears to bind whole platelets after treatment with U46619, rhodocytin and CRP-XL, at least through the early part of the time course. Several studies have implied that upon platelet activation, MPA form (Jungi et al., 1986; Rinder et al., 1991; Christersson et al., 2010). Very few studies have attempted to determine the number of platelets adhering. Xiao and Théroux, (2004) used the MFI of CD42a to determine the number of platelets bound to monocytes. They demonstrated that ~15% MPA formed in untreated control blood and these heterotypic aggregates had up to 3 platelets bound. This is in contrast to the findings from our study where untreated whole blood, which was kept under conditions of low shear for up to one hour had ~4% MPA, which never reached the MFI of a resting platelet.

Whole blood treatment with ADP showed an increase to 45% with 4 platelets adhering per monocyte (Xiao and Théroux, 2004). Again, this is in contrast to data from our study where the MFI never reaches that of a resting platelet after treatment with ADP. The study by Xiao et al 2004, was carried out with blood which had been incubated under static conditions rather than being kept under conditions of stirring, as was the case in the current study. Incubating whole blood under static conditions may encourage MPA to form and could explain discrepancies in the data.

This study also showed that after treatment with 3µM U46619 there appeared to be a decrease in CD42b accumulation on both monocyte subsets between 30-60 minutes. It has again been documented that microvesicles can be internalised by monocytes, although it is not yet known whether this is through a process of receptor mediated endocytosis or through fusion of the plasma membranes (Del Conde et al., 2005; Hargett and Bauer, 2013; Yang et al., 2012). This uptake of vesicles is thought to have an important role in cell communication and be a key signalling process, which allows cross talk between platelets and monocytes.

**Conclusions**

In conclusion, we have demonstrated that upon platelet activation through TP, P2Y1, P2Y12, GPVI and CLEC-2 the formation of MPA increases over time. The maximum percentage increase in MPA formation is dependent on the agonist used. Lower concentrations of some agonists were found to be as effective as higher ones, indicating the need for further titration. Our data also suggests that PMV may be responsible for MPA formation rather than whole platelets. Further work needs to be carried out to find out, which receptor platelets or PMV are using to bind to monocytes and whether their formation can be blocked.

# 6. Chapter 6- FORMATION OF LYMPHOCYTE-PLATELET AND NEUTROPHIL-PLATELET AGGREGATES IN RESPONSE TO TREATMENT WITH DIFFERENT PLATELET AGONISTS

### 6.1.0 Introduction

Lymphocyte-platelet aggregates (LPA) have been reported to be at increased levels in patients with chronic inflammatory diseases such as (SLE) compared to healthy controls (Joseph et al., 2001). It has also been suggested that the enhancement of lymphocyte capture by platelets may have a role in the recruitment of lymphocytes during the progression of atherosclerosis amongst other inflammatory diseases (Li, 2008).

A Previous study from our lab has demonstrated that immobilised activated platelets are able to capture lymphocytes from flow (Lalor and Nash, 1995). Experiments carried out both *in vitro* and *in vivo* demonstrate that activated platelets aid in leukocyte capture to endothelial cells, under proinflammatory conditions (Pitchford et al 2005; Diacovo et al. 1998; Diacovo et al. 1996; Kuckleburg et al. 2011). However, there is some debate in the literature as to whether levels of LPA increase upon platelet activation. Rinder et al, (1991) and Jensen et al, (2001) both reported there was no change in levels of LPA after treatment of whole blood with a platelet agonist. Other more recent studies do suggest that lymphocytes can bind to activated platelets, although some lymphocyte subsets are better adapted for this interaction than others (Li et al., 2006; Pitchford et al., 2005; Kuckleburg et al., 2011; Diacovo et al., 1996).

Neutrophil-platelet aggregates (NPA) are thought to have an important role in the progression of inflammatory diseases and increased circulating levels have been shown in connection with RA, SLE, ACS and ischaemic stroke (Ishikawa et al., 2012; Jensen et al., 2001; Joseph et al., 2001; Linden et al., 2007; Nijm et al., 2005). Mickelson et al, (1996) demonstrated patients with progressive angina had a significant increase in NPA following angioplasty, where atherosclerotic plaques are disrupted; a greater increase in NPA was linked to a poor prognostic outcome. Upon activation of platelets in whole blood, NPA have been shown to significantly

increase in number (Jungi et al., 1986; Klinkhardt et al., 2003; Rinder et al., 1991; Xiao and Théroux, 2004). This phenomenon has been demonstrated *in vivo* using baboons; following transfusion with activated platelets (expressing P-selectin) there was a significant increase in NPA formation compared to transfusion with resting platelets (Michelson et al., 2001).

However, there are several different signalling routes for platelet activation. Including activation through GPVI after interaction with collagen, which could occur following atherosclerotic plaque rupture (amongst other forms of mechanical damage) (Libby, 2012). This would trigger thrombosis and therefore thrombin generation, which would also lead to platelet activation (Coughlin, 2000). When platelets become activated they release the contents of δ granules containing ADP and synthesise thromboxane, both of these can increase platelet activation through an autocrine and paracrine fashion (Jin and Kunapuli, 1998; Liu et al., 2012). Oxidised low-density lipoprotein is also present in atherosclerotic plaques and may be accessible to platelets upon plaque rupture and may also activate platelets (Chen et al., 2001, Libby, 2012). Damage to cells leads to the release of histones, which have been demonstrated to activate platelets through TLR2 and TLR4 (Semeraro et al., 2011). All of these different platelet agonists have potential roles in platelet activation following vascular damage (such as atherosclerotic plaque rupture). The route of platelet activation could have an effect on the ability of platelets to bind to lymphocytes or neutrophils. Platelet activation has also been linked to an increase in platelet microvesicle (PMV) release (Chow et al., 2000). This has also been detected in conjunction with inflammatory diseases (Beyer and Pisetsky, 2010; Burton et al., 2013). It is has been demonstrated that PMV can bind to neutrophils and there is potential for them to also bind to lymphocytes, implicating this as a potential route for interaction during heterotypic aggregate formation (Forlow et al., 2000).

The aims for this chapter were;

1) To find out if activation of platelets in whole blood activated with different agonists would lead to the formation of LPA and if the route of activation had any effect on the rate, or efficiency of LPA formation.
2) To find out if NPA formed with different rates or efficiency in response to platelet activation through different receptor pathways.
3) To specifically assess the level of CD42b accumulation by neutrophils following treatment with platelet agonists.

**6.2.0 Methods**

**6.2.1 Leukocyte-platelet aggregate formation in whole blood following treatment with different platelet agonists**

Briefly CPDA anti-coagulated whole blood, was gently stirred and incubated at 37°C with platelet agonists, including 100µM and 10µM TRAP, 10µM and 3µM thromboxane mimetic U46619, 100nM and 30nM rhodocytin, 30µM and 3µM ADP, 1µg/ml CRP-XL, 1mg/ml, calf thymus histones (CTH) or 50µg/ml oxLDL. Analysis of NPA and LPA formed was determined using flow cytometry (**Figure 6.1**). Statistical analysis was carried out using Graph Pad Prism version 5.0. (For further detail see methods section 2.3.1-2.3.3.)

### 6.3.0 Results

#### 6.3.1 The effect of PAR1 signalling on LPA formation in whole blood

Our aim was to find out if platelet activation could lead to lymphocyte-platelet aggregate (LPA) formation in stirred whole blood incubated at 37°C. First, we used the potent platelet agonist TRAP (Par1 peptide, SLFFRN), to assess the effect this had on LPA formation. Whole blood was incubated with 100µM TRAP for up to 60 minutes, there was no significant increase in percentage LPA formation over time (**Figure 6-1 and 6-2**). The maximum LPA formation was detected at 60 minutes with an average of ~5%, however, this was not a significant increase compared to the 0 minute control (**Figure 6-2**).

#### 6.3.2 The effect of other platelet agonists on LPA formation in whole blood

Having determined that platelet activation using 100µM TRAP did not lead to any significant increase in LPA formation in whole blood, we wanted to find if activating platelets through different receptor pathways still showed no effect. Treatment with a range of platelet agonists including thromboxane mimetic U46619, snake venom toxin rhodocytin, ADP, CRP-XL, CTH as well as oxLDL were compared. After whole blood treatment for a period of up to 60 minutes, table 6-1 demonstrates that there is no significant increase in LPA formation, except after treatment with ADP. Indeed, after treatment with CRP-XL, rhodocytin or U46619 a significant decrease in percentage LPA formation could be detected (**Table 6-1**). Although significant, these changes were not large, representing a 2-3 fold increase above a low background level of LPA in control samples. There is no significant increase in LPA formation in untreated blood which has been incubated for up to 60 minutes (**Table 6-1**).

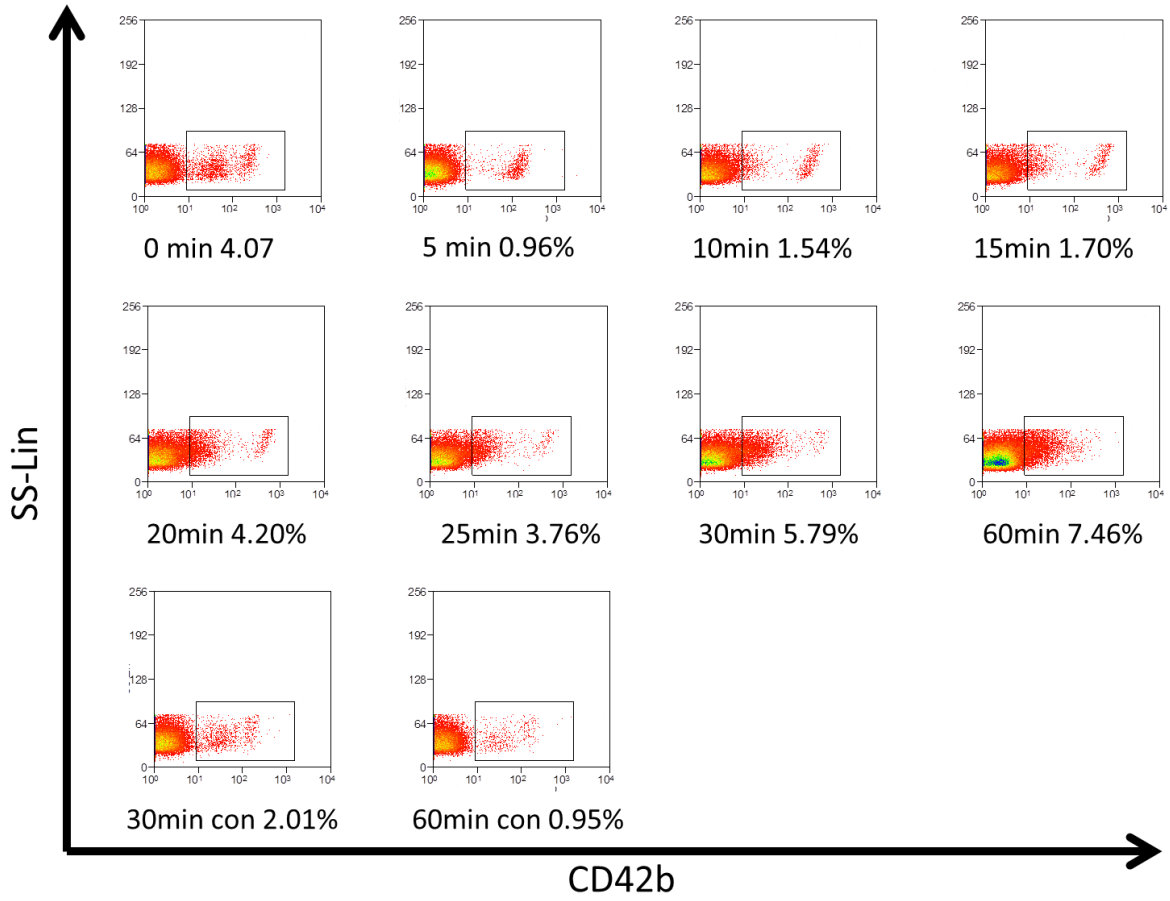


**Figure 6-1: Flow cytometry plots for LPA formation after treatment with 100µM TRAP**

Whole blood was incubated at 37°C with or without 100µM TRAP. The control (0) was fixed prior to any treatment. Lymphocyte platelet aggregates (LPA) were detected using flow cytometry with antibodies against the platelet marker CD42b and granularity (side scatter) of lymphocytes. The flow cytometry plots demonstrate no change in LPA formation over time. (Representative experiment from data set of 3).

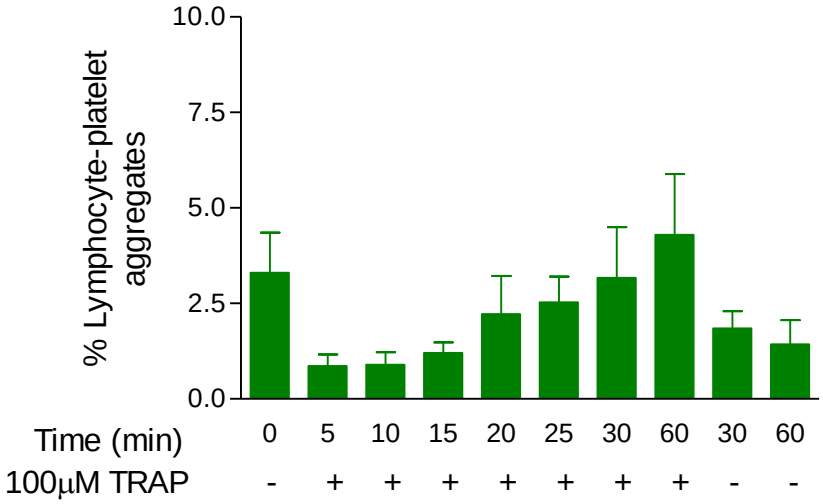


**Figure 6-2: LPA formation in whole blood after addition of 100µM TRAP**

Whole blood was incubated and mixed at 37°C, with or without the addition of 100µM TRAP. The control (0) was fixed prior to any treatment. Data were acquired using flow cytometry. There is no increase in lymphocyte-platelet aggregates over time (ANOVA ns). *,** and *** indicate P<0.05, P<0.01 and P<0.001, respectively, post hoc test Dunnett's. Data are mean +/- SEM of 3 experiments.

| Agonist | Time point 0 | 5 Minutes | 10 Minutes | 15 Minutes | 20 Minutes | 25 Minutes | 30 Minutes | 60 Minutes | 30 Minutes con | 60 Minutes con | ANOVA |
|---|---|---|---|---|---|---|---|---|---|---|---|
| **30µM ADP** | 1.9±0.4 | 0.9±0.1 | 0.9±0.1 | 1.6±0.3 | 2.2±0.5 | 2.1±0.3 | 2.8±0.5 | 1.8±0.2 | 1.6±0.4 | 1.8±0.3 | P< 0.005 |
| **1µg/ml CRP-XL** | 2.3±0.2 ł | 0.8±0.2 | 0.5±0.1 | 0.4±0.1 | 0.4±0.1 | 0.5±0.1 | 0.7±0.1 | 1.1±0.3 | 2.1±0.2 | 2.2±0.3 | P<0.001 |
| **100µM TRAP** | 3.3±1.1 | 0.9±0.3 | 0.9±0.3 | 1.2±0.3 | 2.2±1.0 | 2.5±0.7 | 3.2±1.3 | 4.3±1.6 | 1.8±0.5 | 1.4±0.6 | ns |
| **10µM U46619** | 3.4±0.9ł | 0.9±0.2 | 0.7±0.0 | 0.9±0.1 | 0.9±0.1 | 1.0±0.3 | 1.4±0.3 | 1.3±0.1 | 2.8±0.3 | 2.2±0.5 | P<0.001 |
| **100nM Rhodocytin** | 2.2±0.2ϕ | 1.5±0.5 | 0.6±0.1 | 0.6±0.1 | 0.8± 0.2 | 1.0±0.2 | 1.5±0.5 | 1.5±0.4 | 1.1±0.2 | 1.0±0.2 | P<0.05 |
| **50µg/ml oxLDL** | 2.5±0.6 | 2.9±0.7 | 2.9±0.7 | 2.6±0.5 | 2.8±0.7 | 2.7±0.8 | 2.3±0.6 | 1.4±0.2 | 1.9±0.3 | 2.0±0.6 | ns |
| **1mg/ml CTH** | 1.9±0.4 | 1.2±0.2 | 1.3±0.3 | 1.2±0.4 | 1.5±0.2 | 1.5±0.1 | 1.4±0.2 | 1.3±0.2 | 1.6±0.5 | 1.6±0.2 | ns |

**Table 6-1: Mean percentage LPA formation after treatment with high concentration of various agonists**

Table 6-1 shows the mean percentage lymphocyte-platelet aggregate formation, in stirred whole blood, incubated at 37°C, in response to treatment with different agonists. 30 Con and 60 Con are stirred and incubated at 37°C for 30 and 60 minutes without the addition of any agonist. The control (0) was fixed prior to any treatment. ANOVA indicates a significant increase in Lymphocyte-platelet aggregates (LPA) formation over time, after treatment with ADP. ANOVA indicates a significant decrease in LPA occurs over time after treatment with CRP-XL, U46619 and rhodocytin. Post-hoc test Dunnett's ł indicates 0 minute control is significantly higher than after addition of agonist, ϕ indicates 0 min is significantly higher than after 10-20 minute incubation with agonist. Data are mean +/-SEM; ADP 4-7 experiments, CRP-XL 4 experiments, TRAP 3 experiments, U46619 3 experiments, Rhodocytin 3 experiments, oxLDL 5-6 experiments and CTH 3-4 experiments.

### 6.3.3 The effect of PAR signalling on NPA formation in whole blood

Having found 100µM TRAP has no effect on lymphocyte-platelet aggregate formation in stirred whole blood incubated at 37°C, we now wanted to assess if this agonist had any detectable effect on NPA formation under the same conditions. A significant increase in percentage NPA formation can be detected after 20 minutes TRAP treatment (**Figure 6-3 and 6-4**). A maximum of ~45% NPA formation can be detected at 60 minutes (**Figure 6-3 and 6-4**). There is no significant increase in NPA formation in untreated whole blood incubated for up to 60 minutes (**Figure 6-3 and 6-4**).

### 6.3.4 The effect of other platelet agonists on NPA formation

Having demonstrated that activation of platelets through the PAR1 pathway leads to a significant increase in NPA formation, we now wanted to find out if activation through other platelet receptor pathways would also lead to an increase in NPA over time. The agonists used included thromboxane mimetic U46619, rhodocytin, ADP, CRP-XL, CTH as well as oxLDL. After treatment of whole blood with ADP, TRAP, rhodocytin and U46619 a significant increase in NPA formation could be detected over time (**Table 6-2**). A significant increase in percentage NPA formation can be detected at 20 minutes after treatment with ADP and TRAP and after 30 minutes with U46619 and rhodocytin, compared to untreated, fixed blood (0 minute control) (**Table 6-2**). The most effective agonist which showed maximum NPA formation of ~45% was TRAP, followed by rhodocytin (~25%), ADP (15%) and U46619 (9%), (**Table 6-2**). No significant increase in NPA formation can be detected over time after treatment with oxLDL or CTH (**Table 6-2**). However, a small but significant increase of ~9% can be detected after 60 minute incubation with CRP-XL. No significant increase in percentage NPA formation can be detected in unstimulated blood, which has been incubated at 37°C for up to 60 minutes (**Table 6-2**).

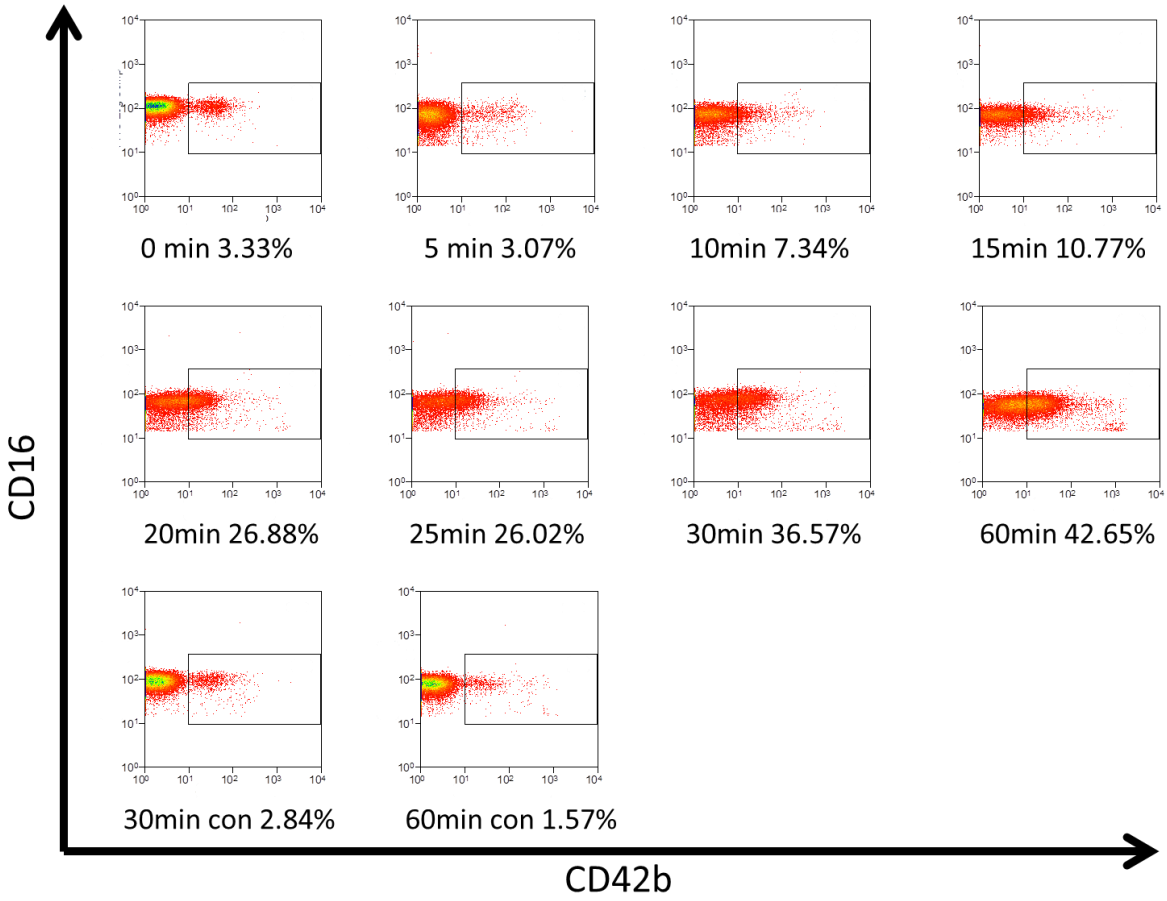


**Figure 6-3: Flow cytometry plots NPA formation after treatment with 100µM TRAP**

Whole blood was incubated at 37°C, with or without 100µM TRAP. The control (0) was fixed prior to any treatment. Neutrophil-platelet aggregates (NPA) were detected using flow cytometry with antibodies against the platelet marker CD42b and neutrophil marker CD16. The data shows an increase in NPA formation over time. (Representative experiment from data set of 3).

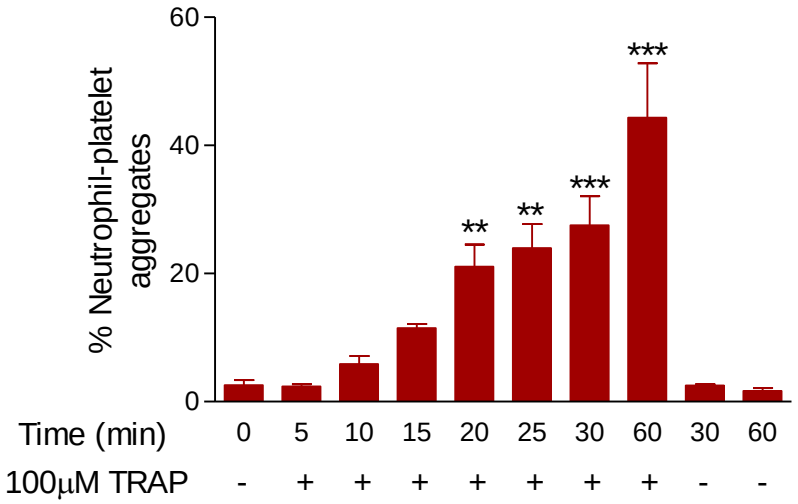


**Figure 6-4: NPA formation in whole blood after addition of 100μM TRAP**

Whole blood was incubated and stirred at 37°C, with or without the addition of 100μM TRAP. The control (0) was fixed prior to any treatment. Data were acquired using flow cytometry. ANOVA ($P<0.001$) reveals a significant increase in neutrophil-platelet aggregate formation over time. There is a significant increase in NPA formation after 20 minute incubation with TRAP compared to 0. (*,** and *** indicate $P<0.05$, $P<0.01$ and $P<0.001$ respectively, post hoc test Dunnett's). Data are mean +/-SEM of 3 experiments.

| Agonist | Time point 0 | 5 Minutes | 10 Minutes | 15 Minutes | 20 Minutes | 25 Minutes | 30 Minutes | 60 Minutes | 30 Minutes con | 60 Minutes con | ANOVA |
|---|---|---|---|---|---|---|---|---|---|---|---|
| **30µM ADP** | 1.9±0.4 | 2.8±1.1 | 2.8±0.3 | 7.9±2.0 | 13.8±5.0 ** | 15.4±3.4 ** | 17.2±2.4 *** | 13.9±3.2 * | 3.3±1.7 | 4.0±2.2 | P<0.0001 |
| **1µg/ml CRP-XL** | 1.5±0.3 | 2.6±0.8 | 2.3±0.7 | 2.1±0.8 | 3.5±1.9 | 3.5±1.5 | 7.6±3.4 | 9.4±3.6 | 2.7±0.8 | 4.1±2.0 | ns |
| **100µM TRAP** | 2.6±0.8 | 2.4±0.4 | 5.9±1.3 | 11.5±0.6 | 21.1±3.4 ** | 24.0±3.7 ** | 27.5±4.6 *** | 44.3±8.5 *** | 2.5±0.2 | 1.7±0.5 | P<0.0001 |
| **10µM U46619** | 2.9±1.0 | 2.5±0.4 | 2.2±0.5 | 2.8±0.7 | 3.5±0.9 | 5.6±0.5 | 7.6±2.1* | 9.0±1.2 ** | 3.3±1.2 | 2.3±0.6 | P<0.001 |
| **100nM Rhodocytin** | 1.7±0.2 | 3.6±0.8 | 3.0±0.8 | 4.7±1.6 | 5.0±1.6 | 13.6±4.7 | 21.7±7.9 * | 25.7±10.7 ** | 1.6±0.5 | 1.4±0.5 | P<0.01 |
| **50µg/ml oxLDL** | 2.2±0.4 | 3.9±1.0 | 3.5±0.7 | 3.8±0.9 | 3.3±0.7 | 3.3±0.6 | 2.9±0.3 | 3.0±1.1 | 2.9±0.8 | 2.4±0.6 | ns |
| **1mg/ml CTH** | 1.6±0.3 | 2.2±0.8 | 2.3±0.7 | 2.2±0.8 | 1.9±0.7 | 2.1±0.7 | 2.5±0.7 | 2.4±0.6 | 1.5±0.3 | 2.2±0.6 | ns |

**Table 6-2: Mean percentage NPA formation after treatment with high concentration of various agonists**

Table 6-2 demonstrates the mean percentage neutrophil-platelet aggregate formation, in stirred whole blood, incubated at 37°C, in response to different agonists over time. 30 Con and 60 Con are stirred and incubated at 37°C without the addition of any agonist. The control (0) was fixed prior to any treatment. ANOVA indicates a significant increase in NPA formation over time, after treatment with either, ADP, TRAP, U46619 or rhodocytin. *,** and *** indicate P<0.05, P<0.01 and P<0.001, respectively, post hoc test (Dunnett's) following a One-way ANOVA. (Data are mean +/- SEM; ADP 4-7 experiments, CRP-XL 4 experiments, TRAP 3 experiments, U46619 3 experiments, Rhodocytin 3 experiments, oxLDL 5-6 experiments and CTH 3-4 experiments).

### 6.3.5 Determining the level of accumulation by neutrophils in response to PAR1 signalling

Having identified the formation of NPA in response to platelet activation with 100μM TRAP we now wanted to determine the accumulation of platelet specific CD42b, by neutrophils, over time (see Methods chapter 2.3.3 for details). Figure 6-5A suggests that very few cells of the neutrophil population have a CD42b MFI equivalent to that of a resting platelet at the 60 minute time point. One explanation for the CD42b MFI being lower than that of a resting platelet is that neutrophils may be accumulating PMV over time, rather than adhering to whole platelets.

A small increase in CD42b MFI in the microvesicle gate was observed, coupled with the increase in percentage of neutrophils in this gate, this suggests that neutrophils could possibly be adhering to PMV, at increasing levels, over time, after treatment with TRAP (**Figure 6-5B, D and Tables 6-3 and 6-5**). The CD42b MFI of the neutrophil population between 5 and 60 minutes in the platelet gate was shown to be almost equal to that of a resting platelet (**Figure 6-5C and Table 6-5**). There was an increase in percentage of neutrophils in this gate over time, suggesting that at least towards the end of the time course (20-60 minutes), whole platelets may also be adhering to neutrophils (**Figure 6-5E and Table 6-6**). The CD42b MFI of untreated neutrophils at the 60 minute time point was also equal to that of a resting platelet but the percentage of events in this gate was low (there was also no significant increase in NPA formation at this time point) making it unlikely that platelets are binding in this instance (**Figure 6-5C, E, Table 6-5 and 6-6**).

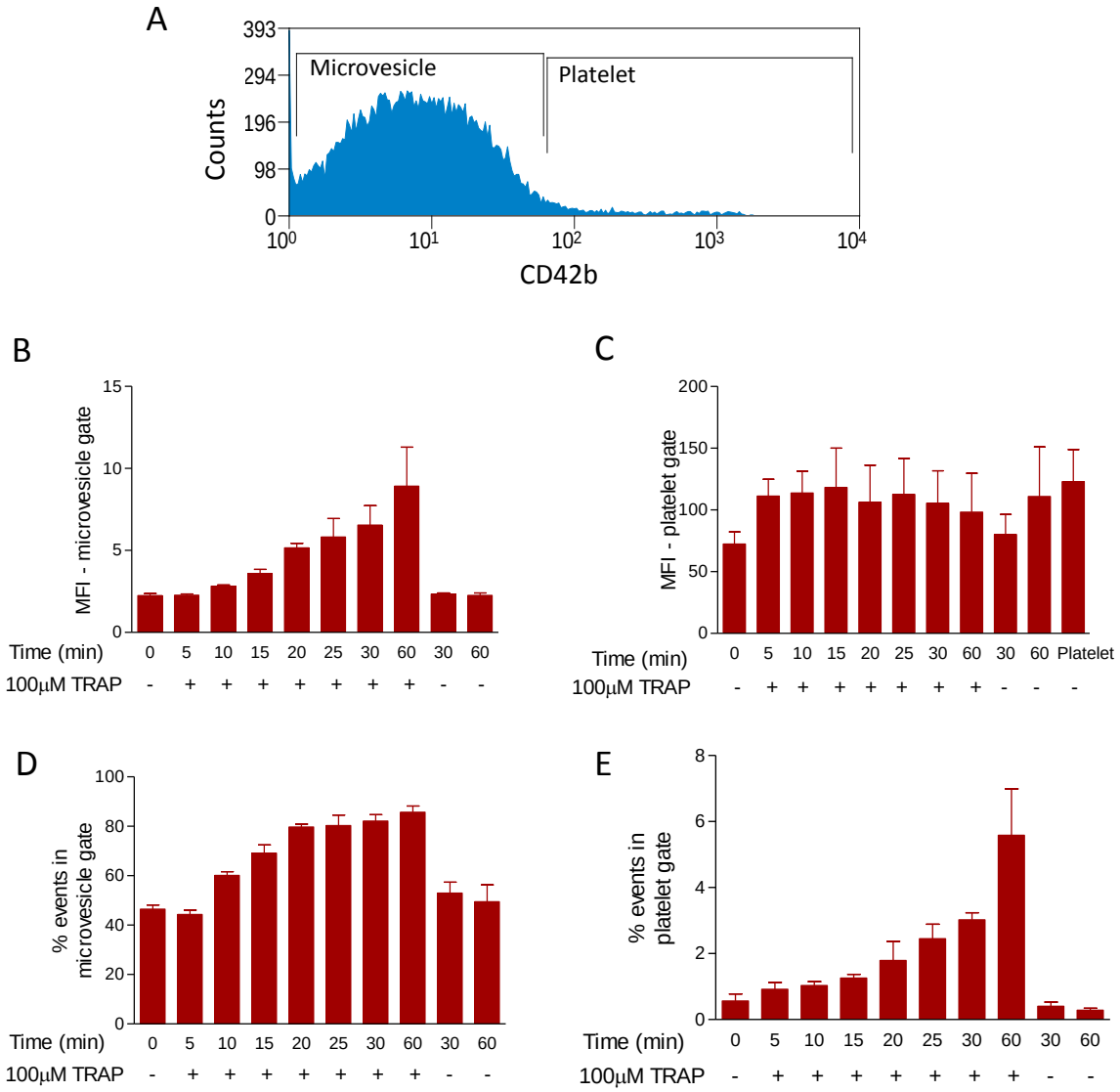


**Figure 6-5: CD42b expression on the neutrophil population after treatment with 100µM TRAP**

Whole blood was incubated and stirred at 37°C with or without the addition of 100µM TRAP. Control (0) was fixed prior to any treatment. Data were acquired using flow cytometry. A) Demonstrates the gating strategy at the 60 minute time point. B) and D) show an increase in the CD42b MFI and percent positive cells in the microvesicle gate, respectively, over time for the neutrophil population. C) Shows the CD42b MFI of neutrophils in the platelet gate. The MFI is close to that of a resting platelet throughout except at 0 minute and 30 minute control. However, E) demonstrates that the percentage of cells in the platelet gate remains low until 20 minutes. Data are mean +/-SEM of 3 experiments.

### 6.3.6 Determining the level of CD42b accumulation by neutrophils; other agonists

The data suggests that neutrophils most likely bind PMV and whole platelets after treatment with 100µM TRAP, we then wanted to repeat this analysis for other platelet agonists. After treatment with 30µM ADP, 10µM U46619 and 100nM rhodocytin there was a small increase in the CD42b MFI of the neutrophils in the microvesicle gate, over time (**Table 6-3)**. There was also an increase in the percentage of neutrophils in this gate over time (**Table 6-4**). The maximum increase in CD42b MFI (accumulation by neutrophils) in the microvesicle gate was seen after treatment with TRAP (~9), followed by rhodocytin and ADP (~5.5) then by U46619 (~4.0) (**Figure 6-5A and C Table 6-3**). Together, with the increase in percentage of neutrophils in the microvesicle gate (**Table 6-4**), this suggests that platelet activation with TRAP leads to the highest level of CD42b accumulation by neutrophils.

After treatment with ADP the CD42b MFI never reaches that of a resting platelet, there was however, an increase in percentage of neutrophils in this gate (**Table 6-5 and 6-6**). In this instance the resting platelet MFI is low, therefore, the data should be interpreted with caution. After treatment with TRAP or rhodocytin the CD42b MFI of neutrophils in the platelet gate was almost equal to that of a resting platelet between 5-60 minutes (**Figure 6-5 B and Table 6-5**). However, the percentage of neutrophils in this gate remained low (**Table 6-6**). Together, the detection of a significant increase in NPA formation and a small increase in the percentage of neutrophils in the platelet gate after 20 minutes, following treatment with either agonist; suggests that up to one platelet may be adhering to a small population of neutrophils between 20-60 minutes (**Figure 6-4 and 6-5 and Table 6-2, 6-5 and 6-6**). Treatment with U46619 also yielded a high CD42b MFI in the platelet gate, but the percentage of neutrophils in this gate

remained stable throughout, suggesting that it is unlikely that platelets are adhering in this instance (**Table 6-5 and 6-6**).

### 6.3.7 The effect of lower concentrations of agonists on NPA formation in whole blood

Having found that treatment of whole blood with high concentrations of agonists TRAP, rhodocytin, U46619 and ADP, lead to CD42b accumulation by neutrophils, which suggested that PMV and platelets were adhering to neutrophils. We decided to test the effect of using lower concentrations of these agonists. The data indicates that 3µM ADP had no significant effect on NPA formation (**Table 6-7**). The most effective agonist was 10µM TRAP which caused a significant increase in NPA formation after 10 minutes (compared to 0 minute control), with a maximum of 65% NPA formation being detected at 60 minutes (**Table 6-7**). Treatment with both 3µM U46619 and 30nM rhodocytin lead to a maximum increase of ~20% NPA, however, this increase was detected at 60 minutes with rhodocytin and after 30 minutes with U46619 (**Table 6-7**). After 60 minute treatment with U46619 percentage NPA formation decreased and was no longer significant compared to the 0 minute control (**Table 6-7**). There was no significant increase in NPA formation in untreated blood, which had been incubated for up to 60 minutes (**Table 6-7**).

| Agonist | Time point 0 | 5 Minutes | 10 Minutes | 15 Minutes | 20 Minutes | 25 Minutes | 30 Minutes | 60 Minutes | 30 Minutes con | 60 Minutes Con |
|---|---|---|---|---|---|---|---|---|---|---|
| **30µM ADP** | 3.4 | 3.7 | 3.9 | 4.5 | 5.5 | 5.4 | 5.4 | 5.6 | 3.6 | 3.7 |
| **100µM TRAP** | 2.2 | 2.3 | 2.8 | 3.6 | 5.2 | 5.8 | 6.6 | 8.9 | 2.3 | 2.3 |
| **10µM U46619** | 2.7 | 2.7 | 2.7 | 3.0 | 3.2 | 3.6 | 3.9 | 4.0 | 2.9 | 3.1 |
| **100nM Rhodocytin** | 2.1 | 2.2 | 2.3 | 2.5 | 2.7 | 3.6 | 4.6 | 5.5 | 2.1 | 2.1 |

**Table 6-3: CD42b MFI on the neutrophil population in the microvesicle gate after treatment with high concentrations of agonist**

Table 6-3 shows CD42b MFI of neutrophil population in the microvesicle gate, following treatment of stirred whole blood, incubated at 37°C with different agonists. Control (0) was fixed prior to any treatment. 30 Con and 60 Con are incubated and stirred at 37°C without the addition of any agonist. Data were acquired using flow cytometry. (Data are means of; ADP 4-7 experiments, TRAP 3 experiments, U46619 3 experiments and rhodocytin 3 experiments.)

| Agonist | Time point 0 | 5 Minutes | 10 Minutes | 15 Minutes | 20 Minutes | 25 Minutes | 30 Minutes | 60 Minutes | 30 Minutes con | 60 Minutes Con |
|---|---|---|---|---|---|---|---|---|---|---|
| **30µM ADP** | 59.6 | 63.7 | 67.7 | 72.1 | 73.7 | 74.1 | 74.8 | 78.2 | 64.3 | 66.4 |
| **100µM TRAP** | 46.4 | 44.3 | 60.1 | 69.2 | 79.7 | 80.3 | 82.1 | 85.7 | 53.0 | 49.5 |
| **10µM U46619** | 52.6 | 53.8 | 53.4 | 59.2 | 64.1 | 69.6 | 74.2 | 77.2 | 65.8 | 72.6 |
| **100nM Rhodocytin** | 45.3 | 46.8 | 52.3 | 58.0 | 60.6 | 72.1 | 77.0 | 84.6 | 47.2 | 47.4 |

**Table 6-4: Percentage of neutrophil population in the microvesicle gate after treatment with high concentrations of agonist**

Table 6-4 indicates percentage of neutrophils in the microvesicle gate, based on CD42b expression, following treatment of stirred whole blood, incubated at 37°C with different agonists. Control (0) was fixed prior to any treatment. 30 Con and 60 Con are incubated at 37°C without the addition of any agonist. Data were acquired using flow cytometry. (Data are means of; ADP 4-7 experiments, TRAP 3 experiments, U46619 3 experiments and rhodocytin 3 experiments.)

| Agonist | Time point 0 | 5 Minutes | 10 Minutes | 15 Minutes | 20 Minutes | 25 Minutes | 30 Minutes | 60 Minutes | 30 Minutes con | 60 Minutes Con | Platelet |
|---|---|---|---|---|---|---|---|---|---|---|---|
| **30µM ADP** | 92.7 | 125.1 | 129.2 | 108.0 | 75.0 | 78.4 | 76.2 | 78.8 | 81.6 | 73.6 | 194.0 |
| **100µM TRAP** | 72.4 | 111.3 | 113.8 | 118.2 | 106.2 | 112.7 | 105.4 | 98.2 | 80.0 | 110.9 | 122.9 |
| **10µM U46619** | 80.8 | 129.0 | 139.0 | 143.0 | 139.1 | 125.5 | 105.5 | 92.1 | 82.1 | 91.9 | 157.7 |
| **100nM Rhodocytin** | 65.6 | 112.3 | 93.3 | 105.2 | 97.9 | 98.7 | 94.3 | 98.4 | 87.3 | 77.6 | 110.3 |

**Table 6-5: CD42b MFI on the neutrophil population in the platelet gate after treatment with high concentrations of agonist**

Table 6-5 shows CD42b MFI of neutrophil population in the platelet gate, following treatment of stirred whole blood, incubated at 37°C with different agonists. Control (0) was fixed prior to any treatment. 30 Con and 60 Con are stirred and incubated at 37°C without the addition of any agonist. (Data are means of; ADP 4-7 experiments, TRAP 3 experiments, U46619 3 experiments and rhodocytin 3 experiments.)

| Agonist | Time point 0 | 5 Minutes | 10 Minutes | 15 Minutes | 20 Minutes | 25 Minutes | 30 Minutes | 60 Minutes | 30 Minutes con | 60 Minutes Con |
|---|---|---|---|---|---|---|---|---|---|---|
| **30µM ADP** | 1.3 | 1.4 | 1.6 | 4.2 | 5.4 | 7.8 | 9.4 | 5.5 | 2.2 | 2.6 |
| **100µM TRAP** | 0.6 | 0.9 | 1.0 | 1.3 | 1.8 | 2.5 | 3.0 | 5.6 | 0.4 | 0.3 |
| **10µM U46619** | 1.3 | 1.3 | 1.2 | 1.0 | 1.0 | 0.9 | 1.2 | 1.2 | 1.1 | 0.5 |
| **100nM Rhodocytin** | 0.5 | 1.7 | 1.0 | 1.2 | 0.9 | 1.6 | 1.8 | 1.2 | 0.4 | 0.3 |

**Table 6-6: Percentage of neutrophil population in the platelet gate after treatment with high concentrations of agonist**

Table 6-6 shows percentage of neutrophil population in the platelet gate, based on CD42b expression, following treatment of stirred whole blood, incubated at 37°C with different agonists. Control (0) was fixed prior to any treatment. 30 Con and 60 Con are stirred and incubated at 37°C without the addition of any agonist. Data were acquired using flow cytometry. (Data are means of; ADP 4-7 experiments, TRAP 3 experiments, U46619 3 experiments and rhodocytin 3 experiments.)

| Agonist | Time point 0 | 5 Minutes | 10 Minutes | 15 Minutes | 20 Minutes | 25 Minutes | 30 Minutes | 60 Minutes | 30 Minutes con | 60 Minutes con | ANOVA |
|---|---|---|---|---|---|---|---|---|---|---|---|
| **3µM ADP** | 4.2±1.1 | 7.8±2.7 | 5.3±1.1 | 5.5±0.8 | 8.9±2.1 | 10.5±2.8 | 10.8±4.1 | 6.3±2.0 | 3.4±1.2 | 2.6±0.9 | ns |
| **10µM TRAP** | 3.8±0.6 | 7.6±3.3 | 20.3±4.2 * | 33.5±5.6 *** | 49.0±7.1 *** | 50.6±3.6 *** | 61.0±2.9 *** | 64.2±2.9 *** | 3.7±0.7 | 3.9±0.7 | P<0.0001 |
| **3µM U46619** | 5.0±0.8 | 4.7±2.7 | 5.8±2.1 | 8.9±1.7 | 14.2±2.1 * | 14.8±2.6 ** | 17.3±2.5 *** | 10.4±2.9 | 3.2±1.0 | 4.0±1.0 | P<0.0001 |
| **30nM Rhodocytin** | 2.9±0.5 | 4.5±1.3 | 2.3±0.4 | 2.8±0.7 | 4.1±0.5 | 8.8±1.6 | 11.5±2.3* | 19.4±5.9** | 1.7±0.2 | 2.6±0.5 | P<0.0001 |

**Table 6-7: Mean percentage NPA formation after treatment with low concentrations of agonists**

Table 6-7 shows the mean percentage neutrophil-platelet aggregate formation, in stirred whole blood, incubated at 37°C in response to different agonists over time. 30 Con and 60 Con are stirred and incubated at 37°C, without the addition of any agonist. The control (0) was fixed prior to any treatment. ANOVA indicates a significant increase in NPA formation over time after treatment with either, TRAP, U46619 or rhodocytin. *,** and *** indicate P<0.05, P<0.01 and P<0.001, respectively, post hoc test (Dunnett's), following a One-way ANOVA. (Data are mean +/- SEM; ADP 5-6 experiments, TRAP 4 experiments, U46619 6-7 experiments, rhodocytin 4-5 experiments).

### 6.3.8 Determining the level of CD42b accumulation by neutrophils in response to lower concentrations of platelet agonists

Having demonstrated that neutrophil-platelet aggregates formed after treatment with 3μM U46619, 10μM TRAP and 30nM rhodocytin we now wanted to assess the accumulation of CD42b by neutrophils over time. The microvesicle gate showed a small increase in CD42b MFI for the neutrophil population after treatment with any agonist (**Table 6-8**). There was an increase in the percentage of neutrophils in the microvesicle gate, over time (except after treatment with 10μM TRAP where the percentage of events decreased at 30 and 60 minutes after treatment with this agonist) (**Table 6-9**). This data suggests that the neutrophils may be binding to platelet derived microvesicles after treatment with TRAP, U46619 or rhodocytin.

After treatment with 10μM TRAP and 3μM U46619 the CD42b MFI of the neutrophils in the platelet gate never approaches that of a resting platelet (**Table 6-10**). There was an increase in percentage of neutrophils in the platelet gate after treatment with 10μM TRAP. However, with the low CD42b MFI observed in the platelet gate and the decrease in percentage of events in the microvesicle gate, this should be interpreted with caution (**Table 6-9, 6-10 and 6-11**). After treatment with rhodocytin or U46619 the CD42b MFI was roughly equal to that of a resting platelet between 5 and 15 minutes (**Table 6-10**). However, the percentage of neutrophils in the platelet gate were low and there was no significant increase in NPA at this time point, making it unlikely that platelet adhesion to neutrophils was occurring (**Table 6-7 and Table 6-11**).

| Agonist | Time point 0 | 5 Minutes | 10 Minutes | 15 Minutes | 20 Minutes | 25 Minutes | 30 Minutes | 60 Minutes | 30 Minutes con | 60 Minutes Con |
|---|---|---|---|---|---|---|---|---|---|---|
| **10µM TRAP** | 2.2 | 2.4 | 3.1 | 4.0 | 4.7 | 5.0 | 4.9 | 5.9 | 2.2 | 2.2 |
| **3µM U46619** | 2.6 | 2.6 | 2.7 | 3.1 | 3.7 | 3.5 | 3.8 | 3.5 | 2.6 | 2.8 |
| **30nM Rhodocytin** | 2.2 | 2.4 | 2.2 | 2.4 | 2.7 | 3.1 | 3.4 | 4.7 | 2.1 | 2.2 |

**Table 6-8: CD42b MFI on the neutrophil population in the microvesicle gate after treatment with low concentrations of agonist**

Table 6-8 indicates CD42b MFI of neutrophil population in the microvesicle gate, following treatment of stirred whole blood, incubated at 37°C with different agonists. Control (0) was fixed prior to any treatment. 30 Con and 60 Con are stirred and incubated at 37°C without the addition of any agonist. 0 min control is untreated and fixed prior to any incubation period. Data were acquired using flow cytometry. (Data are means; TRAP 4 experiments, U46619 6-7 experiments, rhodocytin 4-5 experiments.)

| Agonist | Time point 0 | 5 Minutes | 10 Minutes | 15 Minutes | 20 Minutes | 25 Minutes | 30 Minutes | 60 Minutes | 30 Minutes con | 60 Minutes Con |
|---|---|---|---|---|---|---|---|---|---|---|
| **10µM TRAP** | 49.6 | 55.3 | 66.0 | 70.0 | 63.6 | 63.9 | 54.4 | 57.1 | 56.8 | 57.3 |
| **3µM U46619** | 56.7 | 53.6 | 56.6 | 66.5 | 70.0 | 69.1 | 71.7 | 70.2 | 61.5 | 68.2 |
| **30nM Rhodocytin** | 52.4 | 62.0 | 53.9 | 61.1 | 65.8 | 71.8 | 73.2 | 79.5 | 49.5 | 53.6 |

**Table 6-9: Percentage of neutrophil population in the microvesicle gate after treatment with low concentrations of agonist**

Table 6-9 shows percentage of neutrophil population in the microvesicle gate based on CD42b expression, following treatment of stirred whole blood, incubated at 37°C with different agonists. Control (0) was fixed prior to any treatment. 30 Con and 60 Con are stirred and incubated at 37°C without the addition of any agonist. 0 min control is untreated and fixed prior to any incubation period. Data were acquired using flow cytometry. (Data are means; TRAP 4 experiments, U46619 6-7 experiments, rhodocytin 4-5 experiments.)

| Agonist | Time point 0 | 5 Minutes | 10 Minutes | 15 Minutes | 20 Minutes | 25 Minutes | 30 Minutes | 60 Minutes | 30 Minutes con | 60 Minutes Con | Platelet |
|---|---|---|---|---|---|---|---|---|---|---|---|
| **10µM TRAP** | 31.6 | 42.3 | 33.7 | 33.2 | 38.3 | 38.3 | 43.9 | 39.8 | 30.5 | 36.3 | 62.1 |
| **3µM U46619** | 67.9 | 118.6 | 119.7 | 117.1 | 89.5 | 84.6 | 90.9 | 99.4 | 73.4 | 77.6 | 146.6 |
| **30nM Rhodocytin** | 44.1 | 90.0 | 83.4 | 64.7 | 55.0 | 55.8 | 61.0 | 46.2 | 43.4 | 43.3 | 75.9 |

### 6-10: CD42b MFI on the neutrophil population in the platelet gate after treatment with low concentrations of agonist

Table 6-10 indicates CD42b MFI of neutrophil population in the platelet gate, following treatment of stirred whole blood, incubated at 37°C with different agonists. Control (0) was fixed prior to any treatment. 30 Con and 60 Con are stirred and incubated at 37°C without the addition of any agonist. 0 min control is untreated and fixed prior to any incubation period. Data were acquired using flow cytometry. (Data are means; TRAP 4 experiments, U46619 6-7 experiments, rhodocytin 4-5 experiments.)

| Agonist | Time point 0 | 5 Minutes | 10 Minutes | 15 Minutes | 20 Minutes | 25 Minutes | 30 Minutes | 60 Minutes | 30 Minutes con | 60 Minutes Con |
|---|---|---|---|---|---|---|---|---|---|---|
| **10µM TRAP** | 1.7 | 10.7 | 7.5 | 14.0 | 27.6 | 27.4 | 41.2 | 39.8 | 1.6 | 1.7 |
| **3µM U46619** | 1.8 | 2.6 | 2.3 | 3.1 | 3.8 | 4.0 | 5.1 | 2.4 | 0.9 | 0.8 |
| **30nM Rhodocytin** | 1.5 | 1.6 | 1.1 | 1.1 | 1.2 | 2.6 | 3.4 | 5.0 | 0.7 | 0.8 |

### 6-11: Percentage of neutrophil population in the platelet gate after treatment with low concentrations of agonist

Table 6-11 shows percentage of neutrophil population in the platelet gate based on CD42b expression following treatment of stirred whole blood incubated at 37°C with different agonists. Control (0) was fixed prior to any treatment. 30 Con and 60 Con are stirred and incubated at 37°C without the addition of any agonist. 0 min control is untreated and fixed prior to any incubation period. Data were acquired using flow cytometry. (Data are means; TRAP 4 experiments, U46619 6-7 experiments, rhodocytin 4-5 experiments.)

### 6.3.9 Monocytes form heterotypic aggregates with platelets and PMV with a greater propensity than neutrophils or lymphocytes

The data from this study indicated that all leukocytes are able to form heterotypic aggregates with platelets or possibly PMV. Under certain conditions (treatment with 30µM ADP) a very small increase in LPA formation could be detected in whole blood (**Table 6-2**). A significant increase in NPA formation in whole blood could be detected after treatment with a platelet agonist such as ADP, U46619, rhodocytin or TRAP (**Table 6-2**). Previous data from this study indicated that upon treatment with a platelet agonist MPA form in whole blood (Chapter 4). TRAP was indeed shown to be the most potent agonist, in terms of leukocyte-platelet aggregate formation for both monocyte subsets and neutrophils. However, figure 6-6 demonstrates that upon activation with TRAP, MPA formed with a far greater propensity than NPA. Although here treatment of whole blood with TRAP has been used as an example to demonstrate the increased propensity of MPA formation compared to NPA formation this is indeed the case after treatment with any platelet agonist.

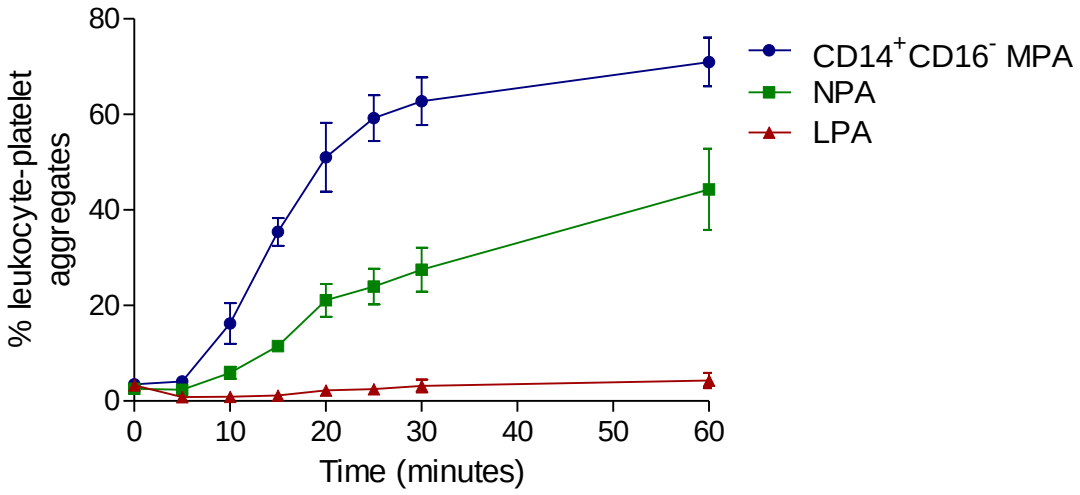


**Figure 6-6: Monocytes show the greatest propensity to form aggregates with platelets and platelet derived microvesicles following treatment with 100µM TRAP**

Whole blood was incubated and stirred at 37°C, with or without the addition of 100µM TRAP. The control (0) was fixed prior to any treatment. Data were acquired using flow cytometry. ANOVA ($P<0.001$ and $P<0.001$) reveals a significant increase in monocyte-platelet and neutrophil-platelet aggregate formation over time (respectively). There is no significant increase in LPA formation (ANOVA ns). Monocytes show a maximum of ~70% MPA formation whereas NPA show a maximum of only ~45%. Data are mean +/-SEM of 3 experiments.

### 6.4.0 Discussion

There was a very small, but significant increase in LPA formation (~2%) over time, after whole blood had been treated with 30µM ADP. However, no significant increase was detected after treatment with any other agonist. Rinder et al, (1991) demonstrated no significant increase in percentage LPA formation over time, after treatment of whole blood with thrombin, however, percentage LPA formation was found to be ~10% throughout the study. This is a higher baseline than the one observed in the present study.

Blood which has been collected (by venepuncture) into CPDA and fixed within 10 minutes prior to any treatment showed an average of ~3% NPA formation. This was not significantly increased when untreated blood was incubated at 37°C for up to 60 minutes. However, after treatment with known platelet agonists 30µM ADP, 100µM TRAP 100nM rhodocytin and 10µM U46619 a significant increase in percentage NPA could be detected over time. The data demonstrates that platelet activation is necessary for NPA to form. This is in agreement with previous studies where an increase in NPA formation has been demonstrated after treatment of whole blood with ADP and TRAP (Rinder et al., 1991; Xiao and Théroux, 2004). The study carried out by Xiao and Théroux, (2004), under static conditions showed a baseline of ~8% NPA formation in healthy controls. Our data implies that under low shear NPA do not significantly increase compared to untreated controls, for a period of up to 60 minutes. The data from these studies implies that neutrophils and platelets have a propensity to aggregate readily under static conditions. This leads us to believe that the high baseline observed under static conditions is an artefact of the experimental procedure rather than a true physiological representation of NPA, which have formed in the circulation.

It was however surprising, that no significant increase in NPA formation could be detected after treatment with CTH. As histones have a key role in activation of both innate immune cells and platelets (Huang et al., 2011; Carestia et al., 2013; Semeraro et al., 2011). Histones also account for an essential part of neutrophil NETS (Carestia et al., 2013). NETS are able to provide a scaffold for thrombus formation (Fuchs et al., 2010). This provides a clear link for histones in inflammation and thrombosis (Xu et al., 2009; Brill et al., 2012). No significant increase in NPA formation being detected during this study could be due to activation of neutrophils and subsequent degranulation, or even formation of very large aggregates with platelets, making it difficult to detect them using flow cytometry.

There were differences in the total percentage NPA formation after treatment with different agonists. Platelet activation through the PAR1 pathway using 100µM TRAP was shown to be the most potent as this lead to ~45% NPA formation, this was followed by activation through CLEC-2 signalling pathway using rhodocytin (~25%), P2Y1, P2Y12 activation through ADP ~(15%) and activation through TP using U46619 (~10%). It is however surprising, that treatment of whole blood with CRP-XL a potent platelet agonist yielded very little NPA formation (only 9% maximum). ADP and thromboxane are released from platelets themselves upon activation and are known to enhance platelet activation (Jin et al., 2002; Paul et al., 1999; Xiao and Théroux, 2004). Whereas activation through PAR-1 and CLEC-2 result in irreversible platelet signalling (Coughlin, 2000; Suzuki-Inoue et al., 2006).

A lower concentration of both 10µM TRAP and 3µM U46619 seemed slightly more effective at inducing NPA formation than higher concentrations. Rhodocytin appeared to be equally as effective at a lower concentration. Previous data has demonstrated that full platelet activation can be achieved using these concentrations of TRAP, rhodocytin and U46619 (Moraes

et al., 2007; Pollitt et al., 2010; Stephens et al., 2005). It is therefore not surprising that they are equally as potent as lower concentrations of these agonists. There was however, an increase in donor variability at low concentrations of agonist. Treatment with a lower concentration of ADP (3µM) showed no significant effect on NPA formation. This indicates that NPA formation responds in a dose dependent manner to ADP. Future work should determine sensitivity of NPA formation to other agonists as the data implies that it may not be necessary for full platelet activation to be achieved for NPA formation to occur in whole blood.

Having demonstrated that in response to platelet activation there is an increase in NPA formation in stirred whole blood. Further analysis of NPA showed that neutrophils accumulate CD42b at lower levels than that observed on a resting platelet. One explanation for this is that neutrophils accumulate PMV, generated upon platelet activation with high concentrations of ADP, TRAP, rhodocytin and U46619. This was also seen after treatment with lower concentrations of U46619, TRAP and rhodocytin. Previous data indicates that activation of platelets through PAR-1 signalling pathway leads to the generation of platelet derived microvesicle (Heijnen et al., 1999; Nygaard et al., 2014). Whole blood sheared at ($10,000S^{-1}$) and treated with TRAP peptide was found to have significantly more microvesicles compare to untreated sheared blood, however, the same study showed that ADP and U46619 had no effect (Chow et al., 2000). This study used flow cytometry to assess microvesicle number, which is not a very accurate way of counting microvesicles as most will be too small to be detected. In agreement with data shown in the current study suggesting that PMV are adhering to neutrophils Forlow et al., (2000) demonstrated that PMV could adhere to isolated neutrophils under conditions of low shear.

After 20 minute treatment with 100μM TRAP or 30 minute treatment with 100nM rhodocytin the data suggests that neutrophils may be binding to platelets in this instance. Although many studies have been carried out to assess the percentage of NPA, which form in whole blood in response to treatment with platelet agonists, very few have assessed the number of platelets adhering per neutrophil. One such study was carried out by Xiao and Théroux, (2004) used the MFI of CD42A to assess the number of platelets adhering to neutrophils. This showed that up to ~8% NPA formed at baseline with up to 2 platelets adhering per neutrophil. This was increased to ~20% with 3 platelets per neutrophil upon treatment with ADP and up to ~70% with 5 platelets per neutrophil upon treatment with TRAP. However, this study was carried out under static conditions, which the data from the current study suggests encourages NPA formation. We would therefore interpret the high level of platelet adhesion which occurs during NPA formation in the study by Xiao and Théroux (2004) as an artefact of the experimental conditions.

In this study we measured CD42b as a platelet marker on neutrophils. Upon platelet activation with thrombin surface expression of CD42b has been shown to decrease (Hourdillé et al., 1992; Schmitz et al., 1998; Hourdillé et al., 1990). This may be indicative of shedding of the receptor on MV after activation. Future studies of NPA formation in whole blood should optimise the use of other markers such as CD41 and/or P-selectin in conjunction with CD42b to determine which of these is the most robust marker of NPA formation.

The data from this study demonstrates that very few LPA form in whole blood in response to platelet activation. However both NPA and MPA form under these conditions, but MPA form with far greater propensity. This is in agreement with several studies which indicate that MPA and NPA formation in patients with chronic inflammatory diseases is increased, but

with higher levels of MPA (Jensen et al., 2001; Joseph E Italiano Jr, Mairuhu Albert T.A., 2010; Michelson et al., 2001; Mickelson et al., 1996; Xiao and Théroux, 2004). It is also in agreement with data where whole blood has been treated with a platelet agonist such as ADP or TRAP (or thrombin) *ex vivo,* treatment with an agonist leads to increased levels of both MPA and NPA but a greater increase in MPA was always observed (Jensen et al., 2001; Jungi et al., 1986; Rinder et al., 1991; Xiao and Théroux, 2004).

**Conclusions**

We have demonstrated that upon platelet activation through PAR1, TP, P2Y1, P2Y12, GPVI and CLEC-2, NPA form, but with a lower propensity than MPA, however, LPA do not. The maximum increase in NPA formed is dependent upon the agonist used. The data suggests that platelet derived microvesicles are binding to neutrophils, although, in some instances whole platelets were thought to adhere as well. Further work needs to be carried out to find out what receptor these platelet derived microvesicles, or platelets, are using to bind to neutrophils and if their adhesion can be blocked.

# 7. Chapter 7- THE ROLE OF P-SELECTIN IN LEUKOCYTE-PLATELET AGGREGATE FORMATION

### 7.1.0 Introduction

Elevated levels of leukocyte-platelet aggregates have been associated with various chronic inflammatory diseases including atherosclerosis (Harding et al., 2004; Htun et al., 2006; Joseph et al., 2001; Shantsila and Lip, 2009; Nijm et al., 2005). The increase in leukocyte-platelet aggregates is often accompanied by an increase in soluble P-selectin levels (Ridker et al., 2001; Xiao and Théroux, 2004). P-selectin is released from activated endothelial cells and activated platelets. Administering anti-platelet therapy, which reduces activation of platelets, significantly reduces levels of soluble P-selectin and levels of MPA in acute coronary syndrome (ACS) patients (Xiao & Théroux 2004). This reduction in platelet activation and P-selectin levels leading to a subsequent reduction in the levels of circulating MPA, implies that this receptor has a role in leukocyte-platelet aggregate formation.

P-selectin is only expressed on the platelet surface upon platelet activation and evidence for its potential role in MPA and NPA formation has been previously demonstrated both *in vivo* and *in vitro*. Upon activation of platelets in whole blood, significantly increased surface expression of platelet P-selectin has been detected along with an increase in MPA and NPA (Jungi et al., 1986; Rinder et al., 1991). Michelson et al, (2001) showed that infusion of thrombin activated platelets (assessed by P-selectin expression) into baboons resulted in an increase in both MPA and NPA compared to control animals infused with resting platelets. Interestingly, the MPA formed upon infusion of thrombin stimulated platelets were detectable *in vivo,* above baseline for up to 2 hours, they were stable for a longer time period than NPA (Michelson et al., 2001). In patients undergoing angioplasty, increased levels of platelet surface P-selectin, MPA and NPA can be detected immediately following plaque rupture, when compared to preoperative levels (Mickelson et al., 1996).

Leukocytes possess the necessary ligand with the highest affinity for interacting with P-selectin, P-selectin glycoprotein ligand-1 (PSGL-1) (Mehta, P. Cummings, 1998). Previous studies have demonstrated that leukocyte PSGL-1 plays an important role in leukocyte-platelet aggregate formation (Théorêt et al., 2001). As activated platelets are known to shed P-selectin positive platelet microvesicles (PMV) from their plasma membrane (Hargett & Bauer 2013; Flaumenhaft et al. 2009). It is possible that these also adhere to leukocytes using P-selectin and PSGL-1 interaction. Evidence to further support this comes from a study which indicated that PSGL-1 positive monocyte derived microvesicles are able to bind to activated platelets (Del Conde et al., 2005). We hypothesised that PMV will bind to leukocytes using surface P-selectin.

**Aims**

The aims for this chapter were;

1) To find out if LPA, NPA and MPA could be detected using P-selectin as a platelet marker and find both the percentage of aggregates formed, as well as the CD62P MFI of the aggregates.

2) To measure surface expression of PSGL-1 on monocytes, neutrophils and Lymphocytes, including after treatment with the platelet agonists CRP-XL and TRAP.

3) To find out if blocking P-selectin interactions prevents NPA and MPA formation in response to treatment with various agonists.

### 7.2.0 Methods

#### 7.2.1 Heterotypic aggregate formation using P-selectin as a platelet marker

Briefly, whole blood was collected into CPDA. Blood was either fixed within 10 minutes (0 minute control) or incubated for 30 minutes, with or without the addition of 30µM ADP, 1µg/ml CRP-XL or 100µM TRAP, at 37°C, on a roller mixer. Whole blood was fixed and incubated with antibodies against monocyte markers CD14, CD16 (also a neutrophil marker) and platelet markers CD42b and CD62P. Red cells were lysed and data were acquired using flow cytometry. (For further details see methods section 2.3.6)

#### 7.2.2 PSGL-1 expression by lymphocytes, neutrophils and monocytes

Briefly, whole blood was collected into CPDA. Blood was either fixed within 10 minutes (0 minute control) or incubated for 30 minutes, at 37°C, on a roller mixer, with or without the addition of 1µg/ml CRP-XL or 100µM TRAP. Blood was fixed and incubated with antibodies against a) CD3, CD20 and PSGL-1, or b) CD14, CD16 and PSGL-1, red cells were lysed and data was acquired using flow cytometry. (For further details see method section 2.3.7)

#### 7.2.3 Heterotypic aggregate formation in the presence of P-selectin blocking antibody

Briefly, Whole blood was collected into CPDA. 20µg/ml of P-selectin blocking antibody (G1) or relevant isotype control was added to aliquots of whole blood some were left untreated at this stage. This was followed by the addition of 30µM ADP, 1µg/ml CRP-XL, 100µM TRAP or 100µg/ml recombinant human histone H4 and 30 minutes incubation at 37°C, on a roller mixer. Blood was fixed and incubated with antibodies against monocyte markers CD14, CD16 (also a neutrophil marker) and platelet marker CD42b. Red cells were lysed and data was acquired using flow cytometry. (For further details see section 2.3.8.)

### 7.3.0 Results

#### 7.3.1 LPA detection using platelet P-selectin as a marker

Lymphocytes are defined in this protocol based only on their size and granularity. It was apparent when using the constitutively expressed platelet marker CD42b, that due to their size some resting platelets were being detected in the lymphocyte gate. To avoid this problem platelets can be identified using a marker which is only expressed upon activation; P-selectin. Untreated blood either fixed within 10 minutes of aliquoting into CPDA or incubated at 37°C for 30 minutes before fixing, showed less than 1% LPA formation (**Figure 7-1**). As previous data has demonstrated that platelet activation is necessary for a significant number of leukocyte-platelet aggregates to form, this suggests that platelets are in their resting state. There was a significant increase in LPA formation, based on the platelet marker P-selectin after whole blood was incubated for 30 minutes with 30µM ADP, 100µM TRAP or 1mg/ml CRP-XL compared to fixed untreated control (0 minute). Although significant increases were observed, these still represent exceedingly modest changes in the percentage of lymphocytes forming LPA, as treatment with any of these agonists does not induce more than a 3% increase in LPA formation (**Figure 7-1**).

#### 7.3.2 PSGL-1 expression - lymphocytes

As the main interaction between leukocytes and platelets has been well documented to be between platelet P-selectin and leukocyte PSGL-1, we decided to measure the PSGL-1 expression on different leukocyte subsets in whole blood using flow cytometry. Figure 7-2 shows the expression of PSGL-1 on lymphocytes. Identified through their size, granularity and CD3 expression, T lymphocytes were found to express PSGL-1 (**Figure 7-2A**). This remained the same even after 30 minutes incubation at 37°C (stirred), either with or without 100µM TRAP or 1µg/ml CRP-XL (**Figure 7-2A**). The MFI of PSGL-1 remains ~300 and is not significantly different

after treatment with either TRAP or CRP-XL showing that the surface expression of this marker is not affected by the addition of these platelet agonists (**Figure 7-2B**). However, figure 7-2 C and D clearly demonstrate that less than 10% of B lymphocytes (identified through size, granularity and expression of CD20) express surface PSGL-1 at very low levels.

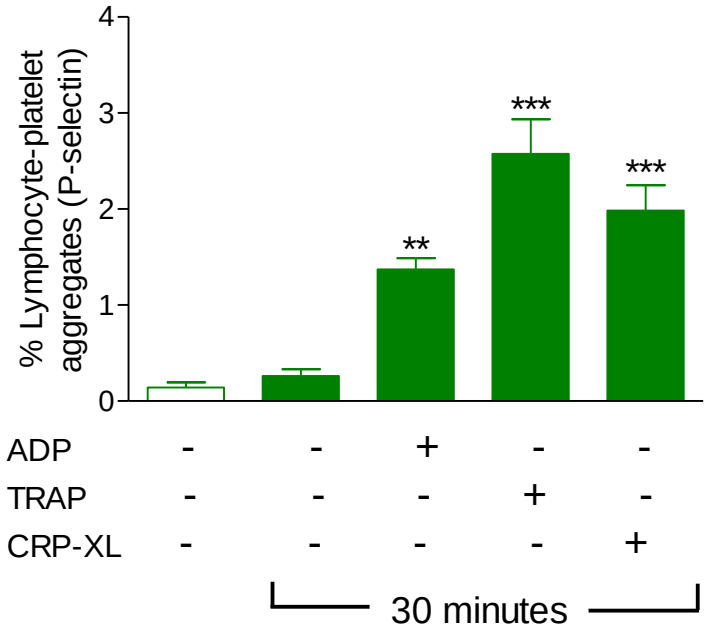


**Figure 7-1: LPA formation using P-selectin as a marker**

Whole blood was incubated at 37°C with 30µM ADP, 100µM TRAP or 1µg/ml CRP-XL or left untreated. As a control untreated whole blood was fixed within 10 minutes of being taken, prior to any treatment (0 minute control). Lymphocyte platelet aggregates (LPA) were detected using flow cytometry against the platelet marker CD62P. Less than 1% LPA form without the addition of an agonist, but a significant increase can be detected after treatment with TRAP, ADP and CRP-XL, although the total percentage LPA formed never goes above 3%. ANOVA ($P<0.0001$) indicates that there is a significant increase in LPA formation after treatment with an agonist. (*,** and *** indicate $P<0.05$, $P<0.01$ and $P<0.001$, respectively, post hoc test Dunnett's).

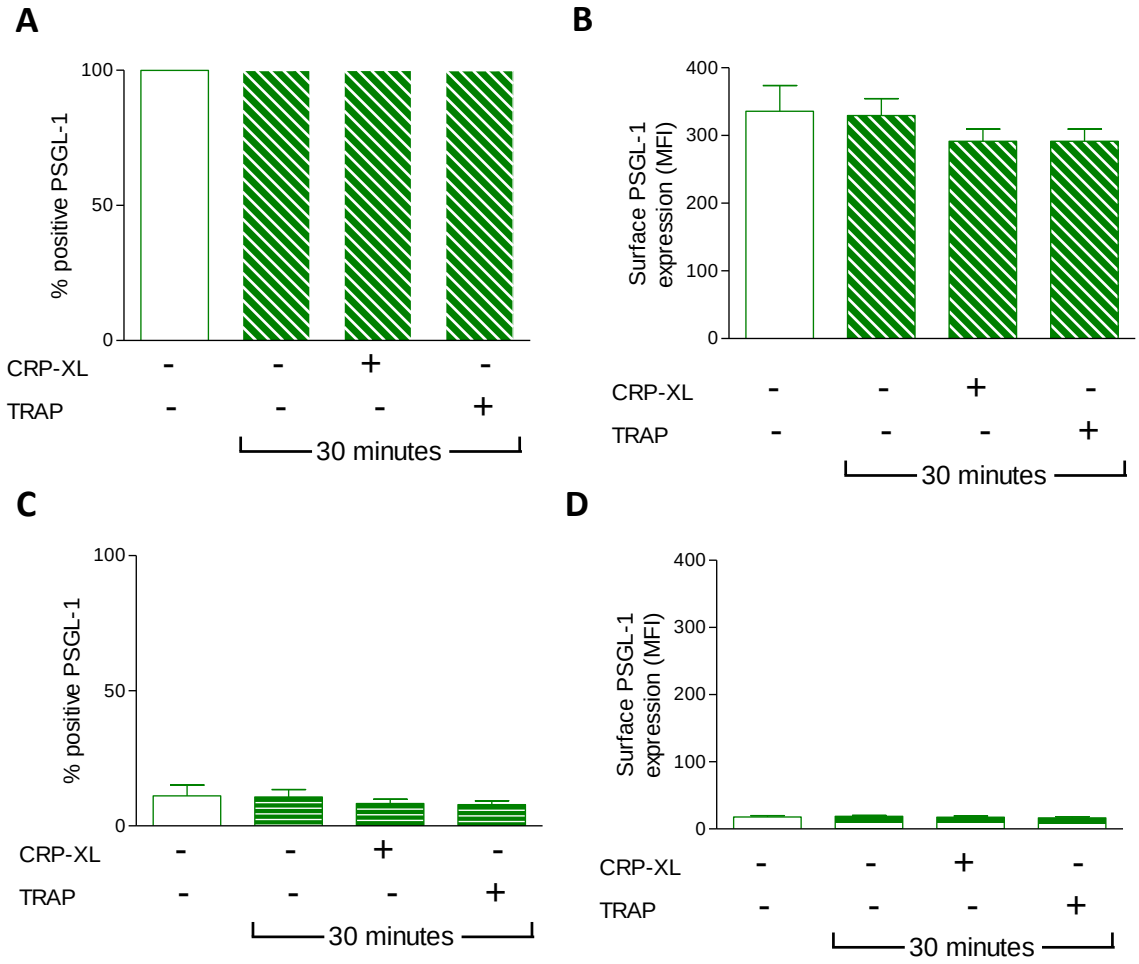


**Figure 7-2: PSGL-1 expression on T and B lymphocytes**

Figure 7-2 shows surface expression of PSGL-1 by lymphocytes in whole blood, which has been fixed prior to any treatment (0 minute control) or incubated at 37°C, following treatment with 100µM TRAP, 1µg/ml CRP-XL or left untreated. Data acquired using flow cytometry. A) Demonstrates that all T-lymphocytes, based on size, granularity and CD3 expression express PSGL-1. B) The high MFI indicates a high level of expression of PSGL-1 per cell. C) Shows that only ~10% of B-lymphocytes (depicted based on their size, granularity and CD20) express PSGL-1 D) with a very low surface expression of PSGL-1 indicated by the MFI. Data are mean +/-SEM 3 experiments.

### 7.3.3 NPA detection using P-selectin as a platelet marker

Previous data has demonstrated that upon platelet activation NPA form in whole blood. As P-selectin interaction with PSGL-1 has a potentially important role in NPA formation, we thought it important to measure the percentage NPA based on P-selectin expression after 30 minute treatment with 30µM ADP, 100µM TRAP and 1µg/ml CRP-XL.

Untreated blood either fixed within 10 minutes of aliquoting into CPDA or incubated at 37°C for 30 minutes, before fixing showed less than 1% NPA formation (**Figure 7-3**). As previous data has demonstrated that platelet activation is necessary for a significant number of NPA to form this suggests that platelets were in their resting state. There was a significant increase in percentage NPA formation in whole blood after 30 minute incubation with ADP, TRAP or CRP-XL compared to fixed, untreated control (0 minute) (**Figure 7-3A**). The maximum increase in percentage NPA formation reached 55% after treatment with TRAP (**Figure 7-3A**). However, the P-selectin MFI of these NPA remained low reaching a maximum of ~15 after treatment with TRAP or CRP-XL, indicating that the amount of P-selectin expression per NPA was low (**Figure 7-3B**).

The percentage of NPA formation based on CD42b expression from the same samples is shown in figure 7-3C. There was ~5% NPA formation observed for untreated whole blood, which had been fixed prior to treatment (0 minute) or incubated at 37°C without the addition of agonist (**Figure 7-3C**). There was a significant increase in percentage NPA formation after treatment with ADP and TRAP (**Figure 7-3C**). However, treatment with CRP-XL did not show any significant increase in NPA compared to the control using CD42b as a marker (**Figure 7-3C**). This is noteworthy, as P-selectin and CD42b are delivering different information about the formation of NPA in response to this agonist.

### 7.3.4 PSGL-1 expression - neutrophils

PSGL-1 expression by neutrophils was also demonstrated in this study. The data suggests that all neutrophils express surface PSGL-1 (**Figure 7-4A**). However, the PSGL-1 MFI is ~ 150 which indicated that surface expression by neutrophils is lower than T-lymphocytes (MFI ~300) (**Figure 7-2B and 7-4B**). Neutrophils also showed a significant reduction in surface PSGL-1 expression, after treatment with either 100µM TRAP or 1µg/ml CRP-XL compared to whole blood fixed prior to any treatment (**Figure 7-4B**). This reduction was not detected in blood, which was incubated without the addition of any platelet agonist (**Figure 7-4B**).

### 7.3.5 The effect of P-selectin blocking antibody on NPA formation

Having determined that neutrophils express PSGL-1, we decided to block its interaction with P-selectin (using P-selectin blocking antibody, G1) in whole blood, prior to any treatment with platelet agonist to see if this reduced the percentage of NPA which formed. As a control, samples were also incubated with relevant (non-blocking) IgG, and formation of NPA was assessed using flow cytometry where NPA formation was based on platelet CD42b expression.

In the presence of control IgG antibody, blood treated with 30µM ADP, 100µM TRAP and 1µg/ml CRP-XL still supported the formation of NPA (**Figure 7-5**). However, NPA formation was decreased in the absence of IgG control antibody, after treatment with TRAP and CRP-XL, this was not significant (compared to IgG normalised control) (**Figure 7-5**). There was a significant decrease in percentage NPA formation after treatment with ADP, TRAP and CRP-XL in the presence of P-selectin (G1) blocking antibody (**Figure 7-5**). This demonstrates that P-selectin is important for the formation of these aggregates.

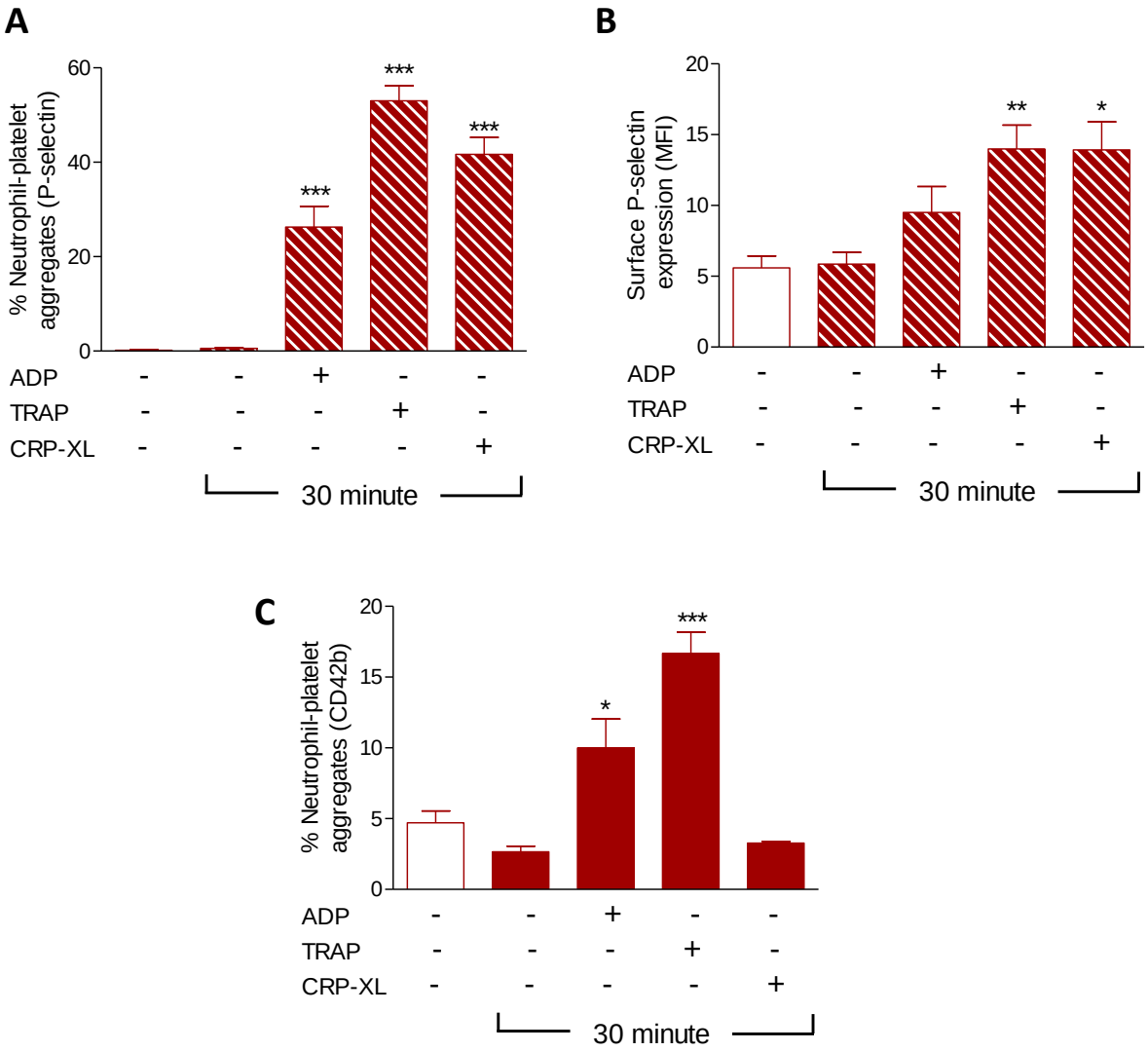


**Figure 7-3: NPA formation based on platelet P-selectin or CD42b expression**

Whole blood was incubated at 37°C with 100µM TRAP, 30µM ADP, 1µg/ml CRP-XL or was left untreated. For a control whole blood was fixed within 10 minutes of aliquoting into CPDA (0 minute control). NPA were detected using flow cytometry against the neutrophil marker CD16 and the platelet marker CD62P (A and B) or CD42b C). A) Indicates there is ~1% NPA formed in untreated whole blood, a significant increase is observed after treatment with TRAP, ADP and CRP-XL compared to 0 minute control. ANOVA ($P<0.0001$) suggests there is a significant increase in percentage NPA formation after treatment with an agonist. B) Shows a significant increase in surface expression of P-selectin indicated by the MFI after treatment with TRAP or CRP-XL, ANOVA ($P<0.005$). C) There is a significant increase in percentage NPA formation based on CD42b expression after treatment with ADP or TRAP compared to 0 minute control (ANOVA $P<0.0001$). (*,** and *** indicate $P<0.05$, $P<0.01$ and $P<0.001$, respectively, post hoc test Dunnett's.) Data are mean +/-SEM 3 experiments.

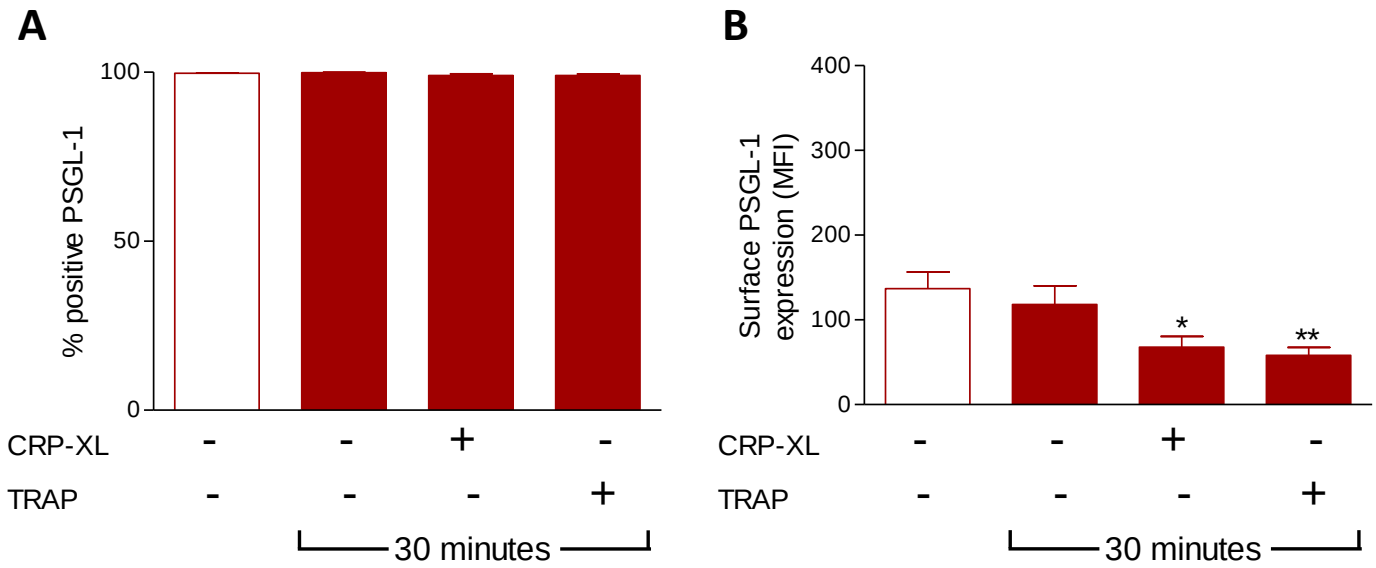


**Figure 7-4: PSGL-1 expression on neutrophils**

Figure 7-4 shows surface expression of PSGL-1 by neutrophils in whole blood, which has been fixed prior to any treatment (0 minute control) or incubated at 37°C, following treatment with 100µM TRAP, 1µg/ml CRP-XL or left untreated. Data were acquired using flow cytometry. A) Demonstrates that neutrophils based on their size, granularity and CD16 expression, express surface PSGL-1. B) Indicates that surface expression of PSGL-1 is significantly reduced after 30 minute treatment with CRP-XL or TRAP compared 0 minute control. 30 minute incubation alone showed no effect (ANOVA $P<0.01$). (*,** and *** indicate $P<0.05$, $P<0.01$ and $P<0.001$, respectively, post hoc test Dunnett's.) Data are mean +/- SEM 3 experiments.

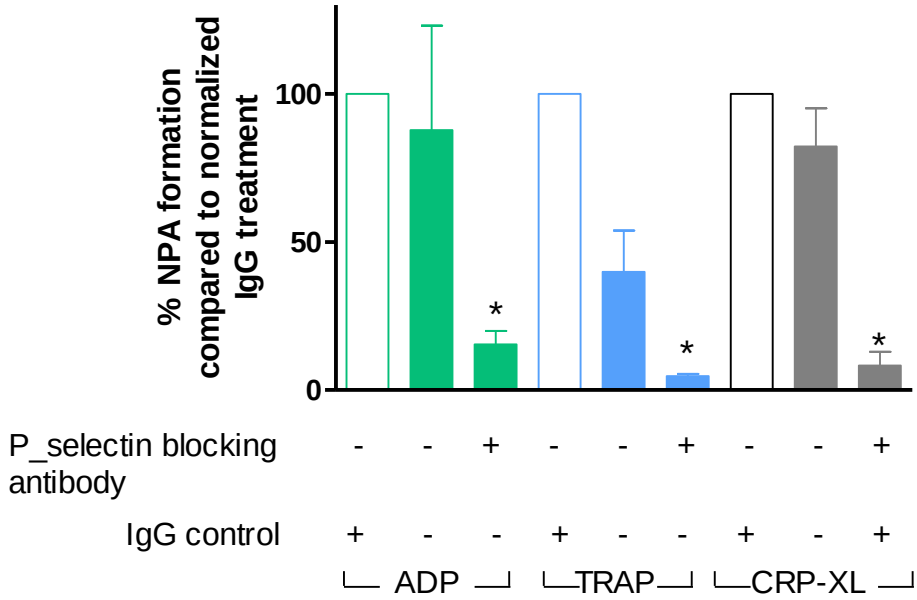


**Figure 7-5: NPA formation in whole blood after pre-treatment with P-selectin blocking antibody**

Whole blood was pre-treated with 20µg/ml of P-selectin blocking antibody (G1) or (non-blocking) unlabelled mouse IgG, or treated with agonist alone. Samples were incubated at 37°C with 100µM TRAP, 30µM ADP, 1µg/ml CRP-XL, NPA were detected using flow cytometry against the neutrophil marker CD16 and the platelet marker CD42b. Data was normalised to the IgG control. Pre-treatment with P-selectin blocking antibody shows a significant decrease in NPA formation after treatment with ADP, TRAP or CRP-XL compared to normalised IgG control (ANOVA ($P<0.005$). (*,** and *** indicate $P<0.05$, $P<0.01$ and $P<0.001$, respectively, post hoc test Bonferroni). Data are mean +/- SEM for 3 experiments.

### 7.3.6 MPA detection using P-selectin as a platelet marker.

Platelets are known to express P-selectin upon activation with an agonist. This ligand is thought to be important for MPA formation. Untreated blood either fixed within 10 minutes of aliquoting into CPDA or incubated at 37°C for 30 minutes before fixing showed ~5% MPA formation (**Figure 7-6A and B**). This suggests that platelets were in their resting state. Figure 7-6A and B demonstrated that whole blood treated with ADP, TRAP and CRP-XL significantly increase MPA formation, using P-selectin as a platelet marker, compared to blood fixed prior to any treatment (0 minute). This occurred for both the monocyte subsets and both subsets showed nearly all of the monocytes were positive for P-selectin (**Figure 7-6A and B**). The MFI for P-selectin on both subsets reached a maximum of 60 with TRAP and CRP-XL, although ADP is a lesser agonist in this respect. For comparison we include the levels of MPA formation measured using CD42b as a platelet marker (**Figures 7-6E and F**). Interestingly, there is a large discrepancy in the reported formation of MPA using this marker compared to P-selectin, with the later indicating far more robust MPA formation than our previous data indicated.

### 7.3.7 PSGL-1 expression - monocytes

Monocytes are known to express PSGL-1 the highest affinity ligand for platelet P-selectin. However, flow cytometry data from whole blood demonstrates that differences occur between monocyte subsets. Figure 7-7A and B demonstrate that both monocyte subsets express surface PSGL-1. However, monocytes in untreated blood, either instantly fixed (0 minute) or incubated for 30 minutes at 37°C showed differences in the levels of surface expression of PSGL-1; with the $CD14^{+}CD16^{-}$ subset showing a higher level of surface expression (MFI ~450) than the $CD14^{+}CD16^{+}$ subset (MFI ~350) (**figure 7-7C and D**). Figure 7-7C also indicates that PSGL-1 may be shed from the $CD14^{+}CD16^{-}$ monocyte surface after whole blood has been treated with TRAP or CRP-XL.

Interestingly however, the $CD14^{+}CD16^{+}$ subset do not demonstrate such a response (**Figure 7-7D**).

### 7.3.8 The effect of P-selectin blocking antibody on MPA formation

Having determined that monocytes express the ligand PSGL-1, we decided to block the interaction with P-selectin (using P-selectin blocking antibody, G1) prior to any treatment with platelet agonist. As a control, samples were also incubated with (non blocking) IgG and formation of MPA was assessed using flow cytometry with CD42b as a platelet marker.

Figure 7-8A and B shows a significant reduction in MPA formation in the presence of an anti-P-selectin blocking antibody, after treatment with; ADP, TRAP, CRP-XL or histone H4 for both monocyte subsets. A decrease in MPA formation is detected with agonist treatment alone compared to IgG control, however, this is not statistically significant with the exception of the effect of TRAP treatment on the $CD14^{+}CD16^{-}$ subset (**Figure 7-8A**). In this instance there is a further decrease in MPA formation on addition of P-selectin blocking antibody (**figure 7-8A**).

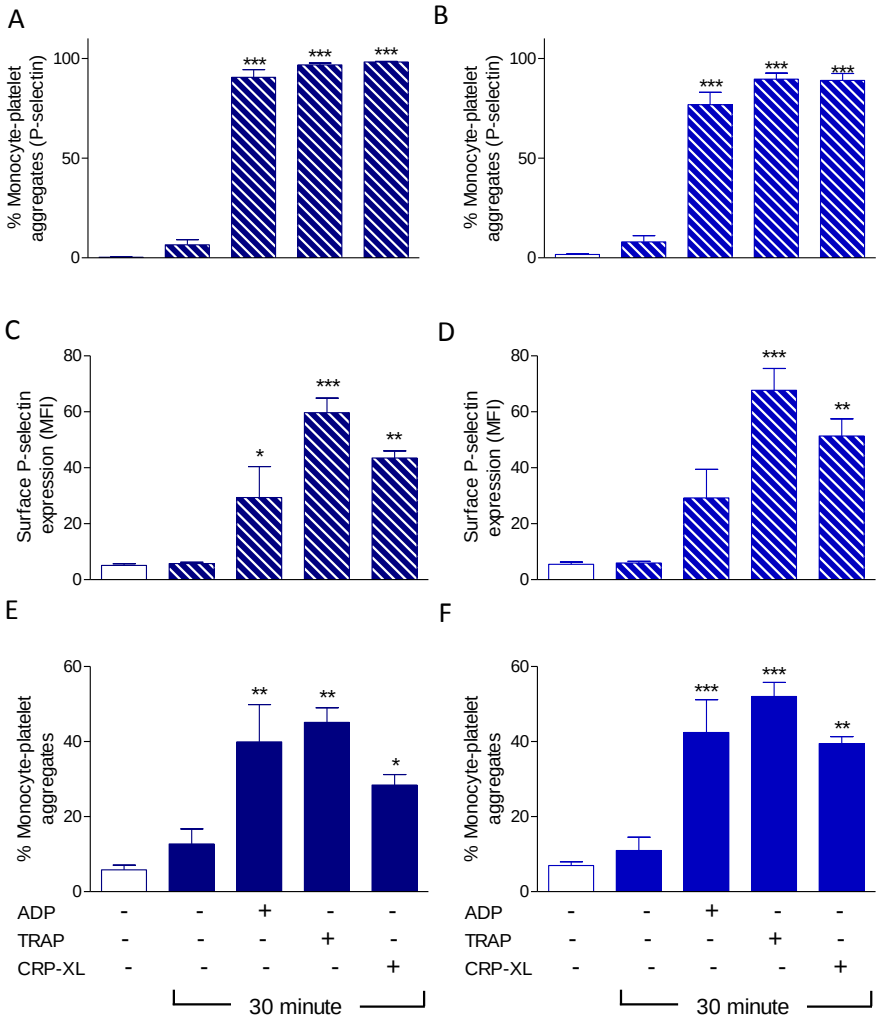


**Figure 7-6: MPA formation based on platelet P-selectin or CD42b expression**

Whole blood was incubated at 37°C with 100µM TRAP, 30µM ADP, 1µg/ml CRP-XL or untreated. For a control whole blood was fixed within 10 minutes of aliquoting into CPDA (0 minute control). Monocyte-platelet aggregate (MPA) were detected using flow cytometry against the monocyte markers CD14 and CD16 and the platelet marker CD62P (A, B, C and D) or CD42b (E and F). A, C and E show the monocyte subset $CD14^{+}CD16^{-}$ and B, D and F show the $CD14^{+}CD16^{+}$ monocyte subset. A and B) Demonstrate that MPA formation for both monocyte subsets is significantly increased, upon addition of a platelet agonist (ANOVA $P<0.001$). C) indicates that surface expression of P-selectin is significantly increased on $CD14^{+}CD16^{-}$ MPA compared to 0 minute control after treatment with all agonists (ANOVA $P<0.001$). D) shows surface expression of P-selectin $CD14^{+}CD16^{+}$ monocyte subset is significantly increased after treatment with TRAP and CRP-XL (ANOVA $P<0.001$). E) and F) demonstrate a significant increase in percentage MPA formation based on the platelet marker CD42b, after treatment with any agonist, compared to 0 minute control, (ANOVA $P<0.01$ and $P<0.001$, for E and F, respectively). *,** and *** indicate $P<0.05$, $P<0.01$ and $P<0.001$, respectively, compared to 0 minute control, blood fixed prior to treatment, post hoc test Dunnett's). Data are mean +/-SEM of 3 experiments.

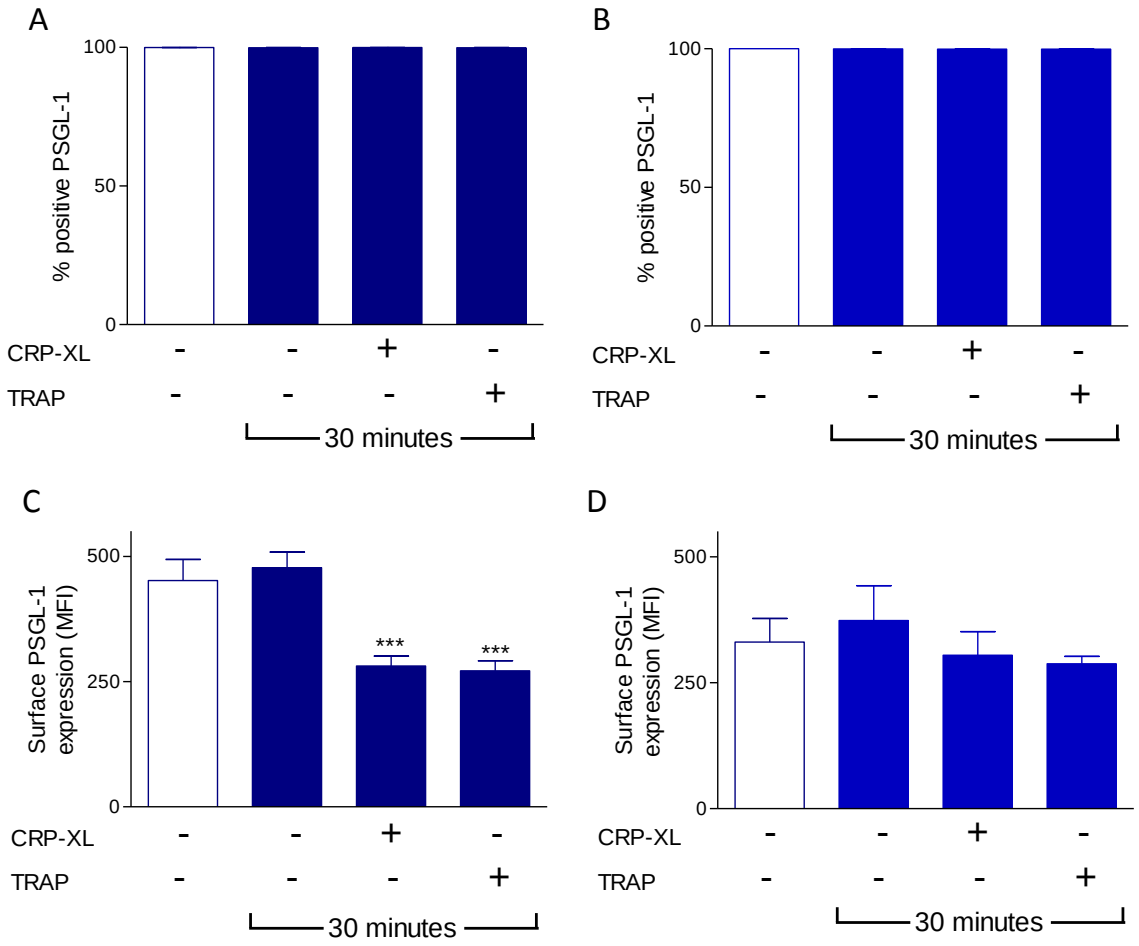


**Figure 7-7: PSGL-1 expression on monocyte subsets**

Figure 7-7 shows surface expression of PSGL-1 by monocytes in whole blood, which has been fixed prior to any treatment (0 minute control) or incubated at 37°C following treatment with 100µM TRAP, 1µg/ml CRP-XL or left untreated. Data were acquired using flow cytometry. A) and B) demonstrates that PSGL-1 is expressed by both $CD14^{+}CD16^{-}$ and $CD14^{+}CD16^{+}$ monocytes, respectively. C) Demonstrates $CD14^{+}CD16^{-}$ subset in untreated blood has a high surface expression of PSGL-1 (MFI ~500), which is significantly reduced upon addition of a platelet agonist (MFI ~250) (ANOVA $P<0.001$). D) Demonstrates $CD14^{+}CD16^{+}$ subset also express high levels of surface PSGL-1 (~300). *,** and *** indicate $P<0.05$, $P<0.01$ and $P<0.001$, respectively, compared to 0 minute, blood fixed prior to treatment, post hoc test Dunnett's.) Data are mean +/- SEM of 3 experiments.

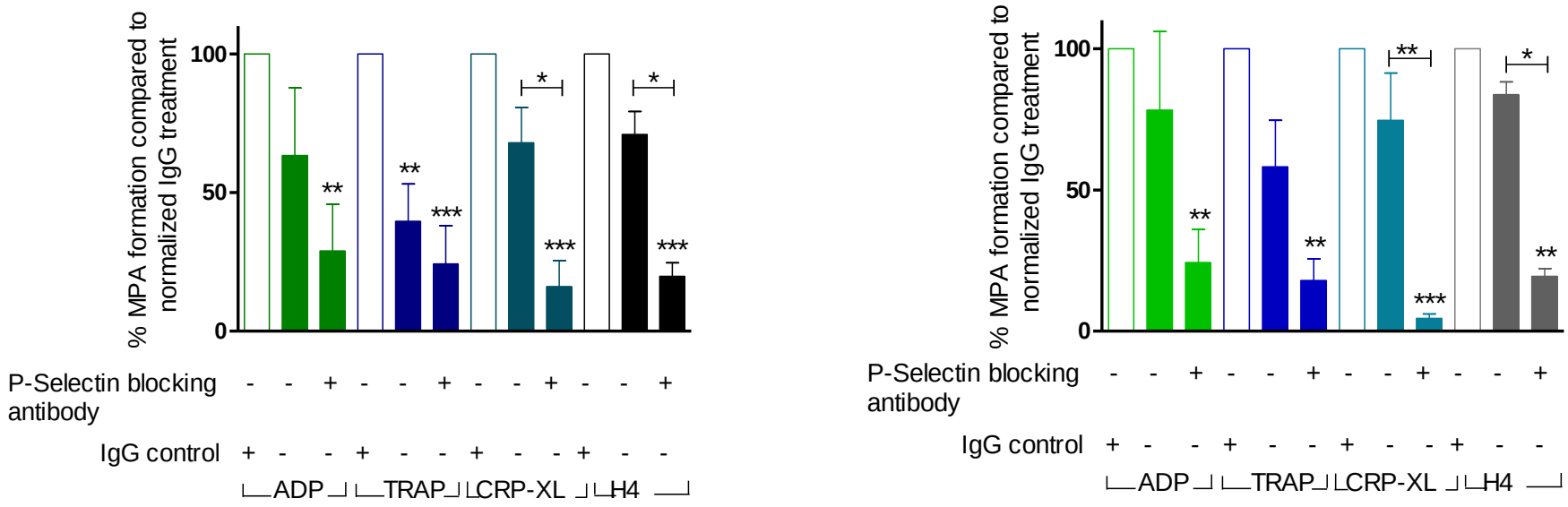


**Figure 7-8: Reduction in MPA formation in whole blood after pre-treatment with P-selectin blocking antibody**

Whole blood was pre-treated with 20µg/ml of P-selectin blocking antibody (G1), unlabelled mouse IgG or agonist alone. Samples were then incubated at 37°C with 100µM TRAP, 30µM ADP, 1µg/ml CRP-XL or 100µg/ml H4. Monocyte-platelet aggregates were detected using flow cytometry against the monocyte markers CD14, CD16 and the platelet marker CD42b. Data was normalised to the IgG control. A) Shows MPA formation for the $CD14^{+}CD16^{-}$ monocyte subset is significantly reduced after pre-treatment with P-selectin blocking antibody (ANOVA P<0.001). B) shows MPA formation for the $CD14^{+}CD16^{+}$ monocyte subset is significantly reduced after pre-treatment with P-selectin blocking antibody (ANOVA P<0.001). *,** and *** indicate P<0.05, P<0.01 and P<0.001, respectively, compared to normalised IgG control for each agonist, post hoc test Bonferroni).

**7.4.0 Discussion**

A small but significant increase (<3%) in LPA formation was detected (using P-selectin as a platelet marker) in whole blood after 30 minute treatment with ADP, CRP-XL and TRAP compared to blood fixed prior to treatment (0 minute control). Incubation at 37°C alone had no significant effect on LPA formation. This demonstrates that platelet activation is necessary for a significant level of LPA to form. This small increase is in agreement with data showing little to no change in LPA formation using the platelet marker CD42b (Chapter 6). The data is also in agreement with several previous studies. Rinder et al, (1991) demonstrated no significant increase in percentage LPA formation over time after platelet activation with thrombin, however, the baseline percentage LPA formation was found to be ~10% throughout the study. Another study investigated LPA formation by individual lymphocyte subsets after platelet activation in whole blood incubated at 37°C (Li et al., 2006). This study demonstrated that untreated NK, T-lymphocytes and B-lymphocytes had a baseline ~3% LPA. After treatment with 10µM ADP, the percentage of LPA for the NK subset significantly increased to ~10%, while T-lymphocyte subset significantly increased to 5% and B-lymphocytes showed no change (Li et al., 2006). The differences between subsets would not be detected in our study.

The leukocyte ligand with the highest affinity for P-selectin is PSGL-1. This is thought to be the most important initial interaction in the formation of leukocyte-platelet aggregates. This is in agreement with a previous study; Moore & Thompson, (1992) demonstrated that <2% isolated B lymphocytes were able to bind to purified P-selectin, this data further implies a lack of PSGL-1 expression by this lymphocyte subset. Our data also demonstrates that T-lymphocytes express very high levels of PSGL-1, but paradoxically form very few LPA under the conditions of shear imposed by our assay. A previous study demonstrated that 16.4± 10.4% and 6.0± 5.0%

isolated NK and T lymphocytes bound purified P-selectin respectively (Moore and Thompson, 1992). Indeed, it has been suggested that PSGL-1 needs to undergo post translational modifications before it is able to bind to P-selectin (Ley, 2003). Fucosyltransferase VII (FucT-VII) and Core 2 N-acetylglucosamine transferase (C2GnT) are enzymes, which mediate post translational modifications necessary for PSGL-1 binding to P-selectin (McEver and Cummings, 1997). Only $CD4^+$ and $CD8^+$ Th1 cells have been demonstrated to have these enzymes and bind P-selectin in a PSGL-1 dependent manner (White et al., 2001; Erdmann et al., 2002; Lim et al., 1999; McEver and Cummings, 1997). Data from other studies has indicated that upon T-cell activation there is an increase in expression of both of these enzymes (Erdmann et al., 2002; Vachino et al., 1995).

Thus it may be that PSGL-1 on lymphocytes is not binding to P-selectin, possibly due to inappropriate localisation on the cell surface or lack of appropriate posttranslational processing. Alternatively, P-selectin-PSGL-1 interactions may be transient, with the formation of stable aggregates in other leukocyte subsets dependent upon additional adhesive pathways, which are lacking in lymphocytes. Any interaction between platelet P-selectin and lymphocytes may be through another lymphocyte receptor which binds P-selectin with a lower affinity (Mehta, P. Cummings, 1998).

Lymphocytes are part of the acquired immune system and have a longer half life over 2 months (compared to 6-8 hour half life for neutrophils), (Hellerstein et al., 1999). Although lymphocytes are recruited to sites of inflammation this largely happens at a later stage than recruitment of innate immune cells (Ley et al., 2007). Lymphocytes have been shown to have a role in atherogenesis, however, their recruitment is thought to occur later in plaque development, mainly through interactions with APC such as monocytes and macrophages

(Woollard, 2013). It is possible that the differences in biological function of lymphocytes compared to leukocytes of the innate immune system means they have not evolved to interact with platelets to the same extent.

Data from this study indicates that MPA and NPA both form in whole blood upon addition of a platelet agonist and this is mainly due to platelet derived microvesicles adhering to monocytes or neutrophils, with platelet adhesion to leukocytes being rare events. The incidence of these heterotypic aggregates increases in a time dependent manner. Whole blood incubated without the addition of any agonist showed no significant increase in either NPA or MPA over time. This data strongly suggests that platelet activation is important for these heterotypic aggregates to occur. Upon platelet activation P-selectin is released from α granules and is trafficked to the platelet surface (Rinder et al., 1993). Platelet surface P-selectin interaction with PSGL-1 is thought to have an important role in initial platelet adhesion to leukocytes (Evangelista et al., 2003, 1999; McEver and Cummings, 1997; Théorêt et al., 2001; Zarbock et al., 2007b; Jensen et al., 2001). Platelet derived microvesicles have also been demonstrated to express P-selectin, (Hargett and Bauer, 2013) and so could potentially interact with monocyte or neutrophil PSGL-1.

It was possible to measure percentage MPA and NPA formation in whole blood after treatment with a platelet agonist using platelet P-selectin as a platelet marker. Very few MPA or NPA could be detected in whole blood, which had been fixed shortly after phlebotomy (0 minute control) or in blood which had been incubated for up to 30 minutes, without the addition of any agonist. As data from this study and others have indicated that platelet activation is necessary for a significant increase in either of these leukocyte-platelet aggregates to occur, this implies that platelets are in their resting state (Michelson et al., 2001; Rinder et al., 1991).

However, after incubation with 30μM ADP, 100μM TRAP or 1μg/ml CRP-XL there is a significant increase in NPA and MPA formation compared to untreated controls (using P-selectin as a platelet marker). The increase in percentage MPA formation is greater for both subsets of monocytes (~95% after treatment with TRAP) compared to percentage NPA formation (~50% after treatment with TRAP). The P-selectin MFI also suggested a higher surface expression of P-selectin per MPA compared to NPA. This is in agreement with previous studies where a greater increase in MPA formation compared to NPA formation has been previously demonstrated upon platelet activation both *in vivo* and *in vitro* (Michelson et al., 2001; Rinder et al., 1991). MPA have also been found to be more prominent than NPA in a chronic inflammatory disease setting (such as atherosclerosis), (Joseph et al., 2001; Mickelson et al., 1996). Over all, the most potent agonist which induced the most MPA and NPA was shown to be TRAP. However, for this part of the study a new batch of TRAP was used which did not appear to be as potent as the batch used previously.

Although P-selectin may be a more sensitive marker for both percentage MPA and NPA formation it would be difficult to use the MFI to assess whether platelet or platelet derived microvesicles are binding to platelets. As P-selectin is not expressed on the resting platelet surface, the MFI would be very low and it could not be used to differentiate between platelets and platelet microvesicles. Once an agonist is added and the platelets become activated they undergo shape change, aggregate and release granules making it difficult to identify them in a whole blood sample based on their size and granularity; making a comparison using activated platelets difficult.

Monocytes and neutrophils in untreated, CRP-XL or TRAP treated whole blood were shown to express PSGL-1. Surface expression of $CD14^{+}CD16^{-}$ monocyte subset in untreated

whole blood was highest (MFI~450), followed by $CD14^{+}CD16^{+}$ monocytes (MFI ~350). Neutrophils had a far lower surface expression of PSGL-1 (MFI ~150). Upon treatment of whole blood with the platelet agonist TRAP or CRP-XL there is a significant reduction in surface PSGL-1 expression for both $CD14^{+}CD16^{-}$ monocytes (~250) and neutrophils (~100). This may be due to masking of the PSGL-1 antigen by bound platelets or PMV. However, PSGL-1 can also be shed (proteolytically or on microvesicles). For example, monocyte microvesicles with high concentration of tissue factor have been shown to be positive for PSGL-1 (Del Conde et al., 2005), thus, we cannot exclude that shedding of PSGL-1 plays some role in this reduction.

It has been demonstrated that neutrophils and monocytes possess the enzymes necessary to carry out post translational modifications to PSGL-1 so it is known to be expressed in its active form (McEver & Cummings 1997; Mehta, P. et al 1998). A previous study, in which, isolated platelets and neutrophils (mixed at a 1:2 ratio) infused over intact or damaged endothelium *in vitro,* showed that platelets were activated (P-selectin was expressed) when flowed across a damaged surface and NPA formed (Théorêt et al., 2001). However, pre treatment of isolated platelets (before the addition of neutrophils) with PSGL-1 blocking antibody or P-selectin blocking antibody showed a significant reduction in NPA formation (Théorêt et al., 2001). Konstantopoulos et al, (1998) demonstrated that blocking antibodies against either P-selectin or PSGL-1 decreased NPA formation in sheared ($100S^{-1}$) whole blood. Kuckleburg et al. (2011) demonstrated that platelets adherent to activated EC preferentially recruited monocytes and P-selectin blocking antibody significantly reduced this. This data suggests that neutrophil and monocyte PSGL-1 in its active form plays an important role in NPA and MPA formation.

So far we have demonstrated that upon activation with a platelet agonist MPA and NPA form in whole blood and the increase in these heterotypic aggregates observed after 30 minutes is possibly due to PMV adhesion to these leukocytes. We have also demonstrated the expression of PSGL-1 by both monocytes and neutrophils, which is known to be in its active form. To find out if P-selectin is important for PMV adhesion to monocytes and neutrophils we blocked this interaction using a P-selectin blocking antibody, before activating platelets in whole blood with 30µM ADP, 100µM TRAP or 1µg/ml CRP-XL (or H4 monocytes only). A significant reduction in NPA and MPA formation (for both monocyte subsets) was observed when samples were pre-treated with P-selectin blocking antibody compared to pre-treatment with non-blocking IgG control antibody. This demonstrates that P-selectin is important in MPA and NPA formation. It suggests that platelets (and possibly platelet derived microvesicles) are adhering to monocyte and neutrophils through an interaction involving their P-selectin expression and the leukocyte PSGL-1.

As the data suggests that the initial interaction between the leukocytes and platelets (or PMV) is highly dependent on P-selectin and leukocyte PSGL-1 interaction, this could give a possible explanation as to why monocytes preferentially adhere to PMV rather than neutrophils. Monocytes have much higher surface expression of PSGL-1 than neutrophils, making them more likely to bind to PMV and platelets. However, P-selectin blocking antibody does not completely block either NPA or MPA formation. This may be because other interactions also have a role in heterotypic aggregate formation. The interaction between platelet P-selectin and PSGL-1 has been suggested to activate monocytes and neutrophils (Christersson et al., 2008; Weber and Springer, 1997). Weber and Springer, (1997) demonstrated using neutrophils that an increased expression of CD11b/CD18 occurred in response to PSGL-1 interaction with P-selectin. Evangelista et al, (1999) then demonstrated neutrophils bind to activated platelets using both

PSGL-1 and CD11b/CD18 (MAC-1). It is thought that stable adhesion takes place when active platelet $\alpha_{IIb}\beta_3$ integrin binds neutrophil CD11b/CD18 (Neumann et al., 1999; Furman et al., 2001; Brown et al., 1998). As PMV have been reported to express CD41 and CD61 (which together form the $\alpha_{IIb}\beta_3$) integrin it is also possible they are adhering to monocytes or neutrophils through this mechanism (Beyer and Pisetsky, 2010), future experiments blocking this interaction should be carried out to investigate this.

**Conclusions**

We have demonstrated that upon platelet activation, platelets (and possibly platelet microvesicles) are released and these are able to adhere to monocytes and neutrophils and at very low levels to lymphocytes. Lymphocytes express high levels of PSGL-1 although do not possess the enzymes to carry out post translational modifications, which allow binding to P-selectin. Neutrophils and monocytes, however, express PSGL-1. Data indicates that monocytes express the highest levels of PSGL-1 and form heterotypic aggregates more readily than neutrophils or lymphocytes. Blocking P-selectin significantly reduces platelet (and PMV) adhesion to leukocytes, indicating the importance of this interaction in heterotypic aggregate formation.

# 8. Chapter 8- RECRUITMENT OF MONOCYTE-PLATELET MICROVESICLE AGGREGATES TO VON WILLEBRAND FACTOR

### 8.1.0 Introduction

Platelet adhesion to activated endothelium before the appearance of atherosclerotic plaques has been demonstrated in $APOE^{-/-}$ mice (Burger and Wagner, 2003; Massberg et al., 2002). This is thought to be one of the first stages of the disease, preceding leukocyte infiltration of the artery wall (Ross, 1999). Using *in vitro* flow assays, we have previously demonstrated one of the mechanisms, through which platelets may be captured during the atherosclerotic process. Secretory phenotype SMC, found in atherosclerotic conditions, release plasmin, which is able to cleave TGF-β into its active form by removing the latency associated peptide. Active TGF-β stimulates HUVEC to express vWf on the cell surface (Tull et al., 2006). Von Willebrand factor is able to capture platelets, initially through interactions with CD42b (GPIb), before they become activated in an ADP dependent manner and bind to vWf through $\alpha_{IIb}\beta_3$ integrin (Tull et al., 2006). Activated platelets express P-selectin and are able to aid in initial leukocyte capture through classic selectin based interactions (Kuckleburg et al., 2011).

Other studies have suggested that blocking platelet adhesion or platelet P-selectin expression reduces infiltration of leukocytes into the artery wall, *in vivo* (Massberg et al., 2002; Burger and Wagner, 2003). Kuckleburg et al., (2011) revealed that these platelet-born P-selectin bridges preferentially recruited monocytes rather than other leukocyte subsets. Platelets are known to release RANTES and CXCL4, both have been demonstrated to aid in monocyte activation and subsequent transmigration (von Hundelshausen et al., 2001, 2005; Kuckleburg et al., 2011). As monocytes are amongst the first leukocyte subsets to infiltrate the damaged artery wall during the atherosclerotic disease process (Ross, 1999), the identification of a potential role for platelets in their specific recruitment may be important for developing future treatments.

However, it is also worth noting that under static conditions, cultured endothelial cells have been demonstrated to bind PMV and this is associated with an increase in EC ICAM-1 expression (Barry et al., 1998). This was accompanied by monocyte adhesion, which increased with longer incubation periods (Barry et al., 1998). Another study has suggested that PMV are able to mediate interactions between leukocytes (Forlow et al., 2000). After incubation with an L-selectin blocking antibody to inhibit leukocyte-leukocyte secondary adhesion events, PMV could restore neutrophil capture by other neutrophils under low shear stresses. Importantly, this was reduced in the presence of P-selectin blocking antibody (Forlow et al., 2000). The authors suggest that in this case, the P-selectin on PMV is interacting with leukocyte PSGL-1 to achieve neutrophil recruitment. It has also been suggested that PMV are able to deliver RANTES to the endothelium and aid in monocyte arrest (Mause et al., 2005). Together, these observations indicate that PMV may provide both an adhesive platform and activating stimuli, which could support leukocyte capture in the absence of endothelial expression of these agents.

**Aims**

1) To find out if activating isolated washed platelets leads to a significant increase in PMV, and which is the most potent agonist in this context.

2) To find out if isolated PMV are able to form aggregates with isolated monocytes and whether the route of platelet activation, through which the PMV are generated effects the final number of PMV-monocyte aggregates.

3) To determine whether monocyte-PMV aggregates can be captured by vWf under conditions of low shear stress.

### 8.2.0 Methods

#### 8.2.1 Generating platelet derived microvesicles

Briefly, blood was collected into CPDA and platelets were isolated using theophylline. 2.5ml of 0.15% (w/v) PBSA containing platelets at a concentration of $8x10^8$/ml were incubated at 37°C for 30 minutes either without the addition of any agonist (control) or in the presence of 100µM TRAP, 1µg/ml CRP-XL or 10µM U46619 or both CRP-XL and U46619. Supernatants were collected following centrifugation at 200G for 20 minutes and 13000G for 2 minutes. PMV were collected, 1ml was stored at -80°C (to be incubated with isolated monocytes at a later date) and 1ml was used for determining the concentration and size distribution using the Nanosight. (For further details see methods section 2.4.1 and 2.4.3.)

#### 8.2.2 Generating monocyte-PMV aggregates

Blood was collected into EDTA and monocytes were isolated using a histopaque density gradient followed by incubation with CD14 positive magnetic beads. Monocytes were separated using a magnetic column. $1x10^6$ isolated (mixed) monocytes were incubated at 37°C for 30 minutes in 0.15% (w/v) PBSA or in a previously prepared aliquot of platelet derived microvesicles (which had been stored at -80°C). At the end of the 30 minute incubation period, samples were fixed using 1% (w/v) FA and then incubated with antibodies against CD14, CD16 and CD42b. Data were acquired using flow cytometry. (For further details see methods section 2.4.4 and 2.4.5)

#### 8.2.3 Flow based adhesion assay; monocyte-PMV recruitment to vWf

Platelet derived microvesicles were isolated (as above) using 1µg/ml CRP-XL as a platelet agonist and were stored at -80°C. Monocytes were isolated (as above) and $5x10^5$ monocytes

were incubated with 0.5ml CRP-XL derived PMV or 0.15% (w/v) PBSA for 30 minutes at 37°C before being used in the flow assay.

1mm x 10mm x 0.1mm (width, x length, x height) APES coated, glass microslides were incubated for 2 hours with 100µg/ml vWf, followed by 1 hour with 1% (w/v) BSA (at 37°C). Or for BSA controls, slides were incubated with 1% (w/v) BSA at 37°C for a minimum of 1 hour. In some experiments, slides were incubated with P-selectin blocking antibody (G1) or IgG control for 30 minutes. Monocyte or monocyte-PMV aggregate samples were flowed at 0.1Pa for a total of 3.5 minutes. After 1 minute of initiating perfusion, digital images of the experiment were collected every 340ms over a 17s period, for 6 different fields of view on the slide. Videos were analysed using image pro software. (For further details see method section 2.4.4, 2.4.5 and 2.4.7-2.4.9.)

**8.2.4 Western blot for the detection of P-selectin**

100µg/ml recombinant human P-selectin and 250µg/ml human vWf (vWf used for flow adhesion assays) were heated to 70°C in Laemmli buffer for 10 minutes before being loaded on to a 8% SDS page gel. Following electrophoresis at 200V for 45 minutes, gels were removed from tanks and either stained with coomassie blue, or transferred to PVDF membranes (electrophoresis at 100V for was carried out for 1hour). Membranes were incubated at 4°C overnight in PBS- tween either with or without 0.1µg/ml sheep anti-human P-selectin antibody. The following day, membranes were incubated with donkey anti-sheep HRP conjugated secondary antibody for 1 hour. Membranes were covered with ECL detection mixture and incubated for 5 minutes at RT. Chemiluminescence was detected using photographic film (10s exposure). (For further details see method section 2.5.0.)

### 8.3.0 Results

### 8.3.1 Measuring PMV production after incubation of isolated washed platelets with a platelet agonist

Before monocyte-microvesicle aggregates could be used in flow assays, it was important to determine if PMV could be generated and isolated following treatment of platelets with an agonist. Also, whether treatment with any particular agonist was more effective in this context. To prevent samples being contaminated with leukocyte microvesicles, platelets were isolated prior to any treatment with an agonist. Washed isolated platelets suspended at a concentration of $8x10^8$/ml showed a significant increase in microvesicle production, following 30 minutes incubation at 37°C with either 1µg/ml CRP-XL or 10µM U46619 compared to untreated controls. CRP-XL was found to be the most potent agonist for PMV production, with an average of ~$1.25x10^9$/ml vesicles produced (**Figure 8-1A**). The weakest agonist in this system was surprisingly 100µM TRAP, showing an average of ~$5x10^8$/ml vesicles produced (**Figure 8-1A**). A combination of both CRP-XL and U46619 did not lead to a further increase in PMV production (**Figure 8-1A**). The PMV produced were also shown to be significantly bigger following treatment with CRP-XL, U46619 or a combination of both compared to the untreated control (**Figure 8-1B**).

The size distribution indicates that the majority of PMV produced either from untreated platelets or following treatment with an agonist were between 100-399nm in diameter (**Figure 8-2A-E**). However, after treatment with 1µg/ml CRP-XL or a combination of 10µM U46619 and 1µg/ml CRP-XL there appears to be more PMV produced with a diameter between 400-599nm compared to the controls or treatment with other agonists (**Figure 8-2A-E**).

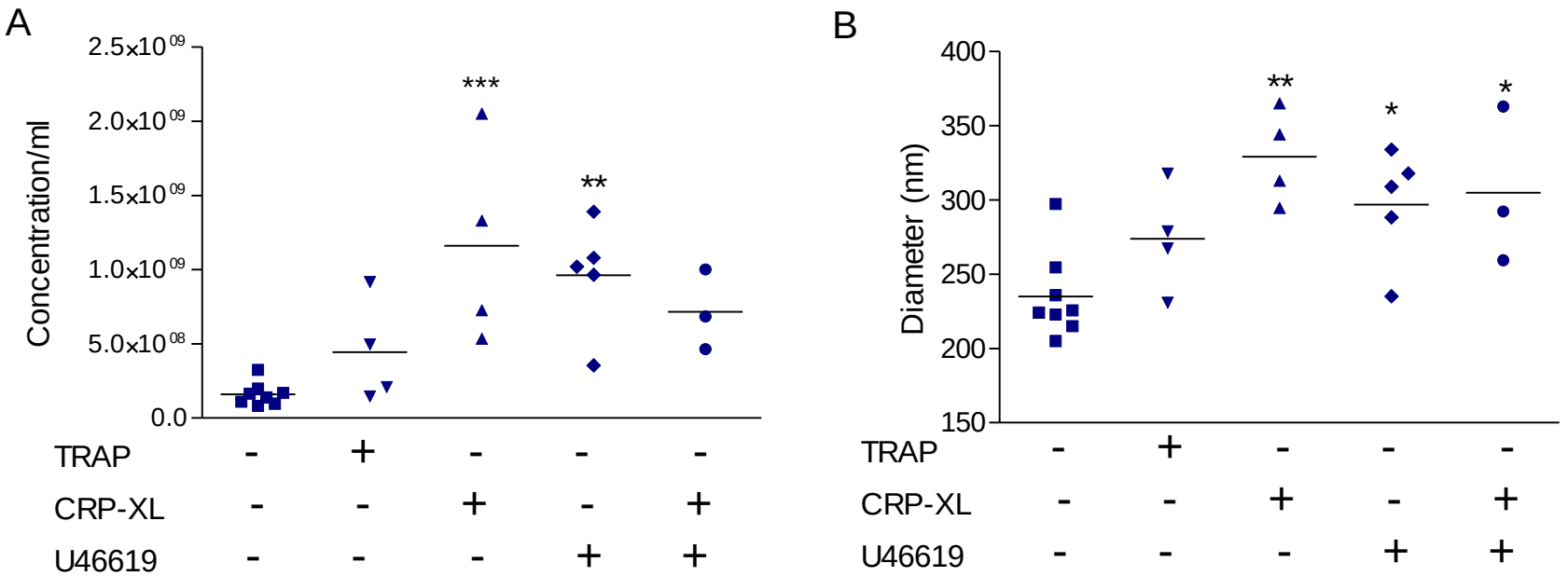


**Figure 8-1: Microvesicle production following stimulation of washed isolated platelets with various agonists**

Washed isolated platelets suspended at $8x10^8$ platelets/ml were incubated for 30 minutes at 37°C, either as untreated (con) or with 100µM TRAP, 1µg/ml CRP-XL or 10µM U46619. Microvesicles were isolated from supernatants following centrifugation for 20 minutes at 2000G and 2 minutes at 13000G, data were acquired using the Nanosight. A) Indicates a significant increase in the number of microvesicles released following treatment with a platelet agonist (ANOVA $P<0.01$). B) shows a significant increase in the size of the microvesicles following treatment with a platelet agonist (ANOVA $P<0.01$) *,** and *** indicate $P<0.05$, $P<0.01$ and $P<0.001$ respectively, post hoc test Dunnett's. Data are means of 3-5 experiments.

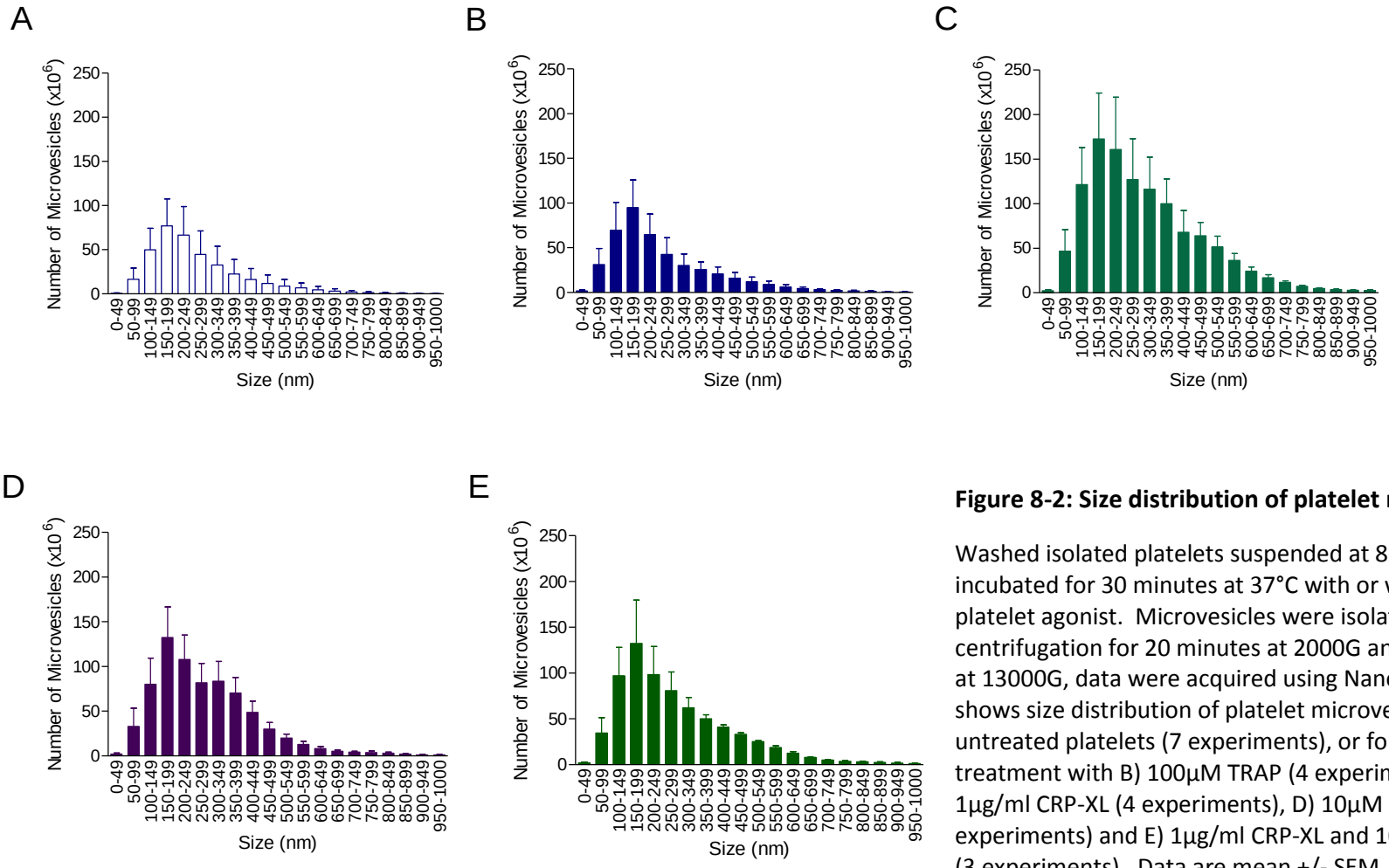


**Figure 8-2: Size distribution of platelet microvesicles**

Washed isolated platelets suspended at $8x10^8$/ml and incubated for 30 minutes at 37°C with or without platelet agonist. Microvesicles were isolated following centrifugation for 20 minutes at 2000G and 2 minutes at 13000G, data were acquired using Nanosight. Data shows size distribution of platelet microvesicles for A) untreated platelets (7 experiments), or following treatment with B) 100µM TRAP (4 experiments), C) 1µg/ml CRP-XL (4 experiments), D) 10µM U46619 (4 experiments) and E) 1µg/ml CRP-XL and 10µM U46619 (3 experiments). Data are mean +/- SEM.

### 8.3.2 Generating monocyte-PMV aggregates through incubation of isolated monocytes with platelet derived microvesicles

Having determined that washed, isolated platelets incubated with an agonist produce PMV we wanted to find out if they would adhere to monocytes when incubated at 37°C under stirred conditions (samples on a roller mixer). $1x10^6$ (mixed) monocytes were incubated with a 1ml aliquot of microvesicles of varying concentrations (**Figure 8-1A**). Using the monocyte markers CD14 and CD16 and the platelet marker CD42b for identification, we demonstrate that up to 75% monocyte-PMV aggregates form for both monocyte subsets after incubation with CRP-XL generated PMV (**Figure 8-3A and B**). The lowest percentage increase in monocyte-PMV formation was seen after incubation with TRAP generated PMV (~60% with both monocyte subsets) (**Figure 8-3A and B**). The ~5% of MPA formed when monocytes are incubated in PBSA control is similar to previously observed data for percentage MPA formed in fixed whole blood.

Figure 8-4A and B demonstrate that the CD42b MFI of the monocyte-PMV aggregates remains low for both monocyte subsets, relative to the CD42b MFI of resting platelets previously observed in whole blood. Monocyte-PMV formed following incubation with PMV, generated using CRP-XL had the highest CD42b MFI, (~30 $CD14^+CD16^-$ subset and ~35 $CD14^+CD16^+$ subset), Monocyte-PMV formed using TRAP generated PMV, had the lowest MFI (~20 both subsets).

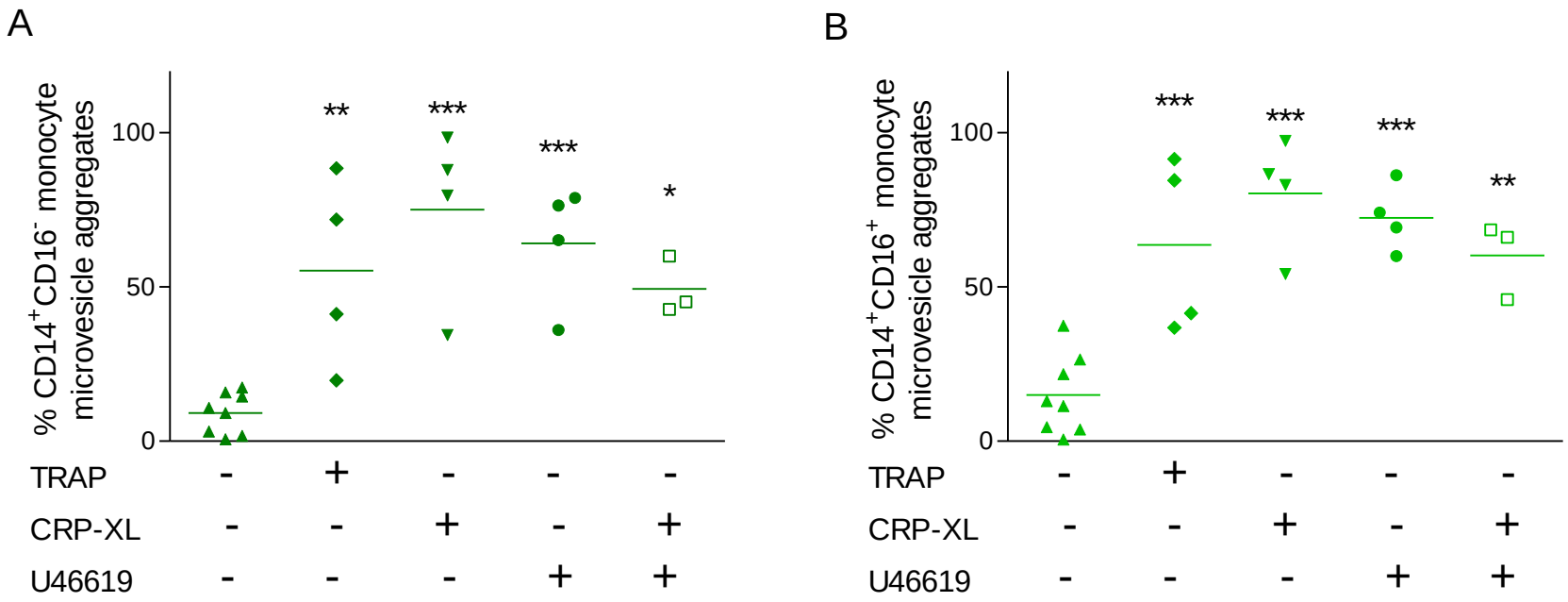


**Figure 8-3: Isolated monocytes incubated with isolated platelet microvesicles**

One million monocytes (mixed subsets) were incubated for 30 minutes at 37°C, either in 1ml 0.15% (w/v) PBSA (control) or in 1ml PBSA containing platelet microvesicles produced from $8x10^8$ platelets, following treatment with 100µM TRAP, 1µg/ml CRP-XL or 10µM U46619 (or both of these agonists together). Samples were fixed and incubated with antibodies against CD14, CD16 and CD42b. Data were acquired using flow cytometry. A) Demonstrates a significant increase in percentage monocyte-PMV formation for the $CD14^+CD16^-$ monocyte subset when monocytes are incubated with platelet microvesicles compared to PBSA control (ANOVA $P<0.001$). B) Indicates this is also the case for the $CD14^+CD16^+$ monocyte subset (ANOVA $P<0.0001$). *,** and *** indicate $P<0.05$, $P<0.01$ and $P<0.001$, respectively, post hoc test Dunnett's. Data are means for 3-4 experiments.

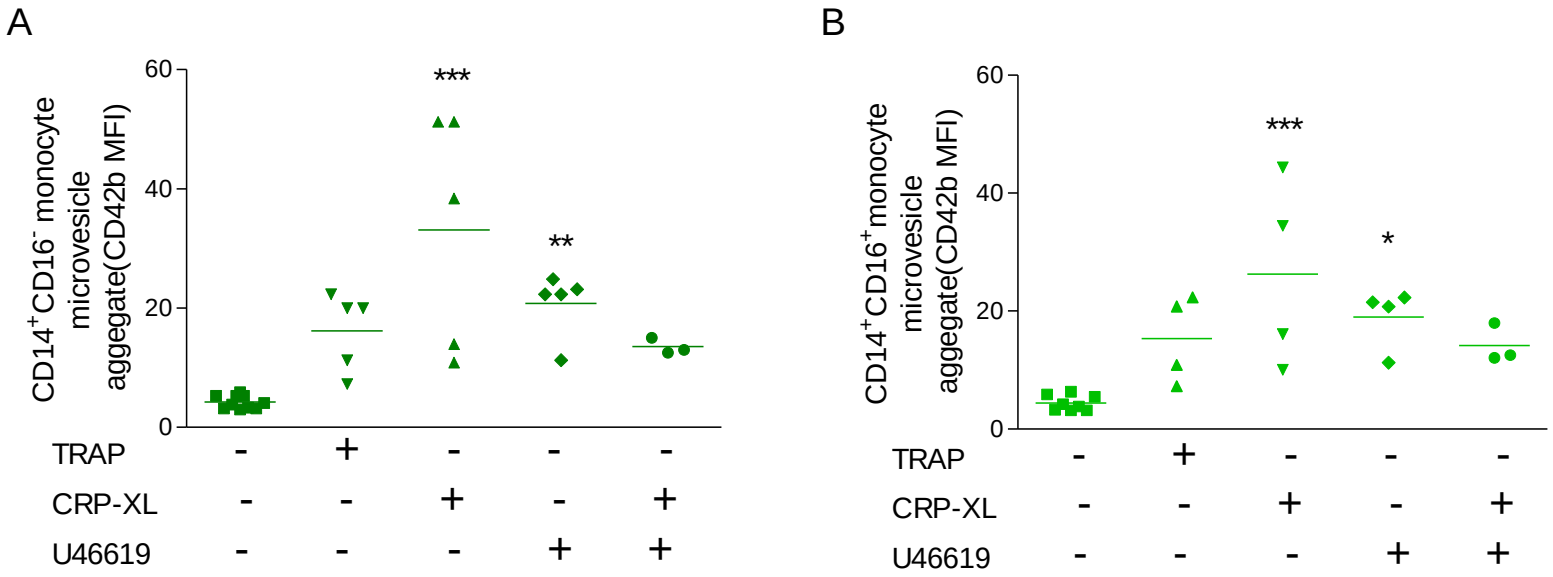


**Figure 8-4: Monocyte-microvesicle aggregates; microvesicle coverage per cell**

One million monocytes (mixed subsets) were incubated for 30 minutes at 37°C either in 1ml 0.15% (w/v) PBSA (control) or in 1ml PBSA containing platelet microvesicles produced from $8x10^8$ platelets, following treatment with 100µM TRAP, 1µg/ml CRP-XL and 10µM U46619 (or both of these agonists together). Samples were fixed and incubated with antibodies against CD14, CD16 and CD42b. Data were acquired using flow cytometry. A) shows a significant increase in platelet marker expression on the $CD14^+CD16^-$ monocyte-PMV aggregates, after treatment with either CRP-XL or U46619 compared to PBSA control, demonstrating more microvesicles are accumulated per monocyte (ANOVA $P<0.001$). B) Indicates this is also the case for the $CD14^+CD16^+$ monocyte subset (ANOVA $P<0.0001$). Data are means for 3-4 experiments.

### 8.3.3 Monocytes roll on vWf under conditions of low shear stress

Flow assays were carried out using APES coated glass microslides, which have been further coated with 100µg/ml vWf and blocked with 1% (w/v) BSA, or for a control, just blocked with 1% (w/v) BSA. Isolated monocytes (mixed subsets) were incubated for 30 minutes at 37°C and flowed across the vWf substrate at a wall shear stress of 0.1Pa. The 30 minute incubation of monocytes without PMV was necessary as in later experiments, where monocyte-PMV aggregates will be used, the cells will be treated thus. Any brief interaction (≥340ms) with the substrate was termed 'rolling', 'stationary adherent' cells were stationary for the full 17s period. The data revealed that there is a significant increase in total monocyte adhesion to vWf compared to BSA control (**Figure 8-5A**). The majority of monocytes were rolling along the vWf (**Figure 8-5B**).

### 8.3.4 P-selectin blocking antibody prevents monocyte adhesion to the vWf substrate

The vWf used for these experiments has been isolated from human plasma. It is well known that soluble P-selectin is present in the plasma as well. The monocyte rolling phenotype observed in the previous experiments lead us to believe that there may be P-selectin contamination of the vWf. Therefore, vWf coated slides were further treated with P-selectin blocking antibody (G1) or non-blocking IgG control. Monocytes were incubated at 37°C for 30 minutes either in (0.15% w/v) PBSA or with PMV generated using CRP-XL. CRP-XL was used as this lead to the highest number of vesicles being produced in isolated platelets; also when incubated with isolated monocytes, the highest number of CD42b positive, monocyte-PMV aggregates. Although the CRP-XL was still present during the experiment, as monocytes do not express GPVI receptor this agonist should not directly affect them.

There was a significant increase in total monocyte adhesion to vWf treated with (non-blocking) IgG antibody, however, treatment with P-selectin blocking antibody (G1) diminished this (**Figure 8-6A**). This suggests that the vWf was contaminated with P-selectin and that it was this P-selectin interaction with monocytes, which lead to monocyte rolling observed throughout these experiments (**Figure 8-6A and B**). Pre-incubating monocytes with CRP-XL derived PMV perfused across either P-selectin blocked or IgG treated vWf substrate, did not lead to a significant increase in monocyte capture compared to BSA control (**Figure 8-6A and B**).

Figure 8-7A demonstrates that the PMV aliquots used in this study were of similar concentrations (~$5x10^9$/ml). Therefore, similar numbers of PMV were added to $5x10^5$ monocytes for each sample used in this study. Figure 8-7B again, indicates that treatment with CRP-XL lead to an increase in PMV size. The majority of PMV were found to be between 100-399nm in diameter, however, there are more PMV between 400-599 after treatment with CRP-XL (**Figure 8-8A and B**).

On completion of the flow assay, samples were fixed and stained with the monocyte markers CD14, CD16 and platelet marker CD42b. CD42b has been well documented to interact with vWf and therefore it was important to determine its presence on PMV. Figure 8-10A and B demonstrate that after 30 minutes incubation at 37°C, monocytes and CRP-XL PMV form monocyte-PMV aggregates, which express CD42b, effectively.

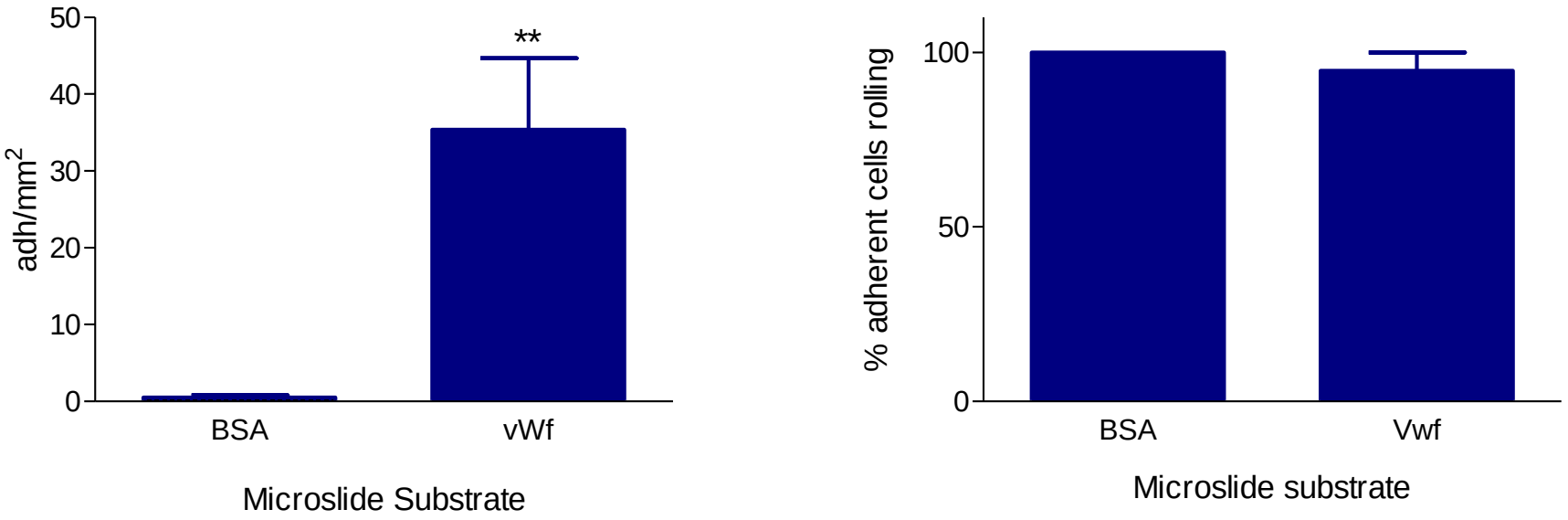


**Figure 8-5: Monocyte capture by vWf substrate compared to BSA control at a wall shear stress of 0.1Pa.**

Isolated monocytes (mixed subsets) incubated for 30 minutes at 37°C (in the absence of PMV) were perfused across either 1% (w/v) BSA or 100µg/ml vWf substrate at a wall shear stress of 0.1Pa. A) There was a significant increase in monocyte capture by vWf compared to BSA control (Unpaired t-test P=0.0028). B) 'Rolling' was defined as interaction with the substrate for at least 1 frame (340ms). ('Stationary adherent' were stationary throughout the 17s period.) The majority (>95%) of monocytes that interacted with either BSA or Vwf 'rolled' along the substrate. Data are mean +/- SEM for 5 experiments.

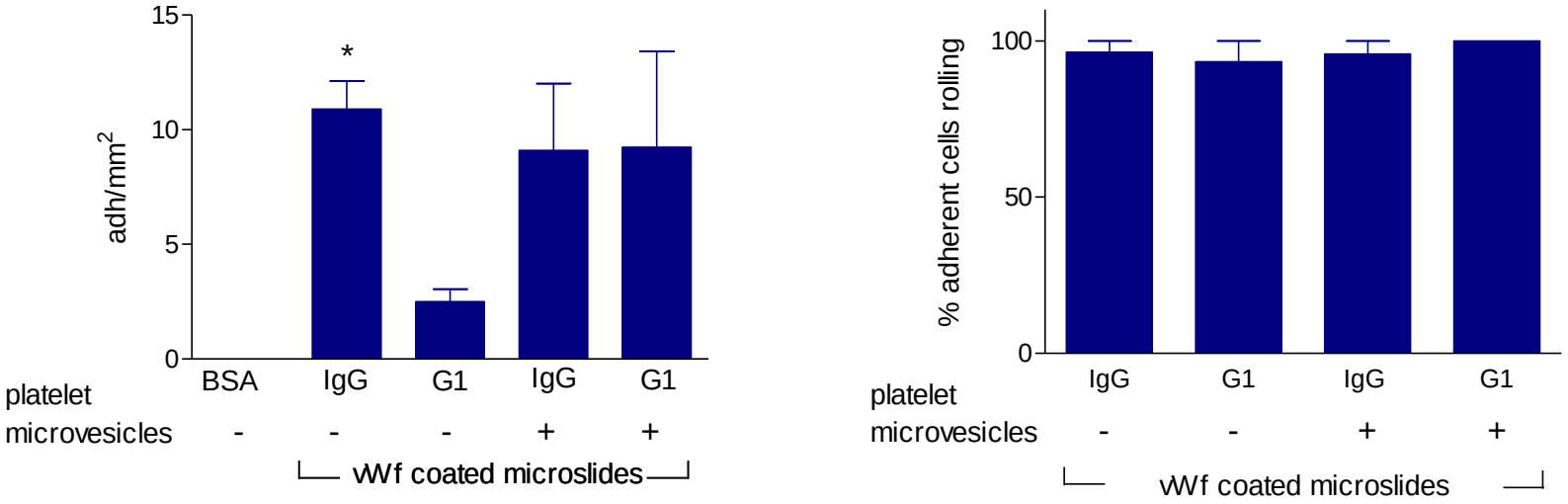


**Figure 8-6: Monocyte capture by Vwf substrate in the presence of P-selectin blocking antibody at a wall shear stress of 0.1Pa**

Isolated monocytes (mixed subsets) were incubated for 30 minutes at 37°C in (0.15% w/v) PBSA or in the presence of platelet microvesicles, which had been previously isolated from $8x10^8$ platelets treated with 1µg/ml CRP-XL and stored (-80°C). Substrates were either 1% BSA controls or 100µg/ml vWf substrate, which had been incubated for 30 minutes at 37°C with P-selectin blocking antibody (G1) or (non-blocking) IgG control. Samples were perfused across substrate at a wall shear stress of 0.1Pa. A) A significant increase can be detected in monocyte capture by vWf incubated with IgG control compared to BSA control. Treatment of vWf with P-selectin blocking antibody (G1) prevents this increase from occurring as does, pre-incubation of monocytes with platelet microvesicles. (ANOVA $P<0.05$), *,** and *** indicate $P<0.05$, $P<0.01$ and $P<0.001$, respectively, post hoc test Tukey's multiple comparison test. B) 'Rolling' was defined as interaction with the substrate for at least 1 frame (340ms). ('Stationary adherent' were stationary throughout the 17s period.) The majority (>95%) of monocytes or monocyte-microvesicle aggregates that interacted with vWf 'rolled' along the substrate. Data are mean +/-SEM 4-5 experiments.

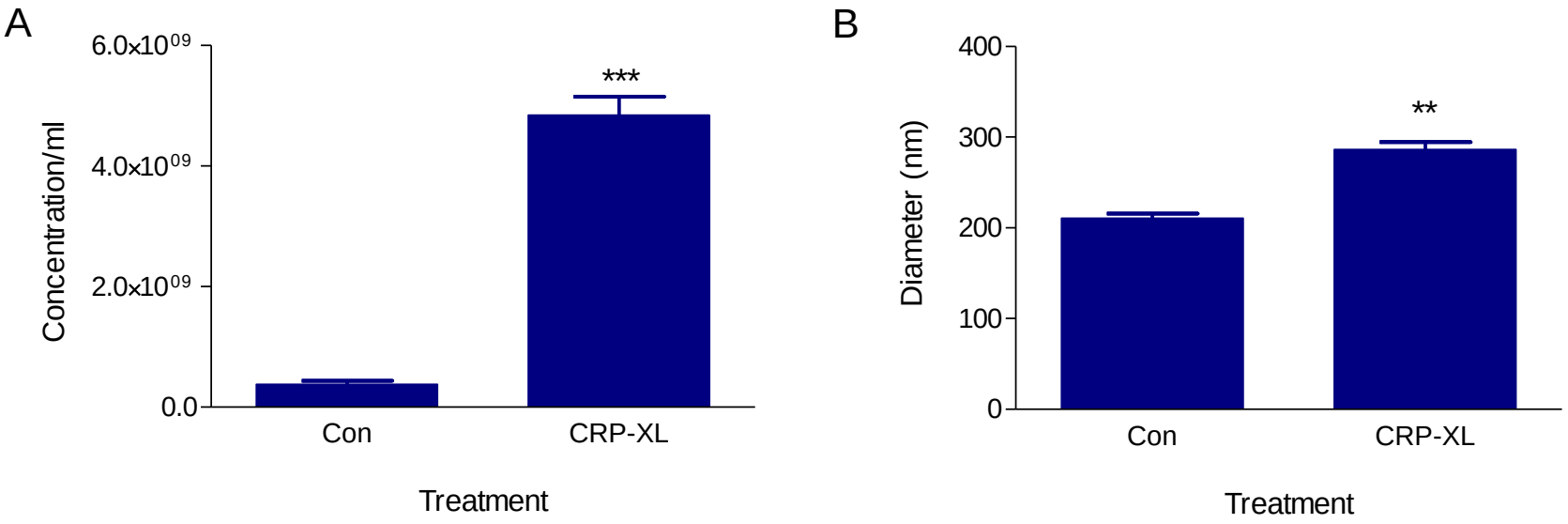


**Figure 8-7: Concentration and size of microvesicles after treatment with 1µg/ml CRP-XL**

Washed isolated platelets were suspended at $8x10^8$/ml and incubated for 30 minutes at 37°C as either untreated (con) or with 1µg/ml CRP-XL. Microvesicles were isolated in supernatants following centrifugation 20 minutes at 2000G and 2 minutes at 13000G. Data were acquired using the Nanosight. A) Indicates a significant increase in the number of platelet microvesicles following treatment with CRP-XL. B) Shows a significant increase in the size of the microvesicles following treatment with CRP-XL. *,** and *** indicate $P<0.05$, $P<0.01$ and $P<0.001$, paired t-test. Data are mean +/-SEM of 5 experiments.

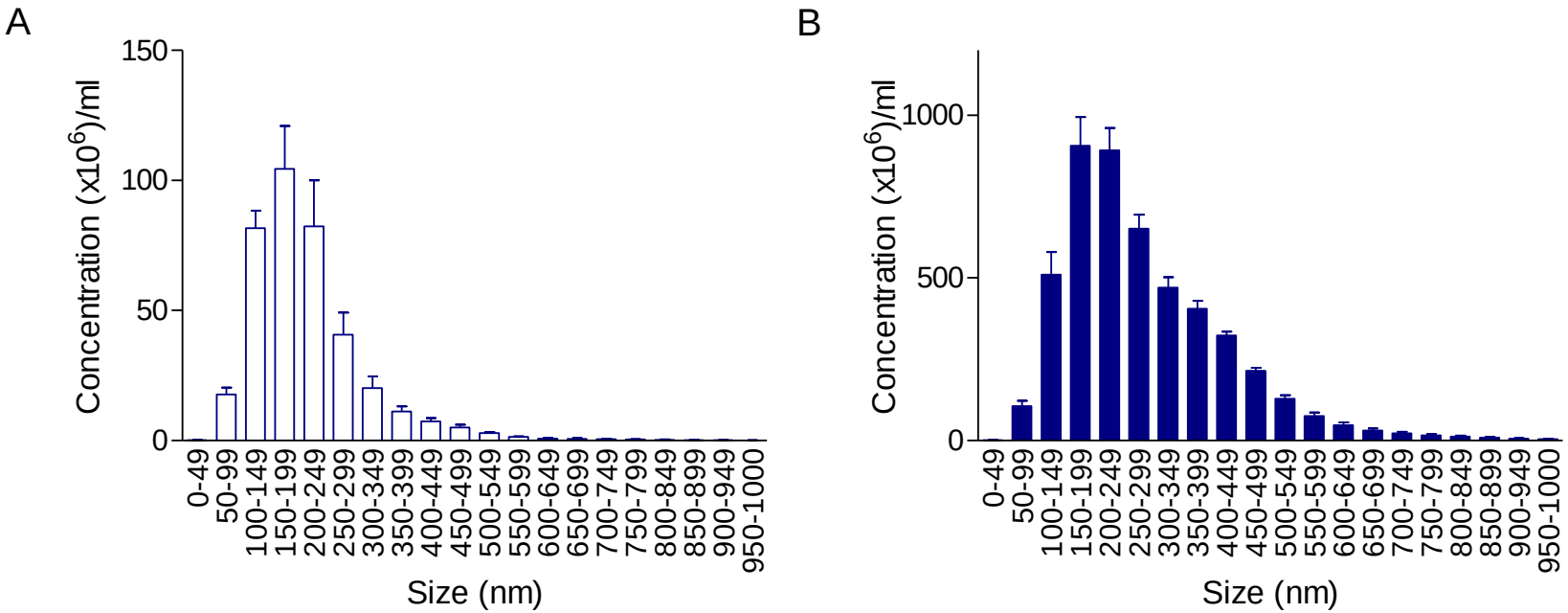


**Figure 8-8: The sized distribution of platelet microvesicles following treatment with 1µg/ml CRP-XL**

Washed isolated platelets suspended at $8x10^8$/ml were incubated for 30 minutes at 37°C with or without platelet agonist. Platelet microvesicles were isolated in supernatants following centrifugation for 20 minutes at 2000G and 2 minutes at 13000G. Data were acquired using the Nanosight. Data shows size distribution of platelet microvesicles for A) untreated platelets or B) following treatment with 1µg/ml CRP-XL . Data are mean +/- SEM for 5 experiments.

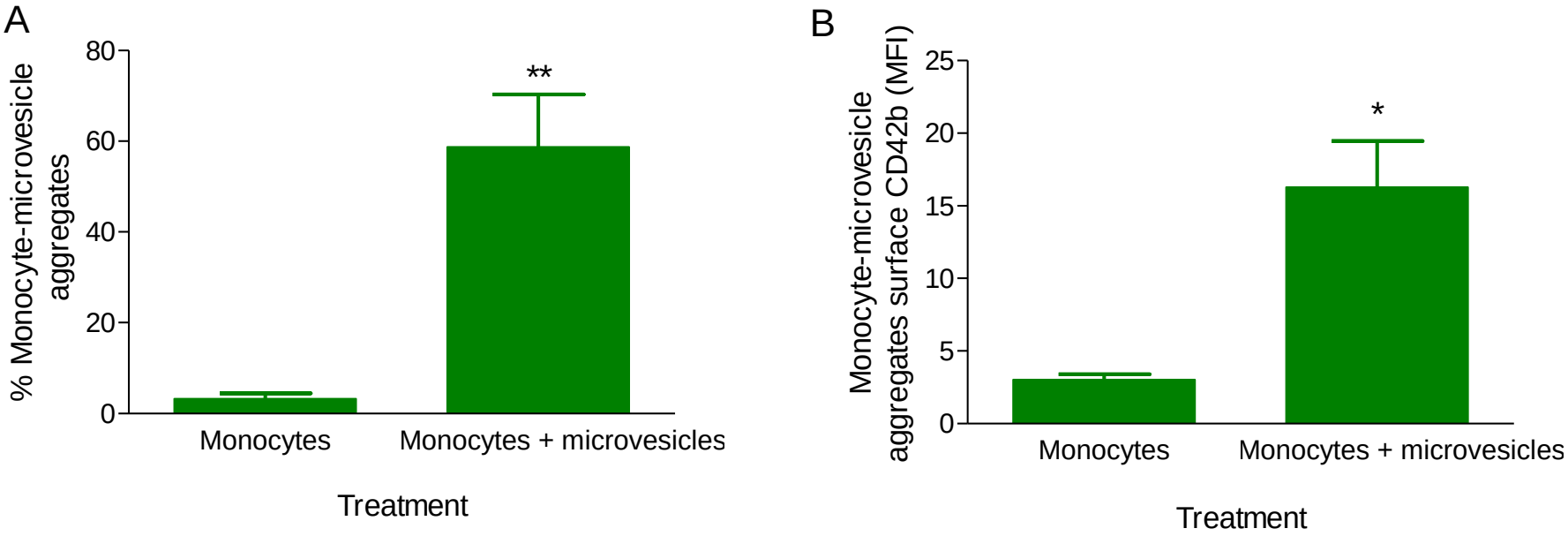


**Figure 8-9: Monocyte-microvesicle aggregates formed for use in flow assays**

$5x10^5$ monocytes (mixed subsets) were incubated for 30 minutes at 37°C either in 0.5ml of 0.15% (w/v) PBSA (control) or 0.5ml PBSA, containing platelet microvesicles produced from isolated washed platelets ($8x10^8$/ml), following treatment with 1µg/ml CRP-XL. Samples were used in flow assays. At the end of the flow assay experiment samples were fixed and incubated with antibodies against CD14, CD16 and CD42b. Data were acquired using flow cytometry. A) Demonstrates a significant increase in percentage monocyte-microvesicle formation for monocytes (mixed subsets) when incubated with platelet microvesicles compared to PBSA control B) shows a significant increase in platelet marker expression on monocytes incubated with platelet microvesicles compared to PBSA control. *,** and *** indicate $P<0.05$, $P<0.01$ and $P<0.001$ paired t-test (pairing not significant). Data are mean +/- 5 experiments.

### 8.3.5 Confirming P-selectin contamination of vWf

Monocyte 'rolling' on vWf was significantly reduced in the presence of P-selectin blocking antibody. This lead us to believe that soluble P-selectin may be contaminating the vWf, which was used as a substrate for flow based adhesion assays, designed to detect monocyte-PMV capture by vWf. To confirm this, a western blot was carried out using an anti-P-selectin antibody. Recombinant P-selectin was used as a positive control. The western blot shows a band between 100 and 150Kda which represents P-selectin, in the recombinant P-selectin lane confirming that the antibody recognises this ligand (**Figure 8-11**). A band of a similar size can also be seen in the vWf lane, confirming the vWf is indeed contaminated with P-selectin (**Figure 8-11**). The coomassie stained gel confirms the presence of both P-selectin and vWf proteins (**Figure 8-10**).

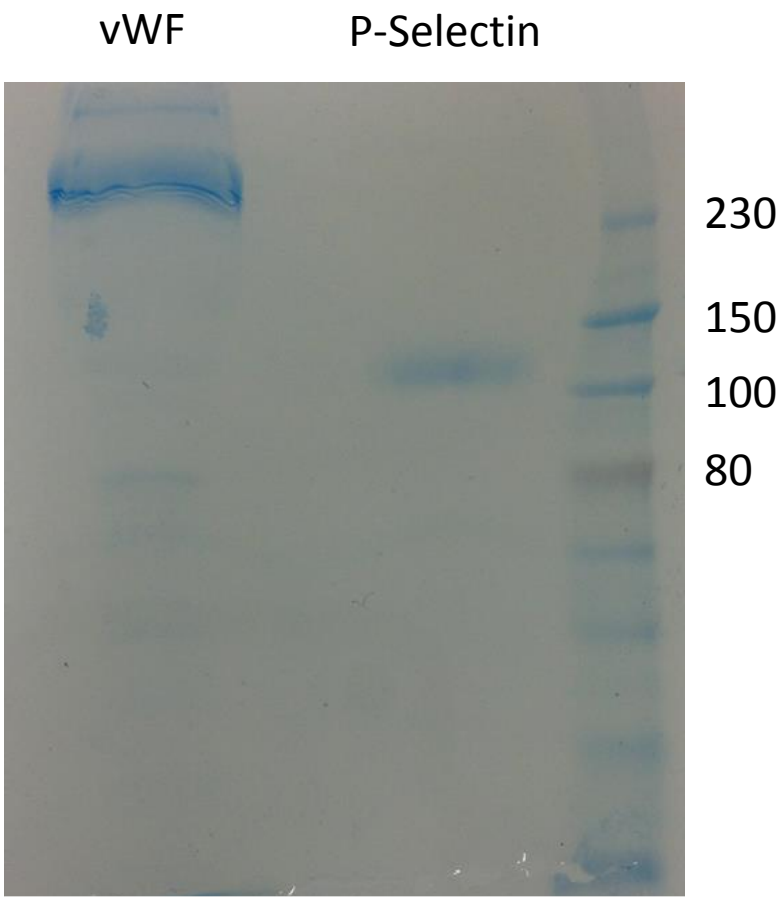


**Figure 8-10: Coomassie blue stained gel showing P-selectin and vWf**

Recombinant P-selectin (100µg/ml) and human vWf (250µg/ml) were incubated at 70°C for 10 minutes in Laemmli buffer and loaded on to an 8% SDS page gel. Electrophoresis was carried out at 200V for 45 minutes. Gel stained with coomassie blue. Von Willebrand factor (monomers 260KDa), a band can be detected in the vWf lane above 250KDa. A faint band can also be seen in this lane between 100-150KDa, which could represent the presence of P-selectin. P-selectin (140KDa), a band can be detected in the (recombinant) P-selectin lane between 100-150KDa.

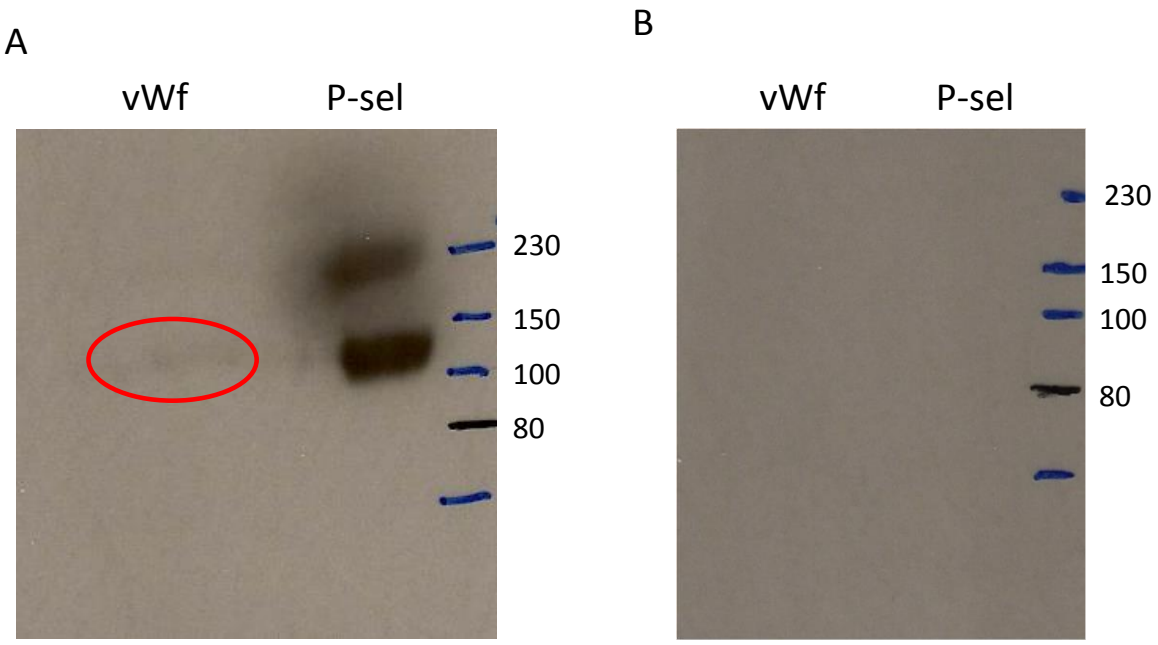


**Figure 8-11: Confirmation of P-selectin contamination of vWf**

Recombinant P-selectin (100µg/ml) and human vWf (250µg/ml) were incubated at 70°C for 10 minutes in Lammeli buffer and loaded on to an 8% SDS page gel. Bands were transferred on to membranes. Membranes were subsequently incubated in PBS-tween overnight, either A) with or B) without the addition of sheep anti-human P-selectin antibody. The following day, membranes were washed and incubated with donkey anti-sheep HRP conjugated antibody. Images are from a 10s exposure of chemiluminescent substrate on photographic film. A) A band can be detected between 100-150KDa in the P-selectin lane, confirming that the antibody detects P-selectin. A faint band (inside red circle) can be detected in the vWf lane between 100-150KDa confirming P-selectin contamination of vWf. B) Confirms there is no non-specific binding of the secondary antibody.

**8.4.0 Discussion**

Here we demonstrate that upon activation through either, PAR-1, GPVI or TP receptor pathways, washed platelets release PMV. Initial data acquired using the Nanosight confirms an increase in particles between 100-1000nm in size after platelet activation compared to unstimulated controls, however, as this technology does not allow the detection of any surface markers it is impossible to tell whether these are microvesicles or exosomes. Washed isolated platelets have been used to prevent contamination from leukocyte microvesicles as without markers these cannot be distinguished. In combination with flow cytometry data showing an increase in the platelet specific surface marker, CD42b, following incubation of these PMV with monocytes, this suggests that PMV are indeed being generated.

Data from the Nanosight suggests that TRAP is a weak agonist in terms of stimulating PMV production from washed isolated platelets. Only a small and non-significant increase, in the number of PMV generated was observed, compared to the unstimulated control. In this system stimulation with CRP-XL through the platelet GPVI pathway resulted in the largest increase in PMV and an increase in the size of the PMV generated. A combination of CRP-XL and thromboxane mimetic (U46619) did not result in an increase in microvesicle production, suggesting that the maximum response was seen with CRP-XL alone. The data from the current study is in contrast to a previous study carried out in whole blood and using flow cytometry to identify PMV generation where TRAP was found to be the most potent agonist for PMV generation (Chow et al., 2000). However, this study was carried out at a high shear rate ($10000s^{-1}$). It could be that a combination of platelet isolation and lower shear rate results in less PMV being produced upon PAR-1 stimulation.

Incubation of PMV with isolated monocytes demonstrated that monocyte-PMV aggregates are able to form. With CRP-XL generated microvesicles forming the highest percentage of aggregates with monocytes. This perhaps isn't surprising as CRP-XL stimulation of washed isolated platelets leads to the highest number of microvesicles being generated. Previous studies have demonstrated that neutrophils and the monocytic cell line THP-1 cells are able to form aggregates with PMV in vitro, the main mechanism for this is thought to be through leukocyte PSGL-1 (Forlow et al., 2000; Jy et al., 1995; Nomura et al., 2001). It is therefore not surprising that primary monocytes form aggregates with PMV as they also express high levels of PSGL-1.

The low CD42b MFI observed for these aggregates is nowhere near the CD42b MFI observed for a resting platelet in whole blood observed in earlier experiments. This is further evidence to support PMV binding to monocytes in whole blood rather than whole platelets. The percentage 'MPA' observed for 30 minutes incubation of monocytes in PBSA is similar to our previous data from monocytes incubated for up to 60 minutes under the same shear conditions in unstimulated whole blood. It is possible that these monocyte-PMV aggregates form in the circulation and survive the monocyte isolation process.

Once we had determined that monocyte-PMV aggregates would form these were ready to be used in flow assays, however, we observed in early experiments that under low shear stress (0.1Pa) monocytes appeared to make transient interactions with vWf, (which we classified as rolling) but not with the BSA control. A previous study has reported that CD170 (Siglec-5) expressed by monocytes, neutrophils and B-lymphocytes can interact with vWf under static conditions (Pegon et al., 2012). Another study demonstrated that at room temperature, leukocyte PSGL-1 can transiently interact with recombinant vWf and that stable adhesion to vWf

can be achieved through β2 integrin (at a shear rate of $50S^{-1}$), (Pendu et al., 2006). However, data from our lab suggests that under conditions of higher shear and at 37°C, leukocyte adhesion to vWf present on the surface of EC is not significantly increased compared to untreated controls (Kuckleburg et al., 2011).

The vWf used throughout this study has been isolated from human plasma, it is well known that soluble P-selectin is also present in the plasma. As previous data from our lab demonstrates that P-selectin can capture leukocytes, allowing them to roll, we decided to incubate the vWf coated slides with P-selectin blocking antibody (G1). This significantly reduced monocyte interactions with vWF compared to vWf coated slides incubated with IgG. This suggests that in this instance, the brief interactions detected in this assay were due to monocyte interaction with contaminating P-selectin rather than vWf itself. Further confirmation of the P-selectin contamination of vWf can be seen from a western blot, where P-selectin is indeed detected in the vWf sample.

Monocyte-PMV aggregates were perfused across vWf coated slides, which had been further treated with P-selectin blocking antibody or (non-blocking) IgG control antibody. The data shows no significant increase in monocyte-PMV aggregate capture by either IgG treated or anti-P-selectin treated vWf. This suggests that vWf is unable to support monocyte-PMV adhesion in the absence of P-selectin. However, further experiments need to be carried out to confirm this.

**Conclusions**

We have demonstrated that upon activation of washed platelets with an agonist PMV are generated. The most potent agonist in terms of PMV generation was CRP-XL, this also lead to larger microvesicles being produced. PMV were able to aggregate with monocytes, the

highest percentage of monocyte-PMV produced was observed after incubation of monocytes with CRP-XL microvesicles, these were positive for the CD42b receptor. When monocyte-PMV aggregates (PMV generated from CRP-XL treatment) were perfused across vWf in the presence of P-selectin blocking antibody there was no significant increase in transient interactions observed than with monocytes alone.

# 9. Chapter 9- GENERAL DISSCUSSION

In this thesis we have demonstrated a role for platelets and platelet microvesicles (PMV) in the inflammatory response. We have shown that in response to inflammatory stimuli (TNFα and TGFβ) platelet adhere to GEnC. Our data also suggests that in response to treatment with different platelet agonists, which activate platelets through a variety of different routes, platelet microvesicles are generated, these, in turn adhere to leukocytes. The data suggests that the only exception to this was activation of platelets with histones which appears to lead to monocytes binding to whole platelets.

Innate immune cells formed aggregates with platelets (and potentially platelet microvesicles) more readily than cells of the acquired immune system, with monocytes preferentially forming heterotypic aggregates compared to neutrophils. Interestingly, lymphocytes did not appear to form heterotypic aggregates. The data also suggests that P-selectin, which is known to be expressed by both platelets and PMV, is the ligand through which aggregates with leukocytes form. PSGL-1, the ligand with the highest binding affinity for P-selectin was found to be expressed by all leukocytes, except B-lymphocytes. The highest levels of PSGL-1 expression were found to be expressed by monocytes, suggesting that this may be the ligand which P-selectin interacts with (although further work will need to be carried out to confirm this).

Platelet recruitment to EC has been shown to be fundamental at an early stage of atherosclerosis disease progression. Previous data has indicated that in response to activation (with TGFβ), HUVEC are able to capture platelets (Tull et al., 2006). However, before our study no one had studied the effect of TGFβ signalling on glomerular endothelial cells and how this affects their ability to capture platelets. Glomerular EC are specialised and line microvascular capillary beds, which have a specialised structure, so that a large volume of blood can be filtered

as it passes through the glomerulus (Miner, 2011; Passerini et al., 2004; Satchell, 2004; White, 2012). This makes GEnC particularly vulnerable to inflammatory disease and platelets may play a key role in early disease progression.

Previous data acquired through the use of a co-culture model has indicated that cross-talk occurs through secretory phenotype SMC and HUVEC (Tull et al., 2006). In this instance, there is an increase in platelet adhesion to HUVEC in response to TGFβ signalling by SMC (Tull et al., 2006). Cross-talk has been demonstrated to occur between podocytes and GEnC (Satchell, 2004). However, no one has yet studied the effect of podocytes on GEnC in the context of platelet adhesion. As primary human GEnC are not readily available, we opted to use a cell line GEnC, which had been previously demonstrated to retain EC markers (Satchell et al., 2006). However, on completion of the first part of our study, where we demonstrated that GEnC were able to adhere to platelets in response to inflammation; new cells were required for continuation of the project. The new batch of cell line GEnC failed to retain EC markers, including vWf (a crucial part of the mechanism for platelet capture by EC in our model), this meant that the project could not be continued and co-culture studies were not carried out.

Both platelet microvesicles and leukocyte-platelet aggregates have been shown to be increased in inflammatory diseases, of particular interest to us is the increase observed in an atherosclerosis disease setting (Burton et al., 2013; Joseph E Italiano Jr, Mairuhu Albert T.A., 2010; Shantsila et al., 2011). Previous studies have demonstrated that NPA and MPA (in particular) are increased in patients with atherosclerosis or in response to treatment with a platelet agonist such as thrombin, TRAP or ADP (Jensen et al., 2001; Klinkhardt et al., 2003; Rinder et al., 1991). However, to our knowledge a thorough screen of so many different platelet

agonists and their effect on leukocyte-platelet aggregate formation has not been carried out before this study.

Several different platelet markers have been used to study MPA/NPA including CD61, CD62P, CD42b, and CD42a (Keating et al., 2006; Basavaraj et al., 2012; Harding et al., 2004; Jensen et al., 2001). The method for identification of leukocytes from flow cytometry data also varies between studies, with some studies using more stringent methods than others (Rinder et al., 1991; Shantsila et al., 2011). The current study adopts a comparatively stringent method for identifying NPA and MPA, based on leukocyte markers CD14, CD16 and the platelet marker CD42b. Another important difference between studies is the use of different anticoagulants for collection of blood samples. The current study uses CPDA, which although chelating calcium, is not efficient, and removes enough to inhibit activation of the coagulation cascade, but leaves sufficient in plasma for the function of adhesion receptors. EDTA is a well known calcium chelator. However, it strips all calcium and magnesium for the plasma inhibiting the function of adhesion receptors. This reduces platelet activation and therefore the number of leukocyte-platelet aggregates (Basavaraj et al., 2012). Whereas, heparin has been shown to significantly increase the numbers of leukocyte-platelet aggregates which form compared to CPDA (Basavaraj et al., 2012).

Although NPA and MPA formation has been well documented, very few studies have determined the number of platelets adhering to these leukocytes. Studies which have indicated platelet adhesion to be occurring to monocytes or neutrophils have reported high numbers of platelets adhering to these leukocytes (Mickelson et al., 1996; Xiao and Théroux, 2004). However, these assays have been carried out under static conditions. In our opinion this promotes the interaction for platelets and leukocytes as an artefact of the methodology and

gives false indications of the incidence of leukocyte-platelet aggregates, which occur (Mickelson et al., 1996; Xiao and Théroux, 2004). Data from the current study suggests that in the main adhesion of platelet derived microvesicles to monocytes and neutrophils occurs upon platelet activation, rather than binding of whole platelets.

Monocytes are known to be a heterogeneous population, which consists of three subsets (Shantsila et al., 2011). Our study also aimed to compare ability of monocyte subsets to form aggregates with platelet microvesicles. Here, we studied two monocyte subsets CD14+CD16$^{-}$ and CD14$^{+}$CD16$^{+}$. However, no differences between monocyte subsets adhering to platelet microvesicles were detected in the current study. The only exception to this generalisation was the adhesion of whole platelets to the CD14$^{+}$CD16$^{+}$ monocyte subset. This phenomenon requires further investigation, as it is unclear why this should be.

Previous data has indicated that leukocyte-platelet aggregates in whole blood are significantly reduced in the presence of P-selectin blocking antibody (Théorêt et al., 2001). PMV are well known to express platelet P-selectin on their surface and are therefore also capable of interacting with leukocytes through this mechanism (Joseph E Italiano Jr, Mairuhu Albert T.A., 2010). Data from the current study suggests that PMV or platelet adhesion to leukocytes is reduced in the presence of P-selectin blocking antibody. To our knowledge no one to date has reported the formation of monocyte-PMV aggregate formation in whole blood in response to platelet agonists, or that this interaction is reduced by P-selectin blocking antibody. Other groups have demonstrated, that the presence of PMV is able to increase interactions between HL-60, which do not express L-selectin and that P-selectin or PSGL-1 blocking antibody, reduces this interaction (Forlow et al., 2000). This suggests that the interaction between PMV P-selectin and leukocyte PSGL-1 is important.

Our study indicates that PSGL-1 is expressed on monocytes and neutrophils. To our knowledge this is the only study to date which measures PSGL-1 expression on leukocytes in whole blood in response to treatment with known platelet activators TRAP and CRP-XL the data reveals that PSGL-1 expression is significantly reduced on both neutrophils and the $CD14^{+}CD16^{-}$ monocyte subset, possibly due to the activation of these leukocytes and subsequent shedding of the receptor. Further studies need to be carried out to confirm this.

The formation of monocyte-PMV aggregates could have a major role in cross-talk during inflammatory disease progression. Atherosclerosis has been shown to be accompanied by high levels of platelet surface and soluble P-selectin, TF and high monocyte expression of CD40L and MAC-1 (Furman et al., 1998; Shantsila and Lip, 2009). Monocyte-platelet aggregate formation through platelet P-selectin, interacting with monocyte PSGL-1, leads to downstream signalling, which results in increased expression of monocyte MAC-1, an inflammatory marker (Evangelista et al., 1999). Importantly, it also results in increased expression of TF by monocytes, this in turn triggers the coagulation cascade, which results in thrombin generation and further platelet activation (Christersson et al., 2008; Coughlin, 2000). This demonstrates a role for cross-talk between these heterotypic aggregates. Evidence also suggests a role for signalling through microvesicle generation. TF has been shown to be transferred from activated monocytes to platelets (Del Conde et al., 2005) or from activated platelets to monocytes through microvesicle generation (Scholz et al., 2002). This occurs through the parent cell generating microvesicles, which contain TF and subsequent adhesion of these vesicles to the recipient cell. The mechanism for delivery of the microvesicle TF cargo is still unknown. It may be either through microvesicle fusion with the recipient cell plasma membrane, or through receptor mediated internalisation.

The data in this thesis, which suggests PMV adhere to monocytes and neutrophils is important. Although PMV are known to be elevated in inflammatory disease it is not yet known how long PMV are stable for, or the mechanism for their clearance. Rand et al, (2006) demonstrated that microvesicles injected into rabbits could not be recovered from the plasma, after 10 minutes. The data from this study implies that the excess microvesicles are cleared through an, as yet, unknown mechanism. The data from the current study suggests that at least one mechanism, which could aid in PMV clearance, is through adhesion of PMV to leukocytes such as monocytes and neutrophils.

Our data, and indeed data from others, demonstrates preferential binding of platelets (or platelet microvesicles) to monocytes (Jensen et al., 2001; Michelson et al., 2001; Rinder et al., 1991). Previous studies in our lab have revealed that activated, adherent, platelets aid in recruitment of monocytes to EC (Kuckleburg et al., 2011). We hypothesised that monocyte-platelet microvesicle aggregates would have an increased chance of recruitment to EC under inflammatory conditions. As the presence of the platelet receptor CD42b, would allow the monocyte-PMV aggregate to adhere to vwf, as well as traditional routes of monocyte capture through interactions with EC expressed selectins. To our knowledge no one has yet studied this. However, data from early experiments indicate that at low shear stress monocyte-PMV recruitment to vWf is not significantly enhanced. It is worth noting however, that the responses were very variable and only a few experiments were conducted. A more stringent study of this aspect of monocyte-microvesicle aggregates should be conducted to clarify this point.

In summary, this study suggests that monocyte-PMV aggregates form in whole blood in response to platelet activation. It also suggests that these aggregates do not aid in monocyte recruitment to the vessel wall under conditions of low shear. However, the importance of these

monocyte-PMV aggregates should not be under estimated. The potential for signalling to occur between these two cell types and the subsequent downstream effects on inflammatory and thrombotic processes could still have a major role in disease progression.

**Further experiments**

The work outlined in this thesis reveals areas that need further investigation. These are listed below;

- Using CD42a as a marker do monocytes and neutrophils still appear to bind PMV?

As CD42a is a non sheddable marker this will confirm whether monocytes and neutrophils are indeed binding PMV, as this thesis suggests.

- Is the levels of PSGL-1 found on monocytes, neutrophils and lymphocytes the reason why more monocytes form heterotypic aggregates than other leukocytes?

This thesis demonstrates that monocytes have the highest levels of PSGL-1 and form the most aggregates with platelets (or even PMV). However, further work needs to be done to confirm that the levels of PSGL-1 expressed are indeed the reason why more of these aggregates form.

- How long are MPA, NPA and LPA stable *in vivo*?

It is important to clarify that these aggregates are able to form *in vivo* and that they are stable. It is also important to find how long they are stable for. There presence *in vivo* may also be an indication of how PMV are cleared from the blood plasma.

- Which receptors are responsible for the stability of MPA and NPA *in vitro* and *in vivo*?

As P-selectin and PSGL-1 are known to only make brief interactions, it is important to determine which receptors are able to aid in the stability of heterotypic aggregates.

- Can monocytes-PMV aggregates be recruited to recombinant vWf at high shear stress?

As platelets are known to aid in leukocyte recruitment and this phenomenon is important at high arterial shear stresses, it is important to determine if monocyte-PMV aggregates can be recruited when subjected to higher shear stresses.

# 10. Chapter 10- REFERENCES

Abbitt, K.B. and Nash, G.B. (2003) Rheological properties of the blood influencing selectin-mediated adhesion of flowing leukocytes. **American journal of physiology. Heart and circulatory physiology**, 285
(1): H229–240
Ait-Oufella, H., Salomon, B.L., Potteaux, S., et al. (2006) Natural regulatory T cells control the development of atherosclerosis in mice. **Nature medicine**, 12 (2): 178–80
Akira, S., Uematsu, S. and Takeuchi, O. (2006) Pathogen recognition and innate immunity. **Cell**, 124 (4): 783–801
Alón, R., Hammer, D. and Springer, T. (1995) Lifetime of the P-selectin-carbohydrate bond and its response to tensile force in hydrodynamic flow. **Nature**, 374: 539–542
Antl, M., von Brühl, M.-L., Eiglsperger, C., et al. (2007) IRAG mediates NO/cGMP-dependent inhibition of platelet aggregation and thrombus formation. **Blood**, 109 (2): 552–9
Barath, P., Fishbein, M.C., Cao, J., et al. (1990) Tumor necrosis factor gene expression in human vascular intimal smooth muscle cells detected by in situ hybridization. **American Journal of Pathology**, 137 (3): 503–509
Barry, O.P., Praticò, D., Savani, R.C., et al. (1998) Modulation of monocyte-endothelial cell interactions by platelet microparticles. **The Journal of Clinical Investigation**, 102 (1): 136–44
Basavaraj, M.G., Østerud, B. and Hansen, J.-B. (2012) Influence of different anticoagulants on monocyte procoagulant functions and monocyte-platelet aggregates formation. **Journal of Thrombosis and Haemostasis**, 10 (8): 1698–702
Beerman, I., Bhattacharya, D., Zandi, S., et al. (2010) Functionally distinct hematopoietic stem cells modulate hematopoietic lineage potential during aging by a mechanism of clonal expansion. **Proceedings of the National Academy of Sciences of the United States of America**, 107 (12): 5465–70
Beisiegel, U., Weber, W., Ihrke, G., et al. (1989) The LDL–receptor–related protein, LRP, is an apolipoprotein E-binding protein. **Nature**, 341: 162–164
Best, L., Martin, T., Russell, R., et al. (1977) Prostacyclin increases cyclic AMP levels and adenylate cyclase activity in platelets. **Nature**, 267: 850–852
Beutler, B. (2004) Inferences, questions and possibilities in Toll-like receptor signalling. **Nature**, 430: 257–63
Bevilacqua, M.P., Pober, J.S., Mendrick, D.L., et al. (1987) Identification of an inducible endothelial-leukocyte adhesion molecule. **Proceedings of the National Academy of Sciences of the United States of America**, 84 (24): 9238–42
Beyer, C. and Pisetsky, D.S. (2010) The role of microparticles in the pathogenesis of rheumatic diseases. **Nature reviews. Rheumatology**, 6 (1): 21–9
Biasucci, L.M., Porto, I., Di Vito, L., et al. (2012) Differences in microparticle release in patients with acute coronary syndrome and stable angina. **Circulation Journal**, 76 (9): 2174–2182
Bixel, M.G., Petri, B., Khandoga, A.G., et al. (2007) A CD99-related antigen on endothelial cells mediates neutrophil but not lymphocyte extravasation in vivo. **Blood**, 109 (12): 5327–36
Blair, P. and Flaumenhaft, R. (2009) Platelet α-granules: basic biology and clinical correlates. **Blood reviews**, 23 (4): 177–89
Blake, R.A., Schieven, G.L. and Watson, S.R. (1994) Collagen stimulates tyrosine phosphorylation of phospholipase C-γ2 but not phospholipase C-γ1 in human platelets. **FEBS Letters**, 353 (6): 212–216
Bobrie, A., Colombo, M., Raposo, G., et al. (2011) Exosome secretion: molecular mechanisms and roles in immune responses. **Traffic**, 12: 1659–68

Boring, L., Gosling, J., Cleary, M., et al. (1998) Decreased lesion formation in CCR2-/- mice reveals a role for chemokines in the initiation of atherosclerosis. **Nature**, 394: 894–897
Boyd, S.D., Liu, Y., Wang, C., et al. (2013) Human lymphocyte repertoires in ageing. **Current opinion in immunology**, 25: 511–5
Braet, F. and Wisse, E. (2002) Structural and functional aspects of liver sinusoidal endothelial cell fenestrae: a review. **Comparative Hepatology**, 1 (1): 1
Brill, A., Fuchs, T.A., Savchenko, A.S., et al. (2012) Neutrophil extracellular traps promote deep vein thrombosis in mice. **Journal of Thrombosis and Haemostasis**, 10 (1): 136–144
Brown, K.K., Henson, P.M., Maclouf, J., et al. (1998) Neutrophil-platelet adhesion: relative roles of platelet P-selectin and neutrophil β2 (CD18) integrins. **American Journal of respiratory cell and molecular biology**, 18: 100–110
Burger, P. and Wagner, D. (2003) Platelet P-selectin facilitates atherosclerotic lesion development. **Blood**, 101: 2661–2666
Burton, J.O., Hamali, H. a, Singh, R., et al. (2013) Elevated levels of procoagulant plasma microvesicles in dialysis patients. **PloS one**, 8 (8): e72663
Carestia, A., Rivadeneyra, L., Romaniuk, M.A., et al. (2013) Functional responses and molecular mechanisms involved in histone-mediated platelet activation. **Thrombosis and haemostasis**, 110 (5): 1035–45
Carlos, T.M. and Harlan, J.M. (1994) Leukocyte-endothelial adhesion molecules. **Blood**, 84 (7): 2068–101
Chan, J.R., Hyduk, S.J. and Cybulsky, M.I. (2001) Chemoattractants induce a rapid and transient upregulation of monocyte α4 integrin affinity for vascular cell adhesion molecule 1 which mediates arrest: an early step in the process of emigration. **The Journal of Experimental Medicine**, 193 (10): 1149–58
Chaput, C., Sander, L.E., Suttorp, N., et al. (2013) NOD-like receptors in lung diseases. **Frontiers in immunology**, 4: 393
Chavakis, T., Keiper, T., Matz-Westphal, R., et al. (2004) The junctional adhesion molecule-C promotes neutrophil transendothelial migration in vitro and in vivo. **The Journal of Biological Chemistry**, 279 (53): 55602–8
Chen, M., Kakutani, M., Naruko, T., et al. (2001) Activation-dependent surface expression of LOX-1 in human platelets. **Biochemical and biophysical research communications**, 282 (1): 153–8
Chigaev, A., Zwartz, G., Graves, S.W., et al. (2003) α4β1 integrin affinity changes govern cell adhesion. **The Journal of Biological Chemistry**, 278 (40): 38174–82
Chirumbolo, S. (2012) State-of-the-art review about basophil research in immunology and allergy: is the time right to treat these cells with the respect they deserve? **Blood transfusion**, 10: 148–64
Choi, M.E. and Ballermann, B.J. (1995) Inhibition of Capillary Morphogenesis and Associated Apoptosis by Dominant Negative Mutant Transforming Growth Factor- Receptors. **The Journal of Biological Chemistry**, 270 (36): 21144–21150
Chotinantakul, K. and Leeanansaksiri, W. (2012) Hematopoietic stem cell development, niches, and signaling pathways. **Bone marrow research**, 2012: 1–16
Chou, T.-C., Lin, Y.-F., Wu, W.-C., et al. (2008) Enhanced nitric oxide and cyclic GMP formation plays a role in the anti-platelet activity of simvastatin. **British Journal of Pharmacology**, 153 (6): 1281–7
Chow, T.W., Hellums, J.D. and Thiagarajan, P. (2000) Thrombin receptor activating peptide (SFLLRN) potentiates shear-induced platelet microvesiculation. **The Journal of Laboratory and Clinical Medicine**, 135 (1): 66–72

Christersson, C., Johnell, M. and Siegbahn, A. (2008) Tissue factor and IL8 production by P-selectin-dependent platelet-monocyte aggregates in whole blood involves phosphorylation of Lyn and is inhibited by IL10. **Journal of thrombosis and haemostasis**, 6 (6): 986–94
Christersson, C., Johnell, M. and Siegbahn, A. (2010) The influence of direct thrombin inhibitors on the formation of platelet-leukocyte aggregates and tissue factor expression. **Thrombosis research**, 126 (4): e327–e333
Cines, D.B., Pollak, E.S., Buck, C. a, et al. (1998) Endothelial cells in physiology and in the pathophysiology of vascular disorders. **Blood**, 91 (10): 3527–61
Clark, A., Federspiel, W.J., Clark, P.A., et al. (1985) Oxygen delivery from red cells. **Biophysical Journal**, 47 (2): 171–181
Del Conde, I., Shrimpton, C.N., Thiagarajan, P., et al. (2005) Tissue-factor-bearing microvesicles arise from lipid rafts and fuse with activated platelets to initiate coagulation. **Blood**, 106 (5): 1604–11
Constantin, G., Majeed, M., Giagulli, C., et al. (2000) Chemokines trigger immediate β2 integrin affinity and mobility changes: differential regulation and roles in lymphocyte arrest under flow. **Immunity**, 13 (6): 759–69
Cooke, B., Usami, S., Perry, I., et al. (1993) A simplified method for culture of endothelial cells and analysis of adhesion of blood cells under conditions of flow. **Microvascular research**, 45: 33–45
Cook-Mills, J.M., Johnson, J.D., Deem, T.L., et al. (2004) Calcium mobilization and Rac1 activation are required for VCAM-1 (vascular cell adhesion molecule-1) stimulation of NADPH oxidase activity. **The Biochemical Journal**, 378: 539–47
Cosemans, J.M.E.M., Angelillo-Scherrer, A., Mattheij, N.J.A., et al. (2013) The effects of arterial flow on platelet activation, thrombus growth, and stabilization. **Cardiovascular research**, 99 (2): 342–352
Coughlin, S.R. (2000) Thrombin signalling and protease-activated receptors. **Nature**, 407 (6801): 258–64
Czepluch, F.S., Kuschicke, H., Dellas, C., et al. (2014) Increased proatherogenic monocyte-platelet cross-talk in monocyte subpopulations of patients with stable coronary artery disease. **Journal of internal medicine**, 275 (2): 144–54
Dahlöf, B. (2010) Cardiovascular disease risk factors: epidemiology and risk assessment. **The American journal of cardiology**, 105 (1 Suppl): 3A–9A
Daniel, J.L., Dangelmaier, C., Jin, J., et al. (1998) Molecular Basis for ADP-induced Platelet Activation: I. evidence for three distinct ADP receptors on human platelets. **Journal of Biological Chemistry**, 273 (4): 2024–2029
Davie, E.W., Fujikawa, K. and Kisiel, W. (1991) The coagulation cascade: initiation, maintenance, and regulation. **Biochemistry**, 30 (43): 10363–70
Devi, S., Kuligowski, M.P., Kwan, R.Y.Q., et al. (2010) Platelet recruitment to the inflamed glomerulus occurs via an αIIbβ3/GPVI-dependent pathway. **The American journal of pathology**, 177 (3): 1131–42
Diacovo, B.T.G., Catalina, M.D., Siegelman, M.H., et al. (1998) Circulating activated platelets reconstitute lymphocyte homing and immunity in L-selectin – deficient mice. **Journal of experimental medicine**, 187 (2): 197–204
Diacovo, T., Puri, K. and Warnock, R. (1996) Platelet-mediated lymphocyte delivery to high endothelial venules. **Science**, 273: 252–255
Ding, G., van Goor, H., Ricardo, S.D., et al. (1997) Oxidized LDL stimulates the expression of TGF-β and fibronectin in human glomerular epithelial cells. **Kidney International**, 51 (1): 147–54

Doan, T., Melvold, R., Viselli, S., et al. (2012) **Immunology. 2nd Edition.** In Lippincott's Illustrated reviews. Philadelphia: Wolters Kluwer Health/Lippincott Williams & Wilkins. p. 17
Dunne, J.L., C.M, B., Beaudet, A.L., et al. (2002) Control of leukocyte rolling velocity in TNF-α-induced inflammation by LFA-1 and Mac-1. **Blood**, 99 (1): 336–341
Eldor, A., Vlodavsky, I., Martinowicz, U., et al. (1985) Platelet interaction with subendothelial extracellular matrix: platelet-fibrinogen interactions are essential for platelet aggregation but not for the matrix-induced release reaction. **Blood**, 65 (6): 1477–83
Erdmann, I., Scheidegger, E.P., Koch, F.K., et al. (2002) Fucosyltransferase VII-Deficient Mice with Defective E-, P-, and L-Selectin Ligands Show Impaired CD4+ and CD8+ T Cell Migration into the Skin, but Normal Extravasation into Visceral Organs. **The Journal of Immunology**, 168 (5): 2139–2146
Eriksson, E., Xie, X., WERR, J., et al. (2001) Direct viewing of atherosclerosis in vivo: plaque invasion by leukocytes is initiated by the endothelial selectins. **The FASEB Journal**, 15: 1149–1157
Etienne-Manneville, S., Manneville, J.-B., Adamson, P., et al. (2000) ICAM-1-coupled cytoskeletal rearrangements and transendothelial lymphocyte migration involve intracellular calcium signaling in brain endothelial cell lines. **The Journal of Immunology**, 165 (6): 3375–3383
Evangelista, V., Manarini, S., Coller, B.S., et al. (2003) Role of P-selectin, β2-integrins, and Src tyrosine kinases in mouse neutrophil-platelet adhesion. **Journal of thrombosis and haemostasis**, 1 (5): 1048–54
Evangelista, V., Manarini, S., Sideri, R., et al. (1999) Platelet/polymorphonuclear leukocyte interaction: P-selectin triggers protein-tyrosine phosphorylation-dependent CD11b/CD18 adhesion: role of PSGL-1 as a signaling molecule. **Blood**, 93 (3): 876–85
Eyles, J.L., Roberts, A.W., Metcalf, D., et al. (2006) Granulocyte colony-stimulating factor and neutrophils-forgotten mediators of inflammatory disease. **Nat Clin Pract Rheum**, 2 (9): 500–510
Falati, S., Gross, P., Merrill-Skoloff, G., et al. (2002) Real-time in vivo imaging of platelets, tissue factor and fibrin during arterial thrombus formation in the mouse. **Nature medicine**, 8 (10): 1175–81
Favero, G., Paganelli, C., Buffoli, B., et al. (2014) Endothelium and its alterations in cardiovascular diseases: life style intervention. **BioMed research international**, 2014: 1–28
Febbraio, M., Podrez, E. a, Smith, J.D., et al. (2000) Targeted disruption of the class B scavenger receptor CD36 protects against atherosclerotic lesion development in mice. **The Journal of Clinical Investigation**, 105 (8): 1049–56
Finger, E.B., Puri, K.D., Alon, R., et al. (1996) Adhesion through L-selectin requires a threshold hydrodynamic shear. **Nature**, 379 (6562): 266–269
Flaumenhaft, R., Dilks, J.R., Richardson, J., et al. (2009) Megakaryocyte-derived microparticles: direct visualization and distinction from platelet-derived microparticles. **Blood**, 113 (5): 1112–21
Forlow, S.B., McEver, R.P. and Nollert, M.U. (2000) Leukocyte-leukocyte interactions mediated by platelet microparticles under flow. **Blood**, 95 (4): 1317–23
Fuchs, T.A., Bhandari, A.A. and Wagner, D.D. (2011) Histones induce rapid and profound thrombocytopenia in mice. **Blood**, 118 (13): 3708–14
Fuchs, T.A., Brill, A., Duerschmied, D., et al. (2010) Extracellular DNA traps promote thrombosis. **Proceedings of the National Academy of Sciences of the United States of America**, 107 (36): 15880–15885
Furman, M.I., Benoit, S.E., Barnard, M.R., et al. (1998) Increased platelet reactivity and circulating monocyte-platelet aggregates in patients with stable coronary artery disease. **Journal of the American College of Cardiology**, 31 (2): 352–8

Furman, M.I., Kereiakes, D.J., Krueger, L. a, et al. (2001) Leukocyte-platelet aggregation, platelet surface P-selectin, and platelet surface glycoprotein IIIa after percutaneous coronary intervention: Effects of dalteparin or unfractionated heparin in combination with abciximab. **American heart journal**, 142 (5): 790–8
Garzetti, L., Menon, R., Finardi, A., et al. (2013) Activated macrophages release microvesicles containing polarized M1 or M2 mRNAs. **Journal of leukocyte biology**, 95: 1–9
Geissmann, F., Auffray, C., Palframan, R., et al. (2008) Blood monocytes: distinct subsets, how they relate to dendritic cells, and their possible roles in the regulation of T-cell responses. **Immunology and cell biology**, 86 (5): 398–408
Geissmann, F., Jung, S. and Littman, D.R. (2003) Blood monocytes consist of two principal subsets with distinct migratory properties. **Immunity**, 19 (1): 71–82
Geremia, A., Biancheri, P., Allan, P., et al. (2014) Innate and adaptive immunity in inflammatory bowel disease. **Autoimmunity reviews**, 13 (1): 3–10
Ghattas, A., Griffiths, H.R., Devitt, A., et al. (2013) Monocytes in coronary artery disease and atherosclerosis: where are we now? **Journal of the American College of Cardiology**, 62 (17): 1541–51
Gibbins, J.M., Okuma, M., Farndale, R., et al. (1997) Glycoprotein VI is the collagen receptor in platelets which underlies tyrosine phosphorylation of the Fc receptor γ-chain. **FEBS Letters**, 413 (2): 255–259
Gkaliagkousi, E., Corrigall, V., Becker, S., et al. (2009) Decreased platelet nitric oxide contributes to increased circulating monocyte-platelet aggregates in hypertension. **European heart journal**, 30 (24): 3048–54
Gkaliagkousi, E., Ritter, J. and Ferro, A. (2007) Platelet-derived nitric oxide signaling and regulation. **Circulation research**, 101 (7): 654–62
Gorski, D.H. and Walsh, K. (1995) Mitogen-responsive nuclear factors that mediate growth control signals in vascular myocytes. **Cardiovascular research**, 30 (4): 585–92
Greene, J.M., Wiseman, R.W., Lank, S.M., et al. (2011) Differential MHC class I expression in distinct leukocyte subsets. **BMC immunology**, 12 (1): 39
Gu, L., Okada, Y., Clinton, S.K., et al. (1998) Absence of monocyte chemoattractant protein-1 reduces atherosclerosis in low density lipoprotein receptor-deficient mice. **Molecular cell**, 2 (2): 275–81
Hanley, W.D., Wirtz, D. and Konstantopoulos, K. (2004) Distinct kinetic and mechanical properties govern selectin-leukocyte interactions. **Journal of cell science**, 117 (12): 2503–11
Harding, S.A., Din, J.N., Sarma, J., et al. (2007) Flow cytometric analysis of circulating platelet-monocyte aggregates in whole blood: methodological considerations. **Thrombosis and haemostasis**, 98: 451–456
Harding, S.A., Sommerfield, A.J., Sarma, J., et al. (2004) Increased CD40 ligand and platelet-monocyte aggregates in patients with type 1 diabetes mellitus. **Atherosclerosis**, 176 (2): 321–5
Hargett, L. a and Bauer, N.N. (2013) On the origin of microparticles: From "platelet dust" to mediators of intercellular communication. **Pulmonary circulation**, 3 (2): 329–340
Heijnen, H.F., Schiel, a E., Fijnheer, R., et al. (1999) Activated platelets release two types of membrane vesicles: microvesicles by surface shedding and exosomes derived from exocytosis of multivesicular bodies and α-granules. **Blood**, 94 (11): 3791–9
Hellerstein, M., Hanley, M.B., Cesar, D., et al. (1999) Directly measured kinetics of circulating T lymphocytes in normal and HIV-1-infected humans. **Nature medicine**, 5 (1): 83–9
Hollopeter, G., Jantzen, H., Vincent, D., et al. (2001) Identification of the platelet ADP receptor targeted by antithrombotic drugs. **Nature**, 409: 202–207

Hourdillé, P., Gralnick, H.R., Heilmann, E., et al. (1992) von Willebrand factor bound to glycoprotein Ib is cleared from the platelet surface after platelet activation by thrombin. **Blood**, 79 (8): 2011–21
Hourdillé, P., Heilmann, E., Combrié, R., et al. (1990) Thrombin induces a rapid redistribution of glycoprotein Ib-IX complexes within the membrane systems of activated human platelets. **Blood**, 76 (8): 1503–13
Htun, P., Fateh-Moghadam, S., Tomandl, B., et al. (2006) Course of platelet activation and platelet-leukocyte interaction in cerebrovascular ischemia. **Stroke; a journal of cerebral circulation**, 37 (9): 2283–7
Huang, H., Evankovich, J., Yan, W., et al. (2011) Endogenous histones function as alarmins in sterile inflammatory liver injury through Toll-like receptor 9 in mice. **Hepatology**, 54 (3): 999–1008
Huang, H., Hao, S., Li, F., et al. (2007) CD4 + Th1 cells promote CD8 + Tc1 cell survival, memory response, tumor localization and therapy by targeted delivery of interleukin 2 via acquired pMHC I complexes. **Immunology**, 120 (2): 148–159
Hughes, C.E., Pollitt, A.Y., Mori, J., et al. (2010) CLEC-2 activates Syk through dimerization. **Blood**, 115 (14): 2947–55
Von Hundelshausen, P., Koenen, R.R., Sack, M., et al. (2005) Heterophilic interactions of platelet factor 4 and RANTES promote monocyte arrest on endothelium. **Blood**, 105 (3): 924–930
Von Hundelshausen, P., Weber, K.S.C., Huo, Y., et al. (2001) RANTES deposition by platelets triggers monocyte arrest on inflamed and atherosclerotic endothelium. **Circulation**, 103 (13): 1772–1777
Hunter, M.P., Ismail, N., Zhang, X., et al. (2008) Detection of microRNA expression in human peripheral blood microvesicles. Lo, Y.M.D. (ed.). **PLoS ONE**, 3 (11): e3694
Huo, Y., Hafezi-Moghadam, A. and Ley, K. (2000) Role of vascular cell adhesion molecule-1 and fibronectin connecting segment-1 in monocyte rolling and adhesion on early atherosclerotic lesions. **Circulation Research**, 87 (2): 153–159
Huo, Y. and Ley, K. (2004) Role of platelets in the development of atherosclerosis. **Trends in cardiovascular medicine**, 14 (1): 18–22
Iiyama, K., Hajra, L., Iiyama, M., et al. (1999) Patterns of vascular cell adhesion molecule-1 and intercellular adhesion molecule-1 expression in rabbit and mouse atherosclerotic lesions and at sites predisposed to lesion formation. **Circulation Research**, 85 (2): 199–207
Ikeda, U. and Matsui, K. (2002) Monocyte chemoattractant protein-1 and coronary artery disease. **Clinical cardiology**, 147: 143–147
Ishikawa, T., Shimizu, M., Kohara, S., et al. (2012) Appearance of WBC-platelet complex in acute ischemic stroke, predominantly in atherothrombotic infarction. **Journal of atherosclerosis and thrombosis**, 19 (5): 494–501
Issekutz, A.C., Rowter, D. and Springer, T.A. (1999) Role of ICAM-1 and ICAM-2 and alternate CD11/CD18 ligands in neutrophil transendothelial migration. **Journal of leukocyte biology**, 65: 117–126
Jaipersad, A.S., Gregory, M., Lip, Y.H., et al. (2014) The role of monocytes in angiogenesis and atherosclerosis. **Journal of the American College of Cardiology**, 63 (1): 1–11
Janssen, E.M., Lemmens, E.E., Wolfe, T., et al. (2003) CD4+ T cells are required for secondary expansion and memory in CD8+ T lymphocytes. **Nature**, 421 (6925): 852–6
Jensen, M.K., de Nully Brown, P., Lund, B. V, et al. (2001) Increased circulating platelet-leukocyte aggregates in myeloproliferative disorders is correlated to previous thrombosis, platelet activation and platelet count. **European journal of haematology**, 66 (3): 143–51

Jin, J. and Kunapuli, S.P. (1998) Coactivation of two different G protein-coupled receptors is essential for ADP-induced platelet aggregation. **Proceedings of the National Academy of Sciences of the United States of America**, 95 (14): 8070–4
Jin, J., Quinton, T., Zhang, J., et al. (2002) Adenosine diphosphate (ADP)-induced thromboxane A2 generation in human platelets requires coordinated signaling through integrin αIIbβ3 and ADP receptors. **Blood**, 99 (1): 193–198
Johnson, Z., Proudfoot, a E. and Handel, T.M. (2005) Interaction of chemokines and glycosaminoglycans: a new twist in the regulation of chemokine function with opportunities for therapeutic intervention. **Cytokine & growth factor reviews**, 16 (6): 625–36
Joseph E Italiano Jr, Mairuhu Albert T.A., and F.R. (2010) Clinical relevance of microparticles from platelets and megakaryocytes. **Current opinion in haematology**, 17 (6): 578–584
Joseph, J.E., Harrison, P., Mackie, I.J., et al. (2001) Increased circulating platelet-leucocyte complexes and platelet activation in patients with antiphospholipid syndrome, systemic lupus erythematosus and rheumatoid arthritis. **British journal of haematology**, 115 (2): 451–9
Jungi, T.W., Spycher, M.O., Nydegger, U.E., et al. (1986) Platelet-leukocyte interaction: selective binding of thrombin-stimulated platelets to human monocytes, polymorphonuclear leukocytes, and related cell lines. **Blood**, 67 (3): 629–36
Jy, W., Mao, W.W., Horstman, L., et al. (1995) Platelet microparticles bind, activate and aggregate neutrophils in vitro. **Blood cells, molecules & diseases**, 21 (3): 217–231
Kahn, M.L., Nakanishi-Matsui, M., Shapiro, M.J., et al. (1999) Protease-activated receptors 1 and 4 mediate activation of human platelets by thrombin. **The Journal of Clinical Investigation**, 103 (6): 879–87
Kanaji, S., Fahs, S., Shi, Q., et al. (2012) Contribution of platelet vs. endothelial VWF to platelet adhesion and hemostasis. **Jouirnal of thrombosis and haemostasis**, 10 (8): 1646–1652
Kataoka, H., Kume, N., Miyamoto, S., et al. (1999) Expression of Lectinlike Oxidized Low-Density Lipoprotein Receptor-1 in Human Atherosclerotic Lesions. **Circulation**, 99 (24): 3110–3117
Keating, F.K., Dauerman, H.L., Whitaker, D. a, et al. (2006) Increased expression of platelet P-selectin and formation of platelet-leukocyte aggregates in blood from patients treated with unfractionated heparin plus eptifibatide compared with bivalirudin. **Thrombosis research**, 118 (3): 361–9
King, C. (2009) New insights into the differentiation and function of T follicular helper cells. **Nature reviews. Immunology**, 9 (11): 757–66
Klinkhardt, U., Bauersachs, R., Adams, J., et al. (2003) Clopidogrel but not aspirin reduces P-selectin expression and formation of platelet-leukocyte aggregates in patients with atherosclerotic vascular disease. **Clinical pharmacology and therapeutics**, 73 (3): 232–41
Konstantopoulos, K., Neelamegham, S., Burns, a. R., et al. (1998) Venous Levels of Shear Support Neutrophil-Platelet Adhesion and Neutrophil Aggregation in Blood via P-Selectin and β2-Integrin. **Circulation**, 98 (9): 873–882
Korporaal, S.J. a, Van Eck, M., Adelmeijer, J., et al. (2007) Platelet activation by oxidized low density lipoprotein is mediated by CD36 and scavenger receptor-A. **Arteriosclerosis, thrombosis, and vascular biology**, 27 (11): 2476–83
Krause, D. (2002) Regulation of hematopoietic stem cell fate. **Oncogene**, 21: 3262–3269
Kuckleburg, C.J., Yates, C.M., Kalia, N., et al. (2011) Endothelial cell-borne platelet bridges selectively recruit monocytes in human and mouse models of vascular inflammation. **Cardiovascular research**, 91 (1): 134–41
Kume, N., Murase, T., Moriwaki, H., et al. (1998) Inducible expression of lectin-like oxidized LDL receptor-1 in vascular endothelial cells. **Circulation Research**, 83 (3): 322–327

Kunjathoor, V. V, Febbraio, M., Podrez, E. a, et al. (2002) Scavenger receptors class A-I/II and CD36 are the principal receptors responsible for the uptake of modified low density lipoprotein leading to lipid loading in macrophages. **The Journal of Biological Chemistry**, 277 (51): 49982–8
Lalor, P. and Nash, G.B. (1995) Adhesion of flowing leucocytes to immobilized platelets. **British journal of haematology**, 89 (4): 725–32
Lerman, A., Holmes, D.R., Bell, M.R., et al. (1995) Endothelin in coronary endothelial dysfunction and early atherosclerosis in humans. **Circulation**, 92 (9): 2426–2431
Levi, M., van der Poll, T. and Büller, H.R. (2004) Bidirectional relation between inflammation and coagulation. **Circulation**, 109 (22): 2698–704
Ley, K. (2003) The role of selectins in inflammation and disease. **Trends in Molecular Medicine**, 9 (6): 263–268
Ley, K., Laudanna, C., Cybulsky, M.I., et al. (2007) Getting to the site of inflammation: the leukocyte adhesion cascade updated. **Nature reviews. Immunology**, 7 (9): 678–89
Li, N. (2008) Platelet-lymphocyte cross-talk. **Journal of leukocyte biology**, 83 (5): 1069–78
Li, N., Ji, Q. and Hjemdahl, P. (2006) Platelet-lymphocyte conjugation differs between lymphocyte subpopulations. **Journal of thrombosis and haemostasis**, 4: 874–81
Libby, P. (2012) Inflammation in atherosclerosis. **Arteriosclerosis, thrombosis, and vascular biology**, 32 (9): 2045–51
Libby, P., Ridker, P.M. and Hansson, G.K. (2011) Progress and challenges in translating the biology of atherosclerosis. **Nature**, 473: 317–25
Lim, Y.C., Henault, L., Wagers, A.J., et al. (1999) Expression of functional selectin ligands on Th cells is differentially regulated by IL-12 and IL-4. **Journal of immunology**, 162 (6): 3193–201
Linden, M.D., Furman, M.I., Frelinger, A.L., et al. (2007) Indices of platelet activation and the stability of coronary artery disease. **Journal of thrombosis and haemostasis**, 5 (4): 761–5
Linsley, P.S., Brady, W., Grosmaire, L., et al. (1991) Binding of the B cell activation antigen B7 to CD28 costimulates T cell proliferation and interleukin 2 mRNA accumulation. **The Journal of Experimental Medicine**, 173 (3): 721–30
Liu, T., Laidlaw, T.M., Feng, C., et al. (2012) Prostaglandin E2 deficiency uncovers a dominant role for thromboxane A2 in house dust mite-induced allergic pulmonary inflammation. **Proceedings of the National Academy of Sciences of the United States of America**, 109 (31): 12692–12697
Lou, O., Alcaide, P., Luscinskas, F.W., et al. (2007) CD99 is a key mediator of the transendothelial migration of neutrophils. **The Journal of Immunology**, 178 (2): 1136–1143
Lu, P., Sodhi, C.P. and Hackam, D.J. (2013) Toll-like receptor regulation of intestinal development and inflammation in the pathogenesis of necrotizing enterocolitis. **Pathophysiology**, 21 (1): 81–93
Luckheeram, R.V., Zhou, R., Verma, A.D., et al. (2012) $CD4^+$T cells: differentiation and functions. **Clinical & developmental immunology**, 2012: 1–12
Mamdouh, Z., Mikhailov, A. and Muller, W. a (2009) Transcellular migration of leukocytes is mediated by the endothelial lateral border recycling compartment. **The Journal of Experimental Medicine**, 206 (12): 2795–808
Marcus, A.J., Broekman, M.J., Drosopoulos, J.H., et al. (1997) The endothelial cell ecto-ADPase responsible for inhibition of platelet function is CD39. **The Journal of Clinical Investigation**, 99 (6): 1351–60
Marshall, B.T., Long, M., Piper, J.W., et al. (2003) Direct observation of catch bonds involving cell-adhesion molecules. **Nature**, 423: 190–3
Masopust, D., Vezys, V., Wherry, E.J., et al. (2007) A brief history of CD8 T cells. **European journal of immunology**, 37 Suppl 1: S103–10

Massberg, S., Brand, K., Grüner, S., et al. (2002) A critical role of platelet adhesion in the initiation of atherosclerotic lesion formation. **The Journal of Experimental Medicine**, 196 (7): 887–896
Matheny, H.E., Deem, T.L. and Cook-Mills, J.M. (2000) Lymphocyte migration through monolayers of endothelial cell lines involves VCAM-1 signaling via endothelial Cell NADPH oxidase. **The Journal of Immunology**, 164 (12): 6550–6559
Mause, S.F., von Hundelshausen, P., Zernecke, A., et al. (2005) Platelet microparticles: a transcellular delivery system for RANTES promoting monocyte recruitment on endothelium. **Arteriosclerosis, thrombosis, and vascular biology**, 25 (7): 1512–8
McAdam, B.F., Catella-Lawson, F., Mardini, I.A., et al. (1999) Systemic biosynthesis of prostacyclin by cyclooxygenase (COX)-2: the human pharmacology of a selective inhibitor of COX-2. **Proceedings of the National Academy of Sciences of the United States of America**, 96 (1): 272–7
McEver, R.P., Beckstead, J.H., Moore, K.L., et al. (1989) GMP-140, a platelet alpha-granule membrane protein, is also synthesized by vascular endothelial cells and is localized in Weibel-Palade bodies. **The Journal of Clinical Investigation**, 84 (1): 92–99
McEver, R.P. and Cummings, R.D. (1997) Perspectives series: cell adhesion in vascular biology. Role of PSGL-1 binding to selectins in leukocyte recruitment. **The Journal of Clinical Investigation**, 100 (3): 485–91
McNicol, A. and Israels, S.J. (1999) Platelet dense granules: structure, function and implications for haemostasis. **Thrombosis research**, 95 (1): 1–18
Mehta, P. Cummings, R.D.M.R.P. (1998) Affinity and kinetic analysis of P-selectin binding to P-selectin glycoprotein ligand-1. **Journal of Biological Chemistry**, 273 (49): 32506–32513
Mellion, B.T., Ignarro, L.J., Ohlstein, E.H., et al. (1981) Evidence for the inhibitory role of guanosine 3', 5'-monophosphate in ADP-induced human platelet aggregation in the presence of nitric oxide and related vasodilators. **Blood**, 57 (5): 946–55
Menon, S. and Valentini, R.P. (2010) Membranous nephropathy in children: clinical presentation and therapeutic approach. **Pediatric nephrology**, 25: 1419–28
Michelson, a D., Benoit, S.E., Kroll, M.H., et al. (1994) The activation-induced decrease in the platelet surface expression of the glycoprotein Ib-IX complex is reversible. **Blood**, 83 (12): 3562–73
Michelson, a. D., Barnard, M.R., Krueger, L. a., et al. (2001) Circulating monocyte-platelet aggregates are a more sensitive marker of in vivo platelet activation than platelet surface P-Selectin: studies in baboons, human coronary intervention, and human acute myocardial infarction. **Circulation**, 104 (13): 1533–1537
Michiels, C. (2003) Endothelial cell functions. **Journal of cellular physiology**, 196 (3): 430–43
Mickelson, J.K., Lakkis, N.M., Villarreal-Levy, G., et al. (1996) Leukocyte activation with platelet adhesion after coronary angioplasty: a mechanism for recurrent disease? **Journal of the American College of Cardiology**, 28 (2): 345–53
Miner, J. (2011) Glomerular basement membrane composition and the filtration barrier. **Pediatric Nephrology**, 26 (9): 1413–1417
Moore, K. and Thompson, L. (1992) P-selectin (CD62) binds to subpopulations of human memory T lymphocytes and natural killer cells. **Biochemical and biophysical research communications**, 186 (1): 173–181
Moore, K.J. and Tabas, I. (2011) Macrophages in the pathogenesis of atherosclerosis. **Cell**, 145 (3): 341–55

Moraes, L. a, Swales, K.E., Wray, J. a, et al. (2007) Nongenomic signaling of the retinoid X receptor through binding and inhibiting Gq in human platelets. **Blood**, 109 (9): 3741–4
Mosmann, T.R. and Sad, S. (1996) The expanding universe of T-cell subsets: Th1, Th2 and more. **Immunology today**, 17 (3): 138–46
Mosser, D.M. (2003) The many faces of macrophage activation. **Journal of leukocyte biology**, 73 (2): 209–212
Mozes, M.M., Böttinger, E.P., Jacot, T. a, et al. (1999) Renal expression of fibrotic matrix proteins and of transforming growth factor-β (TGF-beta) isoforms in TGF-beta transgenic mice. **Journal of the American Society of Nephrology**, 10 (2): 271–80
Muller, W. (2011) Mechanisms of leukocyte transendothelial migration. **Annual review of pathology**, 6: 323–344
Muller, W. a, Weigl, S. a, Deng, X., et al. (1993) PECAM-1 is required for transendothelial migration of leukocytes. **The Journal of experimental medicine**, 178 (2): 449–60
Munday, A.D., Gaus, K. and López, J. a (2010) The platelet glycoprotein Ib-IX-V complex anchors lipid rafts to the membrane skeleton: implications for activation-dependent cytoskeletal translocation of signaling molecules. **Journal of thrombosis and haemostasis**, 8 (1): 163–72
Murphy, J.E., Vohra, R.S., Dunn, S., et al. (2008) Oxidised LDL internalisation by the LOX-1 scavenger receptor is dependent on a novel cytoplasmic motif and is regulated by dynamin-2. **Journal of cell science**, 121: 2136–47
Murray, P.J. and Wynn, T. a (2011) Protective and pathogenic functions of macrophage subsets. **Nature reviews. Immunology**, 11 (11): 723–37
Nahrendorf, M., Swirski, F.K., Aikawa, E., et al. (2007) The healing myocardium sequentially mobilizes two monocyte subsets with divergent and complementary functions. **The Journal of Experimental Medicine**, 204 (12): 3037–47
Neumann, F.J., Zohlnhöfer, D., Fakhoury, L., et al. (1999) Effect of glycoprotein IIb/IIIa receptor blockade on platelet-leukocyte interaction and surface expression of the leukocyte integrin Mac-1 in acute myocardial infarction. **Journal of the American College of Cardiology**, 34 (5): 1420–6
Nieswandt, B., Pleines, I. and Bender, M. (2011) Platelet adhesion and activation mechanisms in arterial thrombosis and ischaemic stroke. **Journal of thrombosis and haemostasis**, 9: 92–104
Nieswandt, B. and Watson, S.P. (2003) Platelet-collagen interaction: is GPVI the central receptor? **Blood**, 102 (2): 449–461
Nijm, J., Wikby, A., Tompa, A., et al. (2005) Circulating levels of proinflammatory cytokines and neutrophil-platelet aggregates in patients with coronary artery disease. **The American journal of cardiology**, 95 (4): 452–6
Nomura, S., Suzuki, M., Katsura, K., et al. (1995) Platelet-derived microparticles may influence the development of atherosclerosis in diabetes mellitus. **Atherosclerosis**, 116 (2): 235–40
Nomura, S., Tandon, N.N., Nakamura, T., et al. (2001) High-shear-stress-induced activation of platelets and microparticles enhances expression of cell adhesion molecules in THP-1 and endothelial cells. **Atherosclerosis**, 158 (2): 277–87
Nygaard, G., Herfindal, L., Kopperud, R., et al. (2014) Time-dependent inhibitory effects of cGMP-analogues on thrombin-induced platelet-derived microparticles formation, platelet aggregation, and P-selectin expression. **Biochemical and biophysical research communications**, 449 (3): 357–363
Oemar, B.S., Tschudi, M.R., Godoy, N., et al. (1998) Reduced Endothelial Nitric Oxide Synthase Expression and Production in Human Atherosclerosis. **Circulation**, 97 (25): 2494–2498

Offermanns, S., Laugwitz, K.L., Spicher, K., et al. (1994) G proteins of the G12 family are activated via thromboxane A2 and thrombin receptors in human platelets. **Proceedings of the National Academy of Sciences of the United States of America**, 91 (2): 504–8
Offermanns, S., Toombs, C.F., Hu, Y.H., et al. (1997) Defective platelet activation in Gαq-deficient mice. **Nature**, 389 (6647): 183–6
Ogle, B. M., Cascalho Marilia, Joao Cristina, Taylor William, W.L.J. and P.J.L. (2003) Direct measurement of lymphocyte receptor diversity. **Nucleic Acids Research**, 31 (22): e139
Ostermann, G., Weber, K.S.C., Zernecke, A., et al. (2002) JAM-1 is a ligand of the β2 integrin LFA-1 involved in transendothelial migration of leukocytes. **Nature immunology**, 3 (2): 151–8
Otsuka, F., Finn, A. V, Yazdani, S.K., et al. (2012) The importance of the endothelium in atherothrombosis and coronary stenting. **Nat Rev Cardiol**, 9 (8): 439–453
Owens, G.K., Kumar, M.S. and Wamhoff, B.R. (2004) Molecular regulation of vascular smooth muscle cell differentiation in development and disease. **Physiological reviews**, 84: 767–801
Passacquale, G., Vamadevan, P., Pereira, L., et al. (2011) Monocyte-platelet interaction induces a pro-inflammatory phenotype in circulating monocytes. **PloS one**, 6 (10): e25595
Passerini, A.G., Polacek, D.C., Shi, C., et al. (2004) Coexisting proinflammatory and antioxidative endothelial transcription profiles in a disturbed flow region of the adult porcine aorta. **Proceedings of the National Academy of Sciences of the United States of America**, 101 (8): 2482–7
Paul, B.Z.S., Jin, J. and Kunapuli, S.P. (1999) Molecular Mechanism of Thromboxane A2-induced Platelet Aggregation: essential role for P2T AC and α 2areceptors. **Journal of Biological Chemistry**, 274 (41): 29108–29114
Pavenstädt, H., Kriz, W. and Kretzler, M. (2003) Cell biology of the glomerular podocyte. **Physiological reviews**, 83 (1): 253–307
Pegon, J.N., Kurdi, M., Casari, C., et al. (2012) Factor VIII and von Willebrand factor are ligands for the carbohydrate-receptor Siglec-5. **Haematologica**, 97 (12): 1855–63
Pendu, R., Terraube, V., Christophe, O.D., et al. (2006) P-selectin glycoprotein ligand 1 and β2-integrins cooperate in the adhesion of leukocytes to von Willebrand factor. **Haemostasis, Thrombosis and Vascular Biology**, 108 (12): 3746–3752
Petäjä, J. (2011) Inflammation and coagulation. An overview. **Thrombosis research**, 127 Suppl: S34–7
Peterson, C.L. and Laniel, M.-A. (2004) Histones and histone modifications. **Current biology**, 14 (14): R546–51
Peterson, D.M., Stathopoulos, N. a, Giorgio, T.D., et al. (1987) Shear-induced platelet aggregation requires von Willebrand factor and platelet membrane glycoproteins Ib and IIb-IIIa. **Blood**, 69 (2): 625–8
Pignone, M. and Williams, C.D. (2010) Aspirin for primary prevention of cardiovascular disease in diabetes mellitus. **Nat Rev Endocrinol**, 6 (11): 619–628
Pirillo, A., Norata, G.D. and Catapano, A.L. (2013) LOX-1, OxLDL, and atherosclerosis. **Mediators of inflammation**, 2013: 1–12
Pitchford S.C, Momi S., Giannini S., Casali L., Spina D., P.C.P. and G.P. (2005) Platelet P-selectin is required for pulmonary eosinophil and lymphocyte recruitment in a murine model of allergic inflammation. **Blood**, 105: 2074–2081
Pollitt, A.Y., Grygielska, B., Leblond, B., et al. (2010) Phosphorylation of CLEC-2 is dependent on lipid rafts, actin polymerization, secondary mediators, and Rac. **Blood**, 115 (14): 2938–46
Rainger, G. and Nash, G. (2001) Cellular pathology of atherosclerosis smooth muscle cells prime cocultured endothelial cells for enhanced leukocyte adhesion. **Circulation research**, 88: 615–622

Rainger, G.E., Stone, P., Morland, C.M., et al. (2001) A novel system for investigating the ability of smooth muscle cells and fibroblasts to regulate adhesion of flowing leukocytes to endothelial cells. **Journal of immunological methods**, 255: 73–82
Rand, M.L., Wang, H., Bang, K.W. a, et al. (2006) Rapid clearance of procoagulant platelet-derived microparticles from the circulation of rabbits [3]. **Journal of Thrombosis and Haemostasis**, 4: 1621–1623
Randolph, G.J., Inaba, K., Robbiani, D.F., et al. (1999) Differentiation of phagocytic monocytes into lymph node dendritic cells in vivo. **Immunity**, 11 (6): 753–61
Ridker, P.M., Buring, J.E. and Rifai, N. (2001) Soluble P-selectin and the risk of future cardiovascular events. **Circulation**, 103 (4): 491–495
Rinder, H.M., Bonan, J.L., Rinder, C.S., et al. (1991) Dynamics of leukocyte-platelet adhesion in whole blood. **Blood**, 78 (7): 1730–7
Rinder, H.M., Snyder, E.L., Bonan, J.L., et al. (1993) Activation in stored platelet concentrates: correlation between membrane expression of P-selectin, glycoprotein IIb/IIIa, and beta-thromboglobulin release. **Transfusion**, 33 (1): 25–9
Rivera, J., Lozano, M.L., Navarro-Núñez, L., et al. (2009) Platelet receptors and signaling in the dynamics of thrombus formation. **Haematologica**, 94 (5): 700–11
Rosenberg, H.F., Dyer, K.D. and Foster, P.S. (2013) Eosinophils: changing perspectives in health and disease. **Nature reviews. Immunology**, 13 (1): 9–22
Ross, R. (1999) Atherosclerosis—an inflammatory disease. **New England journal of medicine**, 340 (2): 115–126
Rothenberg, M.E. and Hogan, S.P. (2006) The eosinophil. **Annual review of immunology**, 24: 147–74
Roy, S., Sato, T., Paryani, G., et al. (2003) Downregulation of fibronectin overexpression reduces basement membrane thickening and vascular lesions in retinas of galactose-fed rats. **Diabetes**, 52 (5): 1229–34
Rzucidlo, E.M., Martin, K. a and Powell, R.J. (2007) Regulation of vascular smooth muscle cell differentiation. **Journal of vascular surgery**, 45: 25A–32A
Saleem, M. a, O'Hare, M.J., Reiser, J., et al. (2002) A conditionally immortalized human podocyte cell line demonstrating nephrin and podocin expression. **Journal of the American Society of Nephrology**, 13 (3): 630–8
Sarma, J. (2002) Increased Platelet Binding to Circulating Monocytes in Acute Coronary Syndromes. **Circulation**, 105 (18): 2166–2171
Satchell, S.C. (2004) Angiopoietin 1 and vascular endothelial growth factor modulate human glomerular endothelial cell barrier properties. **Journal of the American Society of Nephrology**, 15 (3): 566–574
Satchell, S.C., Tasman, C.H., Singh, A., et al. (2006) Conditionally immortalized human glomerular endothelial cells expressing fenestrations in response to VEGF. **Kidney International**, 69 (9): 1633–40
Schenkel, A.R., Mamdouh, Z., Chen, X., et al. (2002) CD99 plays a major role in the migration of monocytes through endothelial junctions. **Nature immunology**, 3 (2): 143–50
Schieffer, B., Schieffer, E., Hilfiker-Kleiner, D., et al. (2000) Expression of angiotensin II and interleukin 6 in human coronary atherosclerotic plaques: potential implications for inflammation and plaque instability. **Circulation**, 101 (12): 1372–1378
Schmid-Schönbein, G., Usami, S., Skalak, R., et al. (1980) The interaction of leukocytes and erythrocytes in capillary and postcapillary vessels. **Microvascular research**, 19: 45–70

Schmitz, G., Rothe, G., Ruf, A., et al. (1998) European working group on clinical cell analysis: consensus protocol for the flow cytometric characterisation of platelet function. **Thrombosis and haemostasis**, 79 (5): 885–96
Schober, A., Manka, D. and Hundelshausen, P. Von (2002) Deposition of platelet RANTES triggering monocyte recruitment requires P-selectin and is involved in neointima formation after arterial injury. **Circulation**, 106: 1523–1529
Scholz, T., Temmler, U., Krause, S., et al. (2002) Transfer of tissue factor from platelets to monocytes: role of platelet-derived microvesicles and CD62P. **Thrombosis and haemostasis**, 88 (6): 1033–8
Schulte, D., Küppers, V., Dartsch, N., et al. (2011) Stabilizing the VE-cadherin-catenin complex blocks leukocyte extravasation and vascular permeability. **The EMBO journal**, 30 (20): 4157–70
Schulz, C., Engelmann, B. and Massberg, S. (2013) Crossroads of coagulation and innate immunity: the case of deep vein thrombosis. **Journal of thrombosis and haemostasis**, 11 Suppl 1: 233–41
Segal, A.W. (2005) How neutrophils kill microbes. **Annual review of immunology**, 23: 197–223
Semeraro, F., Ammollo, C.T., Morrissey, J.H., et al. (2011) Extracellular histones promote thrombin generation through platelet-dependent mechanisms: involvement of platelet TLR2 and TLR4. **Blood**, 118 (7): 1952–61
Serbina, N. and Jia, T. (2008) Monocyte-mediated defense against microbial pathogens. **Annual review of immunology**, 26: 421–452
Serbina, N. V and Pamer, E.G. (2006) Monocyte emigration from bone marrow during bacterial infection requires signals mediated by chemokine receptor CCR2. **Nature immunology**, 7 (3): 311–7
Shai, E., Rosa, I., Parguiña, A.F., et al. (2012) Comparative analysis of platelet-derived microparticles reveals differences in their amount and proteome depending on the platelet stimulus. **Journal of proteomics**, 76: 287–96
Shantsila, E. and Lip, G.Y.H. (2009) The role of monocytes in thrombotic disorders. Insights from tissue factor, monocyte-platelet aggregates and novel mechanisms. **Thrombosis and haemostasis**, 102 (5): 916–24
Shantsila, E., Wrigley, B., Tapp, L., et al. (2011) Immunophenotypic characterization of human monocyte subsets: possible implications for cardiovascular disease pathophysiology. **Jouirnal of thrombosis and haemostasis**, 9: 1056–1066
Shaw, S.K., Ma, S., Kim, M.B., et al. (2004) Coordinated redistribution of leukocyte LFA-1 and endothelial cell ICAM-1 accompany neutrophil transmigration. **The Journal of experimental medicine**, 200 (12): 1571–80
Shaykhiev, R. and Crystal, R.G. (2013) Innate Immunity and Chronic Obstructive Pulmonary Disease: A Mini-Review. **Gerontology**, pp. 1–9
Simss, P.J., Wiedmers, T., Esmon, C.T., et al. (1989) Assembly of the platelet prothrombinase complex is linked to vesiculation of the platelet plasma membrane. **The Journal of Biological Chemistry**, 264 (29): 17049–17057
Sojka, D.K., Bruniquel, D., Schwartz, R.H., et al. (2004) IL-2 secretion by CD4+ T cells in vivo is rapid, transient, and influenced by TCR-specific competition. **The Journal of Immunology**, 172 (10): 6136–6143
Soon Lee, H. (2013) Pathogenic Role of TGF- β in Diabetic Nephropathy. **Journal of Diabetes & Metabolism**, 01 (S9)
St John, P.L. and Abrahamson, D.R. (2001) Glomerular endothelial cells and podocytes jointly synthesize laminin-1 and -11 chains. **Kidney International**, 60 (3): 1037–46

Steinberg, D. (1997) Low density lipoprotein oxidation and its pathobiological significance. **Journal of Biological Chemistry**, 272 (34): 20963–20966
Stephens, G., Yan, Y., Jandrot-Perrus, M., et al. (2005) Platelet activation induces metalloproteinase-dependent GP VI cleavage to down-regulate platelet reactivity to collagen. **Blood**, 105 (1): 186–91
Stirewalt, D.L. and Radich, J.P. (2003) The role of FLT3 in haematopoietic malignancies. **Nature reviews. Cancer**, 3 (9): 650–65
Strauss-Ayali, D., Conrad, S.M. and Mosser, D.M. (2007) Monocyte subpopulations and their differentiation patterns during infection. **Journal of leukocyte biology**, 82 (2): 244–52
Summers, C., Rankin, S.M., Condliffe, A.M., et al. (2010) Neutrophil kinetics in health and disease. **Trends in immunology**, 31 (8): 318–24
Sun, M., Fu, H., Cheng, H., et al. (2012) A dynamic real-time method for monitoring epithelial barrier function in vitro. **Analytical biochemistry**, 425 (2): 96–103
Suzuki, H., Kurihara, Y., Takeya, M., et al. (1997) A role for macrophage scavenger receptors in atherosclerosis and susceptibility to infection. **Nature**, 386: 292–296
Suzuki-Inoue, K., Fuller, G.L.J., García, A., et al. (2006) A novel Syk-dependent mechanism of platelet activation by the C-type lectin receptor CLEC-2. **Blood**, 107 (2): 542–9
Tedder, T.F., Steeber, D.A., Chen, A., et al. (1995a) The selectins: vascular adhesion molecules. **The FASEB Journal**, 9 (July): 866–873
Tedder, T.F., Steeber, D.A. and Pizcueta, P. (1995b) L-selectin-deficient mice have impaired leukocyte recruitment into inflammatory sites. **The Journal of Experimental Medicine**, 181: 2259–2264
Théorêt, J.F., Bienvenu, J.G., Kumar, A., et al. (2001) P-selectin antagonism with recombinant p-selectin glycoprotein ligand-1 (rPSGL-Ig) inhibits circulating activated platelet binding to neutrophils induced by damaged arterial surfaces. **The Journal of pharmacology and experimental therapeutics**, 298 (2): 658–64
Thorin, E. and Webb, D. (2010) Endothelium-derived endothelin-1. **Pflügers Archiv-European Journal of Physiology**, 459 (6): 951–958
Tiwari, S. and Siddiqi, S. a (2012) Intracellular trafficking and secretion of VLDL. **Arteriosclerosis, thrombosis, and vascular biology**, 32 (5): 1079–86
Tobón, G.J., Izquierdo, J.H. and Cañas, C. a (2013) B Lymphocytes: development, tolerance, and their role in autoimmunity-focus on systemic lupus erythematosus. **Autoimmune diseases**, 2013: 1–17
Totani, L. and Evangelista, V. (2010) Platelet-leukocyte interactions in cardiovascular disease and beyond. **Arteriosclerosis, thrombosis, and vascular biology**, 30 (12): 2357–61
Tull, S.P., Anderson, S.I., Hughan, S.C., et al. (2006) Cellular pathology of atherosclerosis: smooth muscle cells promote adhesion of platelets to cocultured endothelial cells. **Circulation research**, 98 (1): 98–104
Turowski, P., Martinelli, R., Crawford, R., et al. (2008) Phosphorylation of vascular endothelial cadherin controls lymphocyte emigration. **Journal of cell science**, 121: 29–37
Twigg, M.W., Freestone, K., Homer-Vanniasinkam, S., et al. (2012) The LOX-1 scavenger receptor and its implications in the treatment of vascular disease. **Cardiology research and practice**, 2012: 1–6
Uematsu, S. and Akira, S. (2006) Toll-like receptors and innate immunity. **Journal of molecular medicine**, 84: 712–25
Vachino, G., Chang, X.-J., Veldman, G.M., et al. (1995) P-selectin Glycoprotein Ligand-1 Is the Major Counter-receptor for P-selectin on Stimulated T Cells and Is Widely Distributed in Non-

functional Form on Many Lymphocytic Cells. **Journal of Biological Chemistry**, 270 (37): 21966–21974
Vyas, J.M., Van der Veen, A.G. and Ploegh, H.L. (2008) The known unknowns of antigen processing and presentation. **Nature reviews. Immunology**, 8 (8): 607–18
Wang, J.M., Sica, A., Peri, G., et al. (1991) Expression of monocyte chemotactic protein and interleukin-8 by cytokine-activated human vascular smooth muscle cells. **Arteriosclerosis, Thrombosis, and Vascular Biology**, 11 (5): 1166–1174
Wang, P. and Zheng, S.G. (2013) Regulatory T cells and B cells: implication on autoimmune diseases. **International journal of clinical and experimental pathology**, 6 (12): 2668–74
Weber, C. and Springer, T.A. (1997) Neutrophil accumulation on activated, surface-adherent platelets in flow is mediated by interaction of Mac-1 with fibrinogen bound to αIIbβ3 and stimulated by platelet-activating factor. **The Journal of Clinical Investigation**, 100 (8): 2085–93
Wegmann, F., Petri, B., Khandoga, A.G., et al. (2006) ESAM supports neutrophil extravasation, activation of Rho, and VEGF-induced vascular permeability. **The Journal of Experimental Medicine**, 203 (7): 1671–7
Welsh, G., and Saleem, M.. (2010) Nephrin—signature molecule of the glomerular podocyte? **The Journal of pathology**, 220: 328–337
Van Wetering, S., van den Berk, N., van Buul, J.D., et al. (2003) VCAM-1-mediated Rac signaling controls endothelial cell-cell contacts and leukocyte transmigration. **American journal of physiology. Cell physiology**, 285 (2): C343–52
Weyrich, A.S., Elstad, M.R., McEver, R.P., et al. (1996) Activated platelets signal chemokine synthesis by human monocytes. **The Journal of Clinical Investigation**, 97 (6): 1525–34
White, K.E. (2012) Research into the structure of the kidney glomerulus-making it count. **Micron**, 43 (10): 1001–9
White, S.J., Underhill, G.H., Kaplan, M.H., et al. (2001) Cutting edge: differential requirements for Stat4 in expression of glycosyltransferases responsible for selectin ligand formation in Th1 cells. **The Journal of Immunology**, 167 (2): 628–631
Whitelaw, D. and Bell, M. (1966) The intravascular lifespan of monocytes. **Blood**, 28: 455–464
Witko-Sarsat, V., Rieu, P., Descamps-Latscha, B., et al. (2000) Neutrophils: molecules, functions and pathophysiological aspects. **Laboratory Investigation**, 80 (5): 617–653
Woodfin, A., Voisin, M.-B., Imhof, B. a, et al. (2009) Endothelial cell activation leads to neutrophil transmigration as supported by the sequential roles of ICAM-2, JAM-A, and PECAM-1. **Blood**, 113 (24): 6246–57
Woollard, K.J. (2013) Immunological aspects of atherosclerosis. **Clinical Science**, 125: 221–235
Xiao, Z. and Théroux, P. (2004) Clopidogrel inhibits platelet-leukocyte interactions and thrombin receptor agonist peptide-induced platelet activation in patients with an acute coronary syndrome. **Journal of the American College of Cardiology**, 43 (11): 1982–8
Xu, J., Zhang, X., Pelayo, R., et al. (2009) Extracellular histones are major mediators of death in sepsis. **Nature medicine**, 15 (11): 1318–21
Yanaga, F., Poole, A., Asselin, J., et al. (1995) Syk interacts with tyrosine-phosphorylated proteins in human platelets activated by collagen and cross-linking of the Fcγ-IIA receptor. **The Biochemical journal**, 311: 471–478
Yang, C., Xiong, W., Qiu, Q., et al. (2012) Role of receptor-mediated endocytosis in the antiangiogenic effects of human T lymphoblastic cell-derived microparticles. **American journal of physiology. Regulatory, integrative and comparative physiology**, 302 (8): R941–R949
Yoshida, T. and Tuder, R.M. (2007) Pathobiology of cigarette smoke-induced chronic obstructive pulmonary disease. **Physiological reviews**, 87: 1047–1082

Zarbock, A., Lowell, C.. and Ley, K. (2007a) Syk signaling is necessary for E-selectin-induced LFA-1-ICAM-1 association and rolling but not arrest. **Immunity**, 26 (6): 773–783
Zarbock, A., Polanowska-Grabowska, R.K. and Ley, K. (2007b) Platelet-neutrophil-interactions: linking hemostasis and inflammation. **Blood reviews**, 21 (2): 99–111
Zhao, B., Rickert, C.H., Filler, T.J., et al. (1995) Adhesion of washed blood platelets in vitro is advanced, accelerated, and enlarged by oxidized low-density lipoprotein. **American Journal of Hematology**, 49: 177–182
Zhou, X., Nicoletti, A., Elhage, R., et al. (2000) Transfer of CD4+ T cells aggravates atherosclerosis in immunodeficient apolipoprotein E knockout mice. **Circulation**, 102 (24): 2919–2922
Zibara, K., Chignier, E., Covacho, C., et al. (2000) Modulation of expression of endothelial intercellular adhesion molecule-1, platelet-endothelial cell adhesion molecule-1, and vascular cell adhesion molecule-1 in aortic arch lesions of apolipoprotein E-deficient compared with wild-type mice. **Arteriosclerosis, Thrombosis, and Vascular Biology**, 20 (10): 2288–2296
Ziegler, T., Silacci, P., Harrison, V.J., et al. (1998) Nitric oxide synthase expression in endothelial cells exposed to mechanical forces. **Hypertension**, 32 (2): 351–355
Zlotnik, A. and Yoshie, O. (2012) The chemokine superfamily revisited. **Immunity**, 36 (5): 705–716